ASPECTS OF THE BIOLOGY OF SMALL FREE-LIVING AND FACULTATIVE PARASITIC AMOEBAE

NAKISAH MAT AMIN

B.Sc., National University of Malaysia (UKM), MALAYSIA
M.Sc., Michigan State University (MSU), USA

Thesis submitted for the
Degree of Doctor of Philosophy
January 1994

Laboratory For Biochemical Parasitology

DEPARTMENT OF ZOOLOGY
UNIVERSITY OF GLASGOW
GLASGOW, SCOTLAND.
UNITED KINGDOM.

© N. Mat Amin, 1994

ProQuest Number: 13818563

All rights reserved

INFORMATION TO ALL USERS
The quality of this reproduction is dependent upon the quality of the copy submitted.

In the unlikely event that the author did not send a complete manuscript
and there are missing pages, these will be noted. Also, if material had to be removed,
a note will indicate the deletion.

ProQuest 13818563

Published by ProQuest LLC (2018). Copyright of the Dissertation is held by the Author.

All rights reserved.
This work is protected against unauthorized copying under Title 17, United States Code
Microform Edition © ProQuest LLC.

ProQuest LLC.
789 East Eisenhower Parkway
P.O. Box 1346
Ann Arbor, MI 48106 – 1346

Abstract

Aspects of the biology of small, naked, free-living amoebae which include some facultatively parasitic forms have been studied with emphasis on two selected genera, *Naegleria* and *Hartmannella*. In the former genus, non-pathogenic *Naegleria gruberi* (CCAP strain 1518/1A), as well as the closely related pathogenic *Naegleria fowleri*, have been investigated.

A combination of fluorescence and electron microscopy techniques have been employed to investigate mitosis in *N. gruberi* with special reference to the distribution of chromosomes/DNA and the possible existence of the microtubule organising centres. In transmission electron micrographs, the nucleolus appeared to persist during nuclear divison but its electron density changed during the course of nuclear division. During most of stages of nuclear division, chromosomal elements could not be distinguished with certainty from nucleolar material. Possible chromosomal structures could be observed as electron dense spherical profiles or as fluorescent dots only when the nucleus was at metaphase or anaphase stages.

Intranuclear microtubules have been detected by transmission electron microscopy in most stages of nuclear division in *Naegleria*. Their profile length seemed to vary according to the stage of nuclear division and it is argued that this might reflect their function; the long microtubule profiles might represent continuous fibres responsible for the elongation of the nucleus in anaphase-telophase and the short microtubules may be important in transporting chromosomes to the poles i.e. the kinetochore microtubules. Both kinds of microtubule were observed in associations with the poles; the kinetochore microtubules were most evident when the nucleus was in metaphase. By both transmission microscopy and light microscopy, stages in both anaphase A (the moving apart of nuclear material to the daughter cells) and in anaphase B (the elongation of microtubules in order to move the poles apart) could be observed clearly.

Colchicine-treatment was used to induce synchronous division in *Naegleria* cells. During colchicine treatment, *Naegleria* cells stopped dividing but resumed division almost synchronously ~1 to 2 h after the drug was removed from the medium. Staining of such cells by α-tubulin antibody makes detection of microtubule structures in cells possible. A centrosome with associated microtubules was found by immunofluorescence using anti-tubulin-conjugated antisera to be present in the cytoplasm of *Naegleria* during nuclear division and this finding contradicts the previous idea that this organelle does not exist in *Naegleria.* The centrosome appeared to divide during prophase but it could not be detected later at metaphase-telophase. Moreover, transmission electron microscopy did not detect this organelle, though crystalloid structures possibly induced by the colchicine treatment were found near the nuclear envelope in early stages of division.

The presence of proteinases in *Naegleria* spp. and their relation to the life cycle was also investigated. These enzymes were found in all three stages of the amoeba's life cycle; trophozoite, cyst and flagellate. At pH 5.5 in the presence of DTT (dithiothreitol) at least 5 enzymes could be detected in gelatin SDS-PAGE gels for actively multiplying trophozoites; they were named bands A, B, C and DE enzymes . The apparent M_r of band A was ~200 kDa, band B was ~148 kDa, band C was ~ 116 kDa, band D was ~98 kDa and band E was ~92 kDa. Bands DE were the most prominent in gels. Flagellates appeared to posses enzymes A and DE, and cysts only band C. Amoebae grown on agar with living bacteria exhibited fewer proteinase bands than those grown in axenic medium; bacterised amoebae lacked bands B and C.

The individual proteinases present in *Naegleria* were characterised on the basis of inhibitor studies, apparent molecular weight, substrate preferences and pH optimum. Band A which was inconsistently observed in gelatin SDS-PAGE gels, had a wide pH range of activity (pH 5.5 to 8.0) but its acitvity was higher at alkaline pH and inhibited by APMSF (4-(amidinophenyl)methanesulphonyl fluoride). Bands B and C were active only at slightly acidic pH (5.5 to 6.0), indicating they are lysosomal in origin; their activity was DTT-dependent, inhibited by E-64 (L-3-carboxy-2,3-*trans*-epoxypriopionyl-leucylamido-(4-guanidino) butane) and markedly inhibited by antipain, so they could be cysteine proteinases. Doublet DE enzymes, which were membrane-associated, exhibited bimodal activities; at lower pH, their activities were stimulated by DTT but at alkaline pH their activities were higher and not stimulated by DTT. Their activities were inhibited by APMSF, EDTA (ethylenediaminetetraacetic acid) , E-64 and antipain. Band B and C enzymes hydrolysed only the fluorogenic peptidyl-amido methylcoumarin substrate, H-Pro-Phe-Arg-NHMec, in contrast to doublet DE enzymes which hydrolysed substrates H-Pro-Phe-Arg-NHMec, Z-Pro-Arg-NHMec, Bz-Phe-Val-Arg-NHMec and Z-Arg-Arg-NHMec.

A similar pattern of proteinases (in SDS-PAGE gelatin gels) was expressed by different stages of growth of amoebae in axenic culture but the intensity of each band appeared to be different and this may have been due to the condition of the trophozoites in cultures during growth. Cysts, which increase in number in older cultures are not so readily lysed by Triton-X-100-treatment as trophozoites, and flagellates revert to the amoeboid stages so quickly they probably did not contribute to the number and intensity of proteinase bands on these gels. The increase in number of non-viable cells in older cultures did not appear to affect the pattern of proteinases observed on gels.

Axenically grown *N. gruberi* (strain 1518/1A) secreted proteinases (apparent M_r 92 kDa, 90 kDa and 75 kDa) into the culture medium and these enzymes could be essential for food predigestion outside the cell. The secretion of these enzymes perhaps together with membrane-associated enzymes (doublet DE enzymes) might also be related to the cytopathogenicity of this amoeba *in vitro* reported by other workers. Other strains of *N. gruberi* (CCAP strains 1518/7 and 1518/G) were used for comparison of proteinase patterns. Different patterns of proteinases on gels were observed for different strains of *N. gruberi* and these may be indicative of genetic, physiological and morphological heterogeneity within the species. Some of the enzymes (bands of apparent M_r 148 kDa and M_r 98 kDa in strain 1518/1G, bands of apparent M_r 148 kDa and M_r 92 kDa in strain 1518/7, and bands of apparent M_r 148 kDa and M_r 98 kDa and M_r 92 kDa in strain 1518/1A) however, appear to have been conserved in all strains and were not detected in *N. fowleri*, so they could be used in defining the species *Naegleria gruberi*.

Pathogenic *N. fowleri* (strain NF3) lysate was found to posses at least two proteinase activities whose apparent M_r was 170 kDa and 128 kDa. The band of 128 kDa-enzyme is membrane-associated and its activity is higher at alkaline pH than at lower pHs; at lower pHs its activity was greatly stimulated by DTT. The activity of band 170 kDa enzyme was higher at pH 5.5 and stimulated by DTT, its activity was destroyed at pH 8.0, suggesting it is a lysosomal enzyme. The activity of this enzyme was inhibited by antipain and slightly inhibited by E-64 indicating that it belongs to the cysteine proteinase group. *N. fowleri* and *N. gruberi* do not share common proteinase enzymes.

Another free-living amoeba, *Hartmannella sp.*, isolated from a contact lens case, has been identified and designated as *Hartmannella vermiformis* (WI isolate) in this study. Its morphology (both trophozoites and cysts) and measurements were identical to a designated strain of *H. vermiformis* (CCAP 1534/7A). The possible invassiveness of the amoeba to human cornea *in vitro* was tested. *H. vermiformis,* (WI isolate) was observed to cause removal of the corneal epithelium 24 h after inoculation. The amoeba did not invade the corneal stroma in contrast to *Acanthamoeba castellanii* (isolated from human cornea biopsy) with which experiments were performed in parallel. *Acanthamoeba* was observed to bind to and invade the corneal stroma without necessarily damaging the epithelium. The results of this study suggest that *Hartmannella* and *Acanthamoeba* have a different mechanism for destroying human cornea *in vitro.*

List of Contents

Page

Title page ... i
Abstract ... ii
List of Chapters ... vi
List of Figures ... xii
List of Tables ... xiv
Acknowledgements ... xv
Declaration ... xvii
List of Abbreviations ... xviii

List of Chapters

1.0. INTRODUCTION AND LITERATURE BACKGROUND

1.1. INTRODUCTION ... 1
1.2. IDENTIFICATION AND CLASSIFICATION OF *NAEGLERIA* SPP ... 5
1.3. MORPHOLOGY AND BIOLOGY OF VARIOUS STAGES IN THE LIFE CYCLE OF *NAEGLERIA* SPP ... 8
  Stages in life cycle ... 8
  Trophozoite ... 9
  Flagellate ... 12
  Cyst ... 13
1.4. MITOSIS IN *NAEGLERIA GRUBERI* ... 15
  Stages of mitosis ... 16
  The properties of microtubules and methods of detection in whole cells ... 17
  The mitotic spindle ... 20
  Spindle fibre action and chromosome movement ... 20
  Effect of microtubule poisons ... 23
1.5. LYSOSOMAL AND NON-LYSOSOMAL ENZYMES IN *NAEGLERIA* SPP ... 24
  The nature of lysosomes ... 25
  Lysosomal function related to cellular digestion ... 25
  The lysosomal enzymes ... 27
  Proteinases ... 28
  Classification of proteinases ... 30
  Non-lysosomal enzymes ... 31

1.6. PATHOGENICITY OF *NAEGLERIA* SPP AND OTHER FREE-LIVING AMOEBAE 32

Pathogenicity of Naegleria spp 32

Pathogenicity of other free-living amoebae 35

1.7. AIMS OF PROJECT 39

2.0. MITOSIS IN *NAEGLERIA GRUBERI*

2.1. INTRODUCTION 40

2.2. MATERIALS AND METHODS 41

- 2.2.1. Cultivation of amoebae 41
  - *Cultivation of amoebae on solid media with bacteria* 41
  - *Axenic cultivation of amoebae in liquid medium* 41
  - *Preparation of heat-killed Escherichia coli suspensions* 42
- 2.2.2. Maintenance of cultures 42
- 2.2.3. The culture medium 43
  - *Bath-Spa medium:* 43
  - *Modified Neff's amoeba saline solution (PAS)* 44
- 2.2.4. Counting the amoebae in cultures 44
  - *Using random number quadrats* 44
  - *Using a haemocytometer* 44
- 2.2.5. Calculating the population doubling time of *Naegleria gruberi* grown in Bath-Spa medium at 32°C 45
- 2.2.6. Obtaining synchronous division in *Naegleria gruberi* 46
- 2.2.7. Preparation for transmission electron microscopy 47
  - *By conventional methods* 47
  - *Techniques for preserving the microtubules* 47
- 2.2.8. Preparation for fluorescence microscopy 48
  - *DNA and RNA staining* 48
  - *Microtubule staining* 49

2.3. RESULTS 50

- 2.3.1. Observation of *Naegleria gruberi* growth in Bath-Spa medium medium at 32°C 50
- 2.3.2. Transmission electron microscopy observations on mitosis in *Naegleria gruberi* 54
- 2.3.3. Fluorescent microscopy study of mitosis in *N. gruberi* 64
  - *Detection of DNA-containing material in cells* 64
  - *Nuclear division in colchicine-treated Naegleria* 67

2.3.4. Observation of the cytoplasmic microtubules in colchicine-treated cells by transmission electron microscopy ... 76

2.4. DISCUSSION ... 79

2.4.1. Population doubling time of *N. gruberi* grown in Bath-Spa medium ... 79

2.4.2. Nuclear division in *Naegleria gruberi* ... 80

The behaviour of nucleolar materials in various stages of the nuclear division ... 81

Do chromosomes exist as individually-discernible structures? ... 82

Are MTs visible in the dividing nucleus of N. gruberi ... 84

Are kinetochores and their related chromosomal fibres discernible? ... 85

Are MTOCs discernible at the poles of the spindle, either inside or outside of the persisitent nuclear envelope? ... 85

Effect of colchicine on cell division in N. gruberi ... 87

2.4.3. General problems and conclusions ... 89

2.5. SUMMARY ... 92

3.0. PROTEINASES IN *NAEGLERIA* SPP

3.1. INTRODUCTION ... 94

3.2. MATERIALS AND METHODS ... 96

3.2.1. Source of samples ... 96

Strains of Naegleria spp used ... 96

Growth conditions ... 97

Modified Chang's medium ... 98

Trophozoite form of amoeba ... 99

Flagellate form of amoeba ... 99

Cyst form of amoeba ... 102

3.2.2. Sample preparations for enzyme extraction ... 102

3.2.3. Protein content determination ... 103

3.2.4. Proteinase assays ... 104

Spectrophotometric assays ... 104

Electrophoretic analysis ... 105

Inhibitor studies to characterise the enzymes ... 107

3.2.5 Enzyme fractionation by gel filtration technique ... 107

3.2.6 Detection of membrane-associated enzymes ... 108

3.2.7 Detection of extracellular enzymes ... 109

3.2.8 Detection of proteinases in different phases of growth in cultures 109

3.2.9 Proteinases detection in *Naegleria gruberi* grown on agar with bacteria 110

3.2.10. Proteinases in different strains of *N. gruberi* and pathogenic *Naegleria fowleri* 110

3.3. RESULTS 111

3.3.1 Proteinases in *Naegleria gruberi* CCAP strain 1518/1A 111

Detection of proteinases in trophozoites, flagellates and cysts using gelatin-SDS-PAGE gels 111

Detection of membrane-associated enzymes 112

Characterisation of individual proteinases in trophozoite samples of N. gruberi 116

Effect of DTT and pH on band appearances 116

Inhibitor study to characterise the enzyme on gelatin gels 117

Spectrophotometric assays of proteinase activity in Naegleria crude lysate 122

Activity towards substrate Bz-Pro-Phe-Arg-Nan 122

Comparison of lysate proteinase activity towards different substrates 122

Effect of inhibitors on *Naegleria* lysates towards Bz-Pro-Phe-Arg-Nan 125

Separation of Naegleria proteinases by FPLC gel filtrations 126

Activity towards Bz-Phe-Pro-Arg-Nan 126

Band pattern on gelatin SDS-PAGE gels 126

Activity on fluorogenic H-Pro-Phe-Arg-NHMec 127

Detection of extracellular enzymes 131

Proteinases at different phases of growth in cultures 131

3.3.2 Proteinases in different strains of *Naegleria gruberi* 136

Proteinase patterns on gelatin SDS-PAGE gels in different strains of N. gruberi 136

Characterisation of individual proteinases in strains 1518/7 and 1518/1G of N. gruberi 138

Effect of pH and DTT on enzyme activity on gelatin gels 138

Inhibitor studies to characterise the proteinases on gelatin SDS-PAGE gels 139

Substrate preferences of the proteinases
from different strains of *N. gruberi* ... 139

3.3.3 Proteinases in pathogenic *Naegleria fowleri* ... 144

On gelatin gels ... 144

Effect of inhibitors on the enzymes ... 144

3.4. DISCUSSION ... 147

3.4.1. Proteinases in *Naegleria gruberi* CCAP strain 1518/1A ... 147

Detection of membrane-associated enzymes ... 148

Characterisation of individual proteinases in the trophozoite samples of N. gruberi ... 149

Activity of Naegleria lysates on peptide nitroanilides and fluorogenic amidomethylcoumarin substrates ... 151

Presence and role of proteinases in different stages of the life cycle ... 152

Enzymes secreted by N. gruberi ... 153

Proteinases in different phases of growth ... 154

3.4.2. Proteinases in different strains of *Naegleria gruberi* ... 155

3.4.3. Proteinases in pathogenic *Naegleria fowleri* ... 157

3.5. SUMMARY ... 160

4.0. PATHOGENICITY OF *HARTMANNELLA SP.*

4.1. INTRODUCTION ... 163

4.2. MATERIALS AND METHODS ... 164

4.2.1. Isolation and identification of the amoeba. ... 164

Method of isolation ... 164

Identification ... 165

4.2.2. Cultivation of *Hartmannella sp.* ... 166

Monoxenic cultivation ... 166

Attempts at axenic cultivation ... 166

ATCC medium 1034 ... 166

4.2.3. Pathogenicity study ... 167

Preparation of amoebae ... 167

Human cornea ... 168

Light and transmission electron microscopy ... 168

Scanning electron microscopy ... 169

4.3. RESULTS ... 169

4.3.1. Identification of *Hartmannella sp.* ... 169

Trophozoites of the amoeba ... 170

Cysts of the amoeba 173
4.3.2 Evidence of pathogenicity 176
Control corneas 177
Experimental corneas 180
Incubated with *Hartmannella sp.* 180
Incubated with *Acanthamoeba castellanii* 187
4.4. DISCUSSION 191
4.4.1. Identification of *Hartmannella sp.* 191
4.3.1. Evidence of pathogenicity 193
4.5. SUMMARY 197
5.0. LIST OF REFERENCES 198

List of Figures

Figure 1.1. *Life cycle of Naegleria gruberi* 9

Figure 1.2. *Substructure of a microtubule.* 19

Figure 2.1. *A phase constrast micrograph of N. gruberi CCAP 1518/1A* 51

Figure 2.2. *Determination of population doubling time of N. gruberi* 52

Figure 2.3. *Transmission electron micrographs (TEM) showing various stages of nuclear division* 57

Figure 2.4. *Fluorescence microscopy of Naegleria cells stained with DAPI and PI* 65

Figure 2.5. *Cytokinesis in N. gruberi observed by fluorescence microscopy.* 66

Figure 2.6. *Organisation of a centrosome (MTOC) during nuclear division* 70

Figure 2.7. *Immunofluorescence staining of Naegleria cells.* 74

Figure 2.8. *Studies on nuclear division in N. gruberi under fluorescence microscopy* 75

Figure 2.9. *TEM of Naegleria cells after treatment with colchicine* 77

Figure 2.10. *Paracrystalline extranuclear structures observed in Naegleria after colchicine-treatment* 78

Figure 3.1. *Glass bead column* 101

Figure 3.2A. *Photographs of gelatin SDS-PAGE gels of proteinases in trophozoites, flagellates and cysts of N. gruberi.* 113

Figure 3.2B. *Phase micrograph of Lugol's iodine-fixed flagellates of N. gruberi* 114

Figure 3.2C. *Scanning electron micrograph (SEM) of cysts of N.gruberi* 114

Figure 3.3. *Detection of membrane-associated enzyme in N. gruberi.* 115

Figure 3.4A. *Effect of pH of the gel incubation buffer and DTT on band appearances in supernatant of Triton X-100-lysed cells of N. gruberi* 118

Figure 3.4B. *Effect of pH buffer on band A enzyme activity in N. gruberi lysates* 119

Figure 3.5A. *Effect of the inhibitor APMSF on enzyme activity on gelatin gel.* 120

Figure 3.5B. *Effect of various inhibitors on enzyme activity of N. gruberi crude lysates* 121

Figure 3.6. *Specific activity of N. gruberi crude lysates towards Bz-Pro-Phe-Arg-Nan* 124

Figure 3.7A. Fractionation of N. gruberi crude lysate by gel filtration 128
Figure 3.7B. Elution of N. gruberi crude lysate from gel filtration by FPLC 129
Figure 3.7C. Detection of enzymes in the fractions of N. gruberi crude lysate from gel filtration by FPLC on gel incubated in substrate H-Pro-Phe-Arg-NHMec 130
Figure 3.8. Secreted enzymes detected in the medium. 132
Figure 3.9. Proteinase activity of N. gruberi on gelatin gels during growth 133
Figure 3.10. Culture composition of N. gruberi grown in Bath-Spa medium 135
Figure 3.11. Proteinase patterns produced by different strains of N.gruberi on gelatin gels 137
Figure 3.12. The effect of pH and DTT on enzyme activity on the gelatin gels of N. gruberi strains 1518/7 and 1518/1G. 141
Figure 3.13. Effect of the inhibitors on proteinases produced by N. gruberi strains 1518/7 and 1518/1G 142
Figure 3.14. Proteinase pattern produced by different strains of N. gruberi on gels incubated in different fluorogenic substrates 143
Figure 3.15. Proteinases in pathogenic Naegleria fowleri. 145
Figure 3.16. Effect of the inhibitors on proteinases of N. fowleri 146
Figure 4.1. Cysts and trophozoites of Hartmannella sp. (WI isolate) observed on agar 171
Figure 4.2. TEM of flattened and elongated profiles of Hartmannella sp.... 172
Figure 4.3. Section through whole cyst of Hartmannella sp. 175
Figure 4.4. Light micrographs of cysts of H. vermiformis CCAP strain 1534/7A 176
Figure 4.5. Light micrographs of sectional view of control human cornea. 178
Figure4.6. TEM showing three layers of intact epithelial cells of control human cornea 179
Figure 4.7. SEM of control human corneal surface 182
Figure 4.8. Light micrographs of thick vertical section of human cornea incubated with Hartmannella sp.. 183
Figure 4.9. TEM of human cornea (A to C) when incubated with Hartmannella sp. 184
Figure 4.10. SEM of human corneal surface when incubated with Hartmannella 186
Figure 4.11. Light micrographs of thick vertical sections of human cornea after incubation with Acanthamoeba castellanii. 188
Figure 4.12. TEM of human cornea (A to D) showing evidences of Acanthamoeba intrusion in the corneal stroma 189

List of Tables

Table 1.1. *Nomenclature and interrelationship of components of the lysosomal system* 26

Table 1.2. *Classification of proteinases by use of inhibitors* 30

Table 1.3. *Free-living amoeba infections in vertebrate animals* 38

Table 2.1. *Population doubling time of Naegleria gruberi* 53

Table 3.1. *The history of Naegleria spp. isolates* 97

Table 3.2. *Specific activity of Naegleria gruberi (strain 1518/1A) crude lysates towards Bz-Pro-Phe-Arg-Nan* 123

Table 3.3.. *Comparison of the specific activity of Naegleria gruberi (strain 1518/1A) crude lysates towards Bz-Pro-Phe-Arg-Nan, Bz-Arg-Arg-Nan and D-Val-Ser-Arg-Nan* 125

Table 3.4. *Culture composition of N. gruberi (strain 1518/1A) grown axenically in Bath-Spa medium at 32°C for 7 days* 134

Table 4.1. *Comparative measurement for trophozoites and cysts of Hartmannella vermiformis (CCAP strain 1534/7A) with Hartmannella sp. (WI isolate)* 174

Acknowledgements

Alhamdullilah, despite being in such difficult situations and subjected to so many constraints, I have managed to finish and complete this thesis; all by *His Will and Help*.

I am very grateful to my supervisor, Professor Keith Vickerman for advice and supervising especially during writing-up this thesis. Through him also, I came to know so many people who work with small free-living amoebae and related fields.

I have had the chance to discuss problems of my work with so many people and I am very grateful to get such good feedback from them; Dr Joe Irvine, Dr. Dave A. Scott, and Dr. Colin D. Robertson for proteinase work; Dr. Laurence Tetley and Dr. Max Huxham for electron microscopy work; Dr. Andrew Campbell, Department of Bacteriology, Stobhill Hospital, Glasgow, Dr. Johan F. De Jonckheere, Department of Microbiology, Instituut voor Hygiëne en Epidemiologie, Brussel, Belgium, and Mr. Simon Kilvington, Public Health Laboratory, Bath, UK., for working with pathogenic *Naegleria*.

I would like to express my gratitude to Dr. Colin D. Robertson and Dr. Dave A. Scott for reading the chapter on proteinases; to the Head Department of Microbiology, University of Glasgow for allowing me to use the containment lab while working with pathogenic *Naegleria;* to Professor Colin M. Kirkness, Department of Ophthalmology, Western Infirmary, Glasgow for supplying the human corneas; to Dr Huw Smith, Department of Parasitology, Stobhill Hospital, Glasgow and Mr Simon Kilvington for supplying pathogenic *Naegleria fowleri*; to Dr. Trevor Sherwin, Department of Biochemistry and Molecular Biology, University of Manchester, for giving anti α-TAT1 tubulin antibody; to Dr. Alan G. Williams, Hannah Research Institute, Ayr, for allowing me to use some of his chemicals and equipment in proteinase studies; and lastly to Professor Graham H.

Coombs, the Head Department of Zoology, University of Glasgow and the Head Unit of Laboratory for Biochemical Parasitology, for allowing me to use facilities at his unit premises throughout my study.

I would like to acknowledge assistance in various aspects of my work from Margaret Mullin, Liz Denton, Maurine Gardner and Peter Rickus. I also would like to thank almost everybody in Department of Zoology, University of Glasgow for their kindness and friendliness which made my stay in Glasgow is a memorable one.

I also wish to thank the Malaysian Government for financial support and Universiti Pertanian Malaysia for study leave. Lastly I would like to thank my family and close friends who always encourage me '*not to quit*' and '*be done with it*', it is therefore appropriate here to dedicate this thesis to them.

Declaration

The content of this thesis is of my original work

except where otherwise stated.

List of Abbreviations

AIDS	Aquired Immunodeficiency Syndrome
AMP	Adenosine monophosphate
APMSF	*p*-APMSF, 4-(amidinophenyl)methanesulphonyl fluoride
ATP	Adenosine triphosphate
BSM	Bath-Spa medium
Bz	*N*-benzoyl
CLS	centriole-like structures
CPE	cytopathic effect
DAPI	4',6-diamidino-2-phenylindole
3,4-DCI	3,4-dichloroisocoumarin
DFP	di-isopropylfluorophosphate (DipF)
DTT	dithiothreitol
E-64	L-3-carboxy-2,3-*trans*-epoxypriopionyl-leucylamido-(4-guanidino) butane
EDTA	ethylenediaminetetraacetic acid
EGTA	ethyleneglyco bis-aminoethyl ether-*N*, *N'* tetraacetate
FITC	fluorescein isothiocyanate-labelled goat anti-mouse immunoglobulin
FPLC	fast protein liquid chromatography
GAE	granulomatous amoebic encephalitis
GDP	guanosine diphosphate
GTP	guanosine triphosphate
GTP_e	GTP which is exchangeable with depolymerised tubulin
GTP_n	non-exchangeable GTP
H	histidine
HV	high-virulence
kDa	kilodalton
kMT	kinetochore microtubule
LV	low-virulence
M_r	relative molecular weight
MT	microtubules
MTOC	microtubule organising centre
NACM	*Naegleria* amoeba cytopathogenic material
Nan	4-nitroanilide

NHMec	7-(4-methyl) coumarylamide
nkMT	non-kinetochore microtubule
PAGE	polyacrylamide gel electrophoresis
PAME	primary amoebic meningoencephalitis
PAS	Page's amoeba saline
PBS	phosphate buffered saline
PDT	population doubling time
PI	propidium iodide
PIPES	piperazine *N,N'*-bis(2-ethane sulfonic acid)
PMSF	phenylmethylsulphonyl fluoride
PPG	proteose peptone glucose
PP_i	inorganic pyrophosphate
PP_i-PFK	pyrophosphate-dependent phosphofructokinase
psi	pounds per square inch
RER	rough endoplasmic reticulum
R_f	relative mobility
SCL	soft contact lens
SDS	sodium dodecyl sulphate
SEM	scanning electron microscope
TEM	transmission electron microscope
TLCK	L-1-chloro-3-[4-tosylamido]-7-amino-2-heptanone·HCl
TPCK	L-1-chloro-3-[4-tosylamido]-4-phenyl-2-butanone
(v/v)	volume per volume
(w/v)	weight per volume
Z	*N*-benzylocarbonyl

Chapter 1

Introduction and Literature background

Chapter 1

INTRODUCTION AND LITERATURE BACKGROUND

1.1. INTRODUCTION

Small, naked, free-living amoebae are ubiquitous in Nature. Different types can be distinguished from one another by their morphology, locomotive form and behaviour, cyst morphology, and ability to transform into flagellates, also by physiological characters such as ability to grow at higher temperatures (Page, 1988) and pathogenicity in experimental animals or mammalian cell cultures (De Johnckeere, 1979; Marciano-Cabral and Fulford, 1986). Although in their natural environment, these amoebae feed mainly on bacteria, some of them can become tissue feeders and facultative pathogens of the human brain and eye. One of these amoebae, *Naegleria fowleri* causes lethal primary amoebic meningoencephalitis (PAME) in healthy humans. This amoeba belongs to a group of amoebae, the so called amoeboflagellates, which have the ability to transform into flagellates in adverse environments. Another amoeba, *Acanthamoeba*, which belongs to different group of free-living amoebae, infects the eye and the central nervous system (CNS) in immunodepressed hosts, inducing a subacute or chronic granulomatous amoebic encephalitis (GAE) (Martinez, 1985). These amoebae gain access to the CNS of the host directly through the olfactory-submucosal nervous plexus in the case of *N. fowleri*, and indirectly via the blood stream, particularly from lungs, in case of *Acanthamoeba*. Infection of the cornea with *Acanthamoeba* is serious and vision threatening. Reports on the association of *Acanthamoeba* keratitis with contact lens wear reveal that this infection is due to the lens having been contaminated with this amoeba (Auran *et al.*, 1987, Stehr-Green *et al.*, 1989).

Free-living naked amoebae, including the two genera mentioned, are classified in the Phylum Rhizopoda von Siebold, 1845 (Page, 1987; 1988).

Naegleria and other amoeboflagellates are grouped in the class Heterolobosea Page and Blanton, 1985. The class Caryoblastea Margulis, 1974 contains the single giant amitochondriate amoeba *Pelomyxa palustris* which has non-motile flagella. Other naked amoebae do not produce flagellates and are placed in the class Lobosea Carpenter, 1861. *Acanthamoeba* belongs to the Lobosea as do amoebae of the genus *Hartmannella*; both these genera contain facultative pathogenic forms. Detailed classification of the free-living, naked amoebae is given overleaf.

Among these amoebae, the genus *Naegleria* is of primary interest in the present study. The genus contains free-living species such as *N. gruberi* and facultatively pathogenic species such as *N. fowleri*. This thesis explores aspects of the biology of *Naegleria* spp. relevant to their unusual cellular organisation and lifestyle. In the following sections, details of cell biology including species identification, mitosis, proteinases and pathogenicity of the amoebae belonging to this genus will be discussed and described. For other amoebae, only aspects of their pathogenicity will be reviewed in this chapter (see section 1.6.).

*A modified classification of naked, free-living amoebae by Page (1987; 1988)

PHYLUM RHIZOPODA von Siebold, 1845
Class HETEROLOBOSEA Page and Blanton, 1985
Order SCHIZOPYRENIDA Singh, 1952
Family Vahlkampfiidae Jollos, 1917
Genus *Adelphamoeba, Naegleria, Paratetramitus, Tetramitus Vahlkampfia, Willaertia*
Family Gruberellidae Page and Blanton, 1985
Genus *Stachymoeba*
Order ACRASIDA Schröter, 1886; emend. Page and Blanton, 1985
Family Acrasidae van Tieghem, 1880; emend. L.S. Olive, 1970
Genus *Acrasis*
Family Guttulinopsidae L.S. Olive, 1970
Genus *Guttulinopsis*

Class CARYOBLASTEA Margulis, 1974
Order PELOBIONTIDA Page, 1976
Family Pelomyxidae Schulze, 1877
Genus *Pelomyxa*

Class LOBOSEA Carpenter, 1861
Subclass GYMNAMOEBIA Haeckel, 1862
Order EUAMOEBIDA Lepsi, 1960
Family Amoebidae Ehrenberg, 1838
Genus *Amoeba, Chaos*
Family Thecamoebidae Schaeffer, 1926; emend. Page, 1987
Genus *Thecamoeba, Dermamoeba*
Family Hartmannellidae Volkonsky, 1931; emend. Page, 1974
Genus *Hartmannella, Saccamoeba*
Family Vannellidae Bovee, 1979
Genus *Vannella, Platyamoeba*
Family Paramoebidae Poche, 1913; emend. Page, 1987
Genus *Dactylamoeba, Mayorella*
Family Vexilliferidae Page, 1987
Genus *Vexillifera*

Order LEPTOMYXIDA Pussard and Pons, 1976; emend. Page, 1987
Suborder RHIZOFLABELLINA Page, 1987
  Family Flabellulidae Bovee, 1970
    Genus *Paraflabellula*
  Family Leptomyxidae Pussard and Pons, 1976; emend. Page, 1987
    Genus *Leptomyxa, Rhizamoeba, Balamuthia*
Suborder LEPTORAMOSINA Page, 1987.
  Family Gephyramoebidae Pussard and Pons, 1976
    Genus *Gephyramoeba*
Order ACANTHOPODIDA Page, 1976
  Family Acanthamoebidae Sawyer and Griffin, 1975
    Genus *Acanthamoeba*

* This classification does not include free-living marine amoebae.

1.2. IDENTIFICATION AND CLASSIFICATION OF *NAEGLERIA* SPP

Naegleria gruberi was first identified as *Amoeba gruberi* by Schardinger (1899). The genus was later amended to *Naegleria* by Alexeieff (1912). Members of the genus *Naegleria* have the ability to undergo temporary transformation from amoebae to flagellates. In a modified classification of naked, free-living amoebae (Page, 1987 and 1988), this genus is placed in the Family Vahlkampfiidae Jollos 1917; Order Schizopyrenida Singh 1952; Class Heterolobosea Page and Blanton, 1985 and Phylum Rhizopoda, von Siebold 1845.

The Schizopyrenida are characterised as follows; they exhibit a single pseudopod and move through a series of eruptive, hyaline hemispherical pseudopodial bulges; they are typically uninucleate with a large central nucleolus; nuclear division is promitotic that is the nucleolus persits and divides into two polar masses during division; flagellate stages are present in the life cycle of most species. Other genera included in this group are *Vahlkampfia* Chatton & Lalung-Bonnaire 1912, *Willaertia* De Jonckheere, Dive, Pussard and Vickerman, 1984 and *Tetramitus* Perty 1852. In *Naegleria* spp, mitotic divisions are restricted to the amoeboid phase whereas in *Tetramitus sp.*, feeding and division occur in both amoeboid and flagellate stages. The flagellates of *Willaertia* have four flagella and cell division occurs both in flagellate and amoeboid stages (De Jonckheere *et al.*,1984a). There is no flagellate stage in *Vahlkampfia* spp (Page, 1974).

Morphological features of cyst and trophozoite forms of amoebae including locomotion have been used in earlier stages of generic identification both at light and electron microscope levels (Page, 1974; 1976; Carosi *et al.*, 1977; Balamuth *et al.*, 1983; Page, 1985; Page and Blanton, 1985). Another feature which is useful as a means of species identification when combined with other methods of identification, is the structure of the mitotic figure as suggested by Singh (1950, 1952) and then adopted by others, including Page and Blanton (1985).

The genus *Naegleria* to date comprises six species; *Naegleria gruberi* (Schardinger, 1899), *Naegleria fowleri* Carter, 1970, *Naegleria jadini* Willaert and le Ray, 1973, *Naegleria lovaniensis* Stevens and De Jonckheere and Willaert, 1980, *Naegleria australiensis* De Jonckheere, 1981 and *Naegleria andersoni* De Jonckheere, 1988. The trophozoite forms of these species are morphologically indistinguishable, but they differ in molecular characters as revealed by indirect fluorescent antibody reactions (De Jonckheere *et al.*, 1974), isoenzyme electrophoretic patterns (Nerad and Dagget, 1979; De Jonckheere, 1982; Pernin *et al.*, 1985; Adams *et al.*, 1989) or by free and bound amino acids (Alonso and Zubiaur, 1989). Cyst wall structure of *N. gruberi*, *N. fowleri* and *N. jadini* at the ultrastructural level has been observed to be different (Schuster, 1975a). The cysts of *N. gruberi* have pores with collars which other *Naegleria spp* do not have, hence these structures also can be used to distinguish between *Naegleria* spp. A phylogenetic tree of *Naegleria* spp has been constructed based on sequence analyses of ribosomal DNAs (Clark, 1990).

N. gruberi and *N. jadini* are mesophilic, that is they grow well at the temperature between 20°C to 37°C, are non-pathogenic for mice but are cytopathic for cultured mammalian cells (Marciano-Cabral and Bradley, 1982). *N. fowleri* is thermophilic i.e. grows better at temperatures between 37°C and 45°C, is pathogenic for humans and experimental animals, and cytopathic for cultured mammalian cells (Carter, 1970; Visvesvara and Callaway, 1974). *N. lovaniensis* is an environmental isolate, thermophilic and somewhat related to *N. fowleri* antigenically, but it is not pathogenic for mice (Stevens *et al.*, 1980). *N. australiensis*, originally isolated from flood waters in Australia, exhibits low to moderate pathogenicity for mice but is antigenically and biochemically distinct from *N. fowleri* (De Jonckheere, 1981). And lastly, *N. andersoni* is reported to be non-pathogenic in experimental animals and show no cytopathic effects in cell cultures (De Jonckheere, 1988). Among these species, *Naegleria fowleri* and *Naegleria* *gruberi* have been most studied. *Naegleria gruberi* has been used to study the molecular biology of cellular differentiation (Fulton, 1977) and the pattern of cell division in vahlkampfiid amoebae (Singh, 1952; Page, 1967a; Fulton, 1970; Schuster, 1975b). The ability of *Naegleria fowleri* to cause disease in humans has attracted many workers to study the pathogenesis of this amoeba in experimental animals and tissue cultures and also to find possible determinants of its virulence (Visvesvara and Callaway, 1974; Curson *et al.*, 1978; Hysmith and Franson, 1982; Lowrey and McLaughlin, 1985a; Marciano-Cabral and Fulford, 1986; Dunnebacke and Dixon, 1989).

Since morphology and locomotion of *N. gruberi* are similar to pathogenic *N. fowleri*, for many years, any isolate of *Naegleria* which did not cause disease when intranasally instilled in mice was considered to be *N. gruberi* and every pathogenic *Naegleria* isolate was assumed to be *N. fowleri*. The differences between these two species however, have been confirmed by the techniques mentioned previously and also by the ability of *N. fowleri* to grow at temperatures higher than 37°C (De Jonckheere *et al.*, 1974; De Jonckheere, 1982; Daggett and Nerad, 1983). Although in nature these amoebae are phagotrophs, an axenic medium has been devised by Chang (1974) and used to differentiate not only between pathogenic and non-pathogenic species of *Naegleria* spp., but also between pathogenic and non-pathogenic isolates of *N. fowleri*. Only pathogenic forms can grow in this medium at temperatures above 37°C (De Jonckheere, 1977).

With regard to temperature tolerance in identifying *Naegleria* spp, the pathogenic *N. fowleri* grown on agar with bacteria are able to grow at temperatures up to 45°C (Griffin, 1972). De Jonckheere *et al.* (1975), however, showed that ability to grow at higher temperature is not a characteristic of *N. fowleri* alone. Although one of their *Naegleria* isolates gave a positive reaction with *N. fowleri* antiserum, it did not exhibit pathogenicity in mice. This isolate was designated a non-pathogenic seropositive *N. fowleri* variant (De Jonckheere and Van de Voorde,

1977) but was later found to be different from *N. fowleri* by electron microscopy and immunoelectrophoretic analyses. This isolate was then named *N. lovaniensis* (Stevens *et al.*, 1980). These reports suggest the importance of employing a combination of morphological and non-morphological methods in identifying amoeba species, especially *Naegleria* spp.

1.3. MORPHOLOGY AND BIOLOGY OF VARIOUS STAGES IN THE LIFE CYCLE OF *NAEGLERIA* SPP

Stages in life cycle

For a unicellular organism, *Naegleria sp.* has a complex life cycle (Figure 1.1). It can exist in three states; as a vegetative trophozoite which feeds and divides; as a flagellate which swims vigorously but does not feed or divide; and as a cyst, a resting stage. The only stage which is invasive is the trophozoite. Although the cyst is not invasive, it is potentially infective since it can convert to the vegetative form under appropriate conditions (John, 1982). The trophozoite can transform into either cyst stage or flagellate stage depending on the environmental conditions. There is no direct transformation from cyst to flagellate or flagellate to cyst (Fulton, 1970).

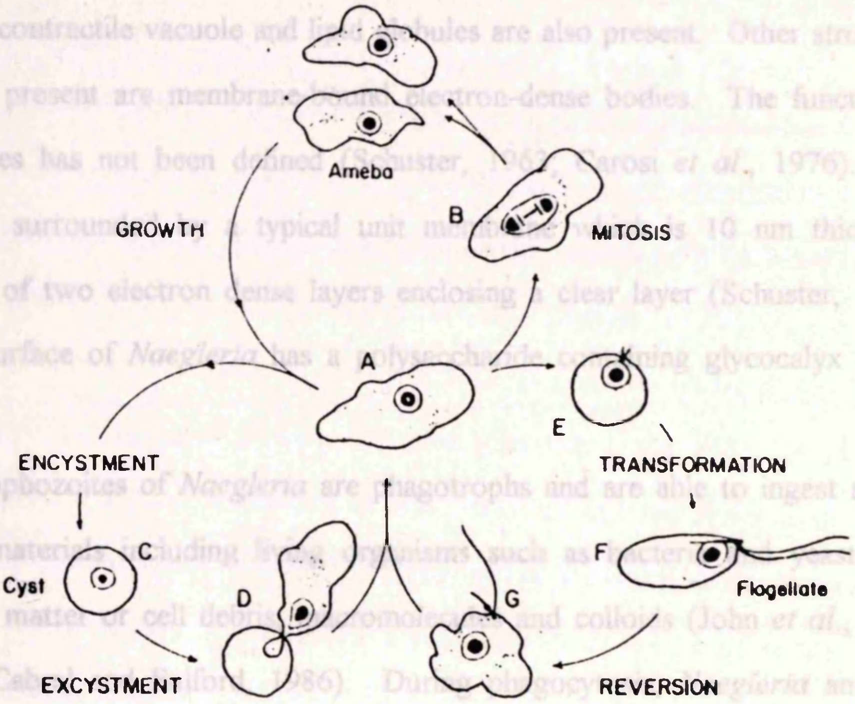
Ameba
GROWTH
B
MITOSIS
A
E
ENCYSTMENT
TRANSFORMATION
C
Cyst
F
Flagellate
D
G
EXCYSTMENT
REVERSION

Figure 1.1. Life cycle of *Naegleria gruberi* (after Fulton, 1970)

Trophozoite

The size of the *Naegleria gruberi* trophozoite is variable and depends on the isolate and conditions of culture. The diameter of the rounded amoeba is 10-20 µm, though smaller and larger amoebae can be found (Page, 1976). The organisation of the *Naegleria* trophozoite is different from other eukaryotic cells in not having a typical Golgi apparatus in the cytoplasm (Schuster, 1963). In some isolates of *N. fowleri* (Stevens *et al.*, 1977) and *N. lovaniensis* (Stevens *et al.*, 1980) a primitive

Golgi-like complex has been reported. Ribosomes, which are often found in clusters, are abundant in the cell. Only small fragments of granular endoplasmic reticulum are found in the cytoplasm. Primary and secondary lysosomes as identified by acid phosphatase staining are dispersed in the cytoplasm (Feldman, 1977). A contractile vacuole and lipid globules are also present. Other structures which are present are membrane-bound electron-dense bodies. The function of these bodies has not been defined (Schuster, 1963; Carosi *et al.*, 1976). The amoeba is surrounded by a typical unit membrane which is 10 nm thick and composed of two electron dense layers enclosing a clear layer (Schuster, 1963). The cell surface of *Naegleria* has a polysaccharide containing glycocalyx (Page, 1988).

Trophozoites of *Naegleria* are phagotrophs and are able to ingest a wide range of materials including living organisms such as bacteria and yeast cells, particulate matter or cell debris, macromolecules and colloids (John *et al.*, 1985; Marciano-Cabral and Fulford, 1986). During phagocytosis, *Naegleria* amoebae exhibit food cups or 'amoebastomes' on their cell surfaces. These food cups are used to capture and ingest particulate foods. They may also serve as attachment organelles. The size and number of the food cups vary depending on the species and strain of *Naegleria* but do not correlate with pathogenicity (John *et al.*, 1984; Marciano-Cabral and Fulford, 1986).

In the laboratory when the amoebae are grown axenically in a liquid medium, the uptake of fluid from the medium is by pinocytosis. Both phagocytosis and pinocytosis are endocytic processes which involve simultaneous invagination of the plasmalemma which then becomes the lining membrane of the vacuole or channel enveloping the ingested materials (Chapman-Andersen, 1973). The initiation of endocytosis depends on the interaction of the glycocalyx with material to be ingested. A study of phagocytosis in *Amoeba proteus* suggests that both chemical and mechanical stimuli are important for the contact between prey and predator (reviewed by Chapman-Andersen, 1973). For pinocytosis, the interaction between inducing solute and the cell surface with subsequent intake of membrane-bound solute (Brandt, 1958) was the initiating phase in the process. The adsorption of pinocytosis inducers depends on the presence of anionic sites in the glycocalyx (Chapman-Andresen, 1973).

The *Naegleria* amoeba projects a single leading blunt pseudopodium when it moves, in the charactersitic slug-like or a 'limax' pattern of locomotion (Page, 1988). The eruption of each subpseudopodium usually occurs near the anterior tip, causing the amoeba to flow in a particular direction (Fulton, 1970; Page, 1988). Adhesion to a substrate is essential for amoeboid locomotion (King *et al*, 1982; King *et al.*, 1983a; King *et al* 1983b). Divalent ions reduce the cell-substrate gap and enhance locomotion. The addition of small amounts of electrolytes such as 10 mM NaCl in deionised water increases adhesion to the substrate and enhances the movement. Other factors which speed the movement of an amoeba are high temperature and for pathogenic forms, the presence of mammalian cells in close proximity (Griffin, 1978; 1983).

Amoeboid movement of *Naegleria*, is assumed to have its basis in actin-myosin interaction (Lastovica and Dingle, 1971). There are two types of microfilaments found in *Naegleria*; the thin, actin-like filaments are concentrated near the plasma membrane and the thick, myosin-like filaments are randomly scattered in the cytoplasm. The interaction between these two filaments has been proposed as the mechanical means by which amoeboid locomotion is accomplished (Lastovica and Dingle, 1971; Lastovica, 1976). During movement, the surface of *Naegleria* makes two types of contacts with the substratum; 'the associated contact', when the amoeba's broad undersurface comes into contact with the substratum, and the 'focal contact' which involves the attachment of amoeba filipodia tips to the substratum (Preston and King, 1978). A recent study showed that cytochalasin B prevents focal contact formation in *N. gruberi* ceases but this drug does not block cytoplasmic streaming and pseudopodium formation, suggesting that the state of actin required for focal contact is different from that required for pseudopodial extension (Preston *et al.*, 1990). At this stage, the details of how an actin-based cytoskeleton in *Naegleria* functions to maintain the cell shape, to develop cell motility, to mediate projection of the pseudopodia and generate cell-substratum interaction, however, remain unknown.

Flagellate

The flagellates have a smooth surface and swim vigorously with the flagella leading (Rafalko, 1947). The number of flagella varies, from 1 to 4 but is usually 2. They measure from 7 to 17 µm in length and are 0.3 to 0.5 µm in diameter (Dingle and Fulton, 1966). The structure of the flagellum and basal body of *Naegleria* are similar to those of other flagellate protozoans. The basal bodies of *Naegleria* flagellates are about 0.2 µm in diameter and about 0.8 µm in length and have the typical centriole-like structure (Fulton and Dingle, 1971). Attached to the basal bodies of flagellated *Naegleria* is a rhizoplast, a striated flagellar rootlet. This structure appears during the amoeba-to-flagellate transformation and is broken down on reversion of the flagellate to the amoeboid form (Gardiner *et al.*, 1981). Rootlets isolated from mature flagellates of *N. gruberi* are ~13 µm long. They taper at both ends with a maximum width of ~0.25 µm. The major protein isolated from the rootlet has an apparent molecular weight of 170-kDa according to Larson and Dingle (1981), 240-kDa according to Gardiner *et al.* (1981). At enflagellation in *Naegleria*, basal bodies, flagella and rhizoplast are assembled *de novo* (Larson and Dingle, 1981).

The transformation of amoebae into flagellates can be evoked *in vitro* by dilution of the nutrient medium with distilled water or dilute buffer solutions (Rafalko, 1947; Schuster, 1963; Fulton and Gruerrini, 1969). The amoebae take between 2 h to several hours to transform into flagellates, depending on the temperature and culture conditions (Fulton, 1970). Several axenically grown *Naegleria gruberi* and *N. fowleri* isolates however, have been found to be incapable of enflagellation when placed in such media (Schuster, 1975b; John, 1982). Axenically grown *N. gruberi* differentiate to flagellates more slowly than bacteria-grown cells (Fulton, 1977). Flagellates revert back automatically to the amoeboid phase if conditions have not changed and then begin to encyst (Rafalko, 1947; Fulton, 1970). The reversion of the flagellate to amoeba does not require ribonucleic acid (RNA) or protein synthesis (Preston and O'Dell, 1973; 1974). Differentiation from amoeboid to flagellate phase is a very rapid process. The process starts as the cytoplasm of the amoeba seems to gel, followed by the rounding up of the cell. As the flagella elongate, they become active causing the cell to tremble, then to spin and suddenly to swim with the flagella leading. Flagellates are thought to represent a means of dispersal in an adverse environment (Fulton, 1970).

Cyst

The cysts of *Naegleria gruberi* are spherical and have three morphological variations; smooth, rough and angular (Page, 1975). The diameter of cysts varies in different strains, ranging from 8.4 μm to 23.0 μm. The common characteristic of all *N. gruberi* cysts is that the wall has pores with collars and sealed with a mucoid plug, through which excystment subsequently occurs (Schuster, 1975a). The mature cyst wall is composed of two layers which join at the region of the cyst pore. The inner layer is about 200-450 nm thick and the outer layer is 25 nm (Schuster, 1963). The outer layer which loosely covers the cyst becomes eroded in old cysts (Schuster, 1975a). Pores vary in number from two to ten and have a maximum diameter of 600 nm (Schuster, 1963; Fulton, 1977). The cysts of pathogenic *Naegleria* are coated with a thick gelatinous layer (Singh and Das, 1970) and varying amounts of this material adhering to the cyst wall gives cysts their rough surface appearance (Lastovica, 1974). The transformation of amoebae to cysts can be induced by washing and suspending the amoebae in distilled water. Although the amoebae transform into flagellates at the beginning of treatment, they revert to the amoeboid stage which eventually forms a cyst (Schuster, 1963).

The resting cysts can survive changes in the environment (such as temperature, drying, pH) which are lethal to amoebae (Fulton, 1977). Cysts of pathogenic *Naegleria* spp are more susceptible to a long period of drying and low temperature than non-pathogenic species. The cysts become non-viable due to a loss of cytoplasmic water that leads to protein denaturation. The cysts of non-pathogenic *N. gruberi* on the other hand, retain their normal appearance and are still viable under the same conditions (Chang, 1978). Cysts of pathogenic species however, are more resistant to heat than cysts of *N. gruberi* (Chang, 1978).

In encysting amoebae, the density of the cytoplasm is increased due to dehydration. The cytoplasmic inclusions become less apparent, except the nucleus which is reduced in size (Schuster and Svihla, 1968). Vacuoles observed in the cytoplasm may contain material for constructing the cyst wall. The endoplasmic reticulum is found closely associated with the elongated mitochondria (Vickerman, 1962; Schuster, 1963) although at this stage in *Schizopyrenus* the mitochondria become rounded perhaps to reduce their volume thus reducing respiratory activity. During excystation, the cytoplasm of the amoeba becomes highly alveolate and appears to be pulled away from the wall. The ejected contents of the food vacuoles are scattered about in this space and remain as a residue in the empty cyst. The amoeba emerges through one of the preformed exit pores after digesting its plug and leaves the empty cyst behind (Schuster, 1963). There are various factors which control the excystment of amoebae eg. the presence of bacteria, increase of pCO_2

(Averner and Fulton, 1966) and increase in hydrostatic pressure (Todd and Kitching, 1973).

1.4. MITOSIS IN *NAEGLERIA GRUBERI*

Mitosis is a process of nuclear division in which chromosomal or genetic material in parent cells is replicated and passed on to two daughter cells. The number of chromosomes received by the daughter cells is identical to that of the parent cell. There are variations among amoebae in how the nucleus divides, and the pattern of cell division has been used to differentiate between groups of amoebae in identification (Page, 1988). *Naegleria gruberi*, has been used to study the peculiar mitosis characteristic of the amoebae in the Schizopyrenida. This species is selected for study because it is widely distributed in nature, is by definition non-pathogenic and is relatively easy to grow in the laboratory either on agar with bacteria or axenically in a liquid medium (Fulton, 1970).

Mitosis in *Naegleria gruberi* has been studied by both light microscopy (Rafalko, 1947; Singh, 1952; Page, 1967a) and electron microscopy (Fulton, 1970; Fulton and Dingle, 1966; 1971; Schuster, 1963; 1975b). Nuclear division in this amoeba is unusual and very different from typical mitosis in animal cells. In the latter, the nuclear envelope breaks down, the nucleolus disintegrates, and chromosomal condensation occurs. In *Naegleria*, throughout nuclear division, the nuclear envelope remains intact, the nucleolus persists, and chromosomes are difficult to distinguish. The term 'promitosis' was first coined for this pattern of division by Nägler (1909) who believed it to be primitive (see Fulton, 1970: Dodge and Vickerman, 1980; Raikov, 1982 for discussion of terminology).

Stages of mitosis

Mitosis in *Naegleria gruberi*, as in other eukaryotes, consists of four phases; prophase, metaphase, anaphase and telophase. Rafalko's (1947) studies on *Naegleria* mitosis with light microscopy of Feulgen-stained material suggested that during interphase, that is the resting stage of the nucleus, DNA-containing chromatin lies around the periphery of the nucleus. As seen by light microscopy, nuclear division begins as the nucleus enlarges and the Feulgen-positive chromosomes condense during prophase. As the chromosomes move towards the equator to assemble at the metaphase plate, the nucleolus elongates and become dumbbell shaped, producing two polar masses. In anaphase, an interzonal body of nucleolar material (Feulgen-negative) connects the two polar masses and separates the diverging bands of daughter chromosomes. Towards the end of anaphase, the interzonal body pinches into two. In late telophase, the interzonal body breaks in half prior to cytokinesis. At the ultrastructural level, chromosomal structures and the nucleolus cannot be distinguished readily. What has been observed is, during division, the nucleolus divides without complete dissolution (Schuster, 1975b; Fulton, 1970; 1977). The nucleolus forms a dumbbell shaped structure along which the two sets of daughter chromosomes appear to be segregated during anaphase. Spindle microtubules have been observed occupying the surface of the nucleolus, especially from metaphase to anaphase. Kinetochores for the attachment of spindle microtubules have not been observed in these studies.

Although during metaphase, spindle microtubules can be observed clearly in transmission electron micrographs of the nucleus, no centrioles or any form of spindle organiser can be found in the cytoplasm near the poles of the dividing nucleus. Spindle microtubules observed in the nucleoplasm of the dividing cell converge on an undifferentiated site on the nuclear envelope. The amoeboid phase of *Naegleria* appears to lack centrioles. The centrioles of mitotic figures and the basal bodies of cilia and flagella are homologous structures and often interchangeable, and so may be designated centriole-like structures (CLS) regardless of their position and function in a cell (see review by Fulton, 1971). Although different buffer combinations were used in order to preserve the possible microtubule structures for transmission electron microscopy and many sections were examined with care, centriole-like structures have not been observed at mitosis in dividing amoebae (Fulton and Dingle, 1971). Not only are centrioles missing from spindle poles, but no centrosphere, i.e. astral arrangement of microtubules extending into the cytoplasm from the poles, has been described.

Microtubule organising centres (MTOCs) are important in typical mitosis, yet they appear to be absent from dividing *Naegleria gruberi*. Is it true that these structures are absent in this amoeba? If it is true, what other organelle could play the role of the MTOCs? If these structures are actually present in *Naegleria*, why are they not detected in the cytoplasm of the amoeba? To answer these questions, we have to understand the properties and behaviour of microtubules. In the following sections, the properties of the microtubules in general and the functions of MTOCs and spindle microtubules will be described in order to help our understanding of the importance of these structures in mitosis.

The properties of microtubules and methods of detection in whole cells

Microtubules (MTs) are proteinaceous organelles, made mainly of dimers of the proteins; α- and β-tubulin (each of molecular weight ~50 kDa) which assemble in alternating sequence into long tubular structures called protofilaments (Figure 1.2). Many properties of MTs proceed from the assembly of tubulins and the so-called microtubule-associated proteins. Each microtubule observed *in vivo* usually consists of 13 protofilaments (Dustin, 1984) although in *in vitro* studies, the number of protofilaments varies from 12 to 16 with 14 as the most abundant (McEwen and

Edelstein, 1980). The average exterior diameter of a microtubule measured by diffraction methods is 30 nm with a central 'hollow' core which is 14 nm in diameter. Variations in diameter observed after negative staining, result in part from the flattening of the MT on the supporting grid (Mandelkow *et al.*, 1977). Length changes occur by assembly or disassembly of its constituent subunits indicating a dynamic instability of the microtubule (Mitchison and Kirschner, 1984). This behaviour is important for rapid MT turnover *in vivo* (Mitchison *et al.*, 1986). The interdimer bond along protofilaments is formed by the N-terminal domain of α-tubulin and the C-terminal domain of β-tubulin (Kirchner and Mandelkow, 1985). Each monomer of tubulin binds one molecule of GTP (guanosine triphosphate). The polymerisation and depolymerisation of tubulin molecules involve GTP (Dustin, 1984). Cross-linking studies have shown that GTP_e (GTP which is exchangeable with depolymerised tubulin) binds to β-tubulin, while GTP_n (non exchangeable GTP) binds to α-tubulin (Geahlen and Haley, 1979; Hesse *et al.*, 1985). Apart from the monomer, tubulin shows three levels of assembly: the dimer, the oligomer and the polymer (Kirchner and Mandelkow, 1985). Besides α- and β-tubulin, a third form, γ-tubulin, has been observed at the spindle poles of *Aspergillus nidulans* (Oakely *et al.*, 1990; Horio *et al.*, 1991). Microtubules in various organelles are structurally similar but have different microtubule-associated proteins (Olmsted and Borisy, 1973).

Various immunohistochemical techniques such as immunofluorescence, immuno-peroxidase, immunoferritin, and immunogold staining have enabled the MTs to be observed in whole cells, particularly in flattened cells cultured *in vitro*. These techniques rely on the use of antibodies against tubulins. Although microtubules are not be visible by conventional light microscopy, it is easy to detect the MTs by fluorescence microscopy. The immunofluorescence technique has been employed to visualise entire arrays of microtubules in whole cells using fluorescent dyes conjugated to specific antibodies (Weber *et al.*, 1975a: 1975b; Yumura and Fukui, 1987; Mullins and Snyder, 1989; Krezel *et al.*, 1990).

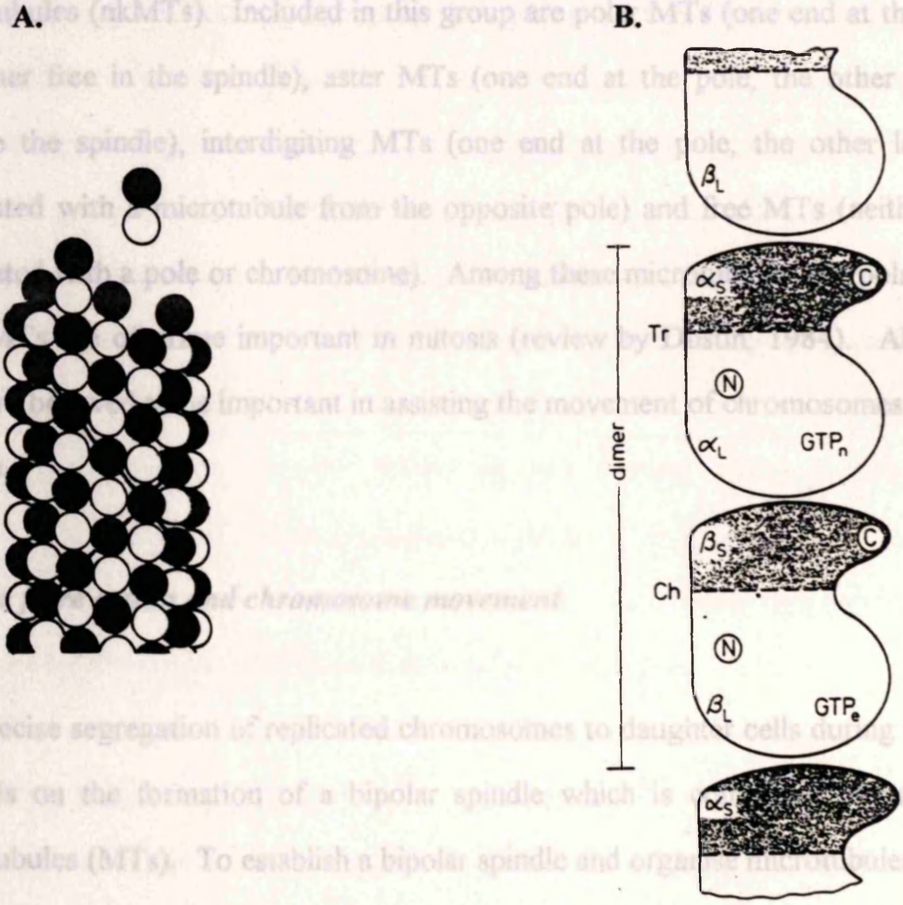

Figure 1.2. Substructure of a microtubule. A. A microtubule assembled from αβ dimers, represented in black and white (from Dustin, 1984, p 24). B. Model of interaction between domains of monomer tubulin along a protofilament as explained in the text (from Kirchner and Mandelkow, 1985).

The mitotic spindle

According to MacDonald (1989), spindle microtubules observed in the dividing nucleus in general, can be classified into two groups according to where they begin and end, relative to other spindle components. The spindle fibres of classical light microscopist represent bundles of microtubules. All spindle microtubules that insert into the kinetochore region of the chromatid are called kinetochore microtubules (kMTs). Other spindle microtubules are referred to collectively as non-kinetochore microtubules (nkMTs). Included in this group are polar MTs (one end at the pole, the other free in the spindle), aster MTs (one end at the pole, the other ending outside the spindle), interdigiting MTs (one end at the pole, the other laterally associated with a microtubule from the opposite pole) and free MTs (neither end associated with a pole or chromosome). Among these microtubules, the polar MTs and kMTs are of prime important in mitosis (review by Dustin, 1984). All these MTs are believed to be important in assisting the movement of chromosomes during mitosis.

Spindle fibre action and chromosome movement

The precise segregation of replicated chromosomes to daughter cells during mitosis depends on the formation of a bipolar spindle which is composed primarily of microtubules (MTs). To establish a bipolar spindle and organise microtubules in the spindle in a mitotic cell, a centrosome or microtubule organising centre (MTOC) is normally required (Vandre and Borisy, 1989). There are many variations in form and distribution of MTOCs in cells. They are often built around centrioles and recognised in electron micrographs as an amorphous pericentriolar material (review in McIntosh and Hering, 1991). MTOCs can also be recognised as forming the poles of the mitotic spindle or bodies of electron-dense material which may be freely dispersed in the cytoplasm (Brinkley, 1985;1990). It has been accepted now that MTOCs specify a place where MT growth will start with the fast growing end (plus-end) distal to the MTOC (review in McIntosh and Hering, 1991). In dividing *N. gruberi* and other cells in which MTOCs have not been observed, it is not clear how the spindle comes to be organised or can play an active part in the segregation of the daughter chromosomes. Schuster (1975b) has suggested that nuclear envelope growth may play an important part in extension of the nucleus, and could be involved in separation of the two sets of chromosomes but attachment of chromosomes to the nuclear envelope during mitosis has not been demonstrated.

During typical mitosis in eukaryotes, spindle fibres interact with chromosomes and with each other to effect the orderly segregation of previously duplicated genome into two distinct regions of the cell. Evidence from previous work has shown that some of these MTs interact with kinetochores of the chromosomes to generate a tension that pulls each chromatid towards one of the spindle poles; other MTs form connections between the poles to maintain and increase the interpolar distance (McIntosh and Hering, 1991). The initial attachment of a chromosome to a spindle fibre occurs when some of MTs which are initiated at the spindle poles or centrosomes are 'captured' at their fast growing end (plus-end) by mature kinetochores (Euteneuer and McIntosh, 1981).

During prometaphase and metaphase, the chromosomes move towards the equatorial position and this motion is accompanied by an elongation of one kinetochore fibre and a shortening of the other. The elongation and shortening processes involve the addition and loss of tubulin subunits respectively, at or near the kinetochore with the cooperation of motor protein molecules which are localised in the kinetochores (Mitchison, 1988). The prometaphase chromosome movement thus results from a kinetochore's motion relative to the MTs to which it is attached, indicating that the forces responsible for movement to the metaphase plate are not generated at the poles or along kMTs. At the metaphase plate, the chromosomes are subject to both pulling and pushing forces caused by MT depolymerisation at the kinetochore, so they oscillate toward and away from the spindle poles until an equilibrium of forces between the two poles is achieved (McIntosh and Hering, 1991).

Anaphase onset is marked by the release of attachment between sister chromatids. Many of the spindle MTs now start to dissolve except the MTs that project into the cytoplasm and those that interdigitate with their counterparts originating from the opposite pole. The length of the interdigitate spindle begins to increase and causes the spindle poles themselves to move apart (anaphase B) (Cande and Hogan, 1989). Two major mechanisms have been proposed for movements in anaphase B. First, in some systems, astral microtubules may exert pulling forces that elongate the spindle. Second, elongation of the interdigitating spindle may result in part from motion of these MTs to reduce their extent of overlap and elongate the distance between their minus-ends (McIntosh and Hering, 1991). This motion is believed to be generated by the motor-driven sliding of antiparallel MTs against each other (Sawin and Scholey, 1991). The chromatids, pulled by their kinetochores move to opposite spindle poles in anaphase A. While the daughter nuclei resume their interphase pattern of chromatin distribution, the kMTs and the aster MTs disappear progressively. These MTs shorten progressively, by a loss of their subunits before disappearing completely (review in McIntosh and Hering, 1991). Following anaphase onset, there is also a decrease in the ability of a centrosome to initiate MTs (Amstrong and Snyder, 1989). At this stage, many changes are required for a return to interphase to be initiated (Forsburg and Nurse, 1991). Despite many studies on the behaviour of microtubules in the mitotic spindle of various types of cells, the form and distribution of these MTs in the mitosis of *Naegleria gruberi* at present is not known.

Effect of microtubule poisons

Microtubule (MT) poisons such as colchicine and some of its derivatives have been employed in studies on microtubule assembly (Olmsted and Borisy, 1973; Gutmann *et al.*, 1989; Binet *et al.*, 1990; Kaufman *et al.*, 1990). Colchicine causes the breakdown of mitotic spindle microtubules of HeLa cells (Borisy and Taylor, 1967) and disassembles cytoplasmic microtubules in adult and foetal rat hepatocytes (Kaufman *et al.*, 1990). In animal cells, colchicine stops division at metaphase and in plants can induce polyploidy (Santavy, 1978). The action of colchicine on the dividing cell is striking since no spindle is formed in the affected cells (Taylor, 1965). These reports have concluded that this drug 'destroys' MTs. The precise mechanism whereby colchicine poisoning of MTs takes place, however, is far from being understood (review in Dustin, 1984). The apparent destruction of MTs may result either from an inhibition of their assembly, from the colchicine-tubulin complexes being unable to form MTs, from slowing down of the assembly of MTs or else disappearance of the MTs may result simply from their continued disassembly. To date, two conflicting theories of colchicine action on MTs have been presented. First, colchicine poisons only the assembly ends of the MTs . This theory supports the 'tip-poisoning' hypothesis proposed by Margolis and Wilson (1977) and is based on the experiments which show that the binding of just a few drug molecules to the growing ends of the MTs could prevent additional molecules from adding on. Second, colchicine-tubulin dimers interfere with assembly with no preference for the ends of MTs. This theory derives from studies which show that colchicine alone is not sufficient to block MT assembly. The presence of colchicine-tubulin dimers block more than half of the MTs from further assembly .

Although in the two theories mentioned, colchicine prevents the formation of MTs, the assembly of tubulin-colchicine (1:1) complexes is possible and leads to the formation of filaments, double rings and paracrystal aggregates. These polymers display several properties of microtubules formed from purified tubulin such as GTPase activity, the need for comparable critical concentrations to form MTs, the apparent free energy change of the reaction, the effects of $Mg^{2+}$and nucleotide binding. Colchicine thus, appears to affect the assembly of tubulin by inducing incorrect bonding geometry between tubulin molecules (Andreu and Timasheff, 1982; Saltarelli and Pantaloni, 1982). The colchicine-tubulin binding, however, appears to be reversible and colchicine can be removed if colchicine-treated cells are resuspended in fresh medium (Taylor, 1965). Band and Mohrlok (1973) used addition of colchicine to culture medium (5 mM colchicine in proteose peptone glucose, PPG) to obtain synchronous mitosis in *Acanthamoeba castellanii*. A burst of synchronous cell divisions was obtained after the drug-containing medium was replaced by fresh PPG. The effect of this drug on *Naegleria* spp. has not been studied, but a similar technique of obtaining synchronous division in these amoebae especially *N. gruberi* could be adopted and employed.

1.5. LYSOSOMAL AND NON-LYSOSOMAL ENZYMES IN *NAEGLERIA* SPP.

Naegleria spp. feed by ingesting food particles which are then digested in food vacuoles through the action of acid hydrolases derived from lysosomes. In some cases, enzymes are secreted to digest the food before ingestion. *Naegleria* amoeba can also produce cytolytic enzymes such as phospholipase A which destroys mammalian cell cultures and host tissues *in vivo* (Hysmith and Franson, 1982) suggesting that these cytolytic enzymes are involved in cellular digestion. In most eukaryotic cells, lysosomes are known to function principally in intracellular digestion since they contain a variety of digestive enzymes (review in Holtzman, 1989). Thus, it is appropriate here to review the nature of lysosomes and their relation to cellular digestion in the following sections.

The nature of lysosomes

Lysosomes are cytoplasmic organelles bounded by a single unit membrane. They usually originate from the Golgi complex but in the absence of this organelle may be derived from the granular endoplasmic reticulum. In *Naegleria* as in other eukaryote cells, they can be distinguished from other cytoplasmic organelles by the presence of acid phosphatases and other acid hydrolases (Feldman, 1977). Lysosomes not only differ in size and shape but also in their enzyme contents. The biochemical heterogeneity of the lysosomes is caused by diversity of the materials to be digested by cells (review in Holtzman, 1989). Since the lysosomes interact with other vacuolar organelles by fusion, and possibly undergo division during recirculation, this heterogeneity is only temporary (Pfeifer, 1987). Several specific types of lysosome are listed in Table 1.1.

Lysosomal function related to cellular digestion

The feeding habits of the amoebae involve two well known processes; phagocytosis and pinocytosis. In both cases, the food is taken into the cells by the invagination of the cytoplasmic membrane to form food vacoules. Phagocytosis is the uptake of solid food by the cells and the vacuoles formed are called phagosomes. In pinocytosis macromolecules such as proteins are taken into the cells, often through the formation of a pinocytosis channel from the cell membrane, followed by the separation of small vacuoles named pinosomes (Mast and Doyle, 1974) from its tip. Pinocytosis is important because these macromolecules cannot pass directly through the cell membrane. The use of methods of enzyme cytochemistry, at both the light and electron microscopic levels reveals the association of these two processes with lysosome fusion in many protozoan cells (Müller *et al.*, 1963).

Table 1.1. Nomenclature and interrelationship of components of the lysosomal system (From Pitt, 1975).

Term	*Synonym*	*Characteristics*
Primary lysosome	Cytosome;pure lysosome; protolysosome; young lysosome	Organelles derived from Golgi and/or ER. Single membrane, contain acid hydrolases
Secondary lysosome	Phagolysosome; digestive vacuole; food vacuole	Body produced on fusion of a primary lysosomes with a food vacoule containing material to be digested
Autophagic vacuole	Cytolysosome; segresome; secondary lysosome	Single or double membrane. Contain recognisable cytoplasmic components in various stages of digestion
Multivesicular body	Late phagolysosome; secondary lysosome	Usually bounded by a single membrane. Contents vacuolated and may represent a late secondary lysosome
Residual body	Dense body; postlysosome storage body, telolysosome	Usually single membrane-bounded, may be double. Contain indigestible remains. Often whorled and containing myelin, etc. Low or no hydrolase activity.

Lysosomal enzyme activity requires a low pH within the digestive vacuole. Cell nutrients resulting from hydrolysis pass through the vacuolar membrane into the cytoplasm, and the undigestible residues are discharged from the cell through exocytosis. Primary lysosomes, when fused with food-containing vacuoles become secondary lysosomes in which digestion takes place (Rodesch *et al.*, 1970). The uptake of foreign materials into the cells is called heterophagy. Under some conditions such as starvation and injury, autophagy may occur where other organelles in the same cell are digested by lysosomal enzymes. The fusion between lysosomes and the membrane of organelle-containing vacuoles (autophagic vacuoles) occurs in the same manner as in heterophagy. Autophagy is thought of as a means of providing nutrients during starvation or as a normal activity in which defective organelles are destroyed (Ericsson, 1969). Sometimes the lysosomal enzymes are secreted extracellularly to digest food outside cells. The liquified food is then absorbed into the cell.

The lysosomal enzymes

Lysosomes contain a rich selection of the proteolytic enzymes (peptidases or proteases) which are necessary for the complete degradation of intracellular or extracellular proteins. These enzymes are synthesised on membrane-bound ribosomes of the rough endoplasmic reticulum (RER) and translocated into or through the RER membrane before moving to their final location (Palade, 1975). These proteolytic enzymes comprise two groups of enzymes; endopeptidases (proteinases) and exopeptidases. These can be differentiated by their different modes of action on proteins. Endopeptidases hydrolyse peptide bonds towards the middle of a polypeptide chain, whereas exopeptidases cleave bonds only near its ends. Protein breakdown mediated by lysosomal enzymes is believed to be initiated by endopeptidase. This process is continued by lysosomal exopeptidases (Kirschke and Barrett, 1987). These enzymes may be released from the lysosomes by the action of homogenisation, freezing and thawing, and detergent, all of which disrupt the single unit membrane of lysosomes. The lysosomal enzymes are found in the supernatant of disrupted cells (Giese, 1979). Since the analysis of lysosomal proteases in cell lysates is complicated by their pH-dependence, oxidative changes of their activity and complex formation with cytosolic inhibitors, a new flow cytometric method has been developed for the intracellular measurements of protease activities in viable cells (Rothe *et al.*, 1992). Examples of lysosomal enzymes detected in *N. fowleri* are acid phosphatase, *N*-acetylglucosamidase, phospholipase and acid protease (Lowrey and McLaughlin, 1985b). Other lysosomal enzymes, cysteine proteinases (endopeptidase), have been detected in some parasitic protozoa (North *et al.*, 1990a).

Proteinases

The major lysosomal proteinases in mammalian cells are cathepsins B, H and L (Barret *et al.*, 1988). Other forms of proteinases have been reported in various unicellular eukaryotic organisms ranging from free-living to pathogenic species. Reports on these enzymes have increased recently especially in parasitic protozoa since evidence of their involvement in many aspects of host-parasite interaction has been forthcoming (McKerrow, 1988). A number of suggestions have been made as to the role of proteinases in other eukaryotic organisms. Apart from their role in general protein turnover, the enzymes play a variety of roles in morphogenesis and differentiation as has been shown for *Dictyostelium discoideum* (North *et al.*, 1988). In *Saccharomyces cerevisiae*, the proteinase level is observed to be increased during sporulation and starvation due to *de novo* synthesis and increased rate of turnover of protein (Klar and Halvorson, 1975; Bezt and Weiser, 1979).

Reports on proteinases of amoebae especially free-living species are very rare. Most studied are the proteinases of the parasitic amoeba, *Entamoeba histolytica* (North *et al.*, 1990a; Tannich *et al.*, 1991). Multiple forms of cysteine proteinase have been observed in the trophozoite form of this amoeba. Two low-molecular weight enzymes are associated with cytoplasmic fraction (cytosol) of this organism, whereas higher molecular weight bands are associated with the membrane fraction (De Meester *et al.*, 1990). There is no difference in the number of proteinase enzymes expressed in pathogenic and non-pathogenic isolates. The amount present of these enzymes, however is higher in pathogenic isolates and may be an important factor in the pathogenicity of *E. histolytica* (Tannich *et al.*, 1991). One enzyme of M_r 56-kDa is secreted by the cells and is believed to be responsible for the cytopathic effect on the host cells (Reed *et al.*, 1989).

Proteinase activity in the pathogenic free-living amoebae, *Acanthamoeba culbertsoni* and *Acanthamoeba rhysodes* has been reported by Auriault and Desmazeud (1979, and review by North, 1982). The enzyme in these amoebae can hydrolyse haemoglobin at pH 3.8. *Acanthamoeba culbertsoni* is reported to release two types of proteases (proteases I and II) in the early phase of excystment and these may be involved in the emergence of the amoeba (Kaushall and Shukla, 1976). Another protease, elastase (which is produced by human leukocytes and is thought to play a part in tissue destruction e.g. in the pathogenesis of pulmonary emphysema), is released by the pathogenic amoebae *Naegleria fowleri, Naegleria australiensis italica* and *Acanthamoeba culbertsoni* (Ferrante and Bates, 1988). The levels of this enzyme are similar in these amoebae. There is also no difference between elastase levels in highly pathogenic *N. fowleri* and in the same organism which has lost its pathogenicity due to long-term axenic maintenance. In *N. fowleri*, enzymes such as phospholipase A and sphingomyelinase, together with a cytolytic and granule-associated cytotoxic activity have been known to be released during invasion of the host (Ferrante and Bates, 1988). Characterisation and sequence determination of some of the cysteine proteinases of the parasitic protozoa have revealed that they are related to papain and the mammalian cysteine proteinases cathepsins L and H suggesting that the parasite enzymes share some characteristics with the proteinases of their hosts (North, 1992).

Classification of proteinases

Proteinases, whether they are lysosomal or non-lysosomal enzymes, are classified by the nature of the essential catalytic group in the active site. Four major classes of proteinases have been identified this way; the serine, cysteine (formerly thiol), aspartic (formerly acid or carboxyl) and metallo proteinases (Barrett and McDonald, 1986). Other proteinases for which the catalytic mechanism is unclear are grouped under unclassified proteinases (Mason, 1991). The mechanistic class of proteinases can be determined by their susceptibility to a group of standard proteinase inhibitors as given in Table 1.2.

Table 1.2. Classification of proteinases by use of inhibitors (modified from North, 1989).

Proteinase type	*Inhibitors (comments)*
Aspartic	Pepstatin A
Cysteine	Iodoacetic acid (not specific), E-64
Cysteine/serine	TLCK (inhibits trypsin-like enzymes), TPCK (inhibit chymotrysin-like enzymes),PMSF (inactivation of cysteine proteinases reversed by reducing agents), Leupeptin & antipain (limited specificity with serine proteinases, inhibited trypsin-like enzymes), chymostatin (limited specificity with serine proteinases, inhibit chymotrypsin-like enzymes).
Serine	DFP, 3,4-DCI, Elastatinal (inhibits elastase-like enzymes).
Metallo-	EDTA, EGTA, 1,10-phenanthroline.

Substrate preference of the proteinases has been used to group the multiple forms of cysteine proteinases in *Leishmania m. mexicana* (Robertson and Coombs, 1990). The specificity of these proteinases determines the amino acid sequence recognised and hydrolysed in the target protein. Several synthetic substrates (both chromogenic and fluorogenic) are available for this purpose. Cleavage of the peptide bond linking the peptides to the chromogenic moiety, such as nitroanilines, leads to an increase in absorbance hence it is easy to quantify the acitivity of the enzymes.

Non-lysosomal enzymes

In *Naegleria fowleri* some of the enzymes detected are associated with specific organelles or membrane in the cells. 5'-nucleotidase is associated with the surface membrane and aspartic aminotranferase is found in the mitochondria. α-D-glucosidase and aminopeptidase are associated with both surface membrane and lysosomal particles (Lowrey and McLaughlin, 1985a). The origin of other enzymes such as β-hydroxybutyrate dehydrogenase, lactate dehydrogenase, leucine aminopeptidase, malic enzyme and superoxide dismutase which have been detected in *Naegleria* spp and have been used for comparing between pathogenic and non-pathogenic isolates and species of *Naegleria* (Nerad and Daggett, 1979; De Jonckheere, 1982; Pernin *et al.*, 1985; Moss *et al.*, 1988; Pernin and Cariou, 1989) are not known since the enzymes are detected in the cell homogenates. A similar problem applies to enzymes glucose phosphate isomerase, phosphoglucomutase and aminotransferase which have been used to distinguish species and strains of *Naegleria* (Warhurst and Thomas, 1978; Kilvington *et al.*, 1984). Other than their significance in identifying *Naegleria* spp, none of these enzymes have been studied from the view point of their actual roles in the biology of these amoebae.

1.6. PATHOGENICITY OF *NAEGLERIA* SPP AND OTHER FREE-LIVING AMOEBAE

Pathogenicity of Naegleria spp

Among *Naegleria* spp., *Naegleria fowleri* was the first known free-living pathogenic form and causes acutely fatal primary amoebic meningoencephalitis (PAME) in man (Fowler and Carter, 1965). Although PAME is a relatively rare disease, reports of its occurrence are worldwide (Martinez, 1985). Patients contracting this disease usually have a history of swimming in pools or freshwater lakes contaminated with this amoeba (Martinez, 1985). Three days after exposure, the patients present with early changes in taste and smell followed by abrupt onset of fever, nausea, vomiting and drowsiness progressing to coma in which most patients survive for less than one week (Martinez, 1985; Ferrante, 1991). Other than swimming, infection with *N. fowleri* can be through face washing, bath-related activity (Anderson *et al.*, 1973; Lawande *et al.*, 1980) and inhalation of dust-borne *Naegleria* cysts (Lawande *et al.*, 1979). This amoeba gains access to the central nervous system of the host through the olfactory-submucosal nervous plexus (Martinez *et al.*, 1971). Examination of sections of brain infected with these amoebae has revealed areas of extensive demyelination with the trophozoites surrounded by a clear halo (Martinez *et al.*, 1971). The production of massive tissue destruction, primarily of neurons, during both human (Chang, 1979) and experimental animal (De Jonckheere, 1979) infection implicates some potent amoeba cytopathogenic mechanism as an integral part of the disease process. Both phagocytosis and pinocytosis of host tissues by *N. fowleri* have been observed (Maitra *et al.*, 1976). *N. australiensis* (De Jonckheere *et al.*, 1984b) is another pathogenic species which causes PAME in experimental animals.

Several properties of *Naegleria fowleri* such as ability to grow above 37°C and up to 45°C (enabling amoebae to survive fever), evasion of the host immune system, possession of cytolytic enzyme activity, phagocytosis of host cells and speed of amoeboid locomotion have been suggested as possible determinants of pathogenesis and virulence (Maitra *et al.*, 1976; Marciano-Cabral and Fulford, 1986; Thong and Ferrante, 1986). In *in vitro* studies of *Naegleria* cytopathogenicity, cell destruction appears to be largely contact-dependent (Brown, 1979; Marciano-Cabral *et al.*, 1982; Lowrey and McLaughlin, 1985b) suggesting a role for amoeba cell surface factors in the cytolytic event. While attaching to the cells, the amoebae produce cytolytic enzymes such as phospholipase and sphingomyelinase to lyse the cells before phagocytosis (Curson *et al.*, 1978). Pathogenic amoebae such as *N. fowleri* and *N. australiensis* and non-pathogenic *N. gruberi* and *N. lovaniensis* produce food cups to ingest the lysed cells (Marciano-Cabral and Bradley, 1982). There are two ways in which *Naegleria* phagocytoses the target cells, by ingesting cell debris after cell lysis or by trogocytosis, a process of piecemeal ingestion of target cells by food cups (Visvesvara and Callaway, 1974; Marciano-Cabral and John, 1983).

Other factors which are associated with the amoeba surface which might also play a role in amoeba pathogenicity are production of *Naegleria* amoeba cytopathogenic material (NACM) which was identified as virus-like particles by Schuster (1969) and cytolysin. NACM is a 35-kDa protein, located at the tips of pseudopodia and in the peripheral cytoplasm of *Naegleria* and is believed to be involved in destroying host cells (Dunnebacke and Dixon, 1989; 1990). This material behaves as an integral component of the amoebae rather than a product released by them. The pattern of morphological change in host cells caused by NACM have been observed to be different from when host cells are phagocytosed by the amoebae or when they are lysed by the enzymes known to be present in amoebal lysates. Cytolysin is a potent, heat-stable cytolytic protein which is associated with the amoeba surface membrane. Its activity is activated by lysosomal enzymes of *N. fowleri* in target cell lysis suggesting an association between lysosomes and the amoeba surface (Lowrey and McLaughlin, 1985b). The properties of cytolysin are different from NACM since the former is not inactivated, even at a temperature of 76°C whereas, NACM is inactivated at 56°C.

Amoeboid locomotion of the *Naegleria* is important for promoting invasion and penetration of tissues and mucus. Pathogenic *N. fowleri* migrates faster than non-pathogenic *N. lovaniensis* and *N. gruberi* on agar surfaces. *N. australiensis australiensis* and *N. australiensis italica* which have been shown to be pathogenic for mice have migration rates similar to highly virulent *N. fowleri* (Thong and Ferrante, 1986). In relation to this locomotion, pathogenic mouse-passaged *N. fowleri* are more responsive to the proximity of mammalian cells than are axenically cultured amoebae (Cline *et al.*, 1986).

Cytopathogenicity *in vitro* may not always correlate with pathogenicity *in vivo*. Non-pathogenic *Naegleria* spp could produce a profound cytopathic effect (CPE) *in vitro*. Not only *N. fowleri,* but other *Naegleria* spp., such as the mildly pathogenic *N. australiensis,* non-pathogenic *N. lovianensis* and *N. gruberi,* also produce CPE in cultured nerve cells on contact (Chang, 1974; Marciano-Cabral and Bradley, 1982; Marciano-Cabral and Fulford, 1986). The cells are lysed after the introduction of these amoebae into the cell cultures. So the ability to kill cells *in vitro*, growth at 37°C in case of non-pathogenic *N. lovaniensis,* and the presence of food-cups on the amoeba surface do not appear to be determinative factors for other *Naegleria* spp. to cause disease as they are in *N. fowleri*.

Although both pathogenic and non-pathogenic *N. fowleri* and non-pathogenic *N. gruberi* produce potentially cytotoxic enzymes, phospholipase A and B, phospholipase A is produced in a greater amount by pathogenic *Naegleria* indicating a role in the different degree of invasiveness and virulence (Curson *et al.*, 1978). Catalase, is produced in abundance by highly virulent *N. fowleri* compared with amoebae of low virulence (Wong *et al.*, 1977). On the other hand, elastase, is expressed in similar amounts both in high and low virulent *N. fowleri* (Ferrante and Bates, 1988) suggesting that difference in amount of enzyme production is related to the role of such enzyme in amoeba pathogenesis. Analyses of the pattern of protein synthesis in *Naegleria* spp indicated that the pattern is related to the amoeba virulence (Hu *et al.*, 1991). Mouse-passaged *N. fowleri* exhibits a different pattern of protein synthesis compared with axenic and non-pathogenic amoebae. The pathogenicity of pathogenic amoebae gradually declines after long axenic maintainance (Biddick *et al.*, 1984) but can be regained by passage of these amoebae in mammalian cell cultures or mice (John, 1982). Attempts to boost virulence of a low-virulent (LV) substrain of *N. fowleri* by serially intracranial passage in mice, does not result in virulence increase to the level of the highly-virulent (HV) substrain of *N. fowleri,* suggesting that LV substrain may differ genetically from the HV substrain (Wong *et al.*, 1977).

Free-living amoebae are commonly considered be aerobic but *Naegleria* spp. especially *N. fowleri* can adapt to grow in thermally polluted waters where oxygen deficiencies have been observed (De Jonckheere *et al.*, 1975). Both *N. fowleri* and *N. gruberi* posses PP_i-dependent phosphofructokinase (PP_i-PFK) which is normally possessed by anaerobic parasitic protozoa such as *Entamoeba histolytica* and *Giardia* (Mertens, 1990; Mertens *et al.*, 1993). In *Naegleria,* PP_i (inorganic pyrophosphate) is used instead of ATP and is regulated by AMP. This evidence suggests that *Naegleria* spp have a wide adaptability to grow in diversified ecosystems, including anaerobic environments in the host.

Pathogenicity of other free-living amoebae

Other free-living amoebae which are known to cause human infections largely belong to the genus *Acanthamoeba.* These amoebae can be distinguished from

Naegleria spp by their non-eruptive pseudopod formation, by the possesion of small spiky acanthopodia and by moving on a broad front, by having angular double-walled cysts and by their dividing by conventional mitosis (Page, 1967b). The form of the *Naegleria* pseudopodium, cyst morphology, and pattern of nuclear division have been described elsewhere in this chapter. *Acanthamoeba* spp. cause a granulomatous amoebic encephalitis (GAE) (Martinez, 1985; Thong and Ferrante, 1987), amoebic pneumonia, and chronic *Acanthamoeba* keratitis of the cornea (Jones, 1986; Wright and Buckley, 1988). These amoebae usually invade the host central nervous system (CNS) by haematogenous spread although they can invade directly via the neuroepithelium as does *Naegleria* (Martinez, 1985). Invasion of the CNS is secondary to the establishment of the organisms in primary sites such as skin lesions, eyes and respiratory tracts (Martinez, 1985; De Jonckheere and Michel, 1988). Immunosupressed people are at high risk. Patients with the Acquired Immunodeficiency Syndrome (AIDS) have been reported with *Acanthamoeba* infection (Wiley *et al.*, 1987). Although *Acanthamoeba* usually causes chronic disease in immunocompromised people, in immunocompetent people, it attacks the cornea causing corneal ulcers and keratitis (Warhurst, 1988).

A. culbertsoni, A. polyphaga, A. castellanii and *A. rhysodes* have been positively identified in human pathological material (Warhust, 1985). The increase of *Acanthamoeba* keratitis recently is due to contact lens wear, especially soft contact lenses (SCL) which have either not been washed properly or have been washed in non-sterile solutions (Mathers *et al.*, 1987). Studies show that the cysts and trophozoites of *A. castellanii* can firmly adhere to new, unworn soft contact lenses (John *et al.*, 1989) and also to human-worn hydrogel contact lenses (John and Desai, 1991). When contaminated lenses are placed on the human cornea, they introduce *Acanthamoeba* to the ocular environment and the amoebae subsequently invade the human cornea either through an intact corneal epithelium or through breaks in the corneal epithelium that are related to SCL-wear (John, 1991). Once introduced to the cornea, *Acanthamoeba* attaches to desmosome-like junctions between the epithelial cell surface membranes. These epithelial cells are pulled from the basement membrane by the trophozoites and penetration is initiated between intact cells which are later phagocytosed by these amoebae thereby destroying the epithelium (Ubelaker, 1990). Since the cysts of *Acanthamoeba* spp. are more resistant to desiccation than those of *Naegleria* spp. (De Jonckheere and Van de Voorde, 1976), air-blown cysts could possibly be infective and cause infection in humans when they alight on the cornea (Martinez, 1983; Brandt *et al.*, 1989).

Besides *Acanthamoeba* and *Naegleria*, other free-living amoebae belonging to the genera *Hartmannella, Vahlkampfia* and *Vexillifera,* have been implicated in diseases in a variety of vertebrate animals as presented in Table 1.3 (Visvesvara and Stehr-Green, 1990). An amoeba, belonging to the order Leptomyxida has recently been discovered associated with encephalitis in man in Argentina, Peru, Australia, Canada, Venezuela and Mexico (Taratuto *et al.*, 1991). This amoeba has been isolated from brain and skin lesions of the patient. Indirect immunofluorescence studies performed on this amoeba ruled-out either *Acanthamoeba* or *N. fowleri*. Its morphology indicated that it belonged to an undescribed genus of amoebae and now it has been named *Balamuthia mandrillaris* (Visvesvara *et al.*, 1993). The associations of *Hartmannella, Acanthamoeba* and *Naegleria* with some pathogenic microorganisms which are ubiquitous in the environments such as *Legionnella pneumophila* (Fields *et al.*, 1986) provide further evidence on their increase in medical importance. Since *Hartmannella* and *Vahlkampfia* have recently shown to cause infections in mammals they have emerged as possible human pathogens (Visvesvara and Stehr-Green, 1990).

Table 1.3. Free-living amoeba infections in vertebrate animals (from Visvesvara and Stehr-Green, 1990 with modifications).

Host	*Amoebae*	*Tissue involved*
Mammals		
1. Gorilla	Leptomyxid	Brain, lungs
2. Baboon (*Papio sphinx*)	Leptomyxid	Brain, lungs
3. Buffalo	*Acanthamoeba sp.*	Lungs, bronchioles
4. Bull	*Acanthamoeba sp.*	Lungs (brain was not examined)
5. Bull	*Acanthamoeba polyphaga*	Preputial cavity
	Acanthamoeba sp.	Preputial cavity
	Vahlkampfia sp.	Preputial cavity
6. Cow	*Acanthamoeba polyphaga*	Vagina
7. Sheep	*Acanthamoeba sp.*	Nasal mucosa and brain
	Leptomyxid	Brain, lungs
8. Sow	*Vahlkampfia inornata*	Nasal cavity
9. Swine	*Vahlkampfia avara*	Nasal cavity
10. Dog	*Hartmannella vermiformis*	Bronchi
	Acanthamoeba sp.	Lungs
	Acanthamoeba castellanii	Brain, lungs, kidney
	Acanthamoeba culbertsoni	Brain, lungs
11. Rabbit	*Acanthamoeba polyphaga*	Liver
Birds		
12. Domestic pigeon	*Acanthamoeba polyphaga*	Intestine
13. Turkey	*Hartmannella vermiformis*	Trachea
	Vahlkampfia enterica	Intestine
	Acanthamoeba polyphaga	Intestine
Fish		
14. Goldfish	*Acanthamoeba sp.*	Kidney, liver, meninges, swim bladder
15. Other fish (11 spp, 8 different genera of fish)	*Acanthamoeba sp.*	Gills, urinary bladder, spleen, gall bladder, blood
	Naegleria sp.	
16. Rainbow trout	*Vexillifera bacillipedes*	

1.7. AIMS OF PROJECT

The aims of this project are to investigate some aspects of the biology of the free-living amoebae, particularly those in the genera *Naegleria* and *Hartmannella*. The main aims are to understand the nature of nuclear division in *Naegleria gruberi* and the significance of the proteinases present in *Naegleria* spp. In this study, the combination of light and electron microscopy techniques are employed and the synchronously dividing cells are used to further investigate mitosis in *N. gruberi*. To investigate the importance of proteinases present in *Naegleria* spp., the presence of these enzymes will be investigated i) in three stages of the amoeba life cycle; that is in trophozoite, cyst and flagellate ii) both intracellularly and extracellularly iii) in other strains of *Naegleria* including pathogenic *N. fowleri* iv) in axenically grown *N. gruberi* and in this amoeba grown on agar with live bacteria. Other aims of this project are to characterise further a poorly known amoeba, *Hartmannella sp.* which has been isolated and identified from a contact lens case and also to test the possibility of its invasiveness to human corneas *in vitro*.

Chapter 2

Mitosis in Naegleria gruberi

Chapter 2

MITOSIS IN *NAEGLERIA GRUBERI*

2.1. INTRODUCTION

Mitosis in *Naegleria gruberi* is interesting for three reasons. First, during division, the nuclear envelope remains intact despite spindle elongation, chromosome movement and the separation of the daughter chromosomes within the nucleus. Second, no microtubule organising centres (MTOCs) have been observed at the spindle poles in the cytoplasm of dividing cells; MTOCs normally initiate spindle microtubule formation prior to nuclear division. And, lastly, kinetochore sites at which the microtubules attach to the chromosomes have not been detected in the *Naegleria* nucleus even at the ultrastructural level (Schuster, 1975b). Despite these anomalies, the objective of mitosis is still achieved; that is the genetic material of the parent cell is replicated and passed on to daughter cells. This type of division is also shared by other heterolobosean amoebae such as *Vahlkampfia* spp., and *Tetramitus* spp. (Raikov, 1982).

Some of the facts mentioned above need to be clarified. The important questions are 1) Do chromosomes exist as individually-discernible structures as Rafalko (1947) depicted them in his papers? 2) Are the daughter chromosomes separated on a conventional microtubule-based eukaryotic spindle despite persistence of the nuclear envelope and division of the nucleolus into polar masses? These questions can be resolved into the following subsidiary questions: i) Are MTs visible in the dividing nucleus and do they form a spindle to which chromosomes are attached? ii). Are MTOCs discernible at the poles of the spindle, either inside or outside of the persistent nuclear envelope? iii). Are kinetochores and their related chromosomal fibres discernible? iv). Are pole-to-pole (continuous) fibres discernible and if so how are the spindle MTs spatially related to the division of the nuclear material?

In this chapter I attempt to answer some of the above questions by studying nuclear division both in log-phase growth and synchronously dividing populations of *Naegleria*. Colchicine treatment was employed to induce synchrony. Non-lethal doses of colchicine have been used to obtain synchronous division in other amoebae (eg. *Acanthamoeba castellanii* (Band and Mohrlok, 1973) and *Entamoeba histolytica* (Orozco *et al.*, 1988)). In addition I have utilised fluorescence microscopy to study the distribution of microtubules and chromosomal material in the dividing nucleus.

2.2. MATERIALS AND METHODS

2.2.1. *Cultivation of amoebae*

Cultivation of amoebae on solid media with bacteria

Naegleria gruberi CCAP strain 1518/1A was obtained from The Culture Collection of Algae and Protozoa, Windermere. The amoebae were grown on non-nutrient agar (NNA), streaked with living *Escherichia coli* strain NCTC W3110, and incubated at 25°C. Subpassaging onto new agar plates was done weekly.

Axenic cultivation of amoebae in liquid medium

Cultures of *Naegleria* about 3 days old were used as a source of amoebae. A block of agar containing several trophic amoebae was transferred into a 50 ml Falcon culture flask containing 5 ml of modified Neff's amoeba saline solution (Page's amoeba saline solution, PAS, Page, 1967)(see 2.2.3.). A few drops of heat-killed *Escherichia coli* suspension (see the following section) were added to the flask as food supply. The flask was placed in an incubator at 32°C. After the amoebae had grown to confluence or semi-confluence, covering the floor of the flask (usually this takes two to three days), the medium was replaced with nutrient Bath-Spa Medium (BSM) with antibiotics (see 2.2.3.). Usually *Naegleria gruberi* took a few days to adapt to BSM, depending on the phase of growth of the amoebae transferred. Once the amoebae had established in BSM, subculturing into new medium was done every three days; the amoebae meanwhile adapt to growth without a bacterial food supply.

Preparation of heat-killed Escherichia coli suspensions

E. coli cultures (strain NCTC W3110) were obtained from the Department of Microbiology, Glasgow University and grown on 1.5% (w/v) nutrient agar slopes at 37°C. Three days after inoculation, the bacteria were removed from the agar surface by flushing 10 ml PAS over the slope with a pasteur pipette. The bacterial suspension was centrifuged once at 500 *g* for 10 min and resuspended in 10 ml of fresh PAS. The bacterial suspension was then placed in a 70°C water bath for 30 min to kill the bacteria. Two drops of heat-killed *E. coli* suspension per tube was found sufficient to support good growth of *Naegleria gruberi* in PAS in this study.

2.2.2. *Maintenance of cultures*

Naegleria gruberi cultures (CCAP strain 1518/1A) were grown either in Falcon culture flasks (basal surface of 25 cm^2) or flat-sided tubes (160 mm x 25 mm) containing 5 ml or 2.5 ml of Bath-Spa medium with antibiotics (Mr Simon Kilvington, Public Health Laboratory, Royal United Hospital, Bath, UK, personal communication, see 2.2.3.) at 32°C. New cultures were initiated by inoculating a few drops of amoeba containing suspension, and subpassaging was done every three days.

2.2.3. *The culture medium*

Bath-Spa medium:

This medium is made up of two components, 1 and 2. Component 1 contains pancreatic casein digest (OXOID) 5 g, proteose peptone (DIFCO) 5 g, yeast extract (DIFCO) 5 g, liver digest (OXOID) 10 g and glucose 5 g all dissolved in 900 ml PAS. All the ingredients were dissolved by gentle heating and the medium sterilised through Millipore membrane filter, pore size 0.22 μm. To avoid the laborious step of membrane filtering, the medium 1 can also be prepared by autoclaving all the ingredients except glucose in 800 ml of PAS at 15 psi. for 20 min. Glucose is dissolved separately in 100 ml of PAS and sterilised by membrane filtration and added later to the autoclaved ingredients.

Component 2 contains haemin 100 mg and triethanolamine 4 ml, made up to 100 ml with 96 ml of distilled water. Haemin was dissolved by heating at 56°C in a water bath and the complete component 2 was sterilised by membrane filtration. To use, all the following components were added together; 90 ml of component 1, 1.0 ml of component 2, 10 ml of heat-inactivated foetal calf serum (GIBCO), 0.5 ml of penicillin (2000 units ml^{-1}) and 0.5 ml of streptomycin (2000 units ml^{-1}). The complete medium was kept at 4°C and used within one month.

Modified Neff's amoeba saline solution (PAS)

Modified Neff's amoeba saline solution (Page's amoeba saline, PAS) made up as follows; NaCl 1.20 g; $MgSO_4.7H_2O$ 0.04 g; $CaCl_2.2H_2O$ 0.04 g; Na_2HPO_4 1.42 g ; KH_2PO_4 1.36 g; each component was dissolved in 100 ml of distilled water and kept as a stock solution; for use, 10 ml of each stock solution made up to one litre with distilled water.

2.2.4. *Counting the amoebae in cultures*

Using random number quadrats

As amoebae grow attached to the flask substratum, the growth of amoebae in BSM was measured following the method of Hendry (1987). The number of amoebae in each flask was counted in five randomly selected fields (taken from the random number table to select microscope coordinates) using an inverted microscope (Diavert, Leitz) whose eyepiece contained a grid graticule. The area measured per field of view was 0.14 mm^2 at a magnification of 32x. The total number of amoebae present in the flask was then estimated from the mean of five fields. In older cultures, the floating cells (not attached to the flask substratum) were counted on a haemocytometer. A 10 μl volume of culture supernatant was taken to count the cells. The total number of the amoebae in a flask was estimated from these two values.

Using a haemocytometer

The cell density of amoebae grown in flat-sided tubes was estimated using an improved Neubauer haemocytometer. The cells were dislodged from the tube surface by flushing gently with the culture medium. At least two counts from each tube were used to estimate the population of amoebae per ml.

2.2.5. *Calculating the population doubling time of Naegleria gruberi grown in Bath-Spa medium at 32°C*

The population doubling time (PDT) of *N. gruberi* grown in Bath-Spa medium at 32°C was determined when the populations were in phase of logarithmic growth. Both Falcon culture flasks with basal surface of 25 cm^2 and flat-sided tubes size 16 mm x 25 mm were used to grow this amoeba. The volume of BSM used in flasks and tubes was 5 ml and 2.5 ml, respectively. The size of inoculum for flasks was $\sim 1.4 \times 10^4$ cells and in flat-sided tubes was $\sim 1.2 \times 10^4$ cells. In one experiment, the initial number of cells inoculated into the flasks was not counted but the cells were counted 4 h after inoculation. The number of cells per flask or per ml (for cultures in tubes) were counted either periodically (every 24 hr) or in some cases, the cells were counted at nonspecific time interval. In all cases, the maximum time for observation was not more than 120 h (5 days).

The PDT was calculated as follows:

The PDT equals $(\log_e 2)/r$

where r is the slope of the curve estimated from an exponential curve, $Y= ae^{bx}$, or when the curve is transformed into a straight line, the equation becomes:

$\ln Y= \ln a + bx$,

where

a, the interception of the line at the Y axis

b, the slope of the line, so b= slope= r.

PDT= $(\log_e 2)/r$ or PDT= $0.693/r$.

The PDTs obtained from this study were analysed by F-test (analysis of variance) to see if the size of culture containers (or the volume of medium used) affects these values. In this test, if the variance ratios (F values) were greater than the critical values of F from statistical tables (at p=0.05) for the required degree of freedom (d.f.), the results were significantly different. In case the PDT values from flasks and flat-sided tubes were significantly different, a further test, Scheffés test (Klugh, 1974) was used to determine which of the means being compared were significantly different.

2.2.6. *Obtaining synchronous division in Naegleria gruberi strain 1518/1A*

To increase the number of mitotic cells, the axenic cultures (~42 h after inoculation) were synchronised by replacing Bath-Spa medium with amoeba saline solution containing 16 mM colchicine. It was observed that a lower concentration of colchicine (5 mM) in Bath-Spa medium did not inhibit the growth of *N. gruberi*. The cultures were left for 18 h in colchicine then released from the inhibitor by replacing it with fresh Bath-Spa medium. The cultures were harvested between one and two hours after the release from the inhibitor.

The sensitivity of amoeba trophozoites to colchicine was tested using the technique of Orozco *et al.* (1988). In this technique, after treatment with colchicine, the viable cells which were determined by trypan blue exclusion, were counted in a haemocytometer. 0.25% (w/v) trypan blue in phosphate buffered saline was used.

2.2.7. *Preparation for transmission electron microscopy*

By conventional methods

Before fixation of the amoebae, the BSM was discarded carefully so as not to disturb the amoebae. The amoebae were then dislodged from the flask wall by flushing with 2% (v/v) glutaraldehyde in 0.1 M phosphate buffer, pH 7.4 at room temperature. Suspended cells were pelleted by centrifugation at 500 *g* for 30 min at room temperature. The pellet formed was rinsed twice with phosphate buffer before adding 3% (w/v) molten gelatin to encase the amoebae and thus prevent disruption of the pellet. The pellets were post-fixed with 0.1 M phosphate buffered 1% (v/v) OsO_4 for 1 h at 4°C, and then after rinsing in distilled water, stained with 0.5% (w/v) aqueous uranyl acetate for 30 min (in the dark). Following dehydration through graded ethanols 30%, 50%, 70% (10 min in each), the pellets were placed in 1% (w/v) *p*-phenylenediamine for 30 min. The dehydration step was continued with 70% ethanol (5 min), 90% ethanol (10 min), 100% ethanol (2 x 10 min) and (dried) dehydrated ethanol (10 min). The pellets were then gradually placed in epoxypropane (3 x 5 min), 1:1 mixture of epoxypropane /araldite (overnight) before being embedded in 100% araldite resin mixture. Araldite blocks were trimmed and cut with glass knives to obtain sections on an LKB ultramicrotome. Only grey and golden colour sections were examined in this study. Sections on copper grids were double-stained with uranyl acetate and lead citrate, and examined in the Zeiss 902 transmission electron microscope operating at 80 kV.

Techniques for preserving microtubules

In order to obtain better preservation of mitotic spindles, the following techniques were employed; 1% (w/v) tannic acid was added to the buffered glutaraldehyde as pre-fixative; post-fixation was with OsO_4; the amoebae were also pre-fixed for 3 h at room temperature with 5% (v/v) glutaraldehyde buffered with mixtures containing 1 mM $MgSO_4$, 2 mM ethyleneglycol bis (β-aminoethyl ether)-*N*, *N'*-tetraacetic acid (EGTA), 1 mM guanosine triphosphate and 100 mM piperazine-*N*, *N'*-bis (2-ethanosulfonic acid) (Luftig *et al*, 1977). 1.0% (v/v) OsO_4 buffered with 0.08 M veronal acetate was used as post-fixative.

2.2.8. *Preparation for fluorescence microscopy*

DNA and RNA staining:

Fluorescent staining of DNA and RNA was carried-out following the method of Kawamoto and Kumada (1987). Two fluorochromes were used. DAPI (4',6-diamidino-2-phenylindole) gives highly specific staining for DNA and PI (propidium iodide) is specific for both DNA and RNA. Both chemicals were from SIGMA.

A drop of *N. gruberi* suspension was placed on a slide, and the amoebae allowed to settle for 5 min before fixation with 70% alcohol for 5 min. After fixing, the slide was stained with a drop of DAPI solution (10 μg ml^{-1} in 0.05 M Tris buffer, pH 7.5 as a stock solution; take 1 ml of stock solution, make up to 100 ml with 99 ml of Tris buffer) for 10 min. A drop of PI solution (10 μg ml^{-1} in 0.05 M Tris buffer, pH 7.5 as a stock solution; take 1 ml of stock solution, made up to 100 ml with 99 ml of Tris buffer) was placed for 10 min on the slide without washing the DAPI out. The stained preparation was then covered with a cover slip, and the edges sealed with nail polish. The staining process was carried out in a humid dark chamber.

Microtubule staining

Microtubule staining was carried-out using an indirect immunofluorescence technique. After the amoeba cells settled on the slides, they were fixed in 70% alcohol for 5 min and washed briefly in phosphate buffered saline (PBS) containing 137 mM NaCl, 2.7 mM KCl, 1.5 mM KH_2PO_4 and 8.0 mM Na_2HPO_4, pH 7.3 (Yumura and Fukui, 1987). The slides were incubated in primary antibody, monoclonal either anti-α-tubulin (raised against microtubules from chicken embryo, SIGMA) or anti-α-TAT1 (kindly supplied by Dr T. Sherwin, Department of Biochemistry and Molecular Biology, University of Manchester; this antibody specifically recognises α-tubulin and cross-reacts with a wide range of species; it was raised in mice against the cytoskeleton of *Trypanosoma brucei*, Woods *et al.*, 1989) at room temperature for 30 min. The slides were rinsed three times for 5 min in PBS (3x5 min) before incubating with secondary antibody, fluorescein isothiocyanate-labelled goat anti-mouse immunoglobulin (FITC) for 30 min. The slides were rinsed again in PBS (3x5 min) and incubated in DAPI solution for 10 min before mounting in glycerol:PBS (Merck, 1:1) as anti bleaching agent. The primary and secondary antibodies were diluted 1:1000 and 1:20 (1:5 for anti-α-TAT1) respectively, in PBS for use. In this study, colchicine-treated cells were used. Non colchicine-treated cells were used as control. The specificity of secondary antibody (FITC) in binding to primary antibody in this staining procedure was tested by using only FITC stained cells as a control.

Mounted slides were examined with a Leitz Ortholux II microscope using incident light fluorescence from an HBO high pressure mercury vapour lamp 2x1 CP490 (exciting), TK 510 (dichroic mirror) and K515 (suppressing) filter used. Photographs were taken using Ilford XPI 400 ASA film, Kodak colour 400 ASA film and Kodak Ektachrome 200 ASA film.

2.3. RESULTS

2.3.1. *Observation of N. gruberi growth in Bath-Spa medium at 32^{o}C*

A phase contrast micrograph of *Naegleria gruberi* CCAP strain 1518/1A is shown in Figure 2.1. The growth curves of this amoeba grown in Bath-Spa medium (BSM) both in flasks and in flat-sided tubes at 32°C are shown in Figure 2.2. The curves represent the log number of cells either per flask or per ml. The population doubling time (PDT) from each culture vessel used in this study was calculated at log-phase growth. The end of this phase is marked with arrowheads in Figure 2.2. The calculated PDTs are presented in Table 2.1. There is no difference ($p<0.05$) in PDT values between flasks and flat-sided tubes (refer to Table 2.1 and Figure 2.2). In both culture vessels, the PDT was between 7 and 8 h. The end of the log-phase in flask A and tube C was ~48 h after inoculation.

In flask B (Figure 2.2B) the growth curve observed was different from the other two observations (in Figure 2.2A and C). In this flask, the cells were counted more frequently at shorter time intervals after every 24 h and the growth curve is J-shaped, indicating that the growth of the amoebae in this flask began with a lag and continued at a linear rate until reaching the end of log-phase which is about 58 h after inoculation. It can be seen that, the time taken for these amoebae to double their number (in log-phase growth) is not affected either by the size of inoculum to initiate the cultures or by the size of culture vessel used.

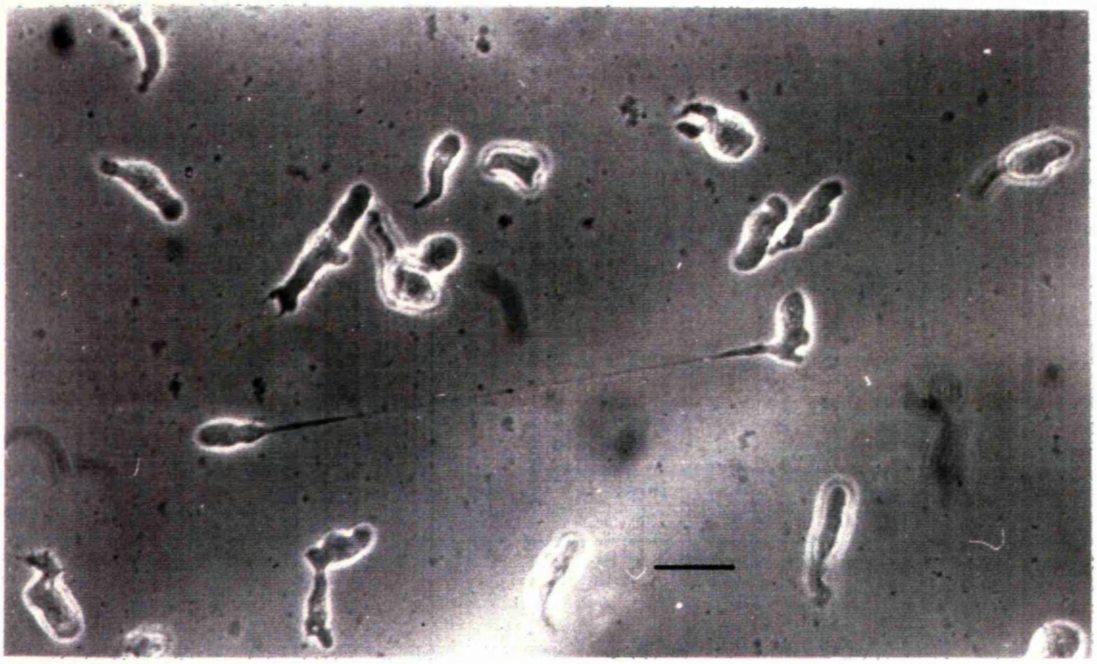

Figure 2.1. A phase constrast micrograph of *N. gruberi* CCAP strain 1518/1A grown in Bath-Spa medium at 32°C. The amoebae exhibit the typical monopodial eruptive mode of progression and movement continues throughout division. A late stage in cytokinesis is prominent at the centre of the micrograph. Scale bar = 20 μm.

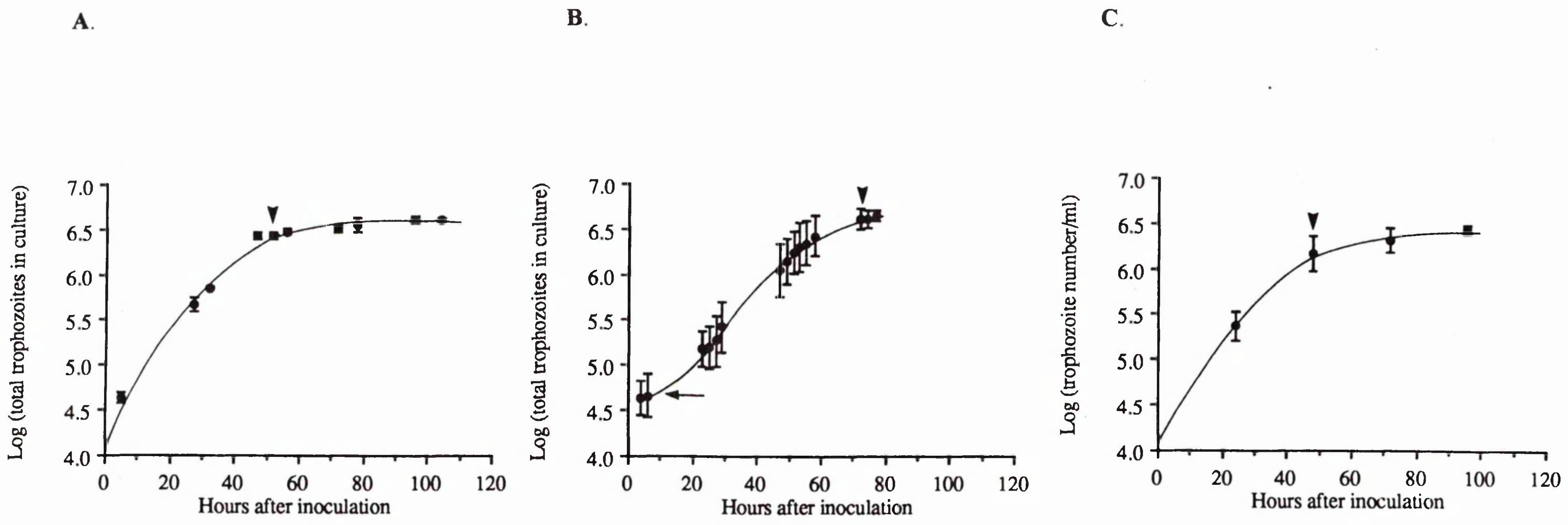

Figure 2.2 . Determination of population doubling time (PDT) of *Naegleria gruberi* CCAP strain 1518/1A grown axenically in Bath-Spa medium (BSM) at 32°C. In panels A and B, the cells were grown in Falcon culture flasks containing 5 ml BSM. In panel C, the cells were grown in flat-sided tubes containing 2.5 ml BSM. The size of inoculum for panels A and C was ~1.4x10^4 cells and ~1.2x10^4 cells, respectively. The number of cells inoculated in flasks in panel B was not counted but the cells were counted for observation 4 h after inoculation. Arrow head in each panel marks the end of log-phase growth and the corresponding hours after inoculation were used as the maximum hours observed for calculating PDTs in Table 2.1. All values plotted are from three observations and represented by means with standard deviations (error bars). Arrow in panel B indicates lag-phase growth of the amoebae.

Table 2.1. Population doubling time (PDT) of *Naegleria gruberi* CCAP strain 1518/1A grown in Bath-Spa medium, at 32°C.

Culture flask/tube	*r (slope)*	*PDT (0.693/r) (hours)*	*Mean±SD*
flask A	0.1005	6.89	
	0.0971	7.14	7.08±0.16[a]
	0.0962	7.20	
flask B	0.0895	7.74	
	0.0882	7.86	7.95±0.26[a]
	0.0841	8.24	
tube C	0.1033	6.71	
	0.1071	6.47	6.97±0.67[a]
	0.0897	7.73	

Key: [a] the means are not significantly different by F-test ($p<0.05$). The calculated F is 4.72 and the value of $F_{(2,6)}$ is 5.14 at $p<0.05$. For flask B, the PDT was calculated between 25 h and 58 h after inoculation. Flasks and tube are labelled corresponding to the graphs in Figure 2.2 for easy reference.

2.3.2. *Transmission electron microscopy observations on mitosis in Naegleria gruberi*

The observations of mitosis in *Naegleria gruberi* by transmission electron microscopy are based on the interpretations of nuclear profiles in sections of pelleted amoebae. In these sections, the nucleus is readily distinguished from other organelles in cells by having a double-membrane nuclear envelope containing pores (~100 nm in diameter) and an electron-dense nucleolus. The profile of resting or interphase nucleus was round and irregular in outline and contained a centrally condensed nucleolus (Figure 2.3A) which sometimes had a central lacuna (Figures 2.3Ba and 2.3Bb). No obvious structures have been observed in the nucleoplasm surrounding the nucleolus.

Patchy electron density and loose appearance of the nucleolus in some circular nuclear profiles have been observed (Figure 2.3C). Careful examination of such nuclei revealed the presence of short microtubules profiles, ranging between 200 nm and 300 nm in the nucleoplasm. In favourable sections of these profiles, the microtubules were seen not to be randomly orientated but to be directional in their distribution, i.e. probably orientated towards opposite poles of the nucleus, and could be construed as representing an early stage in the formation of a spindle.

The elongate nuclear profile with poorly defined nucleolar material (Figure 2.3D, E, G, and H) is believed to represent a later stage in nuclear division. Strongly dense masses whose diameter is between 120 nm and 130 nm are prominent in the nucleoplasm (Figure 2.3Da) and are often seen to be penetrated by microtubules (Figure 2.3Db). These masses are believed to represent chromosomal material and will be refered to as chromatin, their microtubule contact points are construed as kinetochores.

In less-elongate nuclear profiles (Figure 2.3D), the chromatin masses are not evenly distributed in the nucleoplasm, often being clustered around a chromatin-free central space; their relationship with the nucleolar material is less evident. Microtubules are occasionally visible outside the nucleus at what may be interpreted as poles of the now developed spindle apparatus (Figure 2.3Da).

In the most elongate nuclear profiles, chromatin masses are small and more dispersed (Figure 2.3E). Flattened or indented sections of the nuclear envelope are obvious at what may be the poles of an intranuclear spindle (Figures 2.3E and 2.3G). In some nuclear profiles, however the nature of the electron dense masses is enigmatic. Thus, in Figure 2.3F, it is difficult to decide whether the endonuclear mass is chromatin or nucleolar material in the act of constriction into polar masses, though it shows patches of electron density comparable to chromatin masses.

Longer microtubule profiles (the range is between 400 nm and 1000 nm in length) are evident in the most elongate nuclear profiles and this could be due to progressive orientation of spindle microtubules along an axis. Convergence of microtubules upon indented nuclear envelope is evident in some sections (Figures 2.3E, G, H and I).

The relationship between nucleolar material, chromatin and microtubules in the later stages of nuclear division (the equivalent of anaphase/telophase in other eukaryotes) is illustrated in Figures 2.3H to 2.3L. In Figure 2.3H, the chromatin masses form a cluster close to the polar mass of nuclear material and distal to the pole, but chromatin masses also occur peripherally; in Figure 2.3I, microtubules appear almost everywhere in the nucleoplasm, between and alongside the polar masses. In Figures 2.3J to L, microtubules passing between the polar masses and from polar masses to the nearby nuclear envelope are seen; chromatin masses are not in evidence, however, and may be out of the plane of section. An interzonal body of nucleolar material between the polar masses has not been observed.

From transmission electron microscopy of thin sections of unsynchronised cultures, then, only a vague picture of the relationship of chromosomal material to the spindle and the nucleolus can be obtained.

Figure 2.3. Transmission electron micrographs showing various stages (A to L) of nuclear division in *Naegleria gruberi* CCAP strain 1518/1A grown axenically in Bath-Spa medium, at 32°C.

2.3A. The nucleolus (no) which is dense in appearance is in the centre of the nucleus (n). The double-membrane nuclear envelope is irregular in outline with nuclear pores (arrow). Scale bar = 1 μm.

2.3B. Two micrographs (a and b) showing nucleus (n) with nucleolar lacuna (L). The lacuna is more electron dense than the perinucleolar nucleoplasm. Scale bar = 2 μm.

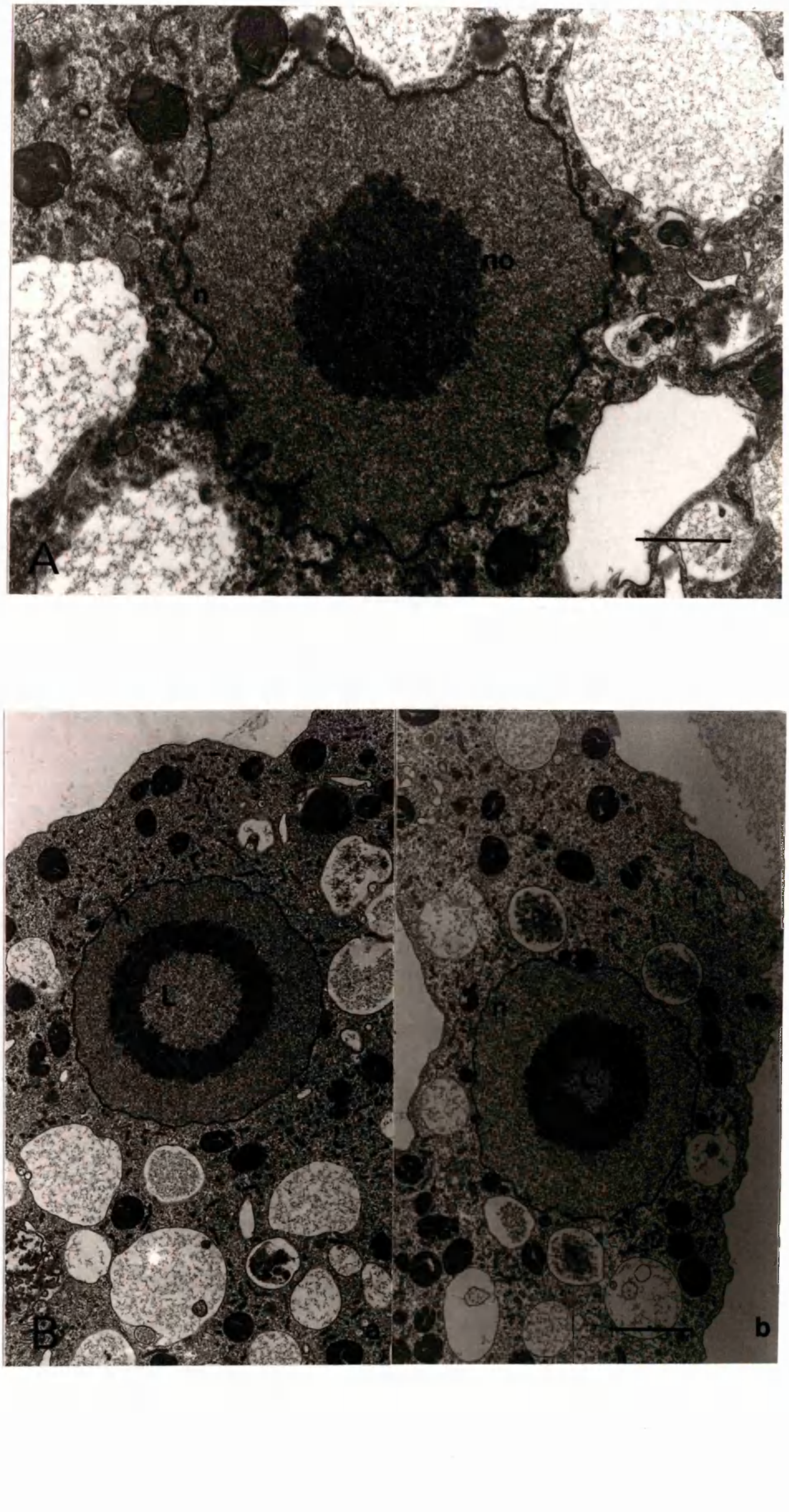
n
no
A
n
L
B
n
b

2.3C. Nucleolar material (nm) has regions of varying density. Microtubules are seen in the nucleoplasm (arrow). From the direction of microtubule formation, one can predict the polar regions (P) of the nucleus. Scale bar = 1 µm

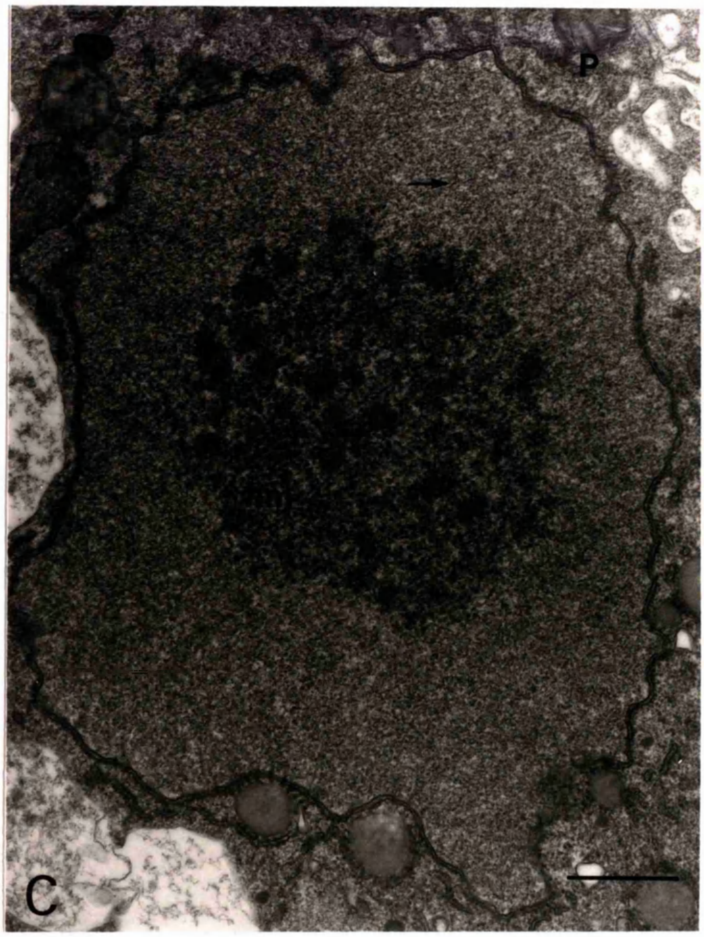
P
C

2.3D. In this specimen, some of the electron-dense nuclear materials are in the middle and at the periphery of the nucleus. In Figure 2.3Da, bundles of microtubules are seen outside of the nucleus at both poles (small arrows). Scale bar = 1 µm. In Figure 2.3Db, some of the intranuclear microtubules appear to insert on the electron dense nuclear material (arrow) suggesting the possible chromosomal kinetochore attachment site. Scale bar = 0.5 µm.

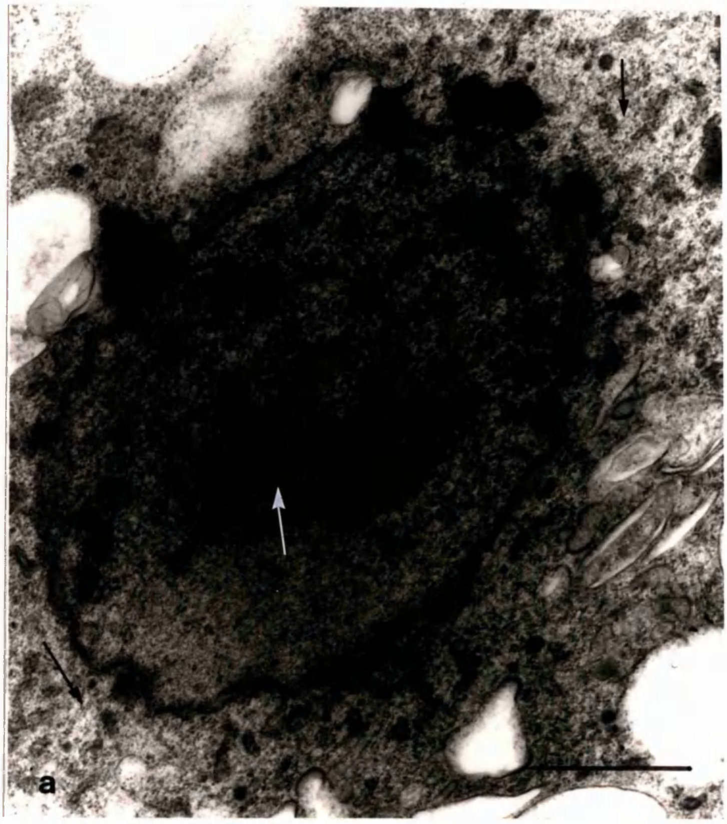
a

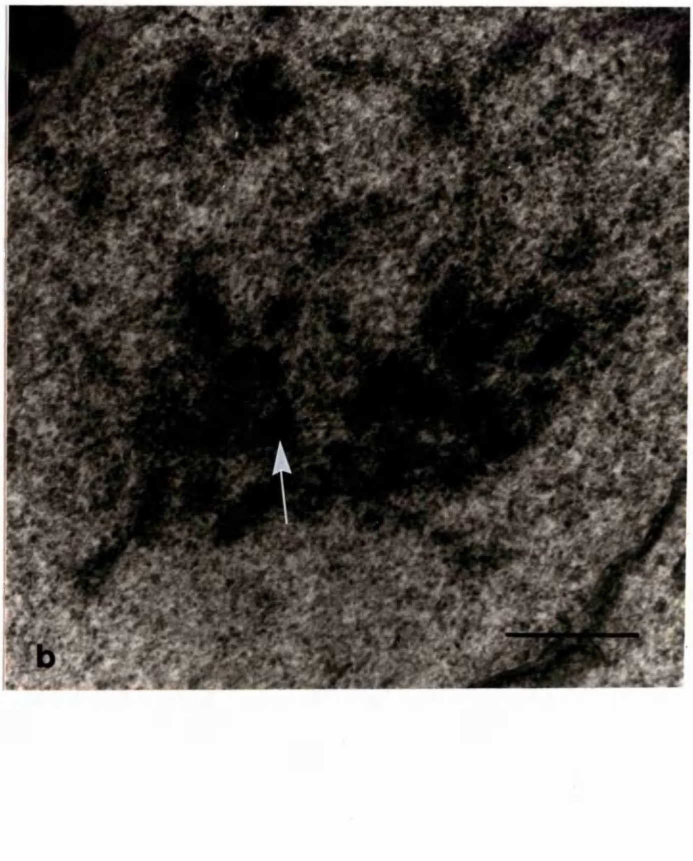
b

2.3E. Nucleus with scattered densely stained material, interpreted as chromatin (arrowheads). The short microtubules (arrows) are mostly seen in the middle section of the nucleus. The nuclear envelope is concave at the pole (left). Scale bar = 0.5 µm.

2.3F. A cross-section of the nucleus. In this specimen, the microtubules (arrow) are seen penetrating the densely stained and compact nucleolar material (possibly a polar mass, nm). Scale bar = 1 µm.

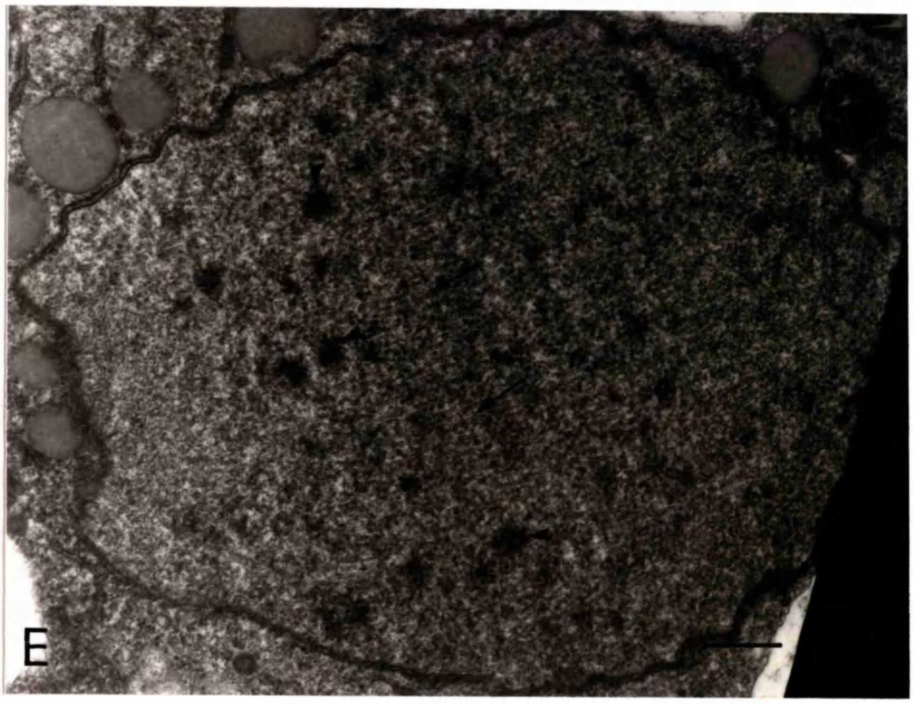
E

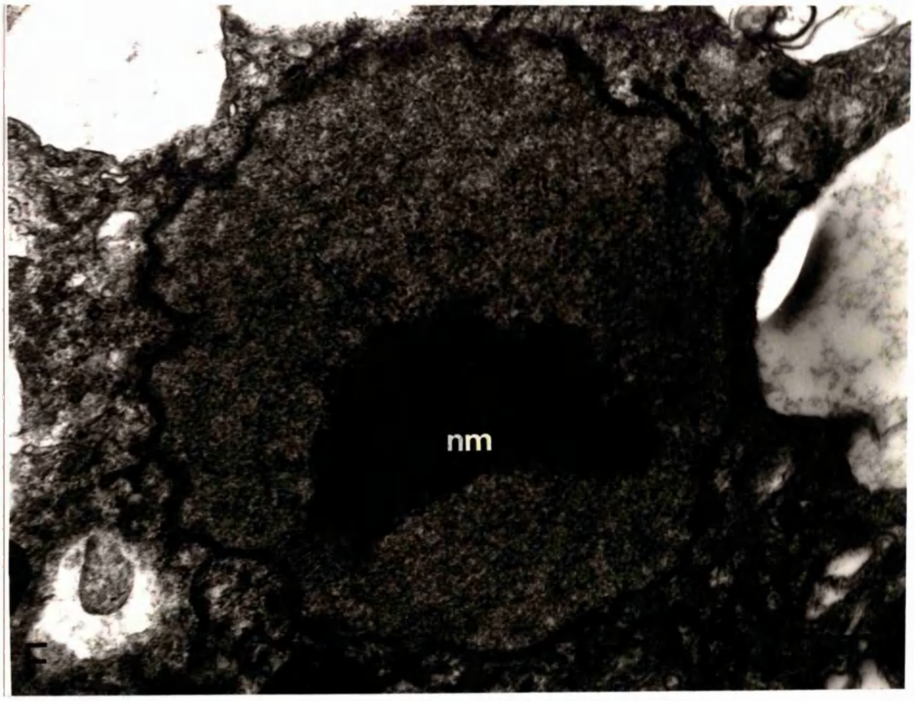
nm
F

2.3G. A tangential section of the nucleus. Bundles of the microtubules (arrows) are seen in areas some distance from the nucleolar material (nm) which may represent a polar mass (left) and interzonal body. The nuclear pole (P) (left) is dented. Scale bar = 1 μm.

2.3H. Nucleus in late division (metaphase-anaphase stage). The polar masses (Pm) lie at the opposite poles (the other polar mass lies outside the plain of the section). The short microtubules (arrows) which are ~160 nm in length are observed occupying the nucleus including the area between polar masses (Pm) and close to the nuclear envelope (at the shorter arrow). The electron dense masses (arrowheads) could represent chromosomal material.
Scale bar = 1 μm.

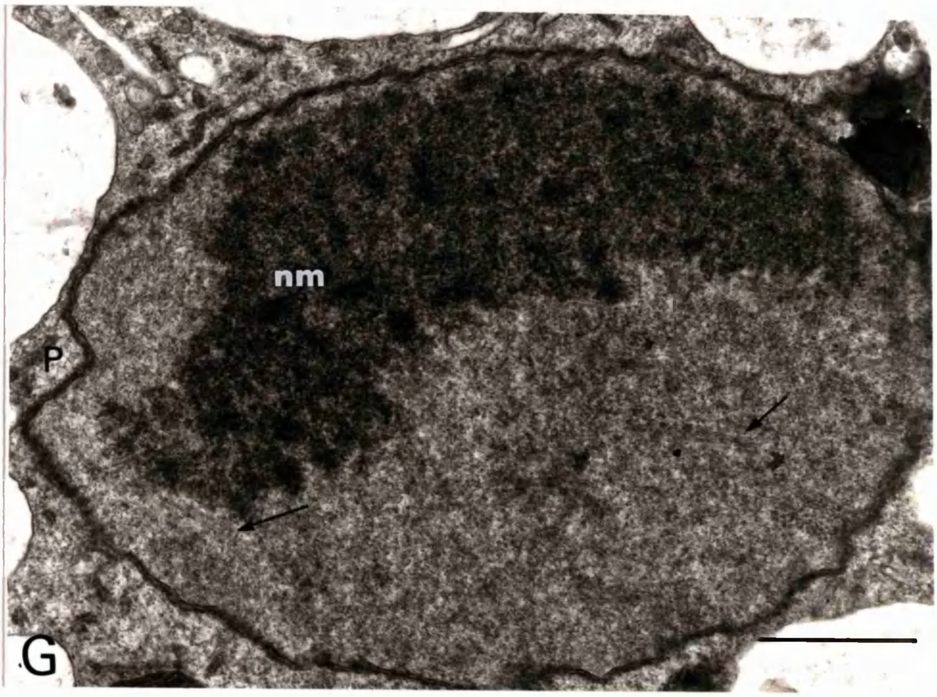
nm
P
G

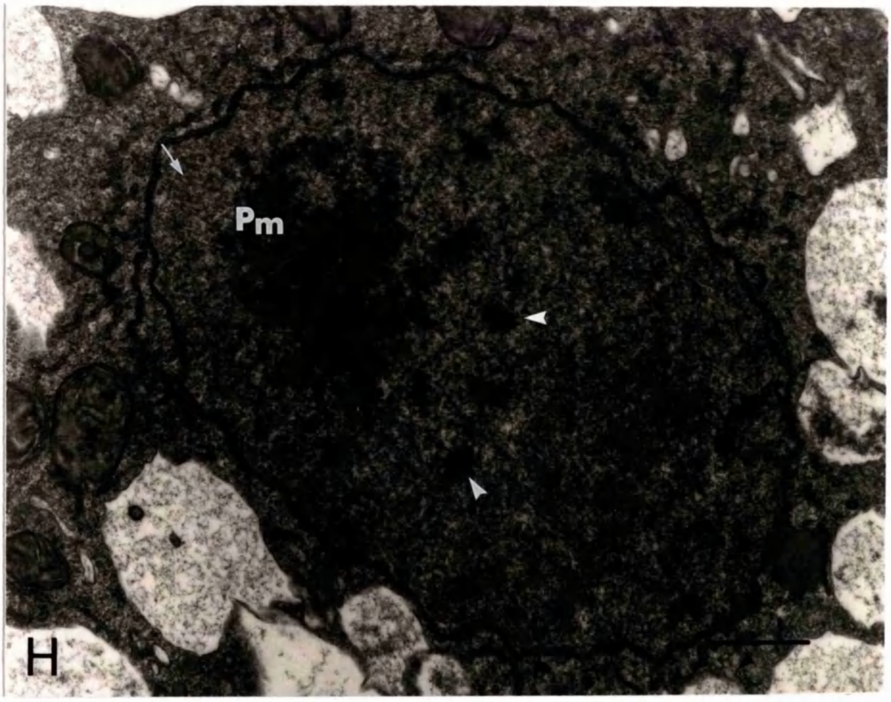
Pm
H

2.3I. Nucleus in anaphase stage. The polar masses (Pm) are at the opposite ends of the nucleus. Microtubule profiles are seen almost everywhere in the nucleoplasm (shown by arrows). Microtubule profiles at the upper pole (left-hand side in this micrograph) are shorter than those at the other pole in this section. Scale bar = 1 µm.

2.3J. Late anaphase stage of nucleus. Polar masses (Pm) are at the opposite ends of the nucleus. The microtubules are clearly seen (arrows), and appear to terminate on the inner membrane of the nuclear envelope (arrowheads). This section may parallel to the interzonal body (which is not visible here). Scale bar = 1 µm.

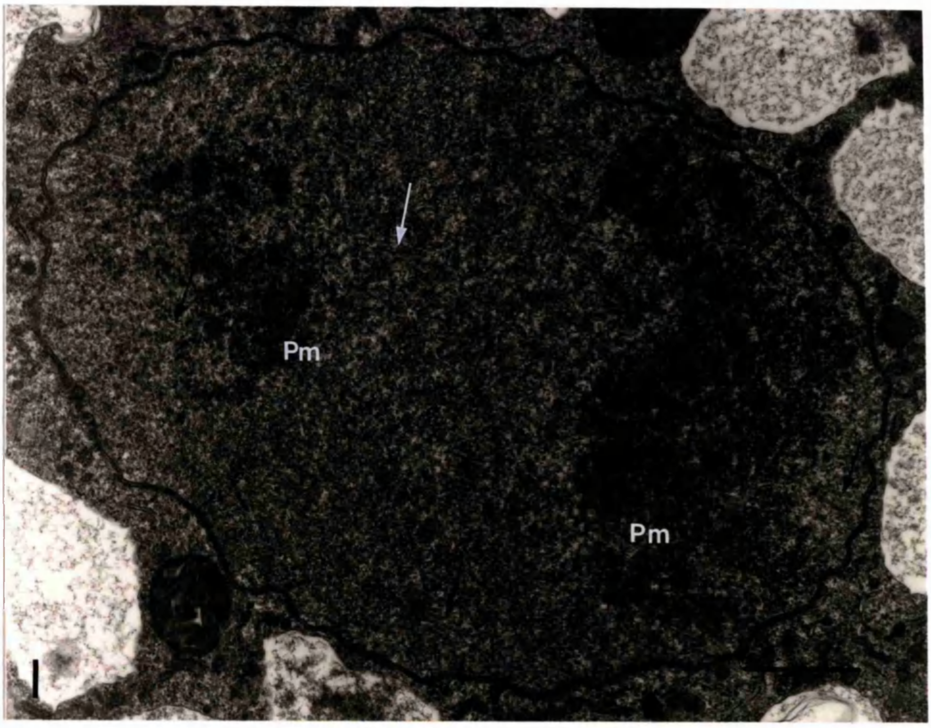
Pm
Pm
I

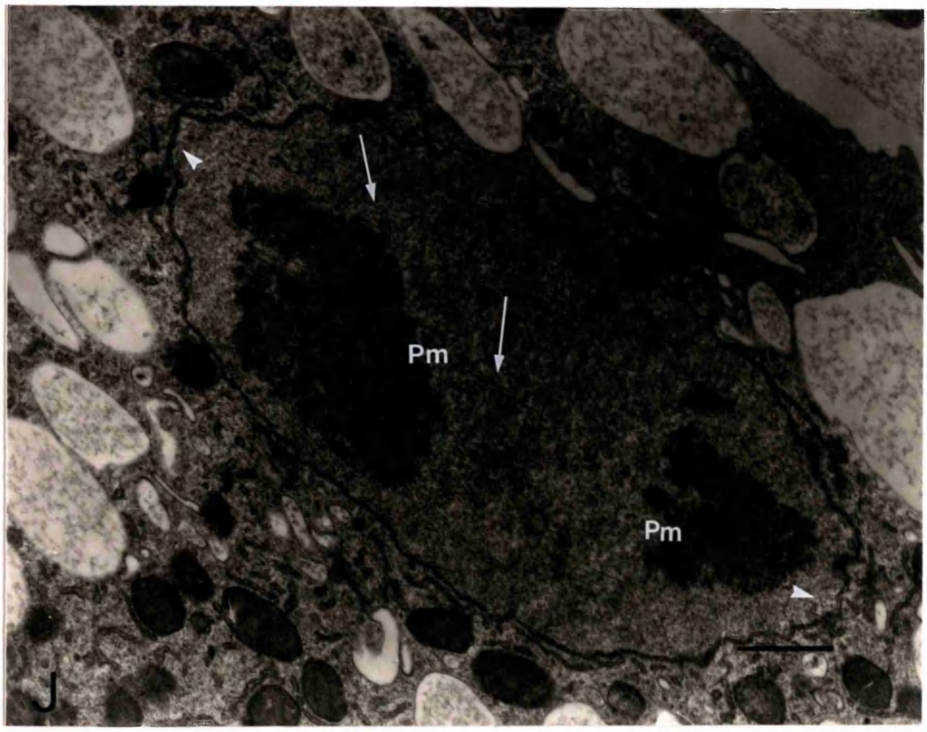
Pm
Pm
J

2.3K and L. The same specimen as in J but enlarged to show the long microtubule profiles (arrows) occupying the nucleus in late anaphase stage. Possible chromosomal structures are not evident in these sections.
Scale bar = 1 μm.

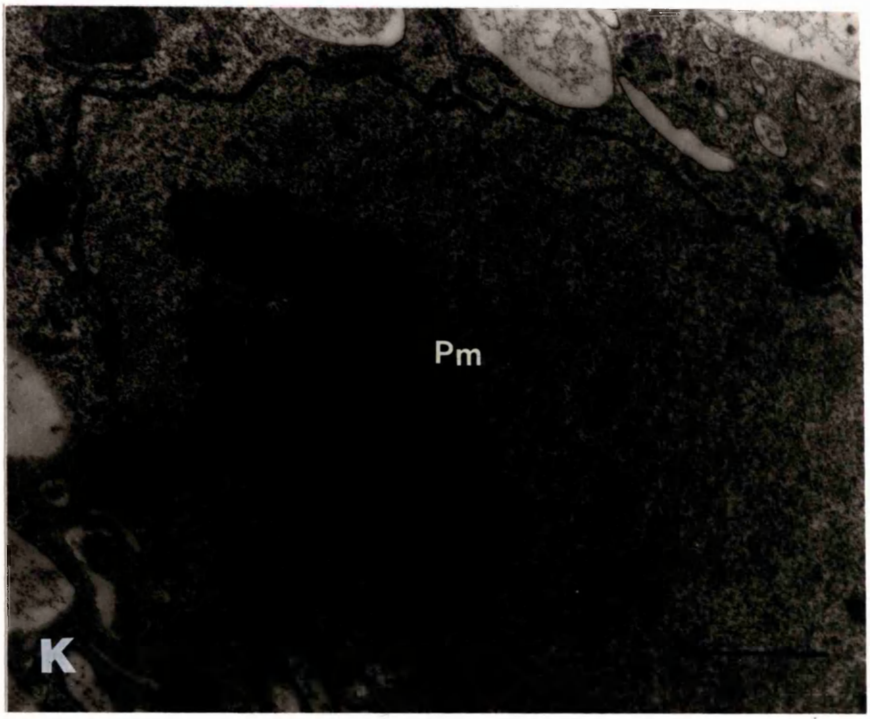
Pm
K

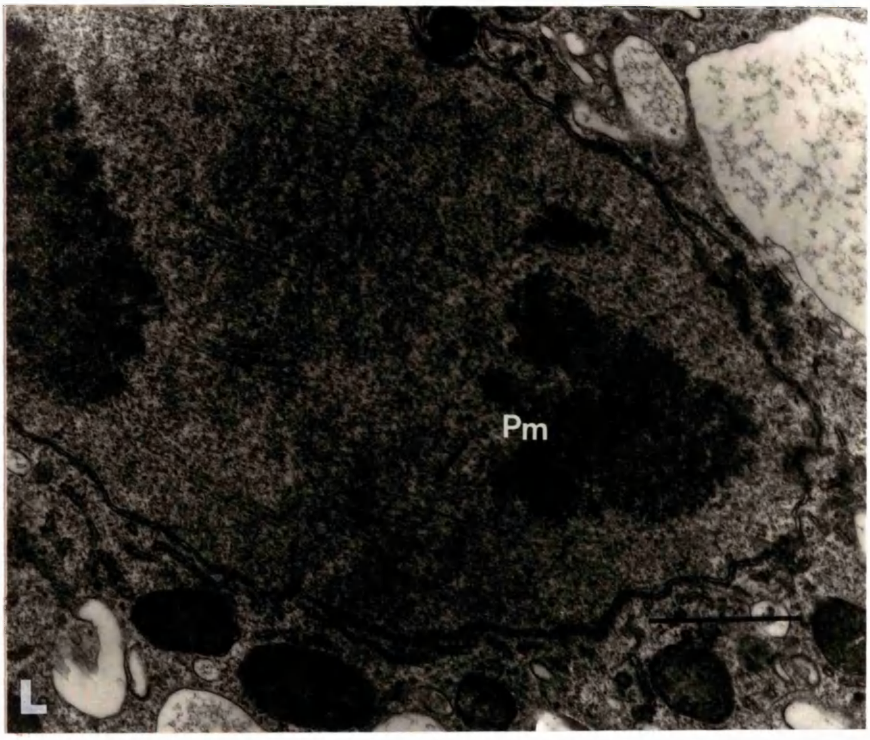
Pm
L

2.3.3. *Fluorescent microscopy study of mitosis in N. gruberi*

Detection of DNA-containing material in cells

In order to shed light on the location and movement of chromosomal material during nuclear division, DAPI, a DNA specific probe was used to locate the distribution of DNA. It was observed that in the non-dividing nucleus, DNA containing material (stained bluish white) occupied the periphery of the nucleus (Figure 2.4A). The nucleolus (located in the middle of the nucleus) was stained red by PI but was not stained by DAPI (Figure 2.4A) indicating that in these cells, chromosomal material (chromatin) was not located in the nucleolus but at the periphery of the nucleus. The chromosomal material however, was atypically observed in the middle of nucleus in a non-dividing cell in Figure 2.4B. In the dividing nucleus, this material was observed at the opposite poles (Figure 2.4B). The morphology of the structures which were stained positive by DAPI in Figure 2.4B could be clearly seen as discrete, small and round objects; they could represent the chromosomes/chromatin of *N. gruberi*.

A puzzling staining pattern is shown in Figure 2.5A; DAPI fluorescence is faintly discernible in what would appear to be the cytoplasmic bulge connecting daughter cells in late cytokinesis, while the daughter nuclei themselves show PI staining only. Figure 2.5B shows the more conventional staining pattern of a cell in late cytokinesis.

Figure 2.4. Fluorescence microscopy of *Naegleria* cells stained with DAPI and PI. A. DNA-containing material stained bluish white by DAPI (arrows) is at the periphery of the nucleus. The nucleolus at the centre of the nucleus is stained red. B. Discrete masses of DNA containing material (arrows) are at oppposite poles in what could represent an anaphase stage in nuclear division, on the right. In the nucleus (n) on the left, the chromatin appears to be central. Scale bar = 20 μm.

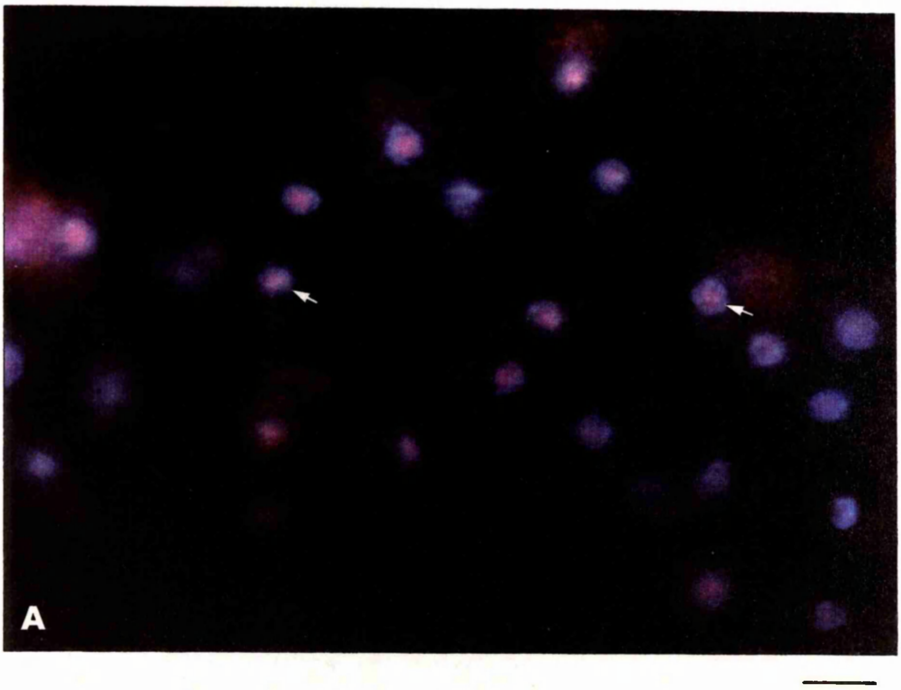
A

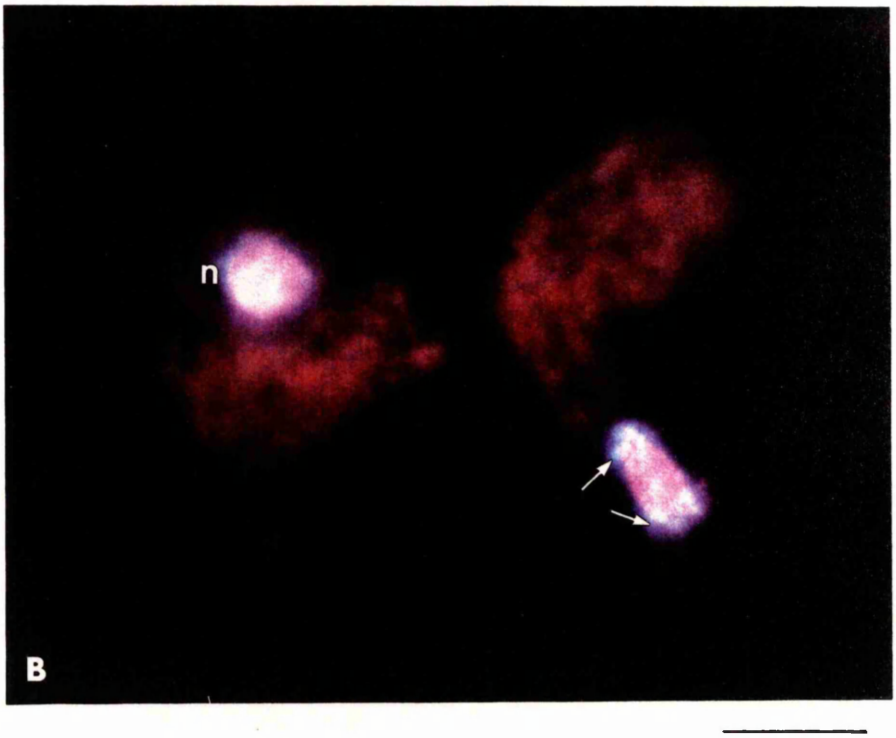
n
B

Figure 2.5. Cytokinesis in *Naegleria gruberi* observed by fluorescence microscopy after DAPI-PI staining. A. DAPI-stained material (arrow) appears to be in the middle of constricting nucleus. Scale bar = 10 μm. B. The cytoplasm which connects the two cells is free of nuclear material. One of the daughter nuclei (n) is in focus. Scale bar = 20 μm.

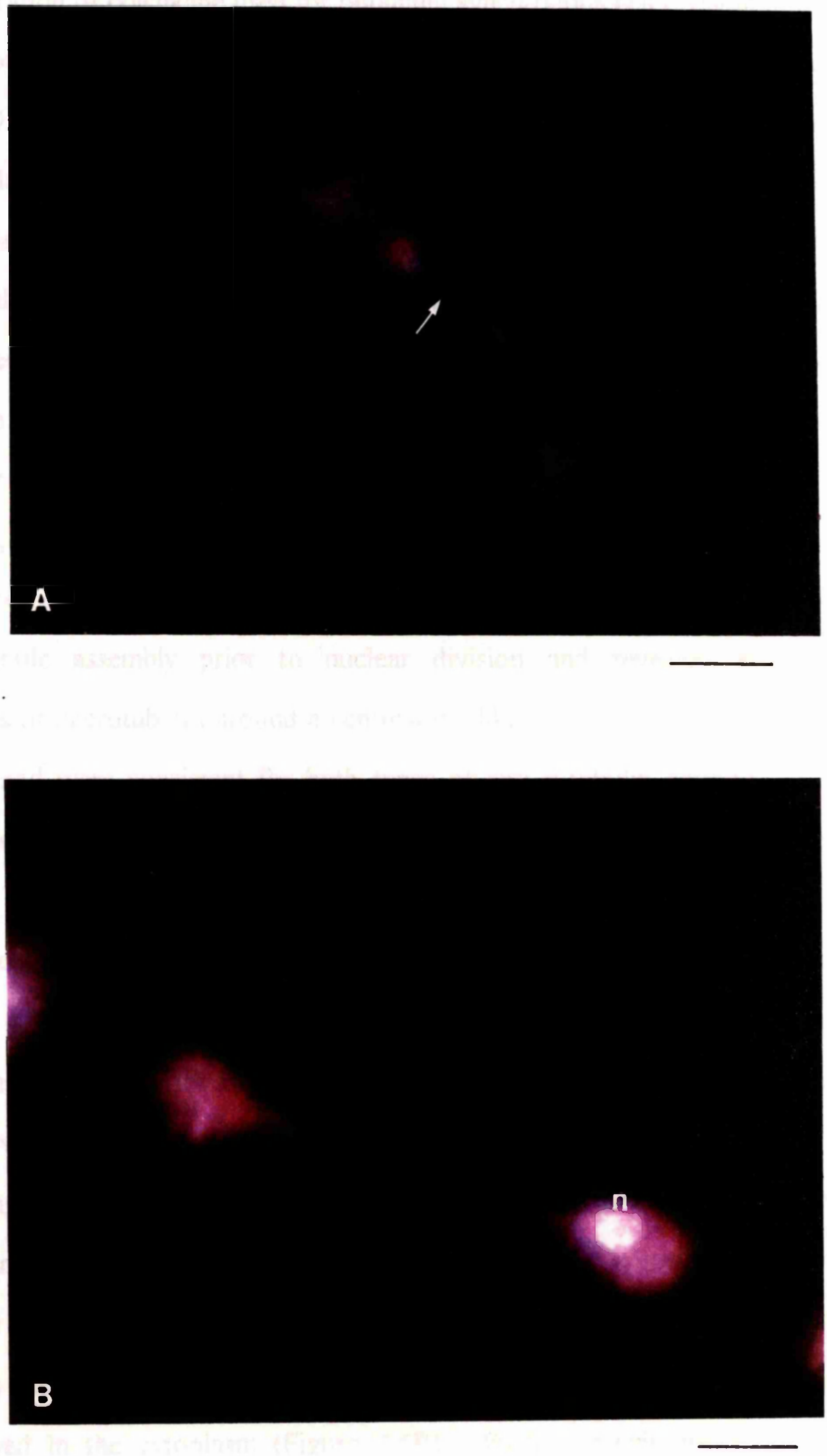
A
B
n

Nuclear division in colchicine-treated Naegleria

The concentration of colchicine used for obtaining synchronous cell division in this study was not lethal to the cells since 100% cells were found to be still viable when tested with 0.25% (w/v) trypan blue. In this study, it was also observed that most cells when placed in Page's amoeba saline without colchicine for 18 h, transformed either into flagellates or cysts whereas in the same amoeba saline, but containing this drug, only a few cells transformed into flagellates. No cysts were observed in these cultures. This observation suggests that in the presence of colchicine, not only did the amoebae fail to multiply but also their transformation either into flagellates or cysts was inhibited.

Cells, released from colchicine treatment and after indirect immunofluorescence staining with anti-α-tubulin antibody, indicated the pattern of the microtubule assembly prior to nuclear division and revealed aster-like arrangements of microtubules around a centrosome-like structure or MTOC. The results obtained were consistent for both types of anti-α-tubulin antibody used. The cells were also stained with DAPI to estimate roughly the location of the centrosome and MTOC in relation to the nucleus. Figure 2.6. shows a reconstructed series of what appear to be events in nuclear division. The colouration of DNA was bluish white and represents either the nucleus or chromosomal material (series in left panels in Figure 2.6) and microtubules were stained yellowish green (series in right panels in Figures 2.6).

A single centrosome with a radiating microtubule network was observed in the cytoplasm (Figure 2.6A) of what may represent the cell in interphase. In a fluorescence micrograph which may depict later stages of nuclear division, two centrosomes each of them forming one MTOC with its microtubule network have been observed in the cytoplasm (Figure 2.6B). Further developments of the centrosome into bipolar microtubule organising centres are illustrated in Figures

2.6A to F and Figures 2.7A and B. In fluorescence micrographs of the same specimens but stained with DAPI, the changes in the nuclear size and shape could be visualised. The nucleus which was observed to be rounded in early stages of division, became elongated in later stages of division (Figures 2.6A to E).

The DNA containing material was observed to be associated with and located in the middle of an elongated bundle of spindle microtubules connecting the nuclear poles (Figures 2.6F and 2.7C); in this image, the cell could be at metaphase with the chromosomes forming an equatorial plate (metaphase plate). The nuclear material in Figures 2.6F and 2.7C was also stained positive by anti-α-tubulin antibody suggesting that the microtubules are present and are associated with the nuclear material/chromosomes. At this stage and later stages of nuclear division, centrosomes and cytoplasmic microtubules were not evident in the cell.

In what are interpreted as much later stages of nuclear division, the association between the mitotic spindles (microtubules) and the chromosomes/nuclear material becomes more evident (Figures 2.6G, H and I). Bundles of microtubules which from their distribution could be described as polar microtubules have been observed extending between the two nuclear poles (Figure 2.6G). The distance between the poles is apparently increased as the nucleus goes further into nuclear division (Figures 2.6H and I) and such cells could be described as representing anaphase B. The appearance of polar masses staining with both DAPI and the antibody at the opposite poles (Figure 2.6H) could be the result of chromosome movement in anaphase A. Although the polar masses have formed at both poles, they are still connected by a bundle of microtubules (Figure 2.6H); these microtubules might represent a midbody (Merdes *et al*, 1991) or interzonal body (Rafalko, 1947) . This midbody was also evident in binucleate amoebae during synchronous nuclear division (Figure 2.6K). The midbody (interzonal body) in later stages of nuclear division appears to become constricted (Figure 2.6I) and then pinched into two, about the time of cytoplasmic cleavage (Figure 2.6J). In fluorescence micrographs, the nuclear envelope was not clearly visible in all mitotic stages of *N. gruberi*.

Colchicine-treatment has been proven to help the detection of not only a spindle but also a centrosome in the cytoplasm of *N. gruberi* during nuclear division. The centrosome or MTOC was visualised only in cells treated with colchicine (Figure 2.8). This structure was not detected in cells which were not treated with colchicine. The intranuclear spindles, however could be detected even in cells not treated with colchicine (Figure 2.8, panel B). The secondary antibody (FITC) used in this study specifically binds to anti-α-tubulin so it selectively binds to the microtubules and tubulin-containing structures. Detectable microtubule structures were absent in cells which were only stained with the secondary antibody (Figure 2.8). The structures observed in colchicine treated cells which are stained positive by anti-α-tubulin and FITC antibodies are therefore microtubules or other tubulin-containing structures.

Figure 2.6. Organisation of a centrosome (MTOC) during nuclear division in *Naegleria gruberi,* visualised under fluorescence microscopy. Left panels; DAPI staining to visualise the nucleus (n). Right panels; anti-α-tubulin staining of the same field to detect the microtubules. Various stages of nuclear division described here are identified by analogy with stages of division in other eukaryotes. A. Interphase: the cytoplasmic microtubule arrays are focussed at the centrosome. B to E. Prophase: two arrays of microtubules (arrows) are present and moving apart. F. Metaphase: all microtubules are associated with the mitotic spindles. Chromosomes (arrows) form a metaphase plate. G to H. Anaphase-Telophase: microtubules are still focussed at the separated spindle poles which later becomes concentrated to form the midbody (arrow in H). I to J. Late telophase: the midbody pinches into two (arrow in I) and cytoplasmic division follows (arrow in J). K. Synchronous nuclear division in a binucleate *Naegleria.* Scale bar = 10 μm.

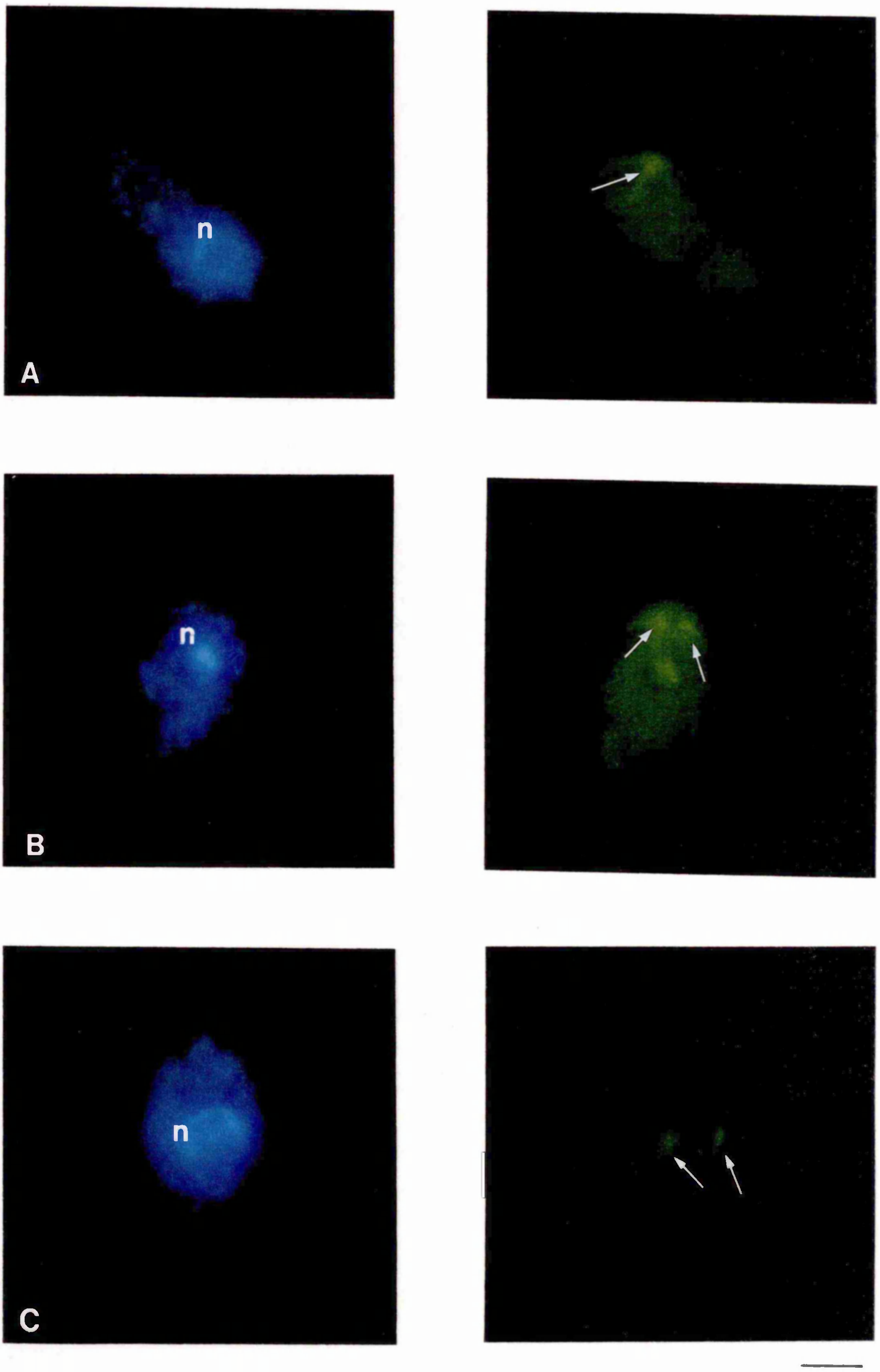
n
A
n
B
n
C

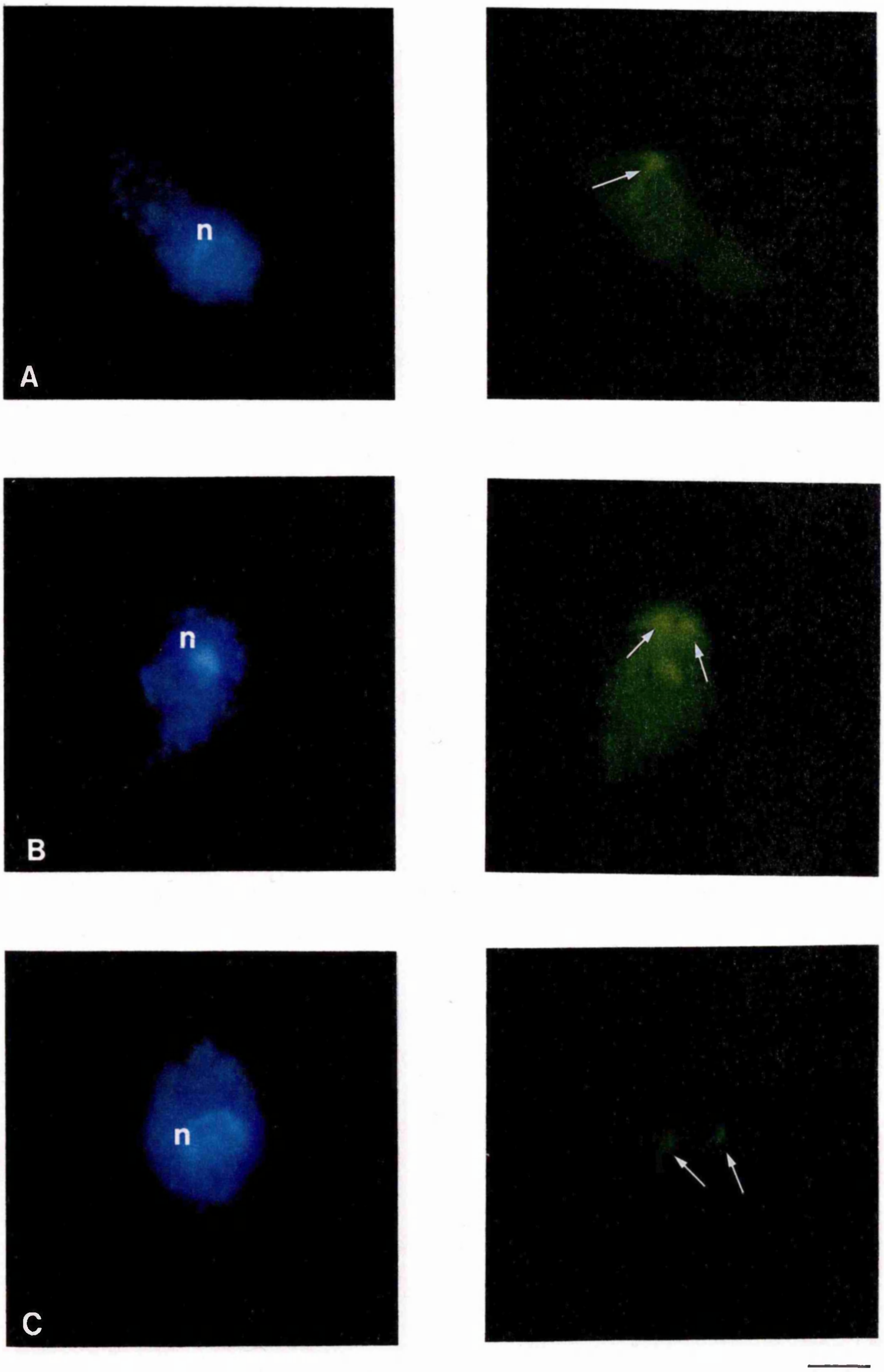
n
A
n
B
n
C

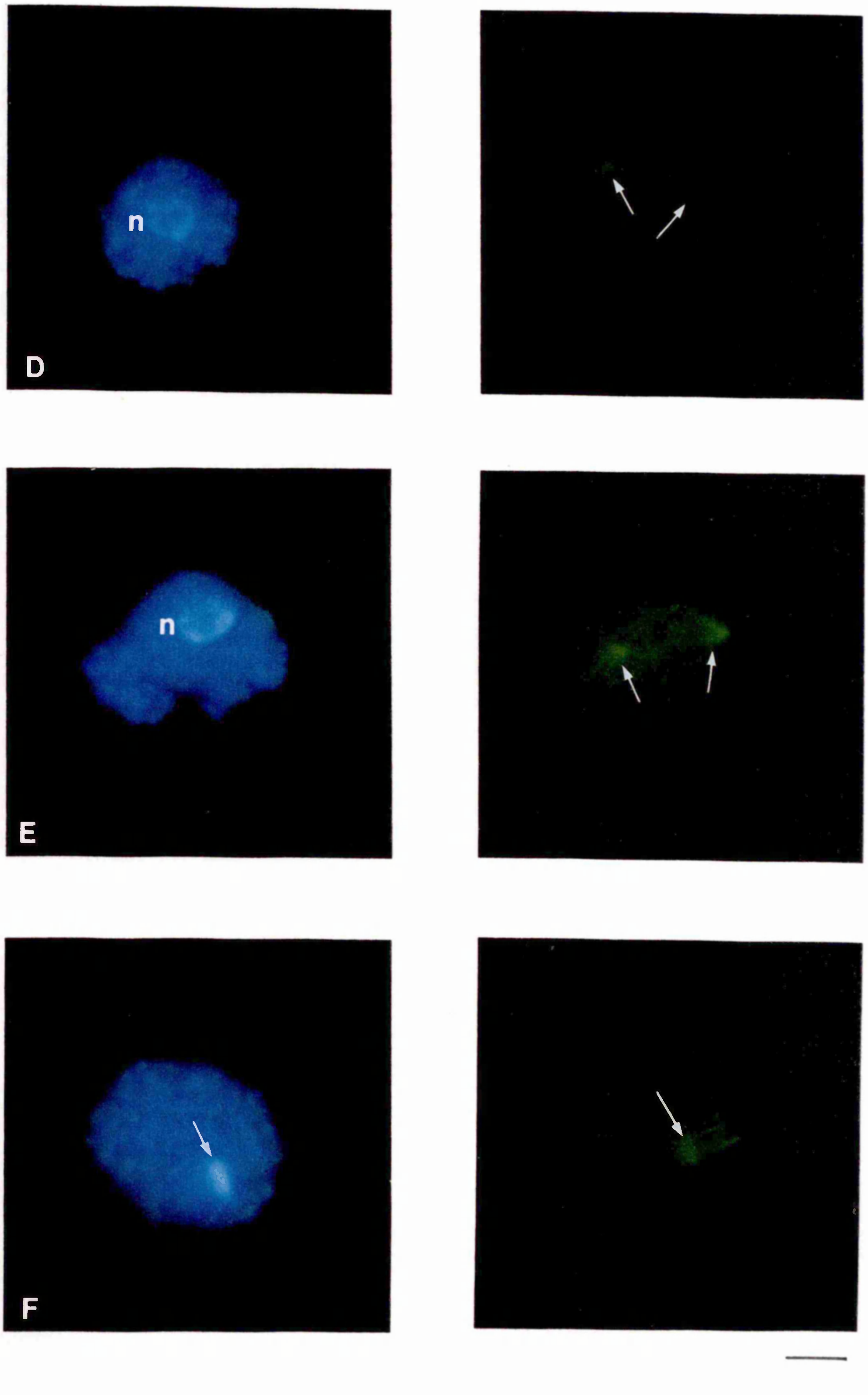
n
D
n
E
F

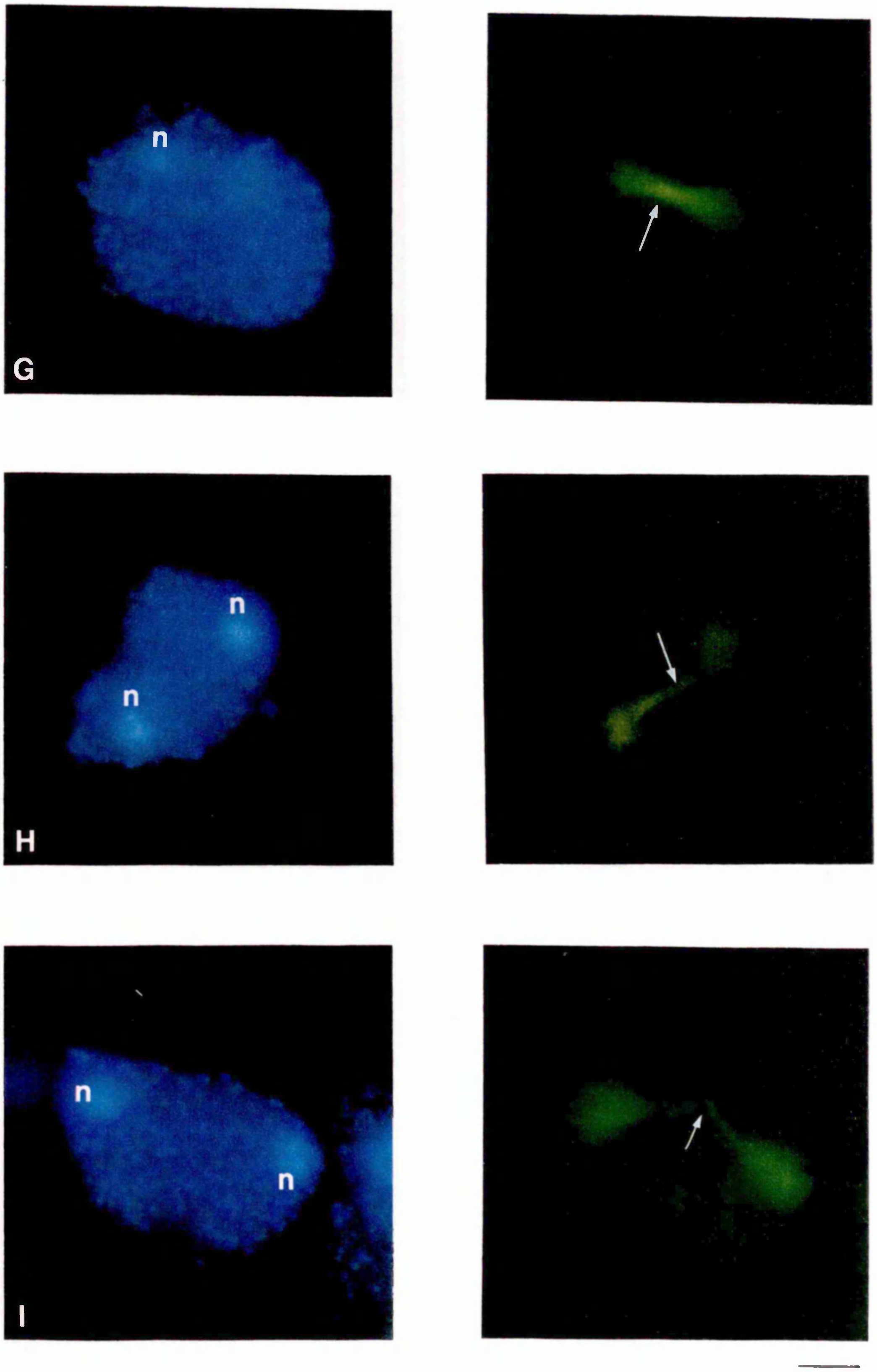
n
G
n
n
H
n
n
I

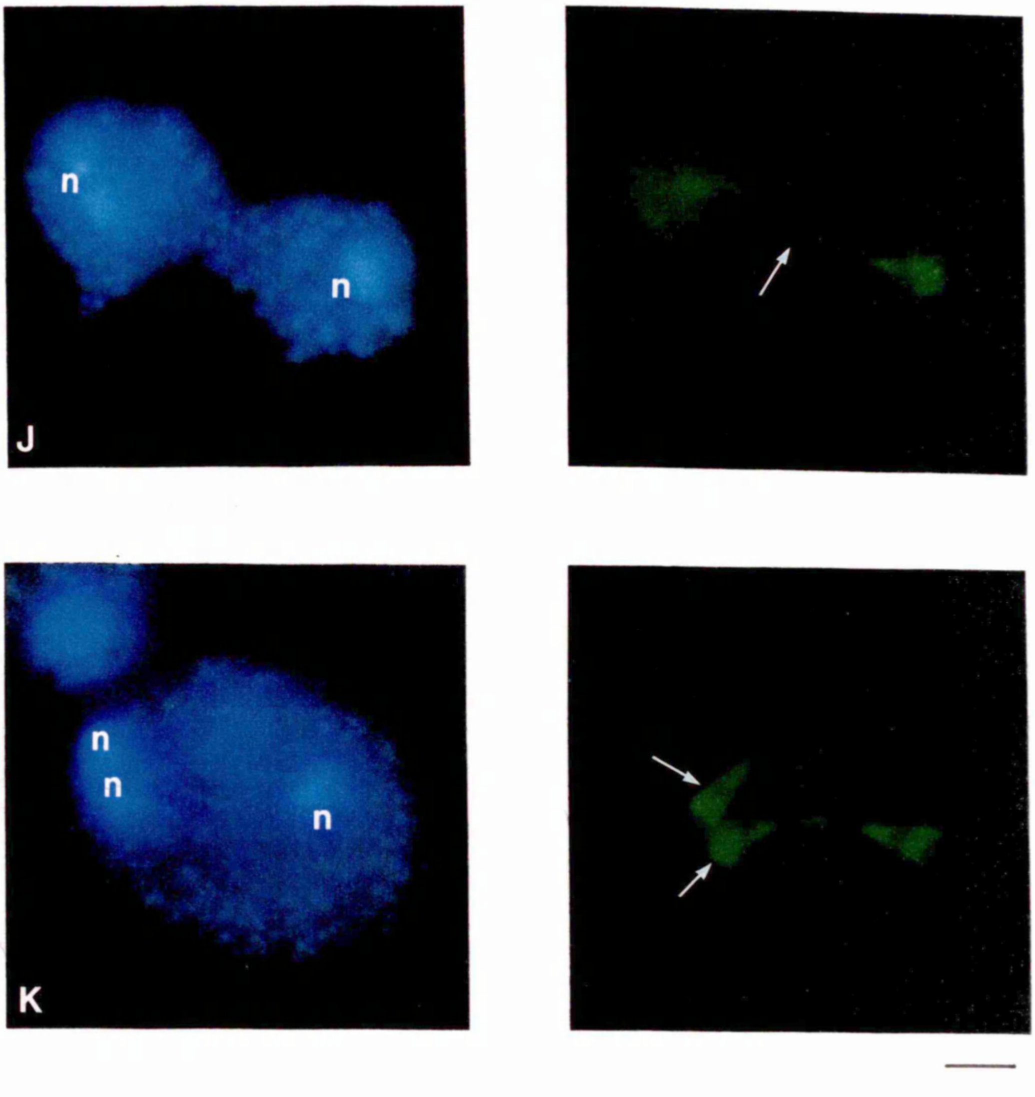
n
n
J
n
n
n
K

Figure 2.7. Immunofluorescence staining of *Naegleria* cells. Left panels; DAPI staining to visualise the nucleus (n). Right panels; anti α-tubulin staining of the same field to detect the microtubules. A. Microtubule arrays originating from a monopolar centrosome. B. Two microtubule arrays are originating from two closely associated MTOCs. C. The nucleus at metaphase. The microtubules form a spindle with sharp nuclear poles and are attached to the chromosomes (arrow). The nuclear envelope could not be visualised at this stage. Scale bar = 20 μm.

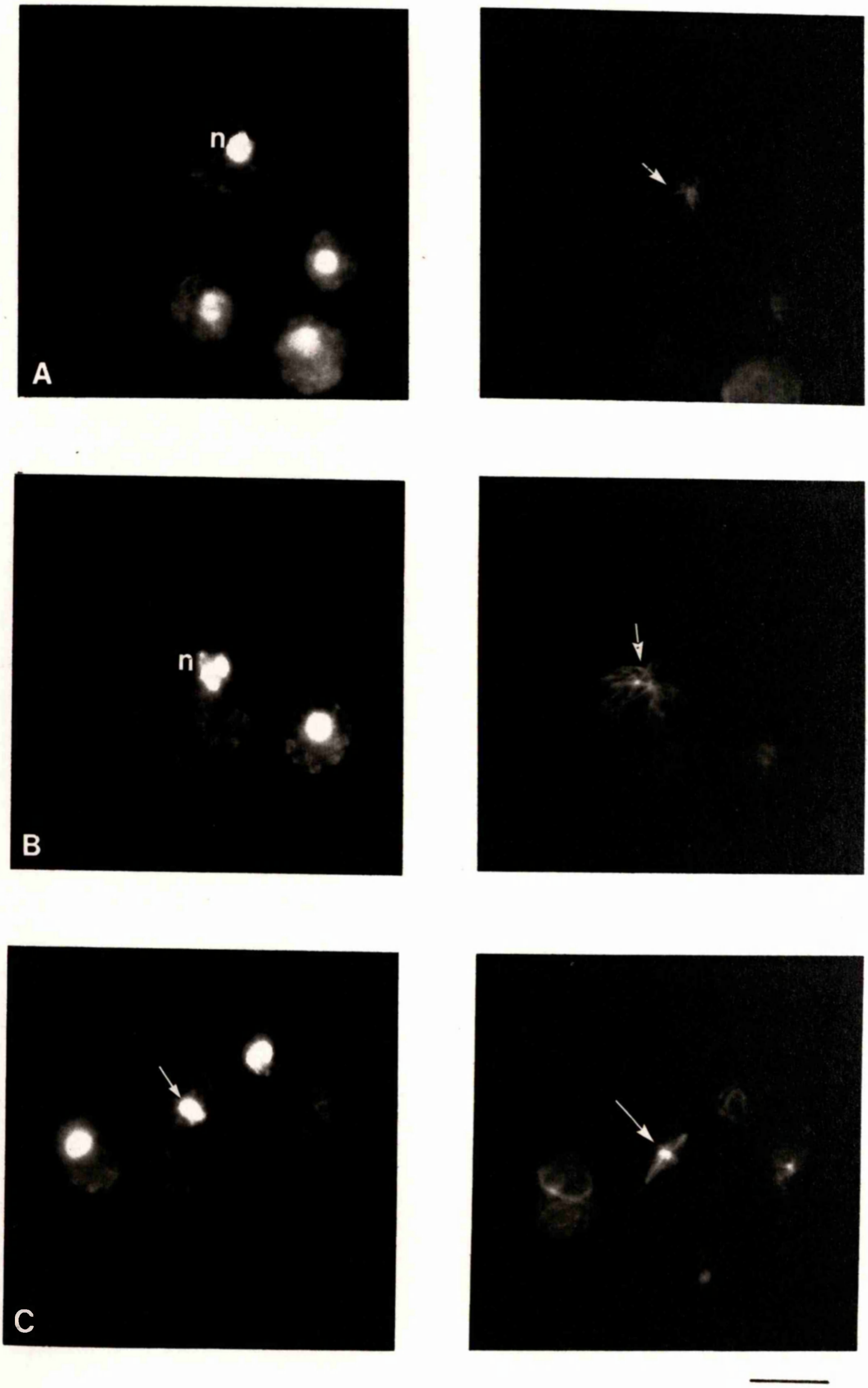
n
A
n
B
C

Figure 2.8. Studies on nuclear division in *Naegleria gruberi* under fluorescence microscopy. Left panels; the cells were stained with DAPI to locate the position of the nuclei in cells. Right panels; the cells were stained with anti-α-tubulin to visualise the microtubules in cells. A. The cells when treated with colchicine. The centrosome like-structures (microtubules, arrows) were observed in most cells. B. The cells were not treated with colchicine. Positive staining of the microtubules was observed only in presumbly dividing nucleus (arrow). C. The cells (colchicine-treated cells) were stained only with a secondary antibody (FITC) to check the specificity of this antibody binding to anti-α-tubulin in A and B. The absence of staining of any structures observed in this study indicating that FITC binds specifically to anti-α-tubulin to stain the microtubules in cells. Scale bar = 20 μm.

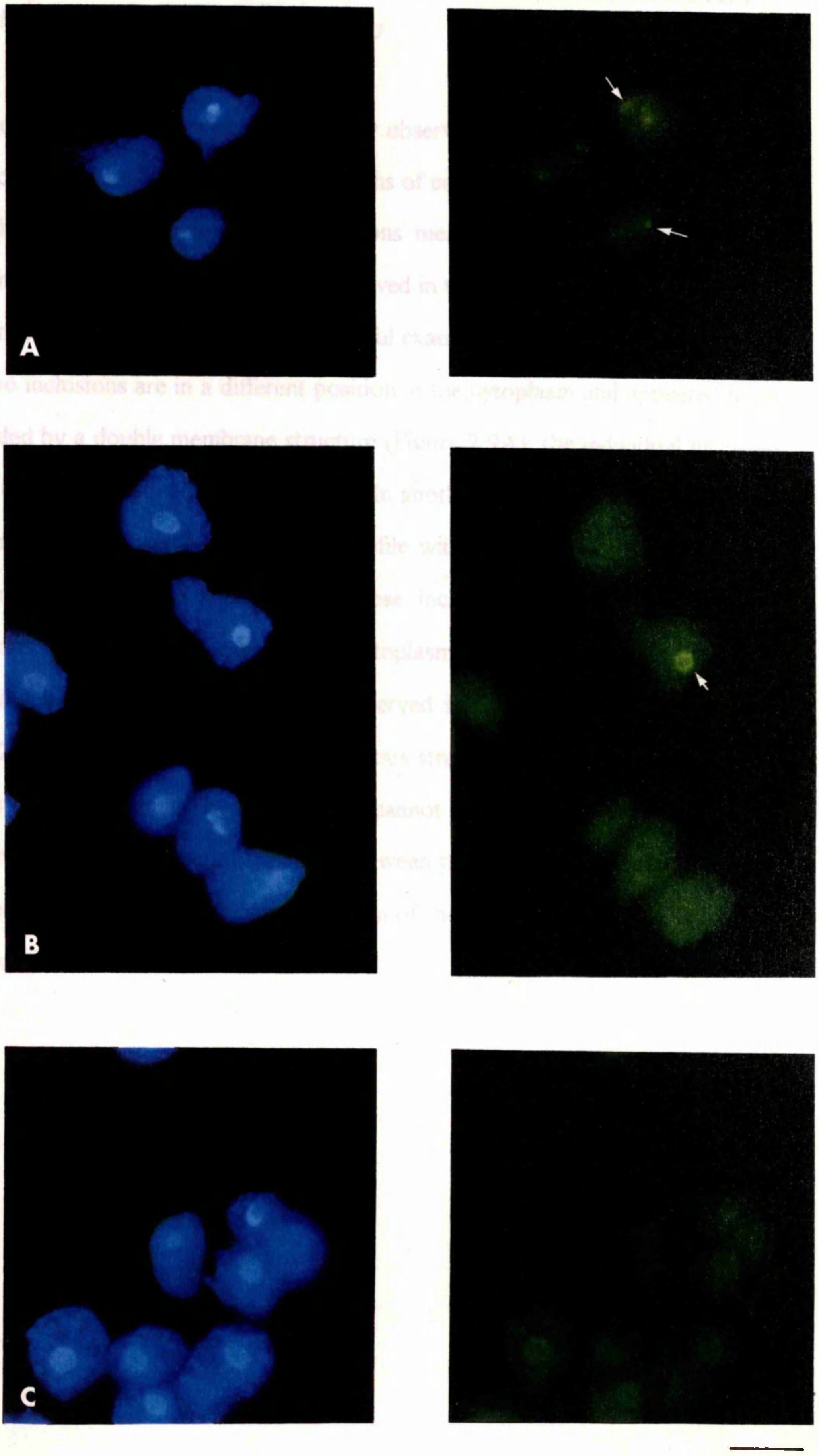
A
B
C

2.3.4. *Observation of the cytoplasmic microtubules in colchicine-treated cells by transmission electron microscopy*

A centrosome or MTOC which was clearly observed in fluorescence micrographs could not be detected in electron micrographs of colchicine-treated cells. A pair of identical, bean-shaped cytoplasmic inclusions measured ~375 nm in length and ~180 nm in width however, have been observed in the cytoplasm of the cell in close proximity to the nucleus (Figure 2.9). Careful examination of this figure shows that these two inclusions are in a different position in the cytoplasm and appeared to be surrounded by a double membrane structure (Figure 2.9A); the individual inclusion seemed to be surrounded by a membrane. In another electron micrograph, one of the inclusions was observed as a longer profile with no evidence of a surrounding membrane (Figure 2.9B). Other than these inclusions, the unusual elongated filamentous structure and other two cytoplasmic inclusions (but not being surrounded by a membrane) were also observed in the cytoplasm of *N. gruberi* (Figure 2.10). The position of this filamentous structure in relation to the nucleus or if it is being surrounded by a membrane cannot be determined with certainty in this figure. The measurement of spacing between parallel lines of the all inclusions (both from tangential and longitudinal section of the inclusions such as Figure 3.0) gave between 10 nm and 13 nm.

Figure 2.9. Transmission elecron microscopy of *Naegleria* cells after treatment with colchicine. A. A pair of bean-shaped paracrystalline cytoplasmic inclusions enclosed in a double membrane structure (possibly the indented nuclear envelope). a, tangential section of the paracrystal; b, different angle of tangential section of the inclusion. Scale bar = 0.25 µm. B. Similar inclusions (big arrows). Small arrows to indicate the direction of the parallel lines of the inclusions. Scale bar = 0.25 µm. C. The same structures in B (arrows) and their location in relation to the nucleus (n). Scale bar = 0.5 µm.

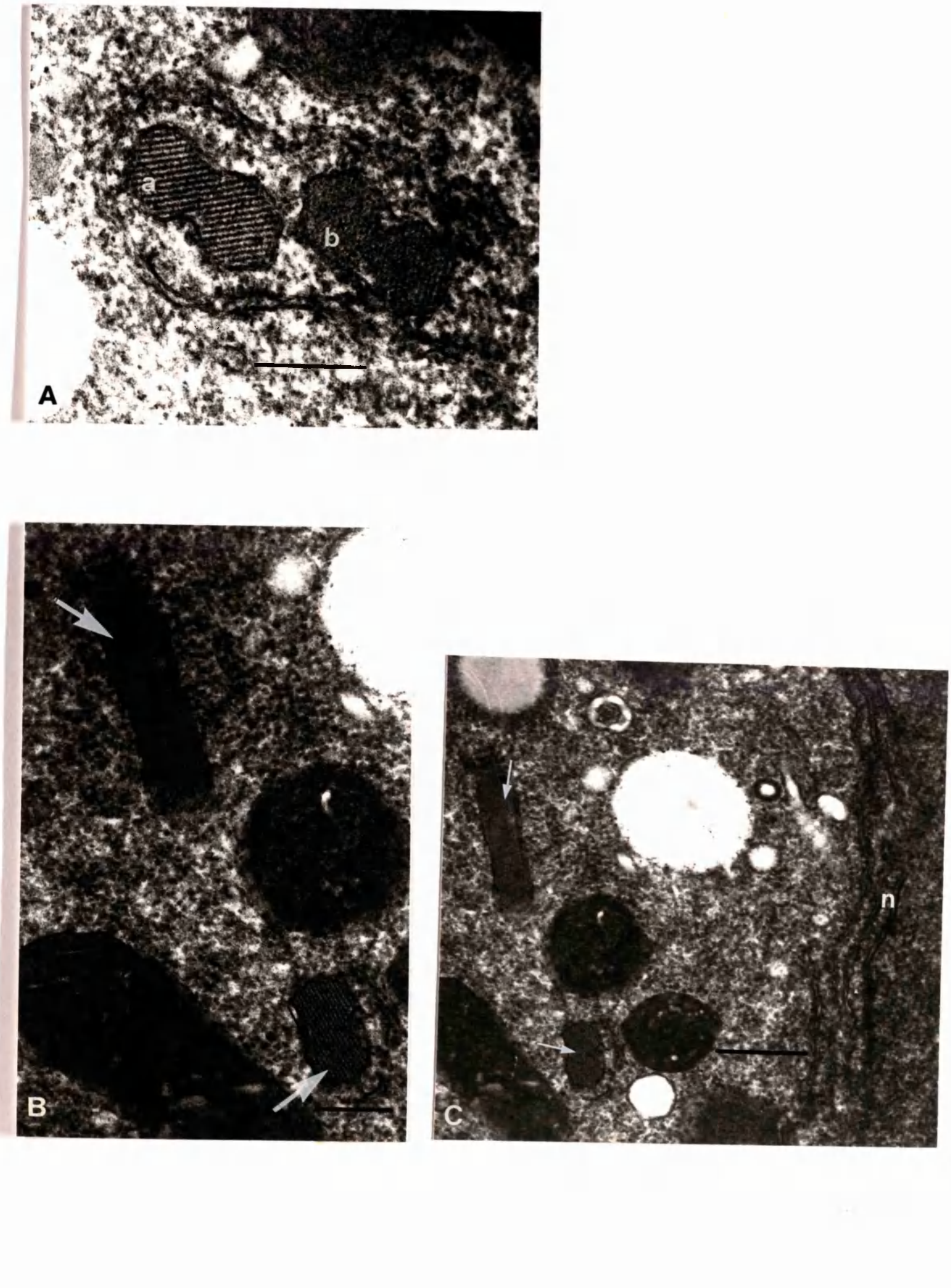
A
a
b
B
C
n

Figure 2.10. Paracrystalline extranuclear structures observed in *N. gruberi* after colchicine-treatment. An elongate form of the paracrystals (big arrow) appeared to be composed of densely packed parallel filamentous structures. Other paracrystalline cytoplasmic inclusions (arrows) which are much smaller in size and do not have a definite shape were seen nearby. Note membrane-like structures are scattered in the cytoplasm especially surrounding.the filamentous paracrystalline inclusion. Scale bar = 1 µm.

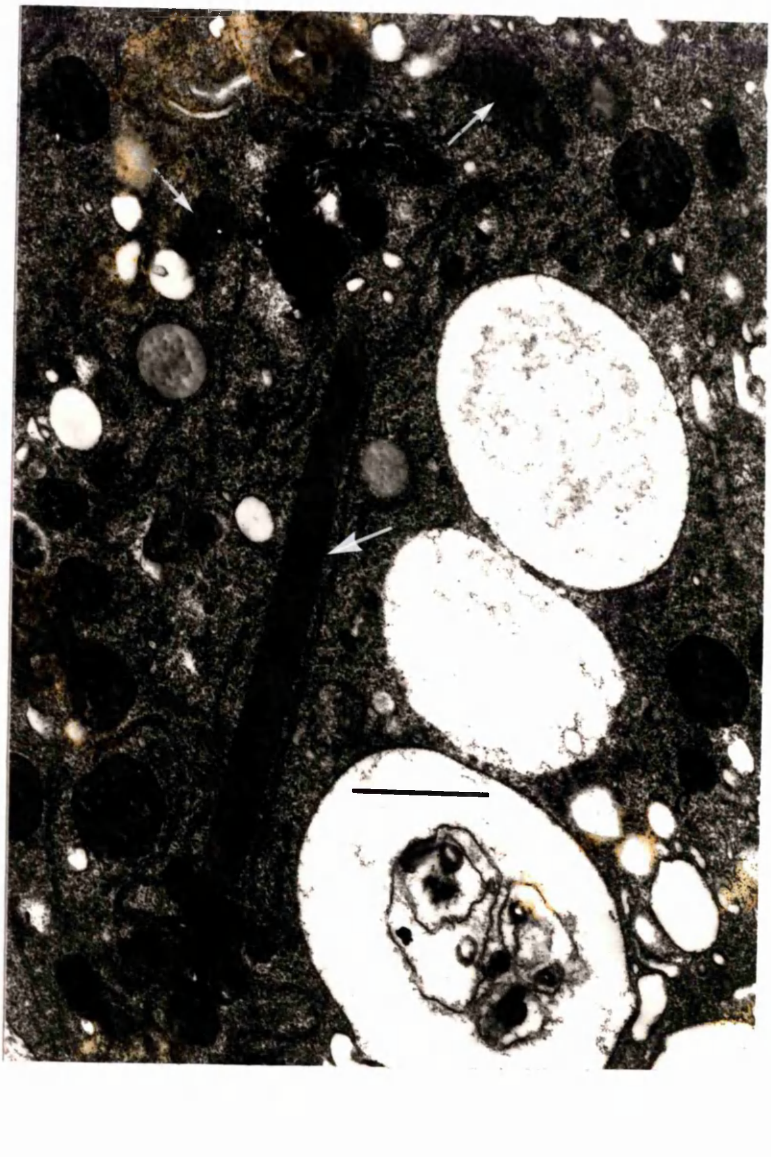

2.4. DISCUSSION

2.4.1. *Population doubling time of Naegleria gruberi grown in Bath-Spa medium*

Various liquid media have been used to grow *Naegleria gruberi* axenically either with killed-bacteria (Schuster, 1961) or without bacteria (Balamuth, 1964; Schuster and Svihla, 1968; Cerva, 1969; Fulton, 1970). The population doubling time (PDT) of log-phase growth of the amoeba in different kinds of media varies between 9 and 12 h. *Naegleria gruberi*, grown in a medium containing 0.5% (w/v) yeast extract, 0.5% (w/v) peptone, 1.0% (w/v) liver concentrate and bacteria *Aerobacter aerogenes* killed by 1 min exposure to 100°C was found to have a doubling time of ~9.4 h (Schuster, 1961). In a medium similar to Schuster's, except that *Aerobacter* was replaced by serum, the doubling time of *Naegleria gruberi* (grown on shaker) was between 6 and 12 h (Balamuth, 1964). In medium containing 0.4% (w/v) powdered skimmed milk, 0.2% (w/v) yeast extract, $MgCl_2$ in Tris buffer and autoclaved *Aerobacter*, and grown in a flask which has been placed in a water bath shaker at 25°C, the doubling time of *N. gruberi* NB-1 was between 4 and 7 h (Fulton, 1970). In this study, *N. gruberi* CCAP strain 1518/1A, the original clone of the strain NB-1 which Fulton used in most of his work, took ~7 to 8 h to double its population size in both culture vessels (Falcon flask or flat-sided tubes). This observation was from non-agitated cultures and grown at 32°C in Bath-Spa medium. The amoeba was grown in this medium after gradual adaptation to grow in saline solution with heat-killed *E. coli* after previously being grown on agar with live bacteria. The composition of Bath-Spa medium is similar to Balamuth's medium except that it contains both serum and haemin. The population doubling time of *N. gruberi* obtained in the present study is therefore within the range of the PDT values reported previously although the amoeba was grown in a different medium and the cultures were not agitated.

Maximal growth profiles of *N. gruberi* at optimum temperature vary between strains according to O'Dell and Brent (1974). Maximal growth of strains PD (from a sewer drainage ditch) and S (an established laboratory line), both grown in TYG medium containing 0.5% (w/v) trypticase, 0.5% (w/v) yeast extract and 1.0% (w/v) glucose with autoclaved *Escherichia coli* added was found to occur at 30°C, whereas maximal growth of strain TS (isolated from a Vero cell culture) took place at 37°C (O'Dell and Stevens, 1973; O'Dell and Brent, 1974). Amoebae which have been sampled from different portions of a growth curve are different in morphology, cell inclusions and volume (Fulton, 1970). In log growth phase, *N. gruberi* consumes 80 ng O_2 min^{-1} mg^{-1} cell protein. At stationary phase, its respiration rate decreases 4-fold and further increase in respiratory rate does not occur despite fresh oxygen supplies (Weik and John, 1977), so knowing the growth phase of the amoeba is important when harvesting the cells for any type of study. In the present study, *N. gruberi* was harvested during log-phase growth (between 48 h to 60 h after inoculation) to study its cell division and most stages of nuclear division have been obtained. For treatment with colchicine to obtain synchronously dividing cells for detection of cytoplasmic microtubules (a centrosome and MTOC), the amoebae were harvested 42 h after inoculation. From the growth curve, this time falls within the actively growing phase of the cell population. The cells were left for 18 h (which was about twice the population doubling time) in the drug-containing saline solution to ensure that all cells had stopped dividing before this solution was replaced with fresh medium.

2.4.2. *Nuclear division in Naegleria gruberi*

Results obtained from both fluorescence and transmission electron microscopy in the present study, give almost a complete picture of mitosis in *Naegleria gruberi*.

Observation on each features involved in this process will be discussed under its relevent heading in the following sections. Unlike previous reports, cell division in *N. gruberi* reported here is from the amoebae which were grown axenically in particle-free liquid medium.

The behaviour of nucleolar materials in various stages of the nuclear division

In electron micrographs, various stages of nuclear division in *N. gruberi* could be recognised. Nucleolar material appears to be persistent although its structure changes (from compact, electron dense to patchy in appearance and then becoming compact again) throughout nuclear division. The significance of the nucleolus stage with a lacuna in *Naegleria* observed in this study, is not clear. The lacuna might indicate a certain event in nucleolar division. In root cells of *Vicia faba*, the lacuna stage of nucleolus has been identified as a prophase nucleus (Lafontaine and Chouinard, 1963). Since chromosomal elements could not be distinguished from nucleolar material in previous electron microscopy studies, the term 'polar masses' which was first used by Rafalko (1947) to describe the nucleolar division in *N. gruberi* under the light microscopy, is used for the dense material which divides into two and moves towards the opposite poles during metaphase-anaphase. When the anaphase nucleus was stained with DAPI (Figure 2.4B), it was found that the nucleolar materials at both nuclear poles (at this stage the nucleus is at anaphase A and the nucleolar materials corresponds to polar masses described above) contained DNA, suggesting that polar masses contain chromosomes. In interphase cells, DNA (stained by DAPI) was found located at the periphery of the nucleus. In these cells, the nucleolus was not stained by DAPI, indicating that it does not contain DNA. This observation is in agreement with Rafalko's (1947) and Singh's (1952) observations on Feulgen-stained cells of *Naegleria* suggesting that chromosomal material and the nucleolus are not the same structures but both are nuclear division of *N. gruberi*.

The DAPI-stained material which was observed connecting the daughter nuclei in Figure 2.5A (this structure could be the interzonal body described by Rafalko (1947)?) contains DNA or chromosomal material. Cytokinesis in *N. gruberi* in this figure seems to fit description of amitosis in *Acanthamoeba castellanii* (Band and Mohrlok, 1973; Byers *et al.*, 1980; Gicquaud and Tremblay, 1991) in which event the nucleus divides into daughter cells in the absence of condensation and regular segregation of chromosomes. This kind of cell division however, was obtained in starved *Acanthamoeba*. It is not known if the Figure 2.5A depicts a real amitosis in *N. gruberi*, and if it does, this observation indicates that amitosis could occur regularly in any amoeba although its significance in amoeba reproduction is not clear.

Do chromosomes exist as individually-discernible structures?

Little is known about the morphology of chromosomes of *Naegleria gruberi*. Their size is minute ranging from 400 kb to over 2 Mb as determined by pulse field gel electrophoresis (Clark, 1990) and they are not easily seen by light microscopy after any staining procedure. Rafalko (1947), however, depicted individual thread-like chromosomes in his drawing of Feulgen-stained amoebae. The observation of the chromosomes by both light and electron microscopy in the present study is difficult since at all stages of nuclear division, the chromosomes are compact in appearance, and nucleolar material and chromosomes are often difficult to distinguish at the ultrastructural level. In electron micrographs, at metaphase-anaphase, the fragmentation of the nucleolus (lightly stained material with no definite structure) has been observed in the middle of the nucleus (Fulton, 1970; Schuster, 1975b). In this study however, the structures depicted in Figure 2.3D have a definite rounded shape and they were observed only at metaphase-anaphase stage of the nucleus. These structures could be chromosomes since similar structures (electron-dense material) have been observed in the giant amoeba *Pelomyxa carolinensis* and *Entamoeba histolytica* nuclei in metaphase and have been termed chromosomes by Roth and Daniels (1962) and by Orozco *et al.* (1988), respectively. In *E. histolytica*, these small structures could be chromosomes as DNA condensation takes place in the karysome (nucleolus) of the amoeba (Albach *et al.*, 1980 and reviewed in Orozco *et al.*, 1988). Although *E. histolytica* is genetically distant from *N. gruberi* according to small subunit rRNA sequence analysis (Clark, 1990), the structures which were observed by fluorescence microsopy in the nucleus of *N. gruberi* in the present study (Figure 2.4) seem to correlate with the structures observed by electron microscopy by being round in appearance. Furthermore when these structures (what might be chromosomes/ chromatin) were observed in the electron micrograph of the nucleus, the nucleolar material was not detected in the same nucleus.

Despite of being small and difficult to visualise, there are many estimates of the number of chromosomes in *N. gruberi* and these range from 3 to 23 (Fulton, 1970; De Jonckheere, 1989; Clark *et al.*, 1990). If the electron-dense materials in Figure 2.3D are considered to be chromosomes, their number is at least 42 and if *N. gruberi* is a diploid organism as suggested by isoenzyme studies (Cariou and Pernin, 1987), the actual number of chromosomes in this amoeba is at least 21. The number 42 can not be the actual number of chromosomes in *N. gruberi* since in Figure 2.3D, the nucleus was at late metaphase-early anaphase stage suggesting that at this stage, the chromosomes were half-way through to the opposite poles; the chromosomes were then observed in one nucleus. This observation is in agreement with karyotype analysis by contour-clamped homogeneous electric field and transverse alternating-field electrophoresis in *Naegleria* spp which gives the chromosomal number between 15 to 23 (De Jonckheere, 1989). From a molecular karyotype construction using pulsed field gel electrophoresis for two strains of *N.*

gruberi, the estimate number of chromosomes in each strain is about 23 (Clark *et al.*, 1990).

Are MTs visible in the dividing nucleus of Naegleria gruberi?

Throughout division, the nuclear envelope is intact, its profile as observed in transmission electron micrographs changes from oval to elongated form and corresponds to the length of its mitotic spindle. The mitotic spindle is visible in the nucleoplasm during nuclear division. Two types of mitotic spindle microtubules profiles were observed. Long microtubule profiles were observed in late metaphase-anaphase (Figures 2.3G, J to L) suggesting their responsibility for nuclear elongation (anaphase B). These long microtubules could be the result of the sliding apart of interdigitating microtubules which overlap in the midzone of the nucleus as in higher Eukaryotic mitosis (Hogan and Cande, 1990). The short microtubules which were always observed associated with the electron dense nucleolar material in the present study, could be the microtubules which are involved in assisting the chromosomes to the spindle poles. The progressive shortening and lengthening of the intranuclear microtubules during nuclear division in higher Eukaryotic cells have been suggested through the activity of an actomyosin system as in muscle contraction, which generates a motile force for chromosome movement, or by the action of the microtubules themselves by repeatedly losing and adding their subunits (Mitchison, 1988).

In most reports on mitosis in *Naegleria*, spindle microtubules were visualised at the metaphase-anaphase stage (Schuster, 1963 and 1975b; Fulton, 1970). During metaphase of higher Eukaryotes, spindle microtubules (which are known to have a very dynamic structure) are at steady state and can stay in that condition for prolonged periods (Mitchison and Sawin, 1990) and this explains why they are observed most frequently at this stage.

Are kinetochores and their related chromosomal fibres discernible?

The uncertainty of chromosomal identity in previous studies mostly due to not being able to detect any microtubule association with the chromosomal material (kinetochore microtubules, kMTs) during division. In this study, the microtubules which were observed penetrating the nucleolar material (probably chromosomes) in the midlle of the nucleus in Figure 2.3D, could be identified as kMTs. These microtubules are very different in arrangement in relation to the nuclear material as compared with the position of microtubules in Figure 2.3E, suggesting these two forms of microtubules could be also different in their function. When stained with anti-α-tubulin antibody, the very elongated spindle microtubules originating from the poles were clearly seen connecting to the chromosomal material at metaphase plate (Figure 2.7C). Whether these microtubules are polar MTs since they appears to originate from the nuclear poles, or are kMTs which might have been captured (c.f. Eutenuer and McIntosh, 1981 for description on structural polarity of kMTs in PtK_1 cells) by chromosomal kinetochores upon their initiation at spindle poles or the combination of both MTs, could not clearly be distinguished. The nuclear material in this figure is also stained positive by anti-α-tubulin, indicating that some of MTs are associated with the nuclear material at this stage of nuclear division. This association might be a proof of the involvement of MTs in transporting the nuclear material/chromosomes/chromatin during nuclear division in *N. gruberi* in this study.

Are MTOCs discernible at the poles of the spindle, either inside or outside of the persistent nuclear envelope?

In most cells, a centrosome or centrioles always appear in the cytoplasm before nuclear division. This organelle is thought responsible for the assembly of spindle microtubules in the nucleus prior to division. In the present work, such an organelle has been observed in the cytoplasm of *Naegleria* before nuclear division. Fluorescent tubulin staining has provided substantial information about the existence and pathways of centrosomal division in the cytoplasm of dividing *Naegleria.* A centrosome which later forms two MTOCs was seen in the cytoplasm prior to nuclear division although previous reports (Fulton and Dingle, 1971; Schuster, 1963; 1975b) denied that this organelle was present in *Naegleria.* After centrosome division, the two MTOCs (with their microtubule arrays) appear to move towards the opposite poles of dividing nucleus (refer to series of Figures 2.6 and 2.7). When the nucleus is at metaphase, the spindle microtubules associated with the chromosomal material and connected to the opposite poles can be observed clearly. At this stage, no more cytoplasmic MTs were observed in the cytoplasm even at the nuclear poles. Whether the cytoplasmic MTs became incorporated into the mitotic spindle or they depolymerised at the nuclear poles needs further investigation. In PtK$_1$ cells, at this stage, the cytoplasmic microtubules breakdown and the fragments of the microtubules are detected in the cytoplasm (Vandre and Borisy, 1989). In electron micrograph of the nucleus which might be equivalent to metaphase-anaphase of Figure 2.6F,G and Figure 2.7C, however, a bundle of cytoplasmic microtubules have been observed at both nuclear poles (Figure 2.3D) indicating the possiblity of both cytoplasmic and mitotic spindle involvement in assisting the movement of chromosomes to the opposite poles.

The presence of the MTOC during nuclear division in *N. gruberi* is to indicate its involvement in initiating the spindle assembly and forming a bipolar spindle. In *Naegleria,* the association between a MTOC and the intranuclear microtubules is not clear since the nuclear envelope remains intact during division. Some of the molecular components of the MTOC in *Naegleria* perhaps induce the spindle assembly indirectly through some enzymatic actions (c.f. Kalt and Schliwa, 1993 for a review on the molecular components of the centrosome).

Effect of colchicine on cell division in Naegleria gruberi

Substoichiometric binding of colchicine to tubulin has been found to prevent further formation or growth of microtubules (Olmsted and Borisy, 1973; Sternlicht and Ringel, 1979) and hence any activity which involve MTs, including mitosis. Different types of cells behave differently when treated with colchicine and related drugs. In some cells, these drugs block cell division only when the drugs are applied before the nuclear envelope breaks down, and not at other stages in division (review in Rieder and Palazzo, 1992). In *N. gruberi* it is not known exactly at what stage of nuclear division (despite the nuclear envelope remaining intact), the mitotic block by colchicine occurs. How the actual mechanism of colchicine poisoning is related to the microtubular polar structures in *Naegleria* cells remains speculative. In this study, the number of *Naegleria* cells apparently did not increase indicating the cells stopped dividing during colchicine-treatment; the cells resume division when they are washed free of the drug.

In this study, the *Naegleria* cells were observed to undergo division ~1 to 2 h after the removal of colchicine from the culture medium, indicating that the colchicine-tubulin bond is not permanent and can be distrupted simply by removing the drug from the medium. When these cells were stained with anti α-tubulin-FITC-DAPI, a centrosome-like structure complete with fluorescing astral rays was detected in the cell cytoplasm. This centrosome was apparently formed from two MTOCs which later appeared to move to opposite nuclear poles (in the fluorescence micrographs). To confirm the existence of a centrosome or MTOC in dividing *Naegleria* cells, cells taken from colchicine-treated populations were processed for transmission electron microscopy. Surprisingly, no detectable normal microtubular structures were observed in the cytoplasm close to the nucleus. What was observed in *Naegleria* were some cytoplasmic inclusions resembling paracrystals of tubulin (Bensch and Malawista, 1969; Schechter *et al*, 1976). One of the electron micrographs depicted a pair of these structures close to the nucleus (Figure 2.9C).

The paracrystalline inclusions observed in colchicine and vinblastin-treated mammalian cells have been found to consist mainly of tubulin. This conclusion is based on the structural resemblance between the tubular subunits paracrystals and normal microtubules (Bensch and Malawista, 1969; Starling, 1976). Colchicine-binding protein was considered to be microtubule protein since this protein is a dimer (M_r ~ 115 kDa) and can be separated by sodium dodecyl sulphate (SDS) acrylamide gel electrophoresis into two subunits; each has M_r of ~55 kDa which correspond to M_r of α- and β-tubulins (Bryan and Wilson, 1971). Furthermore, colchicine-binding activity has the same properties of the normal microtubules derived from the fact that purified tubulin-colchicine complex undergoes *in vitro* polymerisation under the same conditions that promote the assembly of MT from purified tubulin (Andreu and Timasheff, 1982). Both the mitotic apparatus and vinblastin-induced microtubule paracystals in mouse L cells have been observed by fluorescence microscopy using the same anti-tubulin staining indicating that these structures have the same antigens (Nagayama and Dales, 1970). Tubulins from different classes of microtubules share similar antigenic determinants although they probably are not identical molecules (Fulton *et al.*, 1971).

The periodicity between parallel lines of the inclusions in the present study measured between 10 and 13 nm, which is about half the measured diameter of a spindle microtubule measured in *N. gruberi* (~25 nm). Some of the *Naegleria* paracrystals, as shown in Figure 2.9 however, were surrounded by a double-membrane envelope, which has not been observed surrounding the colchicine and vinblastin-induced tubulin paracrystals in previous studies. The cytoplasmic inclusions observed in *N. gruberi* after colchicine treatment could be composed of tubulins but there is no substantial evidence from this study to equate these structures with microtubular structures or MTOCs as have been observed by fluorescent microscopy in *N. gruberi* cells.

The binding of colchicine or vinblastin to tubulins is reversible so the paracrystals dissappear rapidly when placed in medium not containing these drugs (Nagayama and Dales, 1970). The paracrystal structures which were observed only in a few cells of *Naegleria* by the electron microscopy after colchicine-treatment could be the result of some cells which were not being properly washed with fresh medium, leaving the paracrystals intact when the cells were being fixed and processed for transmission electron microscopy. The ability to observe the cytoplasmic paracrystal structures in the present study suggests that they are resistant to both physical and chemical treatments while processing for transmission electron microscopy.

2.4.3. *General problems and conclusions*

In the present study, with the aid of tubulin specific antibodies, tubulin-containing structures (both cytoplasmic and intranuclear microtubules) could be observed by fluorescence microscopy. Although intranuclear microtubules could also be detected by transmission electron microscopy, what appeared to be cytoplasmic microtubules could not readily be detected except in Figure 2.3D. There are a number of reasons why results obtained by electron microscopy sometimes do not agree with those obtained by light microscopy. For study of the cytoskeleton immunofluorescence offers unique advantages over transmission electron microscopy of sections since whole cells rather than sections can be observed and the corresponding antigen which specifically binds to anti-tubulin antibody is easily detected. The diameter of a microtubule is ~25 nm and therefore impossible to resolve by conventional light microscopy, which has a limiting resolution of 200 nm. Visualisation of the microtubule becomes possible by immunofluorescence however, since it is coated by tubulin-specific antibody and by the fluorescein-tagged secondary antibody which presumably increases its diameter to 100 nm or above (Weber *et al.*, 1975a; 1975b). Observation by transmission electron microscopy of thin sections on the other hand, is restricted by small sample size, and serial section analysis is essential to gain information on the three dimensional distribution of the tubulin-containing structures. Furthermore, the plane of section is critical to ease of interpretation of observations (Schuster, 1975b).

During sample preparation for transmission electron microscopy subjecting cells to both physical and chemical treatments might be critical for some organelles of interest. Cytoplamic microtubules are very sensitive to low temperature, high hydrostatic pressure and also to some chemicals (review in Dustin, 1984), and they are readily depolymerised or destroyed by these conditions. Furthermore, if the time taken for microtubule initiation by a centrosome is very short due to probable *de novo* formation of the centrosome during nuclear division in *N. gruberi* as the formation of flagellar kinetosomes (basal bodies) during *Naegleria* differentiation (Fulton and Dingle, 1971), the cells should be processed at a precise time and sample preparation must be completed within a short period in order not to lose the microtubules during processing. These conditions could be major problems in this study and in previous electron microscopy studies of nuclear division in *N. gruberi*. In this study however, the cytoplasmic microtubules which are involved in mitosis in *N. gruberi*, were vaguely observed only in one electron micrograph (Figure 2.3D).

In order to obtain sufficient results either from electron microscopy or light microscopy to reconstruct a picture of the dividing cell, several cells at each stage of division are required. The various stages of cell division can be readily obtained if synchronous division can be induced in cell populations. Techniques by Band and Mohrlok (1973) and Orozco *et al.* (1988) which employ a non-lethal dose of colchicine for inducing synchronous division in *Acanthamoeba castellanii* and *Entamoeba histolytica*, respectively, prove also to work for *N. gruberi*.

Results obtained in this study provide additional information to current understanding of mitosis in *N. gruberi*. It is concluded in the present study that mitosis in *N. gruberi* is not quite so unusual as previously thought; persistence of the nuclear envelope during division which has been termed closed mitosis by Raikov (1982) is common in protists and merely exhibits a variety of nuclear division in eukaryotes. Chromatin structures which are at the nuclear periphery in interphase cells appear to move to the middle of nucleus and then condense during division; such behaviour of chromosomes is common in conventional mitosis (Fulton, 1970). The thread-like chromosomes of *N. gruberi* as reported by Rafalko (1947) were not observed in this study; what was observed was the rounded form of possible chromosomal structures, both under transmission and fluorescence microscopy. Polar masses are probably the combination of both the nucleolar and chromosomal materials since they stain by DAPI. The nucleolus alone was not stained by DAPI and at most stages of nuclear division (due to its persistence throughout nuclear division) cannot be differentiated from chromosomes/chromatin structures unless when (perhaps) chromosomes condense as in Figure 2.3D or when stained by DAPI. The relationship between nucleolar material and chromatin or chromosomes is still not clear in *N. gruberi*. Cytoplasmic and intranuclear microtubules as in other eukaryotic cells, are present and involved during nuclear division in *N. gruberi*. And also, kinetochore microtubules which are observed to be associated with chromosome-like structures are also evident in this amoeba.

2.5. SUMMARY

1 The population doubling time (PDT) of *Naegleria gruberi* strain CCAP 1518/1A, grown in Bath-Spa medium at 32°C, non-agitated either in Falcon culture flasks or flat-sided tubes is ~8 h.

2. During nuclear division, the nuclear envelope remains intact but its shape changes from round (at interphase and early prophase) to elongated form (at anaphase and telophase). In electron micrographs, the nucleolus appears to be persistent during nuclear divison but its structure changes (from compact, electron dense to patchy in appearance and than compact again) during the course of nuclear division. During most of stages of the nuclear division, chromosomal elements could not be distinguished with certainty from nucleolar material.

3. Intranuclear microtubules have been detected in most stages of nuclear division. Their profile length seems to vary and corresponds to the stage of nuclear division. Microtubules are clearly seen when they are parallel to the axis of the nucleus. Elongated microtubules have been suggested by others as well as myself, to be responsible for the elongation of the nucleus in anaphase-telophase. Short microtubules are possibly important in assisting the chromosome movement to the poles. Both microtubules may originate from opposite poles and kinetochore microtubules are particularly evident when the nucleus is at metaphase.

4. Both anaphase A (the moving apart of nuclear material to the daughter cells) and anaphase B (the elongation of microtubules in order to move the poles apart) could be observed clearly by both fluorescent and transmission electron microscopy in mitosis in *Naegleria gruberi*.

5. A centrosome which later forms two MTOCs is present in the cytoplasm of *Naegleria* during nuclear division and this contradicts the previous idea that this organelle does not exist in *Naegleria*.

6. Colchicine has proved to be a useful tool to study the initiation of microtubule assembly in cells. During colchicine treatment, *Naegleria* cells stopped dividing but resumed division almost synchronuosly ~1 to 2 h after the drug was removed from the cell medium. Staining of such cells by α-tubulin antibody, then made the detection of microtubule structures in the cells possible.

Chapter 3

Proteinases in Naegleria spp.

Chapter 3

PROTEINASES IN *NAEGLERIA* SPP

3.1. INTRODUCTION

Proteinases play an important role in general protein turnover in all cells including protozoa. Besides their general intracellular roles, proteinases have been shown to play a part in host-parasite relationships (North *et al.*, 1990a; North, 1992). In *Naegleria* spp which consist of both pathogenic and non-pathogenic free-living forms, the presence of proteinases has not been reported so the significance of these enzymes in the amoebae is not known.

Naegleria spp can exist in three states; as amoebae (trophozoites) which feed and divide; as flagellates which swim for hours but do not feed or divide; and as cysts, resting forms of the organism. These three stages of *Naegleria* often coexist in cultures. In *Naegleria fowleri*, the trophozoite is known to be infective since infection of experimental animals has been achieved with this form alone (Martinez *et al.*, 1971; Maitra *et al.*, 1971). No information is available on whether cysts and flagellates are equally infective. Although cysts of protozoa are widely regarded as resting stages, they may be metabolically active and infective as has been shown for *Giardia* cysts (Jarroll, 1991). The cysts of this protozoan possess enzymes which enable them to continue to catabolise endogenous glycogen reserves. In *Naegleria,* cyst proteinases might be present to aid survival. *In vitro,* enflagellation in *Naegleria* can be stimulated by suspending and agitating the cells in non-nutrient buffer (Fulton, 1970). Although the flagellate stage is important as a means of dispersal, no studies have been undertaken to detect the presence of any enzyme activity in this form of *Naegleria*.

In the natural environment, *Naegleria* phagocytoses bacteria or other particulate matter as a food source. In the laboratory, *Naegleria* has been cultivated on agar with bacteria or grown axenically either in media with killed-bacteria or in particulate-free media (Fulton, 1970). In particulate-free medium, the amoeba takes up nutrients by pinocytosis. The change in diet induced by growth conditions may alter the amoeba's metabolic processes. In intracellular digestion, the ingested 'food' is hydrolysed by digestive enzymes in food vacuoles (secondary lysosomes). Peptidases are amongst the digestive enzymes found in lysosomes (review in Holztman, 1989). Some enzymes are secreted outside the cell to digest the food extracellularly before it is taken into the cell in dissolved form (review in Holztman, 1989). This manner of extracellular digestion seems to be adopted by some parasitic protozoa during invasion in host tissues. *Entamoeba histolytica* for example, secretes a 56-kDa cysteine proteinase which correlates well with the ability of this amoeba to destroy host tissues (Reed *et al.*, 1989). Also the pathogenic free-living amoeba, *Naegleria fowleri* secretes cytolytic enzymes such as phospholipase A into the tissue culture medium before destroying the cells (Curson *et al.*, 1978; Marciano-Cabral and Fulford, 1986). The accumulation of secreted hydrolytic enzymes such as phospholipase A and sphingomyelinase during the log-phase growth of *N. fowleri* suggests that the actively growing amoebae might correspond to invasive stages of the amoeba (Hysmith and Franson, 1982).

The presence of some isoenzymes (alloenzymes) of glucose phosphate isomerase, phosphoglucomutase, aminotransferases, acid phosphatase and superoxide dismutase in *Naegleria* spp has been used to distinguish species, strains, and pathogenic and non-pathogenic forms (Nerad and Dagget, 1979; De Jonckheere, 1982; Kilvington *et al.*, 1984; Pernin *et al.*, 1985; Moss *et al.*, 1988). The proteinases of *Naegleria* spp could be used for a similar purpose.

The main aim of this study was to detect the presence of proteinases in the free-living amoeba, *Naegleria gruberi* strain 1518/1A. Evidence for the presence of proteinases was sought in all stages of the life cycle, in different phases of the growth curve and in amoebae grown monoxenically and axenically. Proteolytic enzymes secreted by the amoebae were also looked for. These enzymes were characterised on the basis of their sensitivity to specific inhibitors, apparent molecular weight, substrate preferences and activity pH optimum. Another aim was to carry-out a comparative study of proteinase zymograms from different strains of *Naegleria gruberi* (CCAP strains 1518/1G, 1518/7 and 1518/1A) and pathogenic *Naegleria fowleri* NF3 in order to obtain a better view of the significance of the proteinases present in *Naegleria* spp.

3.2. MATERIALS AND METHODS

3.2.1. *Source of samples*

Strains of Naegleria* spp *used

Naegleria gruberi CCAP strains 1518/1A, 1518/7 and 1518/1G were used in this study as examples of non-pathogenic strains of *Naegleria* spp. For pathogenic species, *Naegleria fowleri* strain NF3 obtained from Dr Huw Smith, Department of Parasitology, Stobhill Hospital, Glasgow was used. The history of *Naegleria* spp isolates used in this study is provided in Table 3.1. *N. gruberi* strain 1518/1A was used most in this study and also used as a control sample when comparing proteinase patterns from other strains and from pathogenic *N. fowleri*.

Table 3.1. The history of *Naegleria* spp isolates used in this study

**Strains*	*Isolator (year)*	*Origin*
Naegleria gruberi (Schardinger) CCAP 1518/1A[1]	Pringsheim (pre 1950)	unknown
CCAP 1518/1G[2]	Page (1965)	freshwater-public lake Tuskegee, Alabama, USA.
CCAP 1518/7[3]	Page (1965)	freshwater pond, Madison, Wisconsin, USA.
Naegleria fowleri Carter NF3	Kilvington (1983)	thermal spa water, Bath, Avon, England.

Notes:

*The strains are also kept at The American Type Of Culture Collection (ATCC) with different reference number; [1] ATCC 30874, [2] ATCC 30877, this strain was originally strain 48 of Page (1965), [3] originally strain 49 of Page (1965).

Growth conditions

Bath-Spa medium (BSM, see 2.2.3) was used to grow *Naegleria gruberi* CCAP strains 1518/1A, 1518/7 and 1518/1G axenically at 32°C. Upon receipt from The Culture Centre of Algae and Protozoa, strains 1518/7 and 1518/1G were grown axenically in Modified Chang's Medium (MCM, see the following section) at 20°C. The strains were then adapted to grow in MCM at the higher temperature of 25°C. These amoebae were also adapted gradually to grow in BSM at 25°C and 32°C. These strains however, were not able to adapt to growth in MCM at 32°C. Modified Chang's Medium was originally used to grow pathogenic *Naegleria fowleri* at 37°C. De Jonckheere (1977) used growth in Chang's medium at 37°C to distinguish between pathogenic and non-pathogenic strains of *Naegleria fowleri*. Only pathogenic strains grew under these conditions. In this study, however, the MCM used for culturing *N. gruberi* did not support growth of *N. fowleri* strain NF3. This medium was then modified as stated below. All amoebae used in this study, were grown in flat-sided tubes (16 cm x 2.5 cm) containing 2.5 ml of medium, at appropriate temperature as indicated elsewhere.

Modified Chang's Medium

Originally this medium was devised by Chang (1974) and described by De Jonckheere (1977) as Serum-Casein-Glucose-Yeast Extract Medium. This medium was made-up as follows: Casein digest (BBL), 10.0 g; Na_2HPO_4. $7H_2O$, 0.8 g; Yeast extract (DIFCO), 5.0 g; and glucose, 2.5 g, dissolved in 1000 ml distilled water. The pH the of medium was adjusted to 6.9 with 1 N NaOH. The medium was autoclaved at 12 psi. for 15 min. The modified medium has 2.5 g liver digest (OXOID) added to the original recipe (Mr Simon Kilvington, Public Health Laboratory, Royal United Hospital, Bath, UK., personal communication). Before use, heat-inactivated foetal calf serum (GIBCO) was added to the autoclaved medium to a final concentration of 10% (v/v). Penicillin (1000 units) and streptomycin (1000 units) were added per 100 ml medium. The complete medium was stored at 4°C.

The modified medium used to grow *N. fowleri* NF3 (Dr Andrew Campbell, Department of Bacteriology, Stobhill Hospital, Glasgow, personal communication) was as follows: Before use, 1.0 ml of 10% (w/v) liver digest in distilled water (PANMEDE), 5.0 ml of heat-inactivated foetal calf serum (GIBCO), penicillin (200 units) and streptomycin (200 units) were aseptically added to 95 ml of the original Chang's medium.

Trophozoite form of amoeba

The cell pellets of *Naegleria* were prepared as follows; cells were harvested in log-phase growth (which contained mostly healthy trophozoites) at an approximate density of 1-2 x 10^6 cells ml^{-1}. The cells were then pelleted by centrifugation (500 *g*, 10 min) and washed twice in phosphate buffered saline (PBS) (9.5 g NaCl, 3.7 g K_2HPO_4, 1.1 g KH_2PO_4, 1000 ml distilled water, set at pH 7.4 with 0.1 M NaOH). The pellets were kept at -70°C until required.

Only the trophozoite form of the amoebae was used to detect the presence of proteinases in *N. gruberi* CCAP strains 1518/7, 1518/1G and *N. fowleri* NF3. Proteinases were looked for not only in trophozoites but also in flagellates and cysts of *N. gruberi* CCAP strain 1518/1A.

Flagellate form of amoebae

The transformation of *Naegleria gruberi* amoebae to flagellates was induced following the method of Fulton and Gruerrini (1969) with modifications. In late log-phase cultures of amoebae, Bath-Spa medium was replaced by modified Neff's amoeba solution (Page's amoeba saline, PAS) and the culture tubes were placed on a shaker (at 65 revolutions min^{-1}) at 32°C. After 7 h, most cells (~90%) had transformed into flagellates. Flagellates were separated from trophozoites using the bead column technique of Preston and O'Dell (1973) with modifications. The glass bead column was assembled as shown in Figure 3.1. Glass beads (diameter 2 mm) were placed in a column made of a 10 ml plastic syringe (without the piston). A 5 ml syringe was assembled on top of this column, to act as a reservoir. To provide an airtight column, layers of parafilm were used to seal between the two syringes. The flow rate of the fluid through the column was controlled by a burette clip which had been fixed to a silicone rubber tubing, connected to the column, through a 21-gauge needle.

Before separation, the column was washed thoroughly with Page's amoeba solution. Three to four ml of cell suspension containing ~10^6 cells ml^{-1}, mostly flagellates, were layered on to the column. The fluid flow was stopped for ~15 min to let the amoebae attach to the glass surface. The flow of the fluid through the column was continued by gently pushing the piston of the reservoir. Cells were collected from the column periodically and fixed and stained with Lugol's iodine to assess the phenotype of cells. Elutions, drawn off the column, which contained mixture of trophozoites and flagellates were discarded. The flagellates collected were fixed in a centrifuge tube containing the final concentration of 0.001 M $ZnCl_2$ in Page's amoeba saline for about 30 min before centrifuging to form pellets.

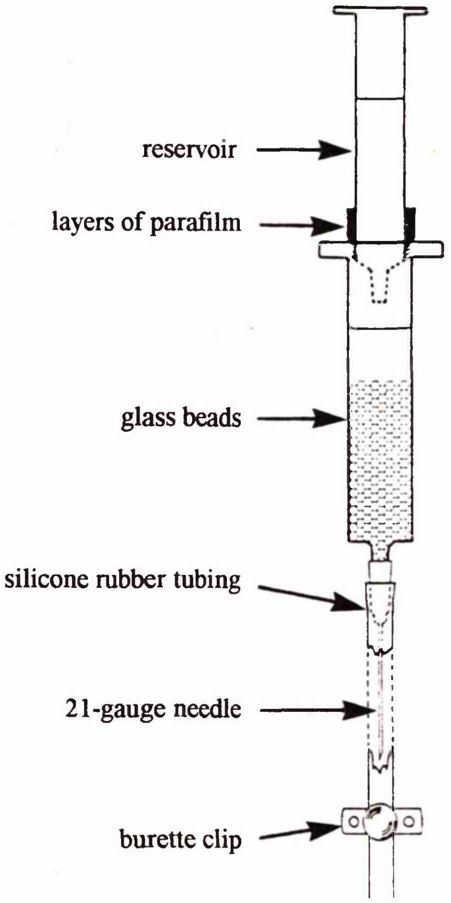
reservoir
layers of parafilm
glass beads
silicone rubber tubing
21-gauge needle
burette clip

Figure 3.1. Glass bead column used in the separation of flagellate *Naegleria* (from Preston and O'Dell, 1973)

Cyst form of amoeba

Transformation of amoebae to cysts was induced by replacing Bath spa medium with Page amoeba saline solution. The induced cultures were left for a few weeks at room temperature. All cysts formed by this technique had a double wall. In order to obtain samples which contained only cysts, non-transformed amoebae were killed by adding a few drops of Triton X-100 solution (0.25% (v/v) Triton X-100 in PBS) to the cyst containing cultures. The cyst pellets were prepared as described for trophozoites.

3.2.2. *Sample preparations for enzyme extraction*

The pellets of trophozoites were lysed in 0.5 ml of PBS containing 0.25 M sucrose and 0.25% (v/v) non-ionic detergent Triton X-100, before centrifuging for 4 min at room temperature in 1.5 ml microfuge tubes at 12000 rpm using an Eppendorf 5415 bench centrifuge. The supernatant sample was used for all proteinase analyses and is referred to as either cell lysate or soluble fraction sample in this study. In some cases, the remaining pellet was resuspended in the same volume of buffer and used for proteinase studies.

Pellets of flagellates were resuspended in PBS containing 0.25% (v/v) Triton X-100, and subjected to alternate freezing and thawing three times (in liquid nitrogen followed by plunging into a water bath at 37°C) then sonicated (at 4°C) in an ultrasonicator (Soniprep 150), with three pulses (10-s per pulse) at maximum power, before centrifugation as above. The supernatant sample was used for study. A similar method of lysis was employed for cyst pellets. Since the cyst wall is resistant to mechanical destruction, the pellets were subjected to six cycles of freezing and thawing and were subjected to six pulses of sonification at maximum power. By doing so, most cysts were ruptured as observed under the microscope.

The cyst suspensions were centrifuged as before and the supernatant samples used for analysis of proteinases samples. In separate experiments, the cysts were lysed by vortexing an equal volume of cell suspension and glass beads (2 mm in diameter). The supernatant sample removed from the beads was centrifuged at 12,000 rpm for 5 min in an Eppendorf bench centrifuge. The soluble fraction was used as cyst sample for proteinase analysis. The pellet was resuspended in 0.25% (v/v) Triton X-100 in PBS, and centrifuged in the same manner as mentioned before. The supernatant sample was also used for study.

3.2.3. *Protein content determination*

The protein content of samples was determined by the method of Sedmak and Grossberg (1977). The Coomassie brilliant blue G-250 dye was dissolved in 0.3 M perchloric acid as a 0.06% (v/v) solution and was filtered through Whatman No. 1 filter paper to remove any undissolved material. The solution gave an absorbance of 1.3 to 1.5 at 465 nm. For standard protein assay, bovine serum albumin (SIGMA) was dissolved in distilled water to cover the concentration range of 0-50 $\mu g\ ml^{-1}$. The assay consisted of 0.5 ml of G-250 dye solution and 0.5 ml of protein solution. A 1:1 mixture of distilled water and dye was used as a control. The absorbance was read both at 620 nm and 465 nm with a Philips UV/VIS scanning spectrophotometer. The ratio of absorbance at 620 nm/465 nm was plotted against protein concentration after the absorbance ratio of a 1:1 dye-water solution was subtracted from the values. This standard curve was used for determination of protein concentration in all samples.

3.2.4. *Proteinase assays*

Spectrophotometric assays

Proteinase activity was quantified by measuring the rate of hydrolysis by cell lysates of the peptidyl-*p*-nitroanilide substrate, Bz-Pro-Phe-Arg-Nan (SIGMA) in a spectrophotometer. Ten µl of Bz-Pro-Phe-Arg-Nan (1 mM) was hydrolysed at 37°C in 1000 µl of buffer supplemented with 10 µl of 0.1 M DTT. The volume of cell lysate used was 10 µl. Activity of the lysates was given in units of nmoles nitroaniline released per minute per ml of lysate calculated from the formula:

$$A = \varepsilon c l$$

where A: absorbance value, c: concentration (Molarity, M); l: length of light path in solution, ε: molar extinction coefficient of nitroaniline. The molar extinction coefficient of 4-nitroaniline was taken to be 9500 $M^{-1}cm^{-1}$ at 405 nm (Pupkis and Coombs, 1984). The specific activity of proteinases in *N. gruberi* was given in nmol nitroanilines released min^{-1} (mg protein)$^{-1}$. Other nitroanilide substrates used were Bz-Arg-Arg-Nan (1 mM) and D-Val-Ser-Arg-Nan (1 mM). All these chemicals are fine grade and available from SIGMA.

To characterise the proteinase activity present in the crude lysates, 3 µl of inhibitor was added to 10 µl of lysate and incubated at 4°C for 30 min before hydrolysis of Bz-Pro-Phe-Arg-Nan was assayed. The activity of the crude lysate in buffer without inhibitor was observed and served as control.

Electrophoretic analysis

Samples for proteinase analysis were subjected to polyacrylamide gel electrophoresis (PAGE) using the SDS discontinuous buffer system (SDS-PAGE). Substrate gelatin (Sigma Type A, from porcine skin) was copolymerised into the separating gel at a final concentration of 0.2% (w/v) (Lockwood *et al*, 1987a). The acrylamide concentration of the separating gels was 7% (v/v). Proteinase samples were mixed with an equal volume of electrophoresis sample buffer (62.5 mM Tris-HCl, pH 6.8, containing 2% (w/v) sodium dodecyl sulphate (SDS), 5% (v/v) 2-mercaptoethanol, 10% (w/v) sucrose and 0.002% (w/v) bromophenol blue) before electrophoresis in gelatin SDS-PAGE gels in a Bio-Rad mini-Protean system. Electrophoresis was carried out until resolution at a constant current of 15 mA per gel.

The resolved gels were incubated with shaking in 2.5% (v/v) Triton X-100 for 30 min at room temperature to remove SDS. The gels were rinsed briefly in distilled water before being incubated. Buffers used were, 0.1 M sodium acetate-acetic acid, pH 5.5; 0.1 M sodium phosphate, pH 5.5, 6.0, 6.5, 7.0, 7.5 and 8.0. The gels were incubated overnight in buffers either at 37°C shaking or at 32°C, without shaking. The gels were fixed and stained with Coomassie Blue dye (0.5 g Coomassie Blue R-250 dye (SIGMA), 100 ml acetic acid and 125 ml *iso*propanol made up to 1000 ml with distilled water). The gels were destained in 10% (v/v) acetic acid solution. Proteinase activity was identified by the presence of clear bands caused by gelatin hydrolysis on the gels. Bands were labelled A, B, C, etc in order of increasing mobility.

Both prestained and non-prestained individual markers were used as protein standards. For non-prestained markers (SIGMA MW-SDS-200) the proteins used were phosphorylase b from rabbit muscle, approximate molecular weight 97,400; β-galactosidase from *Echerichia coli*, molecular weight of 116,000 and myosin from rabbit muscle, apparent molecular weight of 205,000. The proteins were prepared according to the supplier's instructions (SIGMA Technical Bulletin No. MWS-877). β-galactosidase from *E. coli*, α_2-macroglobulin from human plasma (approximate molecular weight 180-kDa), fructose-6-phosphate kinase from rabbit (approximate molecular weight 84-kDa) were used as prestained markers (SIGMA). For both sets of markers, 5 µl of individual marker solution was used and loaded onto gelatin SDS-PAGE gels before electrophoresis. The markers were boiled at 100°C for 3 min before use. A standard curve of relative mobility (R_f) of the protein standards compared to the mobility of the bromophenol blue dye front on the gel was used to calculate the apparent molecular weight of the individual enzymes.

To characterise the proteinases further on gels based on their substrate specificity, fluorogenic peptidyl-amido methylcoumarin substrates such as Z-Pro-Arg-NHMe (5 mM, stock), Bz-Phe-Val-Arg-NHMec (5 mM, stock) , Z-Arg-Arg-NHMec (5 mM, stock) and H-Pro-Phe-Arg-NHMec (5 mM, stock) were used. These chemicals were obtained from Bachem, Bubendorf, Switzerland. 40 µl of fluorogenic substrates were used in 25 ml of gel incubation buffer containing 1 mM DTT. The gels were prepared as previously described but without gelatin. The volume of gelatin had been replaced by distilled water. Also, 2-mercaptoethanol was not included in the sample buffer. The gels were incubated at 37°C and checked regularly by placing the gels on a UV transilluminator until the fluorescent bands appeared. The results were recorded by taking picture using a polaroid camera fitted with grey Wratten 2A gelatin filter (SIGMA).

Inhibitor studies to characterise the enzymes

The inhibitors tested against proteinases detected by spectrophotometric analyses were antipain (reversibly inhibits trypsin-like serine and cysteine proteinases, used at concentration 50 μM), E-64 (irreversibly inhibits cysteine proteinases, used at concentration 10 μM) and APMSF (irreversibly inhibits serine proteinases, concentration used was 50 μM). Other than these inhibitors, 3,4-DCI (irreversibly inhibits serine proteinases, concentration used was 50 μM) , elastatinal (reversibly inhibits elastase-like serine proteinases, concentration used was 50 μM), pepstatin (reversibly inhibits aspartic proteinases, concentration used was 1 μM), EDTA (reversibly inhibits metallo-proteinases, concentration used was 10 mM) were used to characterise the enzymes in the gelatin-SDS-PAGE gels. The gels were incubated after electrophoresis, overnight at 37°C in incubation buffer supplemented with inhibitors. For inhibitor E-64 only, the lysates were also incubated between 20 min to 1 h at room temperature with inhibitor before electrophoresis. The concentrations of the inhibitors used followed the recomendations for commercially available protease inhibitors (Beynon and Salvesen, 1989).

3.2.5. ***Enzyme fractionation by gel filtration technique***

Separation of multiple enzymes present in *Naegleria* cell lysates (*N. gruberi* CCAP strain 1518/1A) according to their molecular weight was by gel filtration on a Pharmacia Fast Protein Liquid Chromatography (FPLC) system using a Superose 12 column (size 30 cm x 1.1 cm). The column was washed thoroughly with 0.1 M sodium phosphate buffer, pH 6.0 before loading the sample.

The supernatant sample from trophozoites' preparation (taken from log-phase population) was filtered through a 0.22 μm Millipore membrane filter. The sample of 250 μl was applied to the column and eluted at a flow rate of 0.75 ml min^{-1}. The fractions between 7.0 ml to 30.0 ml (~1.0 ml each) were collected and the activity of each fraction towards the chromogenic substrate Bz-Pro-Phe-Arg-Nan was observed in microtitre plates, reading the absorbances on a Titertek Multiscan MCC/340 microplate reader at 405 nm (Robertson and Coombs, 1990). Aliquots of fractions from 7.0 ml to 23 ml were run both on gelatin SDS-PAGE gels and on gels without gelatin but incubated in buffer containing the fluorogenic H-Pro-Phe-Arg-NHMec substrate.

3.2.6. *Detection of membrane-associated enzymes*

A pellet of trophozoites was subjected to freeze-thawed lysis as described earlier (section 3.2.2). After centrifugation in an Eppendoff bench centrifuge at 12,000 rpm for 5 min, the supernatant sample was removed and labelled S_A. The pellet was resuspended in the same amount of PBS and recentrifuged. The supernatant formed was removed and labelled S_B. The final pellet was resuspended in PBS buffer and labelled P. All samples S_A, S_B and P were run on gelatin gels to detect the proteinase activities. A fraction of sample P was resuspended in 0.25% (v/v) Triton X-100 before running in the gelatin SDS-PAGE gels to ensure the release of enzymes from the membrane.

3.2.7. *Detection of extracellular enzymes*

The Bath-Spa medium (BSM) from cultures in log-phase growth was analysed for the presence of extracellular proteinases. The culture fluid was collected after filtering twice through a Millipore membrane filter (pore size, 0.22 μm) to remove the cells. The filtered medium was later concentrated in centricon microconcentrators (molecular weight cut off is 10,000 kDa, Amicon), centrifuged at 5000 *g*, at 4°C for 45 min on MSE Europa 24M centrifuge. The technique for obtaining extracellular enzymes as described by North *et al.*, (1990b) was not followed because experience has shown that 2% of *Naegleria* cells are lysed by centrifugation, and that proteinases detected in the medium might not therefore be released by living *Naegleria*. Unused BSM was used as a control. Proteinase activity was assayed by electrophoresis only.

3.2.8. *Detection of proteinases in different phases of growth in cultures*

Only *Naegleria gruberi* CCAP strain 1518/1A was used for this purpose. The amoebae were grown in flat-sided tubes containing 2.5 ml BSM for seven days. The initial inoculum size was ~1.0 x 10^4 cells. The amoebae were harvested on consecutive days after the inoculation. In this study, each day of culture age represents a phase of growth. The number of trophozoites, cysts and flagellates in each sample was counted in a haemocytometer. The samples were processed to obtain pellets as described in 3.2.1. The pH of each culture was also measured at the time of sampling. At least three replicates of each culture were used in this study. The samples were prepared for proteinase study as mentioned in 3.2.2. Detection of proteinases was by electrophoresis only.

3.2.9. *Proteinase detection in N. gruberi grown on agar with bacteria*

N. gruberi strain 1518/1A was grown on non-nutrient agar with live *E. coli* as mentioned in 2.2.1.; the amoebae were harvested four days after inoculation from at least two agar plates. The amoebae were removed from the agar surface by gently washing with phosphate buffer saline (PBS), pH 7.4. To obtain a pellet of amoebae free of bacteria, the cells were washed several times in PBS by centrifugation at 500 *g* at 4°C, for 10 min each wash, until the supernatant was completely free of bacteria as was observed by light microscopy.

The pellet obtained was resuspended in PBS containing 0.25% (v/v) Triton X-100 to lyse the cells, as described for trophozoites in 3.2.2. The supernatant was then used for proteinase analysis by SDS-PAGE electrophoresis.

3.2.10. *Proteinases in different strains of N. gruberi and pathogenic N. fowleri*

Only the trophozoite forms of the amoeba were used to detect the presence of proteinases in other strains of *N. gruberi* and in pathogenic *N. fowleri*. The amoebae were harvested during log-phase growth and processed for enzyme extraction as described in 3.2.2. The technique described in 3.2.5. to detect possible secreted enzymes in the culture medium was followed only for pathogenic *N. fowleri*. Attempts to detect such enzymes however, were aborted since dead /lysed cells were often observed in cultures and these might have released inappropriate enzymes into the culture medium.

3.3. RESULTS

3.3.1. *Proteinases in Naegleria gruberi CCAP strain 1518/1A*

Detection of proteinases in trophozoites, flagellates and cysts using gelatin-SDS-PAGE gels

After incubating a gelatin SDS-PAGE gel at pH 5.5, at least four bands of proteinase activity were observed in trophozoite samples taken from axenic cultures (grown in Bath-Spa medium, BSM). (Figure 3.2A). To facilitate discussion, the bands are labelled A, B, etc. according to increasing mobility of the enzymes in gelatin gels. Trophozoite samples prepared either by resuspending cell pellets in 0.25 % (v/v) Triton X-100 in PBS (lysis buffer) and centrifuging, or resuspending in lysis buffer, then subjecting to alternate freezing-thawing but not to centrifugation, produced similar pattern of enzymes on the gels (Figure 3.2A, panel A, lane 2). More bands however, were observed in the gels when the amount of protein loaded into each well for electrophoresis was more than 20 μg; samples of trophozoites thus produced an additional band as shown in Figure 3.2A (lane 1, panel C compared with lane 1, panel A). Apparent molecular weights (M_r) of proteinase bands A is about 200 kDa and B is about 148 kDa. M_r of band C appears to be around 116 kDa, band D is 98 kDa, and band E is 92 kDa. Since bands D and E are closely associated with each other, they are called doublet DE, in this study. Bands of enzymes A, B, C and doublet DE were observed in the trophozoite samples when the gelatin SDS-PAGE gels were incubated in sodium phosphate buffer, pH 5.5. At pH 8.0, trophozoite samples seemed consistently to produce three proteinase bands; band A and doublet DE.

Trophozoites of *N. gruberi* grown on agar with live bacteria produced at least three proteinase bands (at both pH 5.5 and pH 8.0); band A which appeared to be of very low activity and hardly visible on the gelatin gel at pH 5.5, and doublet DE, whose activity was apparently very high at pH 8.0 (Figure 3.2A, panel C and D).

Flagellate samples (morphology as shown in Figure 3.2B) produced at least three bands, A and DE. Band A which was hardly visible on the gel at pH 5.5 appeared to be very high in activity at pH 8.0 (Figure 3.2A, lane 3 of panels C and D). Cysts (morphology as in Figure 3.2C), produced only one band at pH 5.5. The position of this band on the gelatin gels appeared to be that of a protein of 116-kDa (or of band C in trophozoite samples). At higher pH, i.e. at pH 8.0, no band was observed in the cyst sample (Figure 3.2A, lane 4 of panel D).

Detection of membrane-associated enzymes

The supernatant fraction of the freeze-thawed trophozoite sample (S_A) was observed to have three proteinase activities at pH 5.5 (Figure 3.2A, panel A, lane 4) namely bands B and doublet DE. It was found that the activity of proteinases in sample S_B was very low and that the bands formed in the gelatin SDS-PAGE gels were similar to those in S_A sample, i.e. most proteins were released with the first freeze-thaw, so in later experiments this sample was not run on the gelatin gels. The pellet fraction of freeze-thawed samples which contained membrane-associated enzymes whether or not they had been treated with 0.25% (v/v) Triton X-100 in PBS, seemed to produce only doublet DE at both pH 5.5 and pH 8.0 (Figure 3.2A, panels A and B, lane 3; Figure 3.3, lane 3 and 4). The doublet DE was more abundant in S_A. Band A was not observed in either samples S_A or the pellet. If higher amounts of protein of S_A were loaded onto the wells, four bands, B, C and doublet DE were observed at pH 5.5;(Figure 3.3, panel A, lane 2).

Figure 3.2A. Photographs of gelatin SDS-PAGE gels showing proteinases in crude lysates of trophozoites, flagellates and cysts of *Naegleria gruberi* strain CCAP 1518/1A. Panel A. The gel was incubated in 0.1 M sodium phosphate buffer, pH 5.5. Panel B. The gel was incubated in 0.1 M sodium phosphate, pH 8.0. The amount of protein loaded into each well was 15 µg. Explanation for each lane: 1; trophozoite samples (lysed in 0.25% (v/v) Triton X-100 in PBS), 2; trophozoite samples (suspended in 0.25% (v/v) Triton X-100 in PBS and subjected to alternate freeze-thawing), 3; Pellet of freeze-thawed sample, 4; S_A, the supernatant fraction of freeze-thawed sample. Panel C. The gel was incubated in 0.1 M sodium phosphate buffer, pH 5.5, containing 1 mM DTT. Panel D. The gel was incubated in sodium phosphate buffer, pH 8.0. Explanation for lanes of panels C and D. 1; trophozoite samples (grown in Bath-spa medium and lysed in 0.25% (v/v) Triton X-100 in PBS), 2; trophozoite samples (grown on agar with bacteria and lysed in 0.25% (v/v) Triton X-100 in PBS), 3; flagellate samples, 4; cyst samples. The amount of protein used for each sample was 45 µg, 60 µg, 45 µg and 30 µg, respectively. Relative mobilities of the protein molecular standards are indicated.

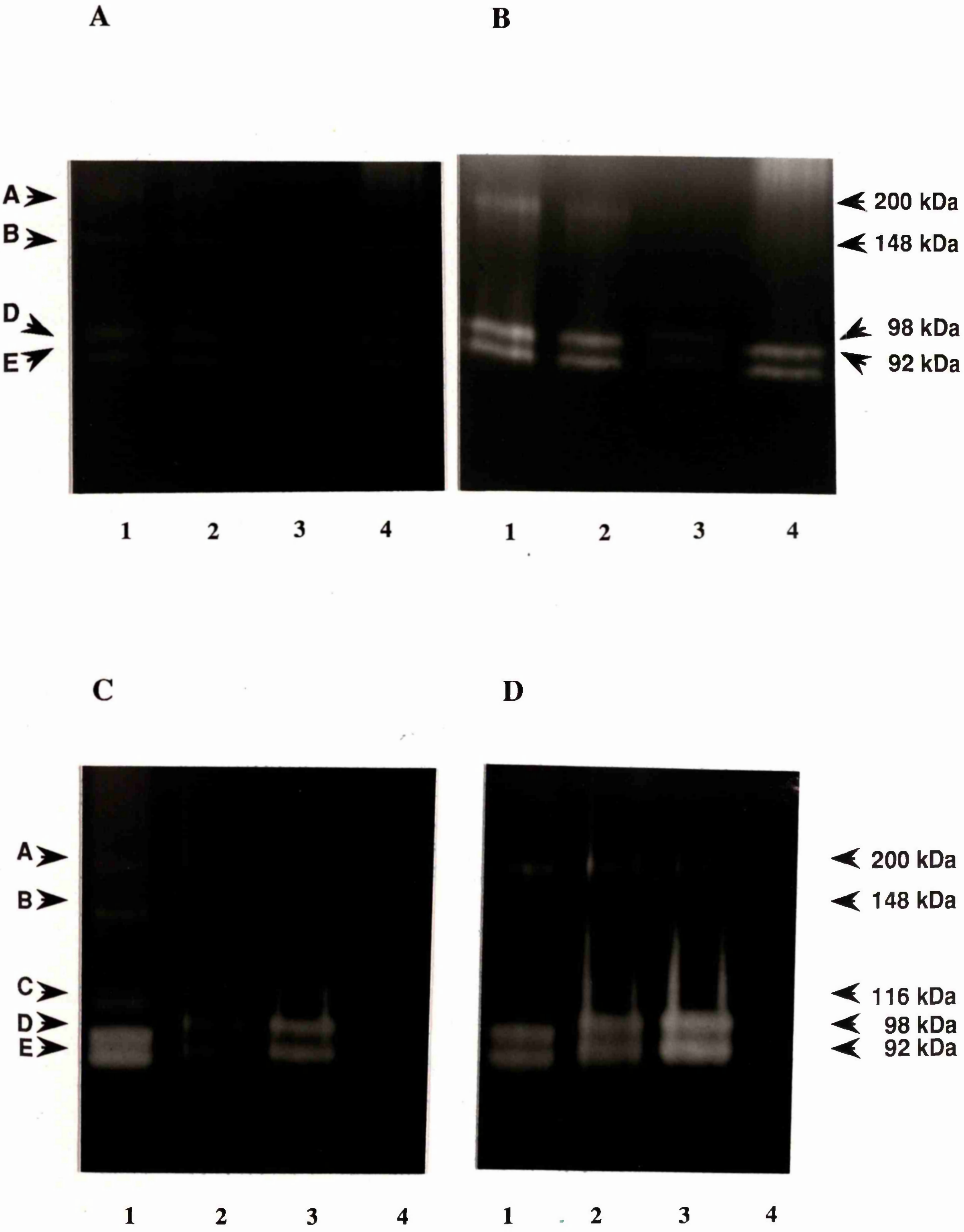
A
B
A
B
D
E
200 kDa
148 kDa
98 kDa
92 kDa
1
2
3
4
1
2
3
4
C
D
A
B
C
D
E
200 kDa
148 kDa
116 kDa
98 kDa
92 kDa
1
2
3
4
1
2
3
4

Figure 3.2B. Phase micrograph of Lugol's iodine-fixed flagellates of *Naegleria gruberi* CCAP strain 1518/1A. The number of flagella appears to vary from two to four. The flagellates were collected through a bead column and processed as described in 3.2.1. for proteinase analysis. Two of the flagellates seem to be in the process of reversion to amoeboid phase (arrowheads).
Scale bar = 20 µm.

Figure 3.2C. Scanning electron micrograph of cysts of *Naegleria gruberi* CCAP strain 1518/1A. Plug pores are clearly seen (arrowheads).
Scale bar = 10 µm.

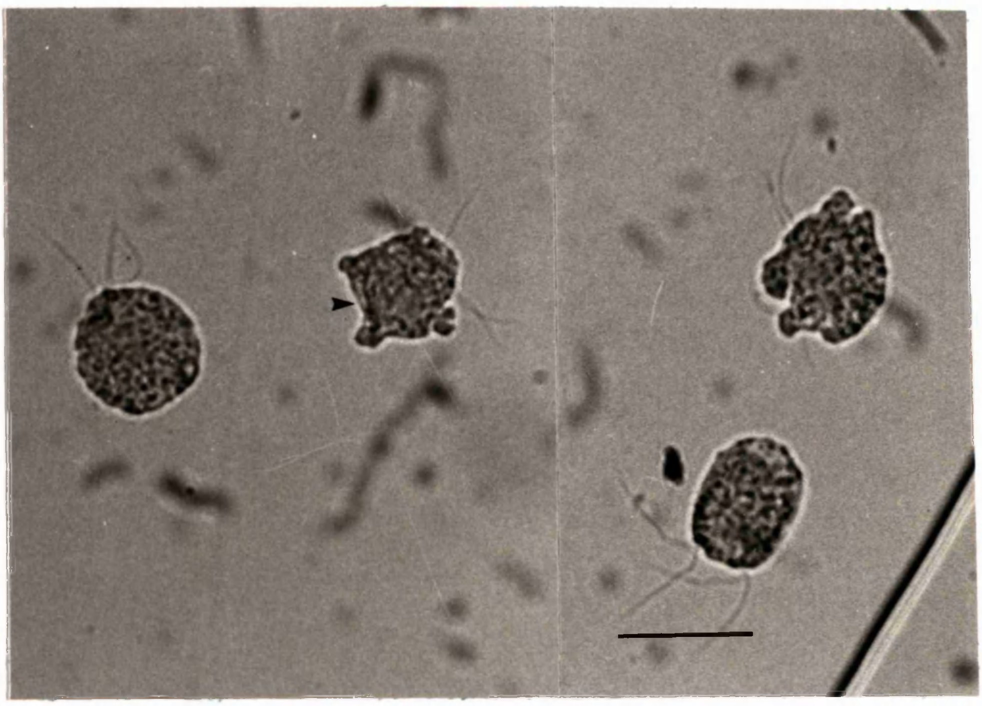

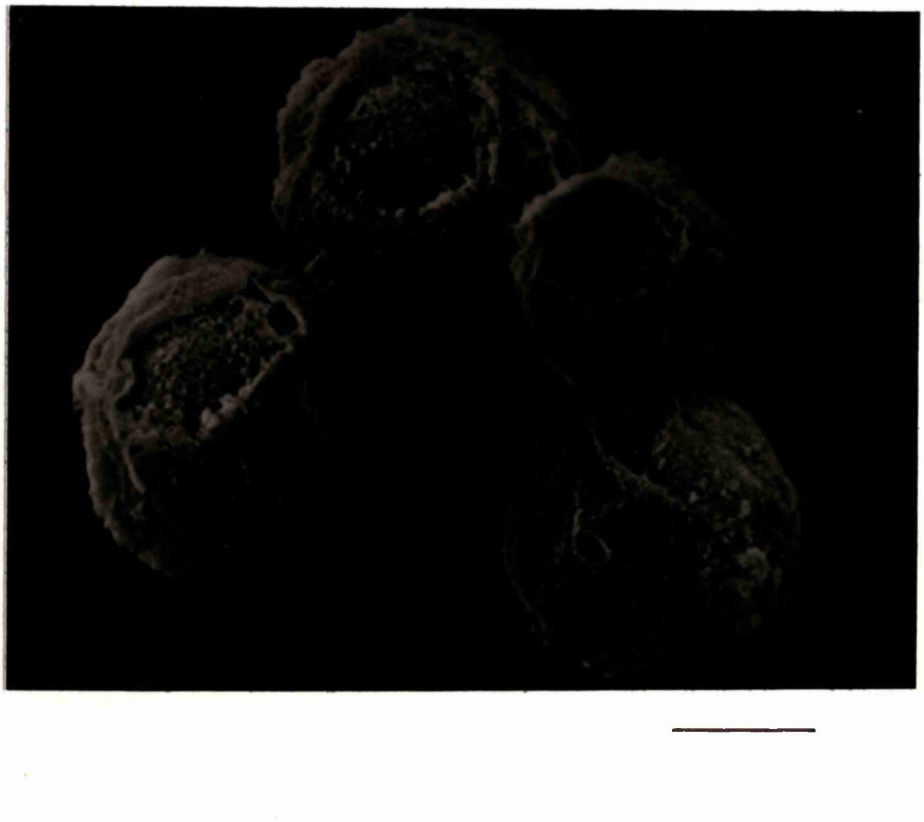

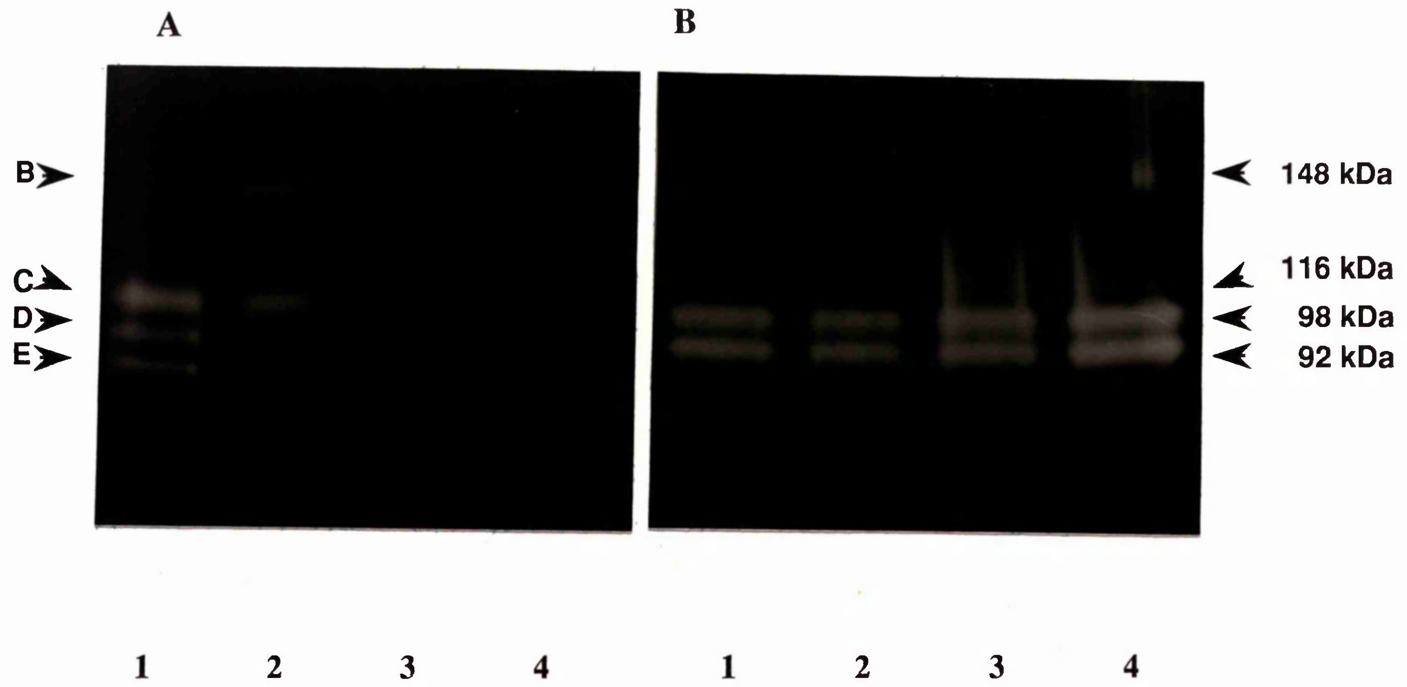

Figure 3.3. Detection of membrane-associated enzymes in *Naegleria gruberi*, CCAP strain 1518/1A. The gels were incubated in 0.1 M sodium phosphate buffer containing 1 mM DTT. Panel A. At pH 5.5. Panel B. At pH 8.0. All gels were incubated in buffers at 37°C. The amount of protein loaded for each lane was 30 μg. Explanation for lanes on each gel: 1; crude lysate of *N. gruberi* prepared by suspending the cells in 0.25% (v/v) Triton X-100 in PBS, used as a control, 2; supernatant of freeze-thawed samples, 3; pellet of freeze-thawed samples, 4; pellet of freeze-thawed sample but suspended in 0.25% (v/v) TritonX-100 in PBS.

Characterisation of individual proteinases in trophozoite samples of N. gruberi

Effect of dithiothreitol (DTT) and pH on band appearances

The effects of the thiol reducing agent DTT on the activity of the individual enzymes in *Naegleria gruberi* strain 1518/1A in this study varied, depending on the pH of the incubation buffer of the gels (Figure 3.4A). At pH 5.5, the presence of DTT enhanced the activities of bands B,C and doublet DE. At pH 6.0, with DTT, only bands C and DE were observed; without DTT the activity of band C was inactivated. The activity of doublet DE appeared to increase at this pH. At pH higher than 6.0, only doublet DE were observed. The presence of DTT at these pHs appeared to inactivate slightly the activity of these enzymes.

The effect of pH in which the gel was incubated on band A enzyme is shown in Figure 3.4B. Samples of cells lysed in 0.25% (v/v) Triton X-100 in PBS and the supernatant fraction of freeze-thawed samples (S_A) were used to see the effect of pH on band A appearance in gelatin SDS-PAGE gels. Band A was only detected in samples of cells lysed in Triton X-100 (Figure 3.4B, lane 1). At pH 5.5 (either in sodium acetate-acetic acid buffer or sodium phosphate buffer) the activity of band A was so low so it was hardly visible on the gels (Figure 3.4B, panel A). With increasing of the buffer pH, the activity of this enzyme was observed to be more active and its band became more distinct. The effect of DTT on band A enzyme activity could not be studied in details due to infrequent detection of this enzyme on the gels. The presence of DTT (at pH 5.5) however, did not inactivate the activity of this enzyme, as has been shown in Figure 3.2A (panel C, lane 1). Since bands B, C and doublet DE enzymes in *Naegleria* were observed with high activity at pH 5.5 with DTT, and bands A and doublet DE enzymes were more active at pH 8.0 without DTT, in the following studies, the proteinase activities were always observed under both conditions.

Inhibitor study to characterise the enzymes on gelatin gels

Preliminary observations have indicated that the effect of some inhibitors on proteinase activities in *Naegleria* lysates was less significant if the enzymes were assayed at pH 5.5 in the presence of 1 mM DTT. In later experiments the inhibition studies thus were made at pH 5.5 without the presence of DTT.

Samples of lysed cells and supernatant (S_A) and pellet of freeze-thawed samples were used to characterise the enzymes by using various inhibitors. APMSF, a serine proteinase inhibitor, slightly inhibited bands A and DE in all samples at pH 8.0; these enzymes are more active at this pH (Figure 3.5A). APMSF also inhibited band A and doublet DE at pH 5.5 and without DTT when the activity of all bands was low on gelatin gel, (Figure 3.5A). When lysed cell samples were treated with other inhibitors, such as 3,4-DCI (a serine proteinase inhibitor), antipain (an inhibitor of serine and cysteine proteinases), pepstatin (an aspartic proteinase inhibitor), elastatinal (an inhibitor of elastase-like enzymes), and EDTA (an inhibitor of metallo-proteinases), only antipain gave inhibition to all bands on the gel. Band B was completely inhibited by antipain whereas other bands (band C and doublet DE) were slightly inhibited by this inhibitor as compared with a control (Figure 3.5B, panel A). This study showed that bands DE were also inhibited by inhibitor EDTA. Inhibitor E-64, a cysteine proteinase inhibitor appears to inhibit slightly bands B and doublet DE in S_A sample and pellet of freeze-thawed sample at pH 5.5 (Figure 3.5B, panel C).

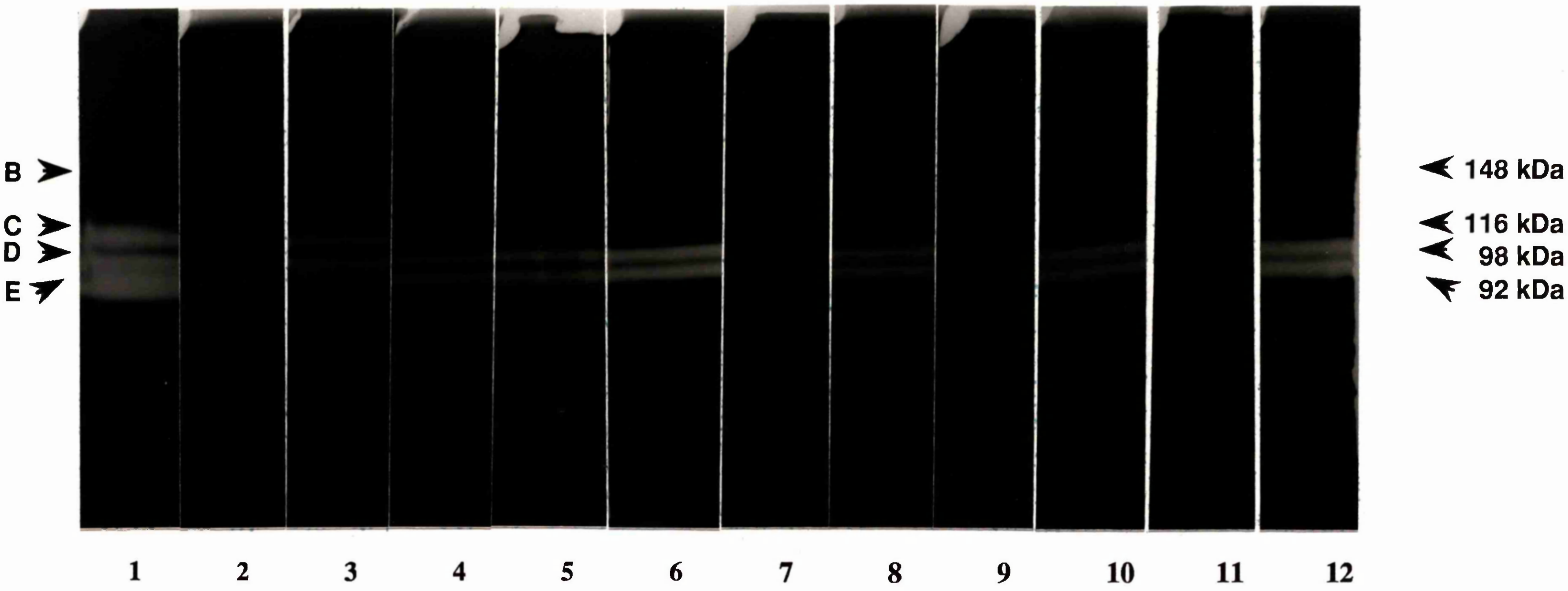

Figure 3.4A. Effect of pH of the gel incubation buffer and DTT on band appearances in supernatant of Triton X-100-lysed cells of *Naegleria gruberi* CCAP strain 1518/1A. All gels were incubated at 37°C in 0.1 M sodium phosphate buffer, pH ranging from 5.5 to 8.0, The amount of protein used for each lane was ~30 µg. Explanation for lanes: 1; pH 5.5, 3; pH 6.0, 5; pH 6.5, 7; pH 7.0, 9; pH 7.5 and 11; pH 8.0, all contained 1 mM DTT. The gels in lanes 2, 4, 6, 8, 10 and 12 were incubated in the same buffers as gels in lanes 1, 3, 5, 7, 9, and 11 respectively, but did not contain DTT.

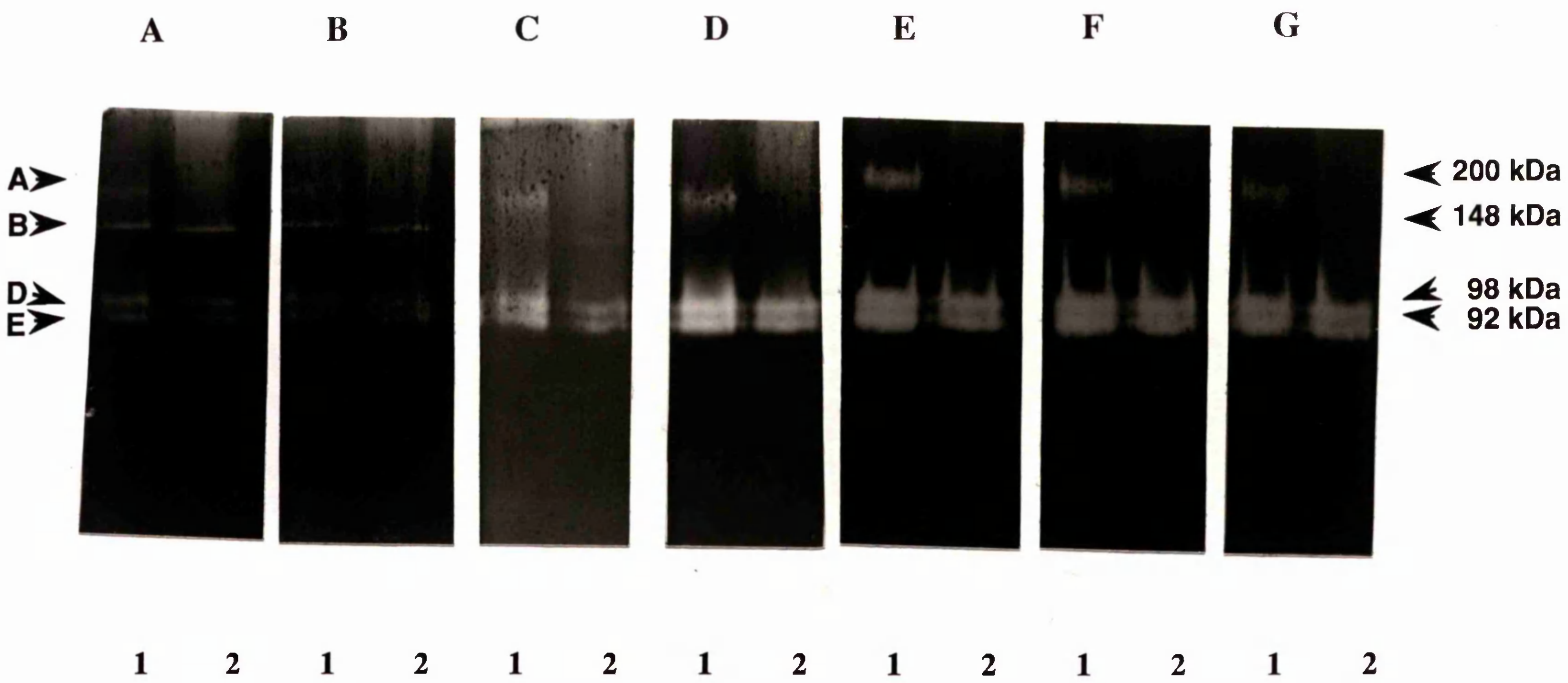

Figure 3.4B. Effect of pH buffer on band A enzyme activity in the supernatant of Triton X-100-lysed cells of *N. gruberi* (lane 1 in each panel) on the gelatin gels. The gels were incubated in buffers at various pHs, at 32°C. Each sample contained 15 µg protein and was loaded onto the wells of gelatin SDS-PAGE gels. Explanation for panels: A. 0.1 M sodium acetate-acetic buffer, pH 5.5; B to G. 0.1 M sodium phosphate buffer, B. pH 5.5, C. pH 6.0, D. pH 6.5, E. pH 7.0, F. pH 7.5, G. pH 8.0. All the incubation buffers did not contain DTT. Lane 2 in each panel contained supernatant of freeze-thawed samples and did not have band A enzyme activity.

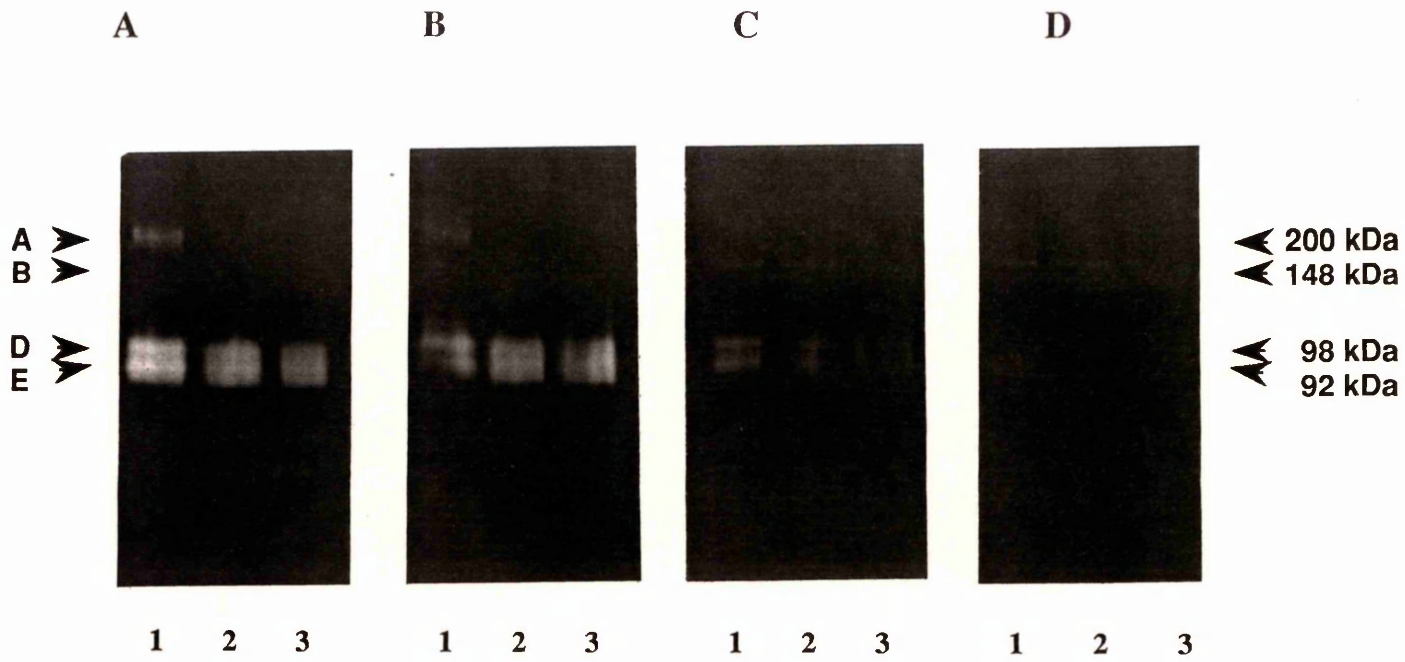

Figure 3.5A. Effect of the inhibitor APMSF on enzyme activity on gelatin SDS-PAGE gel. Each sample contained ~15 µg protein. Panel A. The gel was incubated in 0.1 M sodium phosphate buffer, pH 8.0, without DTT. Panel B. As in panel A but the gel was incubated in buffer containing APMSF. Panel C. The gel was incubated in sodium phosphate buffer, pH 5.5, without DTT. Panel D. The gel was incubated as in C but containing APMSF. Explanation for lanes: 1, supernatant sample of Triton X-100-lysed cells, 2, supernatant of freeze-thawed sample, 3; pellet of freeze-thawed sample.

Figure 3.5B. Panel A. Effect of various inhibitors on enzyme activity of *Naegleria gruberi* crude lysates. The gels were incubated in 0.1 M sodium phosphate buffer, pH 5.5 containing 1 mM DTT, at 37°C. Explanation for lanes: 1; control, the gel was incubated in buffer only, 2; buffer containing inhibitor 3,4-DCI, 3; buffer containing antipain, 4; buffer containing pepstatin, 5; buffer containing elastatinal, 6; buffer containing EDTA. The amount of protein loaded for each sample was 30 µg. Panel B. Effect of inhibitor E-64 on enzymes of *Naegleria gruberi* crude lysate. The gel was incubated at 37°C in 0.1 M sodium phosphate buffer pH 5.5 containing 10 µM inhibitor E-64 without DTT. The samples were also incubated with inhibitor E-64 for 45 min at room temperature prior to electrophoresis. Panel C. The same samples were run on the gelatin gel, incubated in buffer without the inhibitor and used as a control. Explanation of lanes for panels B and C: 1; supernatant of freeze-thawed sample, 2; pellet of freeze-thawed sample and resuspended in 0.25% (v/v) Triton X-100 in PBS.

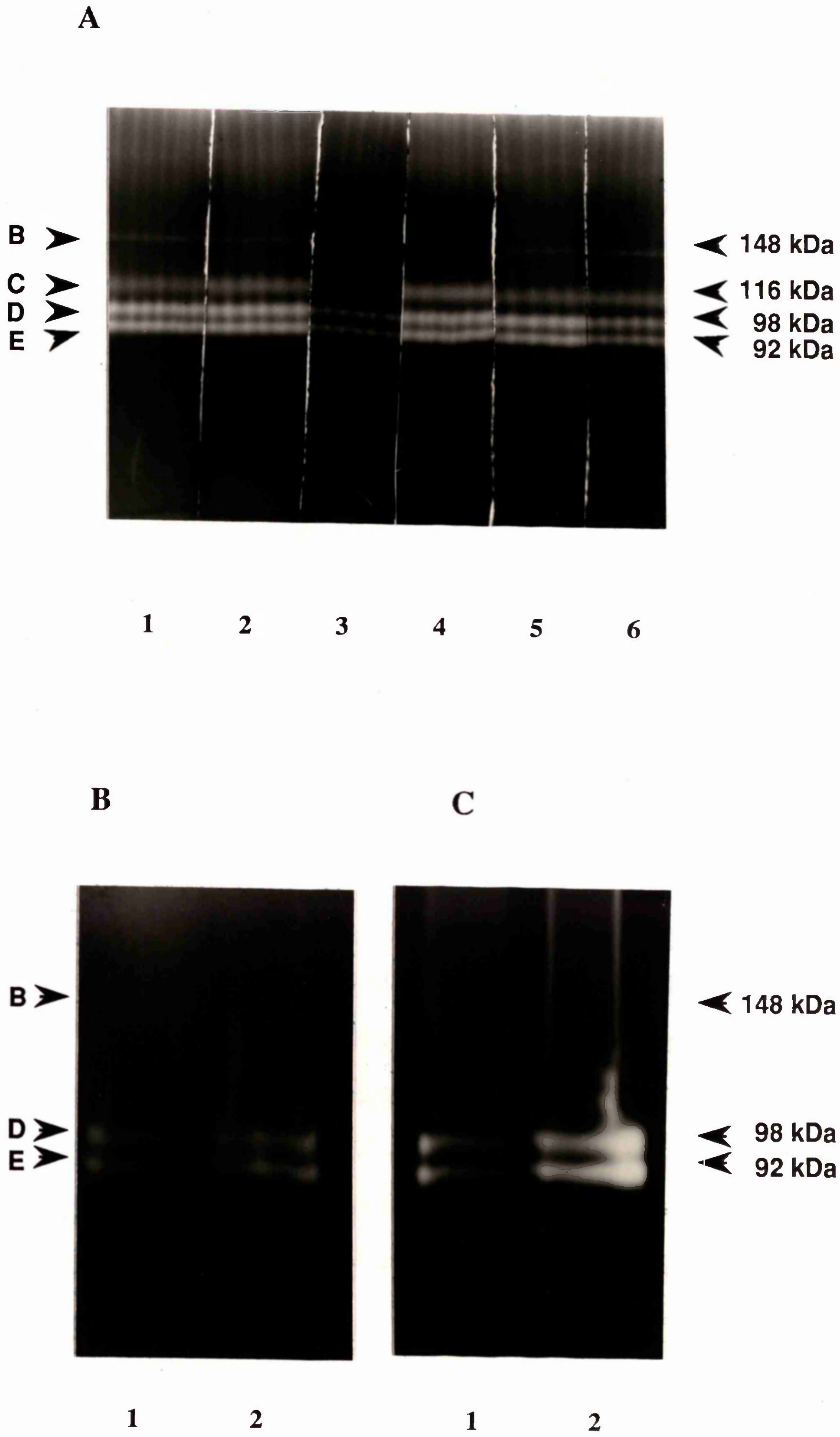
A
B
C
D
E
148 kDa
116 kDa
98 kDa
92 kDa
1
2
3
4
5
6
B
C
B
D
E
148 kDa
98 kDa
92 kDa
1
2
1
2

Spectrophotometric assays of proteinase activity in Naegleria crude lysates

Activity towards substrate Bz-Pro-Phe-Arg-Nan

The activities of proteinases of *Naegleria gruberi* (CCAP strain 1518/1A) crude lysates towards substrate Bz-Pro-Phe-Arg-Nan in 0.1 M sodium phosphate buffer at different pH values are presented in Table 3.2. Lysates of samples taken from log-phase growth which contained mostly trophozoites, were used in this study. The highest value of specific activity of *Naegleria* crude lysates towards Bz-Pro-Phe-Arg-Nan (based on nmol nitroaniline released min^{-1} $(\text{mg protein})^{-1}$ ± standard deviation) is at pH 5.5 and in the presence of DTT (69.55 ± 3.79) (Table 3.2). The lowest activities were observed between pH 7.0 and pH 7.5, and without DTT (15.81 ± 1.86, 16.55 ± 1.89, respectively). DTT seemed to enhance the activities of *Naegleria* crude lysates towards Bz-Pro-Phe-Arg-Nan. Without DTT at all pHs, the activities were markedly reduced (Figure 3.6).

Comparison of lysate proteinase activity towards different substrates

Two other substrates (Bz-Arg-Arg-Nan and D-Val-Ser-Arg-Nan) were used to study further the substrate preferences of *N. gruberi* crude lysates. Activities of the lysates towards other substrates were compared with the activity towards Bz-Pro-Phe-Arg-Nan and the results are shown in Table 3.3. In general, the activity of *N. gruberi* lysates was low towards both substrates (Bz-Arg-Arg-Nan and D-Val-Ser-Arg-Nan), even in the presence of DTT. The hydrolysis of these substrates was only observed at higher pHs (pH 7.0 and pH 8.0); the presence of DTT seemed not to stimulate the ability of *Naegleria* lysates to hydrolyse these substrates.

Table 3.2. Specific activity of *Naegleria gruberi* strain (1518/1A) crude lysates towards Bz-Pro-Phe-Arg-Nan

Condition of assay	*nmol nitroaniline released min^{-1} (mgprotein)$^{-1}$*	*% activity*
Without inhibitors:		
pH 5.5, +DTT	69.55±3.79	100
-DTT	36.91±6.43	53
pH 6.0, +DTT	65.51±0.64	94
-DTT	31.77±1.90	46
pH 6.5, +DTT	62.79±1.92	90
-DTT	21.48±5.06	31
pH 7.0, +DTT	55.56±3.17	80
-DTT	15.81±1.86	23
pH 7.5, +DTT	53.31±3.84	77
-DTT	16.55±1.89	24
pH 8.0, +DTT	58.73±7.08	84
-DTT	22.37±1.27	32
With inhibitors:		*% inhibition*
pH 5.5,+DTT+E-64	0	100
-DTT+E-64	0	100
pH 5.5,+DTT+antipain	0	100
-DTT+antipain	0	100
pH 5.5,+DTT+APMSF	52.86±1.3	24
-DTT+APMSF	19.56±1.1	47

Explanation: The results shown are from three observations and presented as means ± standard deviations.

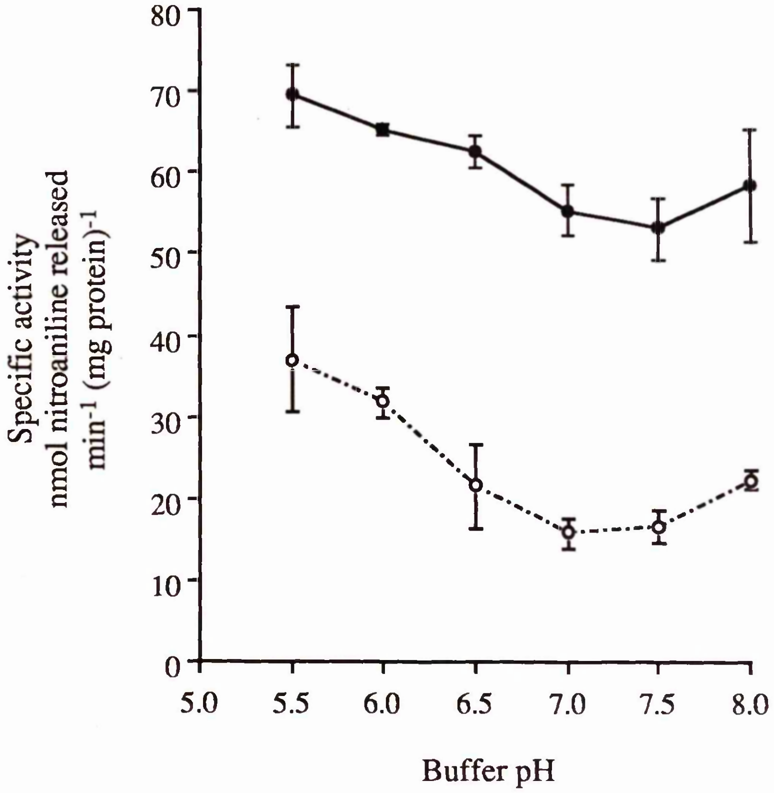

Figure 3.6. Specific activity of *N. gruberi* crude lysates towards Bz-Pro-Phe-Arg-Nan in 0.1 M sodium phosphate buffer at various pH values . Values shown are means with standard deviations (error bars) taken from three observations.
Explanation for symbols: —●— with 1 mM DTT; ···○··· without DTT.

Table 3.3. Comparison of the specific activity of *Naegleria gruberi (*strain 1518/1A) crude lysates towards three substrates; Bz-Pro-Phe-Arg-Nan (PFR), Bz-Arg-Arg-Nan (RR) and D-Val-Ser-Arg-Nan (VSR). (based on nmol nitroaniline released min-^{1} (mg protein)-^{1})

	Substrate peptide moiety (mean ±SD)		
Condition of activity	*PFR*	*RR*	*VSR*
pH 5.5,+DTT	69.55±3.79	0.90±0.10	0.90±0.00
-DTT	36.91±6.43	0	0.89±0.00
pH 7.0,+DTT	55.56±3.17	1.81±0.00	3.16±0.61
-DTT	15.81±1.86	1.35±0.63	4.03±0.63
pH 8.0,+DTT	58.73±7.08	2.26±0.64	3.61±0.10
-DTT	22.37±1.27	2.24±0.64	3.14±0.64

Key:

All values are taken from three observations and presented as means with standard deviations (mean±SD). The background hydrolysis in the assay mixture is zero.

Effect of inhibitors on Naegleria lysates towards Bz-Pro-Phe-Arg-Nan

The sensitivity of the cell lysates proteinase activity to E-64 and antipain is also shown in Table 3.2. Both E-64, the inhibitor of cysteine proteinases and antipain, the inhibitor of serine and cysteine proteinases inhibited completely the crude lysate activity with or without the presence of DTT. APMSF was observed to inhibit the enzyme activity by ~23% when DTT was present, and ~47% when DTT was not present.

Separation of Naegleria proteinases by FPLC gel filtration

Activity towards Bz-Phe-Pro-Arg-Nan

Fractions between 7 ml to 30 ml collected from gel filtration of *N. gruberi* lysates (section 3.2.5) were assayed for activity towards the substrate Bz-Phe-Pro-Arg-Nan. The activity was assayed in 0.1 M sodium phosphate buffer, at pH 5.5 (with DTT) and pH 8.0 at 37°C and the results are shown in Figure 3.7A. The maximum peak of activity was observed in fraction volume of 19 ml (at both pHs) and this peak corresponds to the second peak of the total protein released by the gel filtration. The result shows that the activity of the enzymes in these fractions was higher at pH 5.5 than at pH 8.0.

Band pattern on gelatin SDS-PAGE gels:

To check which of the bands usually seen in gelatin SDS-PAGE gels is responsible for hydrolysis of the substrate in the above study (in Figure 3.7A), the fractions between 7 ml to 23 ml were run on gelatin SDS-PAGE gels. Earlier results (data not shown) indicated that the other fractions did not have any enzyme activity on the gelatin gels so they were not used in this study. All four bands usually found in *Naegleria* lysates (bands A, B and DE) were detected on the gel (Figure 3.7B). Band A was detected in the fraction volumes of 9 and 10 ml. Both bands A and B were observed in the fraction volumes of 15 and 16 ml. Bands A and doublet DE were detected in the fraction volumes between 18 ml to 23 ml but with low activity except in fraction 19 where the enzymes could be observed clearly. The original sample of *N. gruberi* lysate was also run on the gel and used to detect and label the corresponding enzymes in each fraction. From this observation, it can be seen that band A co-fractionates with either band B enzyme or doublet DE enzymes, despite having undergone fractionation, with the exception in earlier fractions where this enzyme was detected singly (in fractions 9 and 10 ml). From this study, doublet DE enzymes could be proposed to be the enzymes which hydrolysed the substrate Bz-Pro-Phe-Arg-Nan and produced a peak in Figure 3.7A. Since there was no peak of activity observed in earlier fractions (fractions 9 and 10 ml) in Figure 3.7A, in which fractions the activity of band A enzyme was detected in gelatin SDS-PAGE gels in Figure 3.7B, the result of this study suggests that band A enzyme did not hydrolyse this substrate.

Activity on fluorogenic H-Pro-Phe-Arg-NHMec

The activity of *Naegleria* crude lysates was studied further by taking the fraction volumes which had the enzyme activity on the gelatin gels and running on gels which later were incubated in buffer containing fluorogenic substrate (H-Pro-Phe-Arg-NHMec). The gels were incubated at 37°C, at pH 5.5 with DTT and pH 8.0. Only the gel which was incubated in buffer at pH 8.0 produced positive result and is shown in Figure 3.7C. Due to low activity of these enzymes (in all fractions), they could not be detected readily on the gel (at both pHs). Doublet DE from a control sample were the only bands detected on the gel in this study.

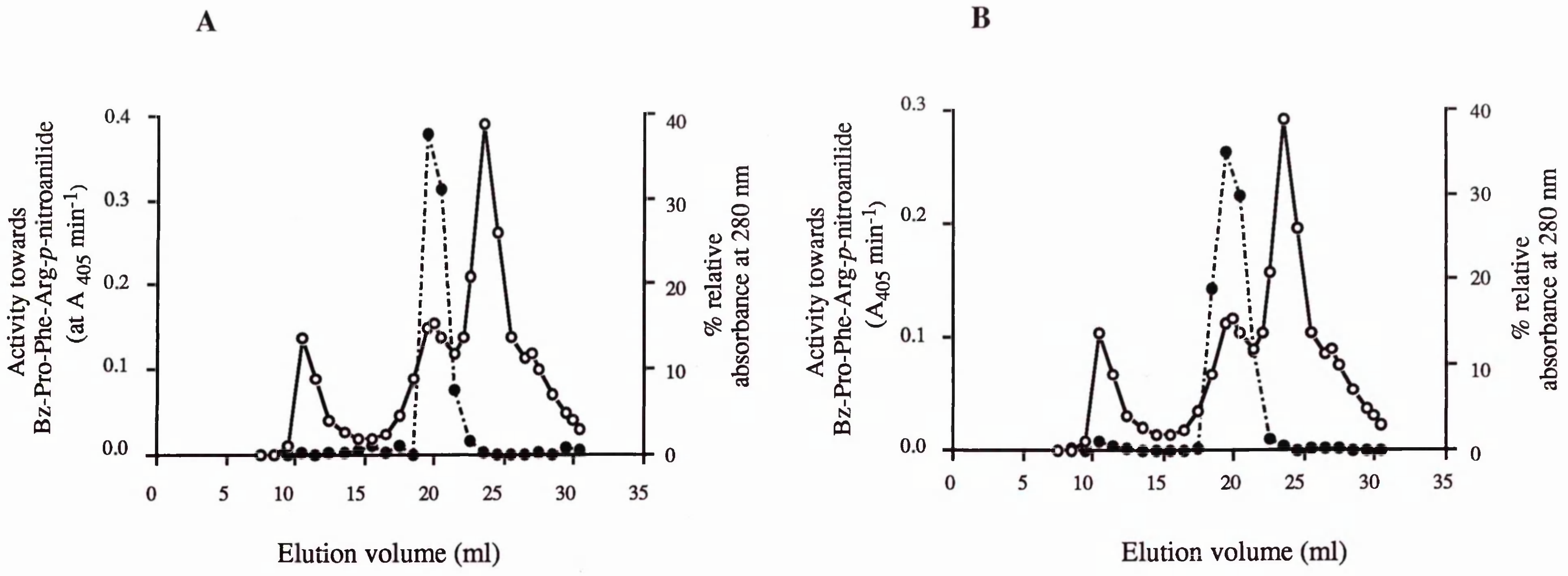

Figure 3.7A. Fractionation of late log-phase *Naegleria gruberi* crude lysate by gel filtration. A 250 µl sample was applied to a Superose 12 column and eluted as described in 3.2.1. Proteinase activity towards Bz-Pro-Phe-Arg-*p*-nitroanilide (● , panel A is at pH 5.5, panel B is at pH 8.0) and relative absorbance at 280 nm (○ , % of full scale) are shown on the elution profile.

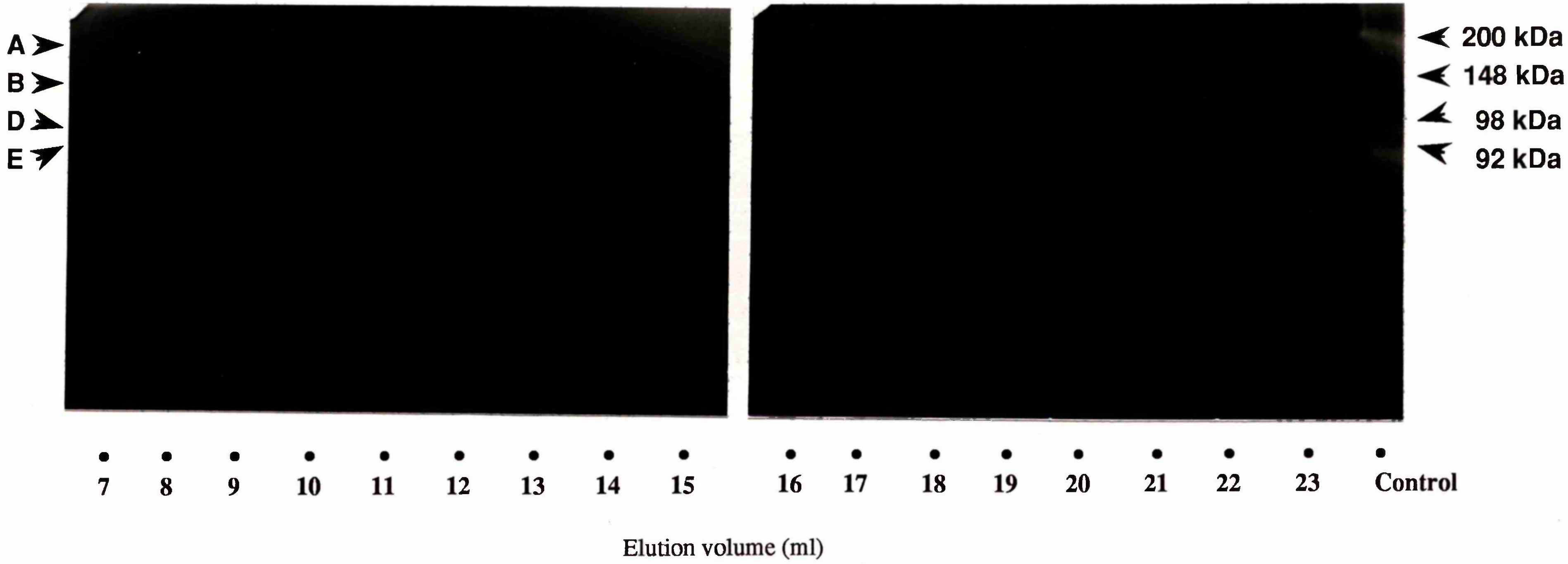
A
B
D
E
200 kDa
148 kDa
98 kDa
92 kDa
7
8
9
10
11
12
13
14
15
16
17
18
19
20
21
22
23
Control
Elution volume (ml)

Figure 3.7B. Elution of late log-phase *Naegleria gruberi* crude lysate from gel filtration by FPLC. A 250 µl volume sample containing supernatant fraction of lysed cells of *N. gruberi* was loaded to the Superose 12 column and 1.0 ml fractions between 7.0 and 30.0 ml were collected. Only fraction from 7.0 to 23.0 ml were run on the gelatin gels. The volume of each fraction used on the gelatin gel was 20 µl. The original sample of *N. gruberi* lysates was used as a control and also run on the same gel.

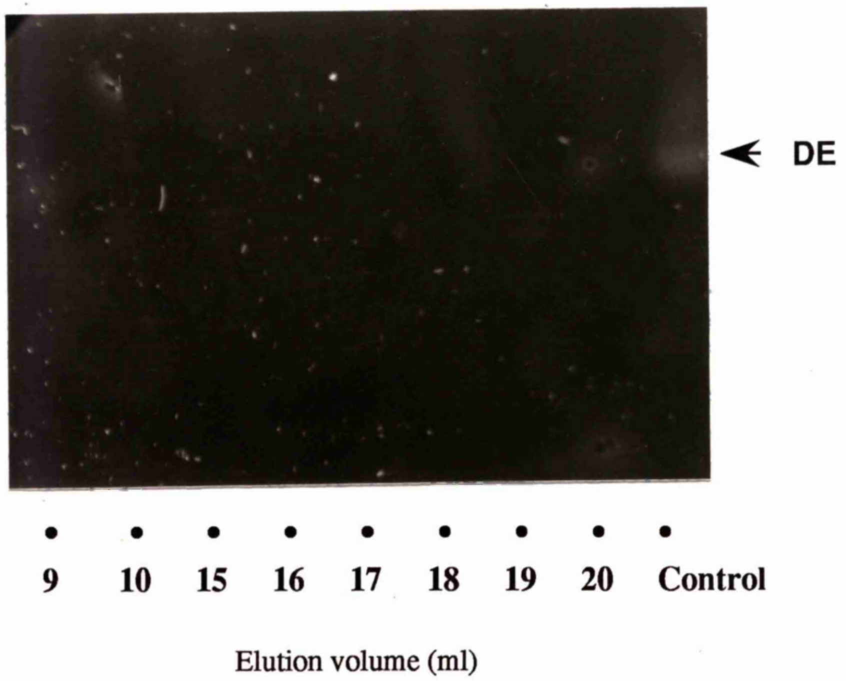
DE
9
10
15
16
17
18
19
20
Control
Elution volume (ml)

Figure 3.7C. Detection of enzymes in the fractions of *Naegleria* crude lysate from gel filtration by FPLC on gel incubated in 0.1 M sodium phosphate buffer, pH 8.0 containing substrate H-Pro-Phe-Arg-NHMec. A 20 µl volume of each fraction sample was loaded in each lane. Only fraction volumes as indicated above were run on the gel. The original sample of *N. gruberi* lysate (10 µl) was also run on the gel and used as a control.

Detection of extracellular enzymes

Naegleria gruberi apparently secretes proteinase activity extracellularly. At pH 5.5 in the presence of 1 mM DTT, at least three proteinase bands were detected by gelatin SDS-PAGE gels in the medium of established cultures of *N. gruberi*. The position of these bands in relation to bands from cell lysates of *N. gruberi* is shown in Figure 3.8 (panel A). Bands of ~92 kDa, ~90 kDa and ~75 kDa enzymes were observed. Only one proteinase band whose apparent M_r is ~90 kDa was observed when the gel was incubated at pH 8.0. The activities of the ~92 kDa and ~75 kDa enzymes thus were inactivated at this pH. Surprisingly, when treated with inhibitor E-64 at pH 5.5 in the presence of DTT, this sample produced at least nine bands of enzymes which hydrolyse gelatin. The position of these bands relative to the protein standards on gelatin gels indicated that their apparent molecular weights are greater than 98 kDa. So they appeared to differ from the secreted enzymes which were observed in samples not treated with E-64. Unused medium did not produce such enzymes when treated with the same inhibitor (Figure 3.8, panel B).

Proteinases at different phases of growth in cultures

Only four bands (A, B and doublet DE) of proteinase activity which were observed in *N. gruberi* crude lysates, were detected by gelatin SDS-PAGE gels in all samples taken from different phases of growth in cultures (Figure 3.9). Band C was not detected in these samples. The bands A, B and doublet DE appeared to be present in all samples although band B in day 1 sample (D_1) was only faintly visible on the gel. Band A, on the other hand, was barely visible in samples of older cultures (D_5 to D_7). Doublet DE was detected in all samples with very high activity especially in samples D_1 to D_4.

Figure 3.8. Secreted enzymes detected in the medium taken from cultures of *Naegleria gruberi* CCAP strain 1518/1A. The medium was sampled and prepared as described in 3.2.5. 10 μl volume of concentrated samples were run on gelatin gels. Unused medium was used as a control. Panel A. The gel was incubated in buffer without inhibitor. Explanation for lanes: 1; unused medium at pH 5.5 containing DTT, 2; used medium at pH 5.5 containing DTT, 3; unused medium at pH 8.0, without DTT, 4; used medium at pH 8.0 without DTT, 5; lysate of *N. gruberi*, at pH 5.5 with DTT, 6; lysate of *N. gruberi* at pH 8.0 without DTT. Panel B. The gel was incubated in buffer with inhibitor E-64. Explanation for lanes. 1; unused medium treated with inhibitor E-64, 2; used medium treated with E-64. The molecular weight of protein standards used as molecular weight markers is indicated. For panel B, the gel was incubated in 0.1 M sodium phosphate buffer, pH 5.5 containing 1 mM DTT at 37°C.

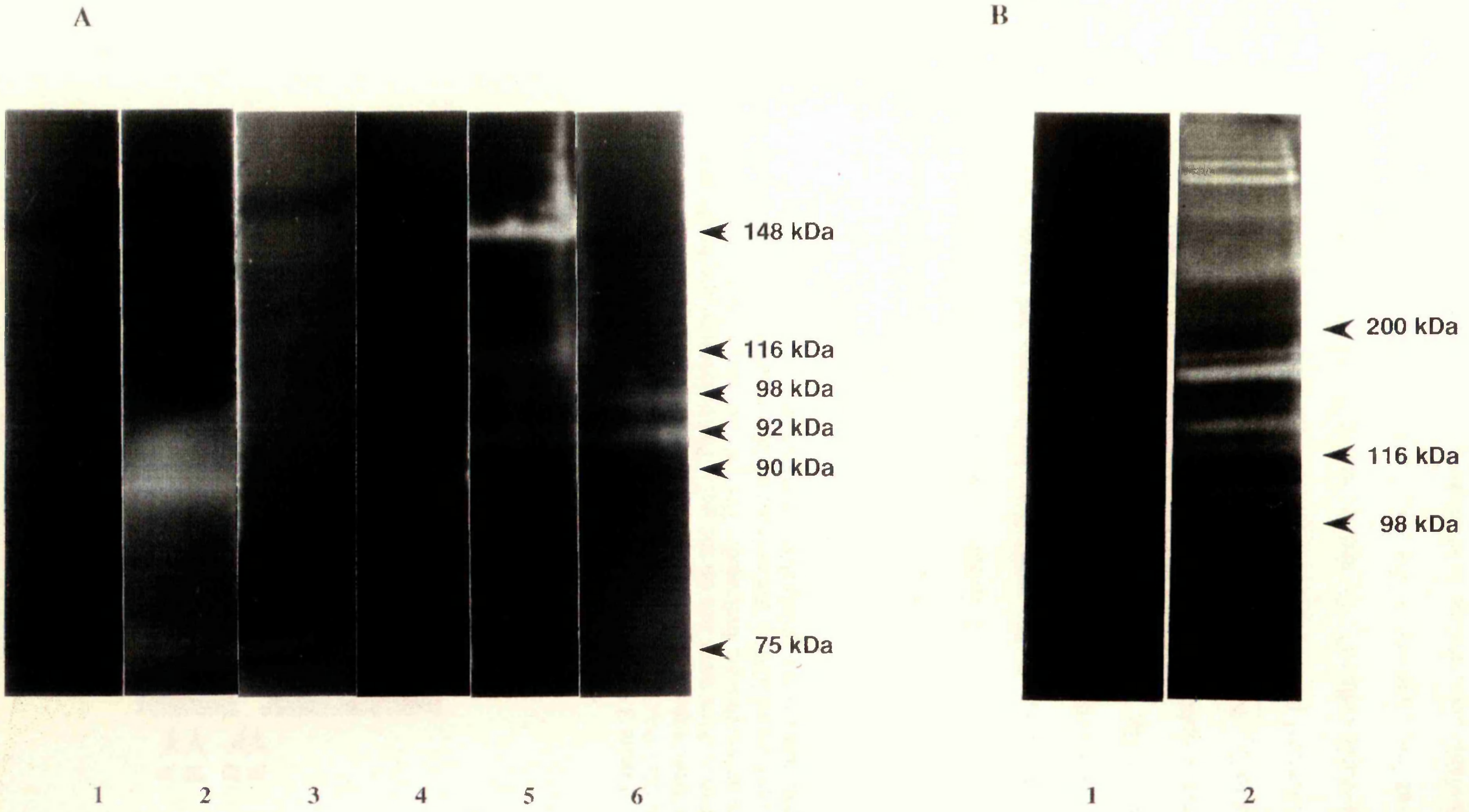
A
148 kDa
116 kDa
98 kDa
92 kDa
90 kDa
75 kDa
1
2
3
4
5
6
B
200 kDa
116 kDa
98 kDa
1
2

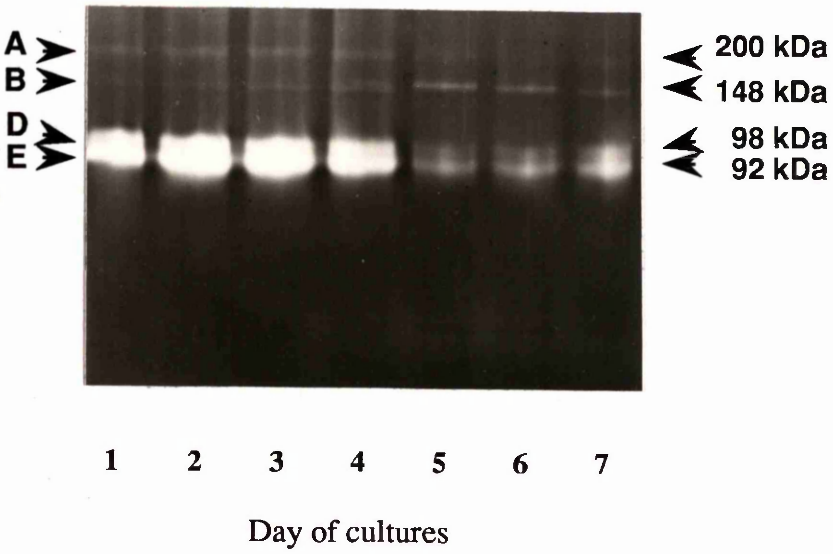

Figure 3.9. Proteinase activity of *Naegleria gruberi* CCAP strain 1518/1A on gelatin SDS-PAGE gels during growth in axenic culture. Sample containing 15 µg of protein from supernatant of cell pellets lysed in 0.25% (v/v) Triton X-100 in PBS on 7 consecutive days were run on the gel. The position of the bands and their apparent molecular weights are indicated. The gel was incubated in 0.1 M sodium phosphate buffer, pH 5.5 at 32°C. The number of lane represents the age of each culture. For example, lane 1 is for sample day 1, and so forth.

The number of proteinase bands produced by each sample on the gel did not reflect the proportion of different stages of the life cycle of *Naegleria* in the cultures (Table 3.4). Sample D_1, apart from having low cell count, only consisted of trophozoite forms of *Naegleria*. This sample produced bands A, band B with low intensity on the gel, and doublet DE. Sample D_2 comprised two forms of *Naegleria;* trophozoites and flagellates. This mixture of forms exhibited similar enzymes to D_1. Non-viable cells were first detected in D_3. This sample exhibited an almost identical pattern of proteinases to D_4, which contained trophozoites, cysts and non-viable cells. D_5, D_6 and D_7 had similar patterns of proteinase bands with band B at high intensity on the gel. These samples contained trophozoites, cysts and non-viable cells; among these samples, only sample D_6 had flagellates.

The maximum number of trophozoites counted in culture grown in flat-sided tubes in this study was in sample D_3 and the number decreased in older cultures (Figure 3.10). Cysts, which started to appear in culture of D_4, reached their maximum number in D_5 and then decreased as the cultures grew older (Figure 3.10). The number of non-viable cells seemed to increase exponentially in older cultures, beginning from culture D_3 (Figure 3.10).

The pH of the medium in cultures seemed to increase (became more alkaline) as the cultures grew older (Table 3.4 and Figure 3.10). The pH appeared to be constant between D_3 and D_4 and constant again between D_5 and D_6 after a slight increase from D_4 to D_5. The same pH of the culture medium on D_3 and D_4, and also between D_4 and D_5 might reflect similar culture conditions, hence exhibit a similar pattern of the enzymes on the gelatin SDS-PAGE gels (Figure 3.9).

Table 3.4. Culture composition of *Naegleria gruberi* CCAP strain 1518/1A grown axenically in Bath-Spa medium in flat-sided tubes for 7 days. The size of inoculum to start the cultures was ~1.0 x 10^4 cells.

Days	*pH*^{a}	*Trophozoites (x* 10^5 *ml*$^{-1}$*)*	*Cysts (x* 10^5 *ml*$^{-1}$*)*	*Flagellates*	**Non-viable cells (x* 10^5 *ml*$^{-1}$*)*
1	6.85±0.01	4.40±0.28	0	nd	0
2	6.94±0.04	7.65±1.20	0	d	0
3	7.06±0.04	15.60±0.71	0	d	0.05±0.07
4	7.04±0.02	10.45±0.78	3.65±1.77	nd	0.25±0.18
5	7.15±0.01	3.75±0.07	9.60±4.95	nd	1.55±0.21
6	7.14±0.04	2.85±0.35	5.15±1.77	d	6.15±1.66
7	7.32±0.01	2.45±0.35	2.35±0.64	nd	11.55±0.07

Explanation for symbols:

^{a}- the pH of fresh Bath-Spa medium is 6.80.

Data for flagellates are presented either as d (detected in cultures) or nd (not detected in cultures) only. *The non-viability of cells was determined by trypan blue inclusion.

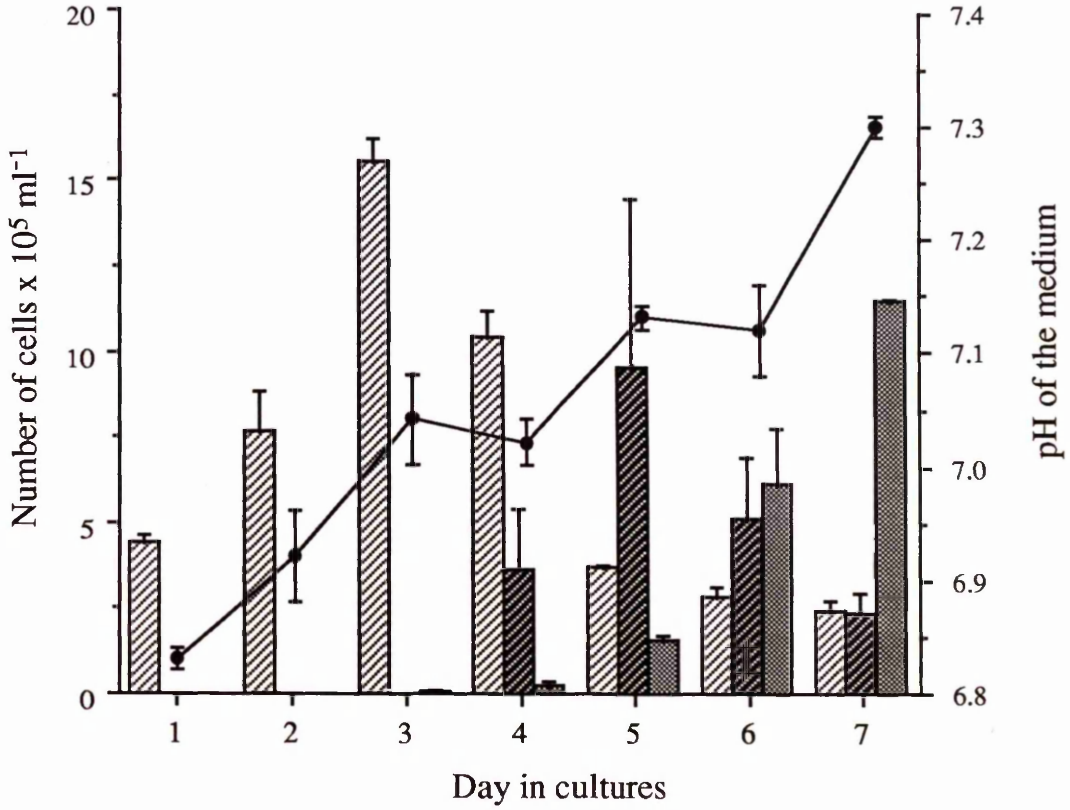

Figure 3.10. Culture composition of *Naegleria gruberi* CCAP strain 1518/1A grown axenically in Bath-Spa medium. The number of trophozoites, cysts, and non-viable cells counted on consecutive days after inoculation. The pH of the medium was also measured during growth. Data represented as mean values with standard deviations (error bars) from three separate experiments.
Explanation for symbols:
—●— pH, ▨ trophozoites, ▩ cysts, ▦ non-viable cells.

3.3.2. *Proteinases in different strains of Naegleria gruberi*

Proteinase patterns on gelatin SDS-PAGE gels in different strains of N. gruberi

Naegleria gruberi CCAP strain 1518/1G produced two bands of proteinase activity at pH 5.5 in the presence of 1 mM DTT (Figure 3.11, panel A). The position of these bands in relation to bands produced by *N. gruberi* CCAP strain 1518/1A is the first (top) band appears to be in the same position as band B (apparent M_r is 148 kDa), and the second band which shows very high activity is almost in the same position as band D in strain 1518/1A which has the same mobility as the ~98 kDa standard protein. *N. gruberi* CCAP strain 1518/7 produced three proteinase bands (Figure 3.11, panel A). The top band (although it is not clearly visible in gel) is about the same position as band B of strain 1518/1A, the second but very prominent band is about the position of band C (apparent M_r is 116 kDa) in strain 1518/1A and lastly a third band with apparent molecular weight of about 84 kDa. At pH 8.0 (without containing DTT) (Figure 3.11, panel B), the activity of band 148 kDa-enzyme in strain 1518/1G was inactivated, indicating its similarity with band B of strain 1518/1A. The activity of band 98 kDa-enzyme on the other hand seemed to be increased; a property which was also exhibited by bands DE of strain 1518/1A. All bands in strain 1518/7 which were observed at pH 5.5 seemed to be inactivated at pH 8.0; a new enzyme activity instead (a band of ~ 92 kDa mobility enzyme), was detected on the gel.

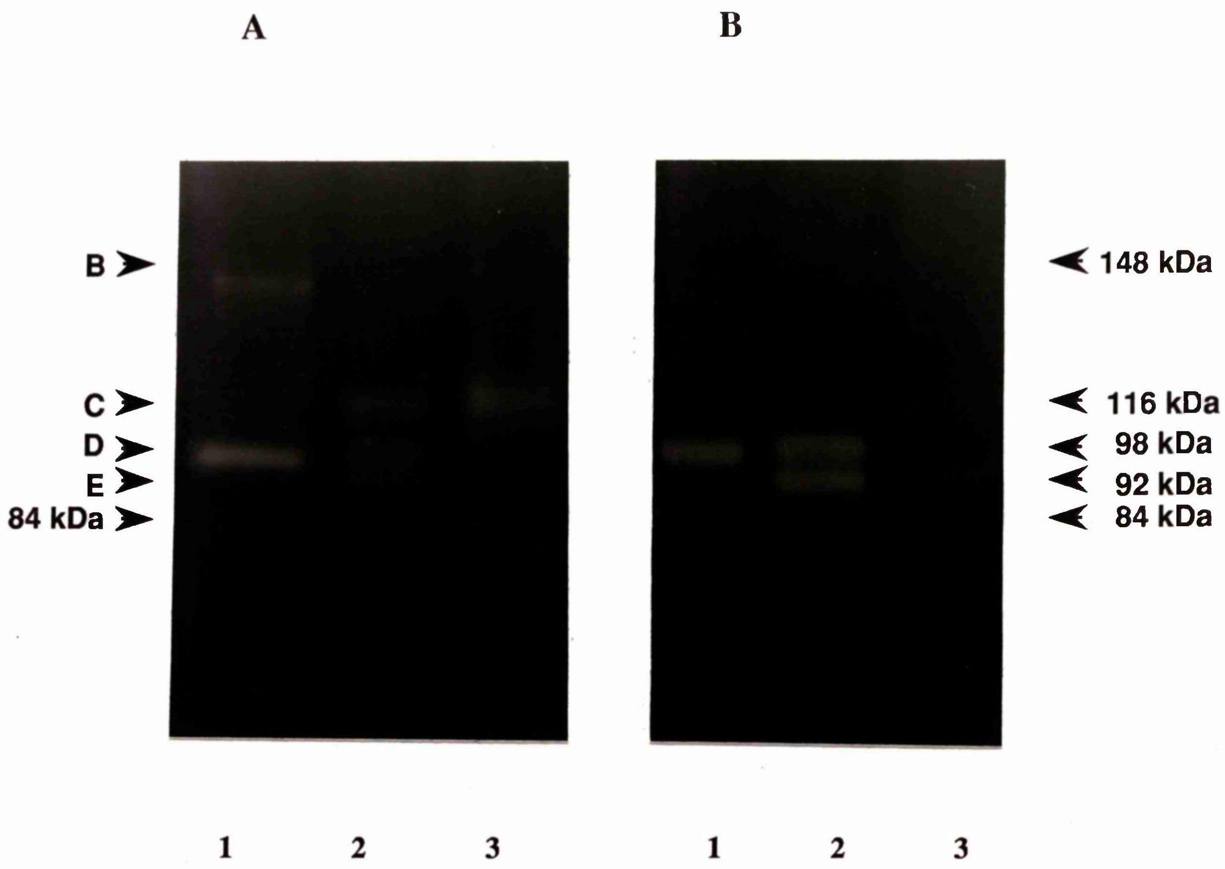
A
B
B
C
D
E
84 kDa
148 kDa
116 kDa
98 kDa
92 kDa
84 kDa
1
2
3
1
2
3

Figure 3.11. Proteinase pattern produced by different strains of *Naegleria gruberi* on gelatin gels. Panel A. The gel was incubated in 0.1 M sodium phosphate buffer, pH 5.5 containing 1 mM DTT. Panel B. The gel was incubated in sodium phosphate buffer pH 8.0, not containing DTT. Explanation for lanes: 1; strain 1518/1G, 2; strain 1518/1A, 3; strain 1518/7. The positions of the bands are indicated. The bands labelled in panel A (B, C, etc) are of strain 1518/1A for reference.

Characterisation of individual proteinases in strains 1518/7 and 1518/1G of Naegleria gruberi

Effect of pH and DTT on enzyme activity on gelatin gels

The effect of pH and DTT on individual bands in the cell lysates of *Naegleria gruberi* strain 1518/7 is striking as shown in Figure 3.12 (panel A). In this figure, the lysate of the amoeba apparently has four enzyme activities and only the top two bands are labelled temporarily as bands *a* and *b* according to increasing mobility of the enzymes on the gelatin gels for convenience in discussion. Careful investigations on the position of these bands on gelatin SDS-PAGE gels compared with bands in Figure 3.11, indicated that the broad band of 116 kDa enzyme was actually the fusion of band *a* and *b*; the other bands are the 92-kDa and the 84-kDa enzymes. All four bands are clearly visible when the gel was incubated in buffer, pH 5.5 containing 1 mM DTT. Without DTT, the intensities of bands *a* and 84-kDa enzyme were noticably reduced (lane 2, Figure 3.12, panel A). The activities of bands *a* and *b* (band of 116-kDa enzyme) seemed to be inactivated at pH higher than 6.5, despite the presence of DTT in the incubation buffer. The activity of band of 92-kDa enzyme on the other hand, was apparently increased by raising the pH especially when DTT was not present in the incubation buffer. The activity of band of 84-kDa enzyme was reduced with increasing pH and its activity apparently was not DTT-dependent. Bands *a*, *b* and 84-kDa enzymes were inactivated at higher pHs, and the only band which was observed in strain 1518/7 sample was band 92 kDa-enzyme. The activity of band 148 kDa-enzyme which was faintly observed in Figure 3.11, was not detected in this gel.

Only one band of enzyme activity (band of ~98 kDa protein) was clearly visible from cell lysate of *N. gruberi*, strain 1518/1G. The activity of this enzyme at pH 5.5 to 6.5 seemed to be enhanced with the presence of DTT (Figure 3.12, panel

B). At pH 7.0 and 8.0, the presence of DTT appeared to inactivate this enzyme, indicating similarity to the properties of band *c* of strain 1518/7 or band E of strain 1518/1A. The activity of band 148 kDa-enzyme is not evident in this figure.

Inhibitor studies to characterise the proteinases on gelatin SDS-PAGE gels

Various inhibitors (3,4-DCI, antipain, pepstatin, elastatinal and EDTA) were used to characterise the proteinase bands in strains 1518/1G and 1518/7 of *N. gruberi*. Bands of 116-kDa enzyme, 92-kDa enzyme and 84-kDa enzyme of strain 1518/7, and band of 98-kDa enzyme of strain 1518/1G in the two strains of *Naegleria gruberi* appeared to be inhibited by antipain (Figure 3.13 lane 3). EDTA appeared to inhibit the 98 kDa-enzyme activity in strain 1518/1G. 3,4-DCI, elastatinal and EDTA seemed to inhibit slightly band ~116 kDa enzyme of strain 1518/7 (Figure 3.13, panel A, lane 2). Since this band is composed of two enzymes (bands *a* and *b* enzymes) and were not always resolved, the inhibition of the ~116 kDa enzyme band by these inhibitors could be also due to the inhibition of one (or more) particular enzyme (s). It is then difficult to analyse the inhibition of band ~116 kDa enzyme by other inhibitors except by antipain which appeared to inhibit all enzymes in strain 1518/7. Band 92 kDa-enzyme in strain 1518/7 appeared to be inhibited by EDTA.

Substrate preferences of the proteinases from different strains of Naegleria gruberi

Four fluorogenic substrates, Z-Pro-Arg-NHMec, Z-Arg-Arg-NHMec, Bz-Phe-Val-Arg-NHMec and H-Pro-Phe-Arg-NHMec were used for this purpose. After electrophoresis, the gels were incubated at 37°C, in buffer, pH 5.5 containing 1 mM DTT. The bands formed on the gels when incubated with substrates Z-Pro-Arg-

NHMec, Z-Arg-Arg-NHMec and Bz-Phe-Val-Arg-NHMec are similar in pattern for all strains including strain 1518/1A which was used for comparing the position of bands in other strains on gels (Figure 3.14). Only a band of 98-kDa enzyme of strain 1518/1G and a band of 92-kDa enzyme of strain 1518/7 seemed to hydrolyse these substrates. The gel incubated with substrate H-Pro-Phe-Arg-NHMec for all strains however, shows more bands. Band of ~148-kDa enzyme (equivalent to band B of strain 1518/1A) and band of 98-kDa enzyme (equivalent to band D of strain 1518/1A) in strain 1518/1G, band of ~148-kDa enzyme, band of 116-kDa enzyme, band of 98 kDa enzyme and band of 84 k-Da enzyme in strain 1518/7 seemed to hydrolyse this substrate. Since the band of 98-kDa enzyme in strain 1518/7 was diffuse, it was difficult to detect the 92-kDa enzyme on the gel.

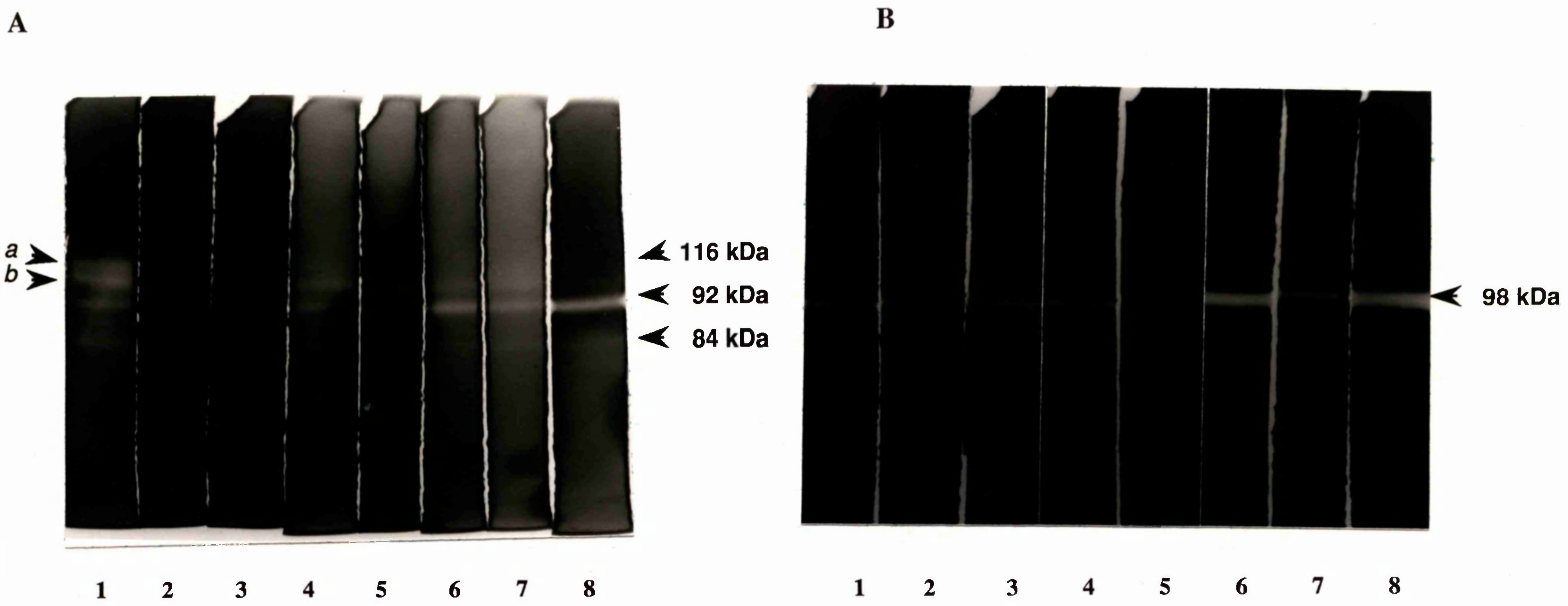

Figure 3.12. The effect of pH and DTT on enzyme activity on the gelatin gels of *Naegleria gruberi* CCAP strains 1518/7 (panel A) and 1518/1G (panel B). Explanation for lanes of panel A: The gel was incubated in buffer with the following treatments; 1; at pH 5.5, with 1 mM DTT, 2; at pH 5.5, without DTT, 3; pH 6.0 with DTT, 4; pH 6.0 without DTT, 5; pH 6.5 with DTT, 6; pH 6.5 without DTT, 7; pH 7.5 with DTT, 8; pH 7.5 without DTT. For lanes of panel B: 1; pH 5.5 without DTT, 2; pH 5.5 with DTT, 3; pH 6.0 with DTT, 4; pH 6.5 with DTT, 5; pH 7.0 with DTT, 6; pH 7.0 without DTT, 7; pH 8.0 with DTT, 8; pH 8.0 without DTT. Note that the 116 kDa enzyme is actually composed of band *a* and *b* enzyme activities (panel A),

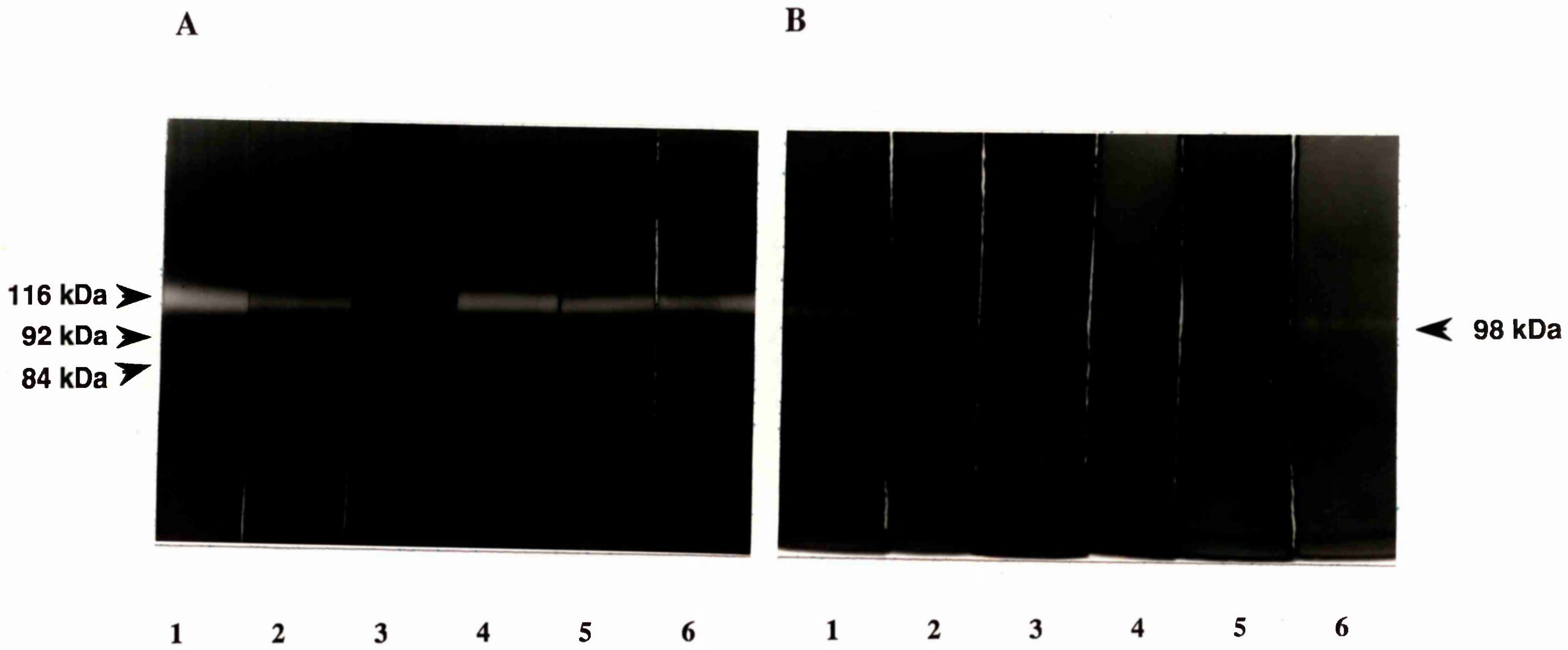

Figure 3.13. Effect of the inhibitors on proteinases produced by *Naegleria gruberi* CCAP strains 1518/7 (panel A) and 1518/1G (panel B). The gels were incubated in 0.1 M sodium phosphate buffer, pH 5.5 overnight, at 37°C. Explanation for lanes in both panels: 1; control, the gel was incubated in buffer only, 2; buffer containing inhibitor 3,4-DCI, 3; buffer containing antipain, 4; buffer containing pepstatin, 5; buffer containing elastatinal, 6; buffer containing EDTA. The amount of protein loaded in each well was 30 μg. The apparent molecular weight of the individual enzymes is indicated.

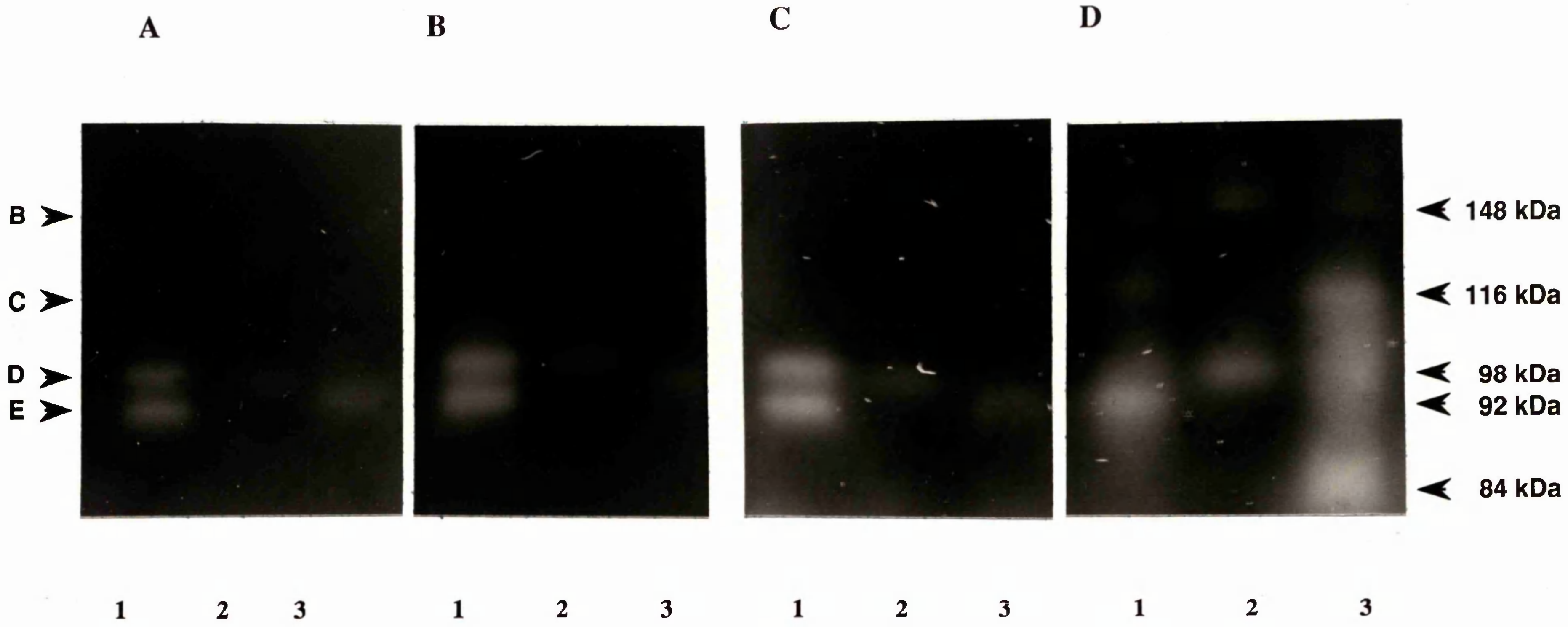
A
B
C
D
B
C
D
E
148 kDa
116 kDa
98 kDa
92 kDa
84 kDa
1
2
3
1
2
3
1
2
3
1
2
3

Figure 3.14. Proteinase patterns produced by different strains of *Naegleria gruberi* on gels incubated in different fluorogenic substrates. The gels were incubated at 37°C in 0.1 M sodium phosphate buffer, pH 5.5 containing 1 mM DTT and fluorogenic substrates. Explanation for panels: A. Substrate Z-Pro-Arg-NHMec. B. Substrate Z-Arg-Arg-NHMec. C. Substrate Bz-Phe-Val-Arg-NHMec. D. Substrate H-Pro-Phe-Arg-NHMec. Explanation for lanes: 1; strain 1518/1A, 2; strain 1518/1G, 3; strain 1518/7.

3.3.3. *Proteinases in pathogenic Naegleria fowleri*

On gelatin gels

Since the freeze-thaw method has been employed to detect various intracellular enzyme activities in protozoa (De Meester *et al.*, 1990), and S_A sample and cell lysates of *N. gruberi* exhibit a similar pattern of proteinases (see 3.3.1.), samples prepared by this method were used to detect proteinases in *N. fowleri*. Two proteinase bands were observed in the supernatant fraction of freeze-thawed sample of pathogenic *N. fowleri* on the gelatin gels when incubated in buffer pH 5.5, containing 1 mM DTT (Figure 3.15). The apparent molecular weight of the top band was ~170 kDa and the lower band was ~128 kDa. A pellet of freeze-thawed sample which represents enzymes associated with the membranes of *N. fowleri* seemed to produce only one band whose apparent molecular weight was ~128 kDa (Figure 3.15, panel A, lane 2). At pH 8.0 but in the absence of 1 mM DTT, only the band of ~128 kDa-enzyme was observed in both samples but its activity seemed slightly higher than at pH 5.5 (Figure 3.15, panel B).

Effect of inhibitors on the enzymes

Inhibitors E-64 and antipain were used to study their effects on proteinases in *Naegleria fowleri*. Only the band of 170-kDa enzyme in *N. fowleri* was observed clearly on the gel incubated in 0.1 M sodium phosphate buffer, pH 5.5 without DTT. This enzyme seemed slightly inhibited by E-64 but completely inhibited by antipain when compared with the band in control (Figure 3.16). The activity of the other enzyme (~128 kDa enzyme) seemed to be low, therefore it could not be detected on the gel even in the control and so no assumptions could be made about inhibitor sensitivity.

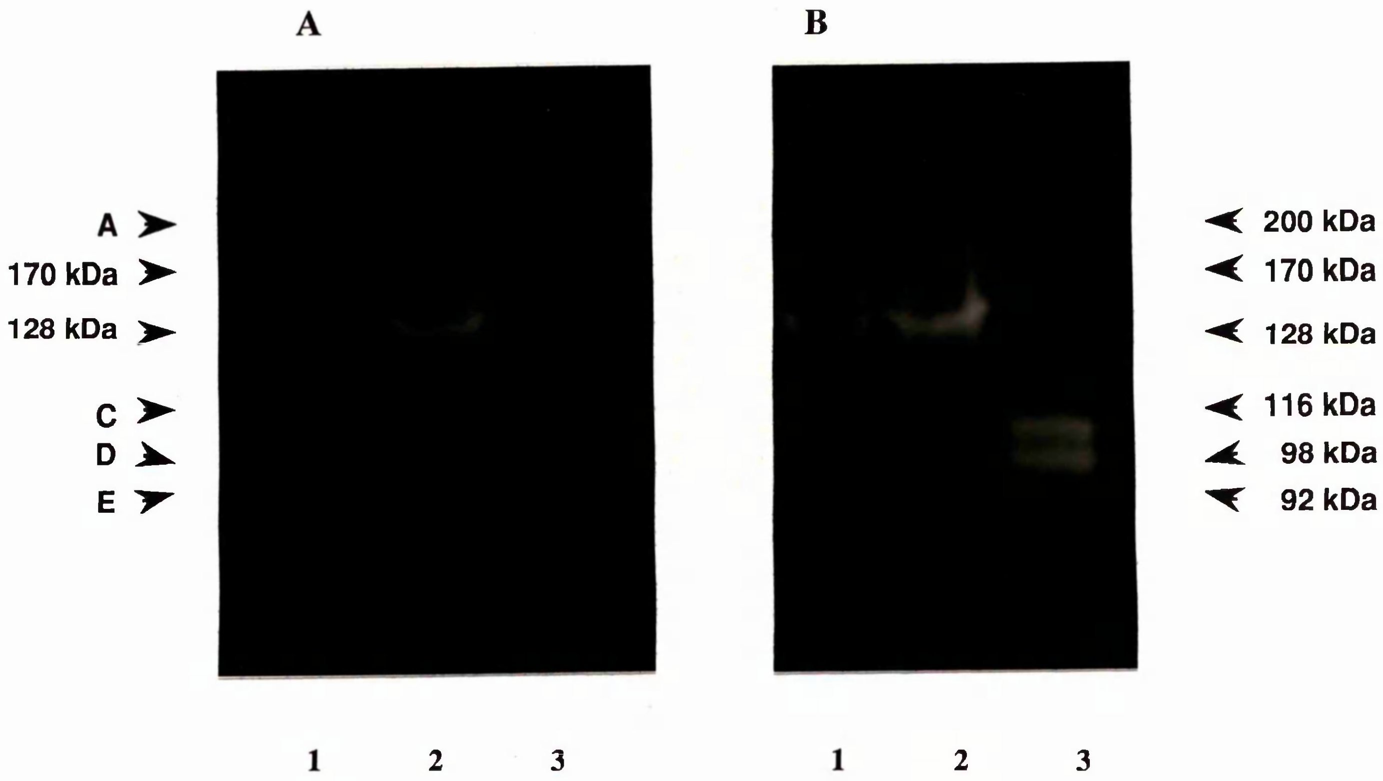

Figure 3.15. Proteinases in pathogenic *Naegleria fowleri*. Supernatant and pellet samples of freeze-thawed cells were run on the gelatin gels. (Cell lysates of non-pathogenic *Naegleria gruberi* CCAP strain 1518/1A were used to compare the position of the proteinase bands in *N. fowleri*). Panel A. The gel was incubated in 0.1 M sodium phosphate buffer, pH 5.5 containing 1 mM DTT. Panel B. The gel was incubated in sodium phosphate buffer pH 8.0, without containing DTT. Both gels were incubated at 37°C. Explanation for lanes: 1; supernatant of freeze-thawed sample, 2; pellet of freeze-thawed sample and resuspended in 0.25% (v/v) Triton X-100 in PBS, 3; cell lysates of *N. gruberi*.

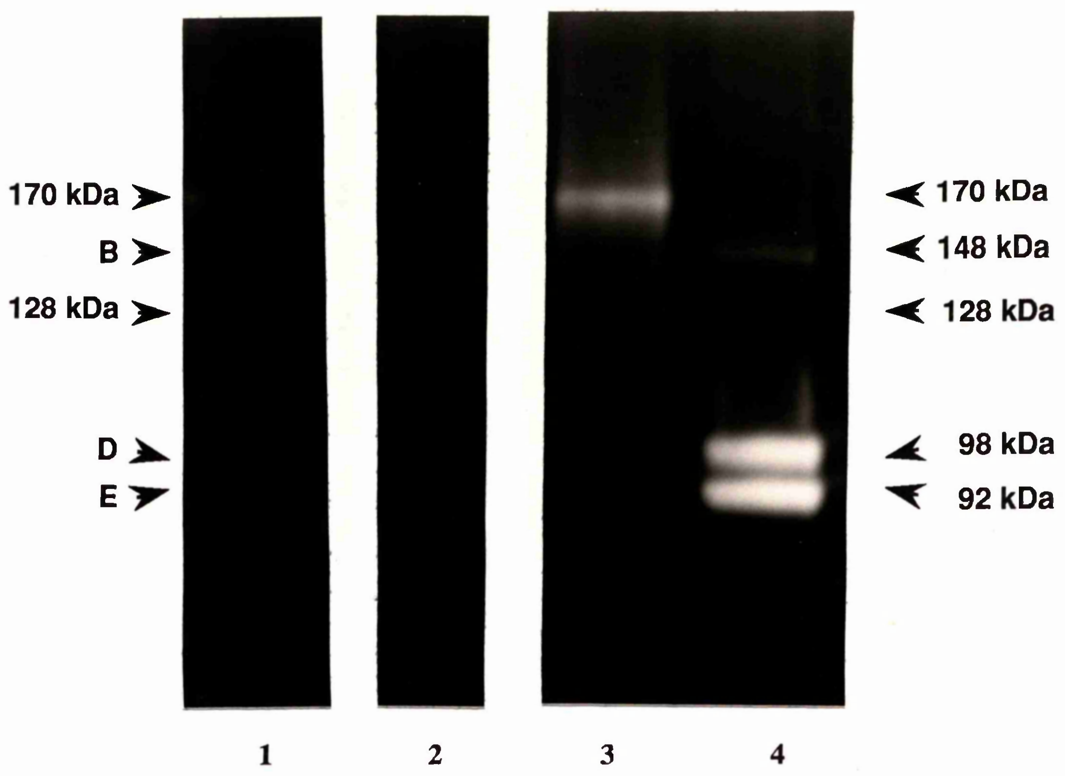
170 kDa
B
128 kDa
D
E
170 kDa
148 kDa
128 kDa
98 kDa
92 kDa
1
2
3
4

Figure 3.16. Effect of the inhibitors on proteinases of *Naegleria fowleri*. The gels were incubated in sodium phosphate buffer, pH 5.5 without containing DTT. Explanation for lanes: 1; inhibitor E-64, 2; antipain, 3; control, 4; cell lysates of *N. gruberi* strain 1518/1A for reference of the position of the bands in *N. fowleri*.

3.4. DISCUSSION

3.4.1. *Proteinases in Naegleria gruberi CCAP strain 1518/1A*

Various techniques were employed to detect the activities of proteinases in *Naegleria gruberi* crude lysates in this study. The proteinase activities were detected either by looking at the rate of hydrolysis of chromogenic substrates or by electrophoresis in the SDS-PAGE gel then incubated with fluorogenic substrates or by observation of the hydrolysis of gelatin in SDS-PAGE gels by lysates of *Naegleria*. Gelatin SDS-PAGE gels have been used sucessfully in the analyses of the proteinases of other protists (Lockwood *et al.*, 1987) and provide better resolution and sensitivity than the haemoglobin gel method (North *et al.*, 1988). Both methods of electrophoretic analysis mentioned above would allow detection and study of the properties of the multiple enzymes in *Naegleria* crude lysate individually, without being purified.

Lysis of trophozoite samples from cultures axenically grown in liquid medium, lysed either by 0.25% (v/v) Triton X-100 in PBS or by freeze-thaw treatment, seemed to produce the same number and pattern of proteinase bands on gelatin gels. Four proteinase activities were usually observed, namely bands A (apparent M_r ~200 kDa), B (apparent M_r ~ 148 kDa) and doublet DE (apparent M_r ~98 kDa and 92 kDa, respectively). The trophozoite samples seemed additionally to have an enzyme of 116 kDa (band C). The absence of band A in some of the trophozoite and S_A (trophozoite supernatant) samples was probably due to its activity being so low it could not be detected readily in the gelatin SDS-PAGE gels. The use of crude lysate to detect the proteinase activities in the present study could cause the impurities to interfere with the proteinase activities especially for a high molecular weight enzyme such as band A enzyme. The appearance of band C in trophozoite samples is associated with the high amount of protein loaded in the gelatin SDS-PAGE wells and also the addition of DTT to the gel incubation buffer at pH 5.5.

Detection of membrane-associated enzymes

The freeze-thaw technique, which involves repeatedly placing the suspended pellet in liquid nitrogen and then thawing in a water bath at 37°C, was employed to detect the possible presence of membrane-associated proteinases in *Naegleria gruberi*. After the removal of the supernatant sample, the remaining pellet was resuspended in 0.25% (v/v) Triton X-100 in PBS to ensure the release of the enzymes from the membrane. Any band observed from this sample thus represents the membrane-associated enzymes. The result was that doublet DE bands were observed in this sample (Figures 3.2A and 3.3). These enzymes were also observed in the supernatant sample although their activities were higher in the pellet sample despite the amount of protein used for the pellet sample being less than that used for the supernatant sample. Doublet DE could therefore be defined as membrane-associated enzymes; more detailed investigations however, are needed to localize these enymes at the subcellular level. Methods as described by Lowrey and McLaughlin (1985b) should be followed in order to screen the whole homogenate of *N. gruberi* to identify the subcellular localization of these enzymes. These methods involved density centrifugation of the cell lysates which separate cytoplasmic inclusions from the cell membrane. Their distribution both in the supernatant and the pellet samples could be suggested to have been associated with both the surface membrane and lysosomal particles of *N. gruberi*. α-D-glucosidase and an aminopeptidase in *N. fowleri* have been shown to have such bimodal activities (Lowrey and McLaughlin, 1985b). *N. gruberi* has been observed to cause tissue destruction *in vitro* and its pathogenicity seems to be contact-dependent

(Brown, 1979), the membrane-associated enzymes such as bands DE enzymes could therefore involved in pathogenesis.

Characterisation of individual proteinases in the trophozoite samples of N. gruberi

Individual proteinases in *Naegleria gruberi* CCAP strain 1518/1A were characterised by their apparent molecular weight (M_r), activity at different pHs with or without the presence of 1 mM DTT, sensitivity to various inhibitors and also substrate preferences. Although the proteinases detected in *N. gruberi* lysates could not be separated individually by gel filtration of FPLC except band A in fractions 9 and 10, they (bands A, B, C and doublet DE enzymes) could be observed on gelatin SDS-PAGE gels. Their activities seemed to be affected by pH and the presence of DTT in the gel incubation buffer. The activity of band A increased with increasing pH and at higher pH its activity was not DTT-dependent. Bands B and C were observed to be reduced in activity at pH higher than 6.0 and without DTT their activities were completely inactivated; these enzymes could possibly be suggested as lysosomal since they are active only at slightly acidic pH (Barrett *et al.*, 1988). The activities of doublet DE appeared to increase with the increasing pH; at these pHs (6.0 to 8.0) their activities were not DTT-dependent. At pH 5.5, in the presence of DTT, the activities of all enzymes appeared optimal since they could be detected clearly on gelatin gels.

Band A was observed to be inhibited by APMSF, suggesting that this enzyme is of the serine proteinase type; this enzyme is also active at higher pHs (6.0 to 8.0). Bands B and C were observed to be inhibited by antipain and probably belong to the cysteine proteinase group, since their activity is high at pH 5.5, and DTT-dependent. The activities of bands DE seemed to be diminished by various inhibitors such as APMSF, E-64 and antipain. At pH 5.5, these enzymes behaved as cysteine proteinase types; DTT-dependent and inhibited by E-64 and antipain.

From inhibitor and pH optimum studies, proteinases in *Naegleria gruberi* can be categorised into four groups: Group 1) Band A proteinase whose apparent M_r is ~200 kDa, is sensitive to APMSF, and active at higher pH; Group 2) Band B proteinase (apparent M_r ~148 kDa) which is sensitive to antipain, slightly inhibited by E-64 but not sensitive to APMSF, active only at lower pHs and its activity is DTT-dependant, and may be a cysteine proteinase; Group 3) Band C proteinase (apparent M_r ~116 kDa), active at lower pH and DTT-dependant, sensitive to antipain could also be a cysteine proteinase; Group 4) Proteinases of bands DE (~98-kDa and 92-kDa enzymes) which are markedly inhibited by antipain and by E-64, slightly inhibited by EDTA and APMSF and are more active at higher pHs. DTT inhibited slightly their activities at these pHs. At lower pHs, their activities are DTT-dependent. All of these enzymes (except group 1) are of the cysteine proteinase type since they are inhibited (partially or completely) by antipain and E-64 and their reactions at lower pHs are DTT-dependent (Coombs and North, 1983; North *et al.*, 1990b).

The properties of bands B and C enzymes in *N. gruberi* seem to fit the properties of mammalian lysosomal Cathepsins B, H and L, examples of typical cysteine proteinases which are active at acidic pH and their activities are stimulated by DTT and sensitive to cysteine proteinase inhibitors (Barrett *et al.*, 1988). Doublet DE enzymes, on the other hand, exhibit both lysosomal cysteine proteinase and serine/metallo-proteinase properties. This finding could be proof that they are associated with both lysosomes and the surface membrane of *N. gruberi*. Metallo-proteinases on the surface of the parasite *Leishmania* have been reported (Bouvier *et al.*, 1990). Further characterisation of group 1 which consists of band A enzyme based on the inhibitor studies, could not be done since this enzyme was not consistently detected in *Naegleria* lysates.

Activity of Naegleria lysates on peptide nitroanilides and fluorogenic amido methylcoumarin substrates

By spectrophotometric studies, using chromogenic substrates such as Bz-Pro-Phe-Arg-Nan, Bz-Arg-Arg-Nan and D-Val-Ser-Arg-Nan, proteinases detected in *Naegleria* lysates seemed to have preference for substrate Bz-Pro-Phe-Arg-Nan when compared with other substrates used in this study. Proteolytic activity of *Naegleria* lysate towards this substrate occurred at all pHs (pH 5.5 to 8.0) and the activity was stimulated by DTT. The activity of the lysate towards other substrates (Bz-Arg-Arg-Nan and D-Val-Ser-Arg-Nan) on the other hand, was not stimulated by DTT and only took place at alkaline environment (pH 7.0 and 8.0). On gels, bands of B, C and doublet DE enzymes seemed to hydrolyse substrate H-Pro-Phe-Arg-NHMec whereas the other substrates (Z-Pro-Arg-NHMec, Bz-Phe-Val-Arg-NHMec and Z-Arg-Arg-NHMec) were being hydrolysed only by doublet DE enzymes. These results are in agreement with those for some other protozoan cysteine proteinases which have preference towards Bz-Pro-Phe-Arg-Nan (North *et al*, 1983; Lockwood *et al*, 1984) suggesting these enzymes may have similar binding sites for the substrate. Substrates which have arginine residues in the P_1 position (as in all fluorogenic substrates used in the present study) are good substrates for mammalian Cathepsin B (Barrett *et al.*, 1988). Only doublet DE enzymes exhibit similar preferences to Cathepsin B. The other proteinases in *N. gruberi* are apparently more selective in hydrolysing the substrates used. Bz-Pro-Phe-Arg-Nan has proved to be a good substrate for detecting proteinases activities in *N. gruberi*.

Presence and role of proteinases in different stages of the life cycle

Trophozoites grown on agar with live bacteria seemed to produce bands A and DE only. They did not appear to possess either band B or band C enzymes despite loading higher amounts of protein onto the gel than those used for trophozoite samples from axenic cultures (Figure 3.2A, panel C). The difference in proteinase patterns of trophozoite samples between the two cultures might therefore reflect the different manner of feeding. On agar, the amoebae phagocytose the live bacteria, whereas in axenic cultures, the amoebae take the complex medium (Bath-Spa medium) into the cells by pinocytosis (Brent, 58). Both bacteria and the medium (the liquid form of food) are then digested by enzymes in the food vacuoles or secondary lysosomes of the amoebae. The possession of band A and doublet DE enzymes seems sufficient for the amoebae to feed on bacteria.

Flagellate samples seemed to produce a similar pattern of proteinases to that of amoebae grown on agar with bacteria, with bands A and doublet DE observed on the gels. The absence of band B in this sample is probably because it is not important in digestion since flagellates are non-feeding stages of *Naegleria* (Fulton, 1970). Cysts, as resting stages of *Naegleria* seem to produce only one enzyme band. The apparent molecular weight of this enzyme (~116 kDa) and its activity being inactivated at pH 8.0 show a similarity to band C in the trophozoite sample; and it could be the same enzyme. The cyst stage of *Naegleria* thus, appears not to have much proteinase activity, suggesting that most cellular activities which involve these enzymes are reduced. The presence of compact, ribosome-like particles in vacuoles in encysting *N. gruberi* (Schuster, 1963) might indicate that autophagocytosis was taking place in the amoeba. Since trophozoites are actively endocytosing the surrounding medium and presumably digesting the proteins it contains, and as endocytosis ceases in the flagellate and in the cyst, the greater number of proteinases in the trophozoite may be related to the feeding process.

Enzymes secreted by Naegleria gruberi

Other than those retained intracellularly, *N. gruberi* strain 1518/1A seems to secrete three bands of proteinase enzymes into the culture medium. Two of the enzymes (whose apparent M_r is 92 and 75 kDa, respectively) appear to be active only at pH 5.5 since only the third band (apparent M_r is 90) was observed at pH 8.0. Attempts to characterise these enzymes were made by using the inhibitor E-64. Interestingly, at least 9 bands of enzymes appeared on the gelatin SDS-PAGE gel after treatment with this inhibitor. A possible explanation for the appearance of these enzymes after E-64 treatment is that the three secreted enzymes which are sensitive to this inhibitor, and therefore could be of the cysteine proteinase type, perhaps inactivate other proteolytic enzymes secreted by the amoebae. Once their activitites were inhibited, the activities of the otherwise inactivated enzymes could be observed on the gelatin SDS-PAGE gels. This phenomenon however, needs further investigation.

The release of proteinases extracellularly by *Naegleria gruberi*, even when the amoeba is grown in axenic liquid medium, might indicate that these enzymes are essential for breaking down the complex components of the medium such as peptone, before they are taken into the cell by pinocytosis. *Euglena gracilis* secretes more extracellular proteinases when peptone is added to the medium (Nakano *et al.*, 1979). Other enzymes (which were retained intracellularly) would then be responsible for further digestion of these complex materials in the cell. The mechanism of release of these enzymes is not known. In *T. vaginalis*, the secreted enzymes are stored temporarily in lysosomes before being released into the environment (D.A. Scott *et al.*, personal communication). The results of this study indicate that *N. gruberi* secretes proteinases primarily for food digestion outside the cell. A similar manner of digestion seems to be adopted by this amoeba or by pathogenic *N. fowleri* when destroying tissue cells *in vitro* (Marciano-Cabral and

Bradley, 1982; Fulford and Marciano-Cabral, 1987). The cytopathic effect of the amoebae is the result of a lytic process followed by phagocytosis of the cellular debris released.

Proteinases in different phases of growth

The results of the gelatin SDS-PAGE gelatin gel analyses have demonstrated that *Naegleria gruberi* lysates contain multiple proteinases; proteinases of bands A, B, C and DE. All bands except band C could be detected in all samples taken from day 1 (D_1) to day 7 (D_7) after inoculation, although differences in intensity of each band were observed. All bands were more clearly observed in samples D_3 and D_4 compared with other samples (Figure 3.9). This corresponds with the higher number of the actively growing trophozoites observed in cultures at this time (Table 3.2 and Figure 3.10). Hence it seems that the four proteinases may be produced by actively growing amoebae.

Cysts alone produced band C enzyme (Figure 3.2A, panel C) and so it was expected that this band would be found in samples D_4 to D_7 due to the increased number of cysts in these cultures (Table 3.2). However, this was not found to be the case. Cysts were later found not to be readily lysed in 0.25% (v/v) Triton X-100 in PBS, if they were not also subjected to mechanical rupture of the walls, so the bands produced by each stage of growth on the gelatin gels in this study do not belong to cysts. Furthermore, the C enzyme is only detected in gels if the amount of protein loaded onto the wells is more than 20 μg and its activity is optimum only at pH 5.5 but in the presence of DTT. Flagellates on the other hand, transform to the amoeboid phase readily unless this transformation was interrupted e.g. as by fixing the flagellates with 0.001M $ZnCl_2$ (Preston and O'Dell, 1973). The bands observed in the gelatin SDS-PAGE gels from cell pellets lysed in Triton X-100, thus could be suggested to be from trophozoites only. The difference in intensity of each band may reflect the state of trophozoites during growth in cultures. In older cultures (such as at D_6), although some trophozoites were still present, they were not in a healthy condition, their size was observed to be reduced and many were transforming into cysts, thus there would be fewer enzymes in the cells. The increase in number of the non-viable cells in older cultures did not change the number of proteinases and the intensity of proteinase bands observed in the gels.

The pH of the medium was observed to increase during amoeba growth in cultures (Figure 3.10; Table 3.4). A similar observation has been reported in *Naegleria gruberi*, strain EG, grown in agitated cultures by Weik and John (1977) who suggested that the pH changes may reflect changes in metabolism and differentiation of the amoebae induced by oxygen depletion and a switch-over to fermentative metabolism. Since the amoebae seem to use glucose in small amounts for growth (Nerad *et al.*, 1983), the pH increase is probably due to deamination of amino acids for an energy source during growth in culture (Weik and John, 1977). Regardless of the phases of at which the trophozoites were harvested for preparing the cell lysates, the bands DE enzymes could be detected clearly in all samples indicating their importance in this amoeba.

3.4.2. *Proteinases in different strains of Naegleria gruberi*

All strains of *Naegleria gruberi* (CCAP strains 1518/7 and 1518/1G including strain 1518/1A) seemed to have multiple forms of proteinases which could be observed on gelatin SDS-PAGE gels. Interestingly, each strain exhibited a different pattern of proteinases either in gelatin SDS-PAGE gels or in SDS-PAGE gels incubated in fluorogenic substrates. Although having different pattern of proteinases, the bands which have the same apparent molecular weight in each strain seem to share common characteristics implying that they could be the same enzymes. Bands of 148 kDa enzyme in all strains of *N. gruberi* (1518/1A, 1518/1G and 1518/7) are active at lower pH and are DTT-dependent, inactivated at higher pH (pH>6.5) and have preference only towards substrate Bz-Pro-Phe-Arg-Nan. Since the detection of this enzyme sometimes was not clear in the gels, its properties based on inhibitor studies could not be investigated.

The band of 116 kDa-enzyme which was observed only in strains 1518/1A and 1518/7, like the band 148 kDa-enzyme, was observed to be active at lower pH and its activity was stimulated by DTT; it only had preference towards substrate Bz-Pro-Phe-Arg-Nan. The activity of this enzyme was inhibited by antipain, elastatinal and EDTA; in strain 1518/7, this enzyme was also inhibited by 3,4-DCI. The activities of bands of 98 kDa and 92 kDa enzymes seemed to be DTT-dependent at lower pH but at higher pH (pH>6.5), their activities were increased and not stimulated by DTT. The 98 and 92 kDa enzymes in all strains seemed to have preference towards substrates H-Pro-Phe-Arg-NHMec, Bz-Phe-Val-Arg-NHMec, Z-Arg-Arg-NHMec and Z-Pro-Arg-NHMec used in this study. Their activities were inhibited by antipain and EDTA.

Different patterns of proteinases in the three strains of *Naegleria gruberi* used in this study might be indicative of genetic, physiological and morphological heterogeneity within the species (refer to Table 3.1) as has been shown by isoenzyme pattern differences between a smooth and a rough cyst strain of *N. gruberi* (Warhurst and Thomas, 1978). Allozyme data for 33 loci of 30 enzymes studied (excluding proteinases) in *Naegleria* isolates however, indicate that *N. gruberi* isolates from culture collection (included also the strains of *N. gruberi* used in this study) formed five single and widely-separated zymodemes which could be interpreted as five separate species; strains 1518/1A, 1518/1G and 1518/7 were found to be in separate groups by this method of identification (Robinson *et al.*, 1992). Restriction endonuclease DNA patterns in *N. gruberi* isolates have also indicated genetic heterogeneity in this species (De Jonckheere, 1987). Although proteinase patterns observed in different strains of *N. gruberi* in this study provide further evidence that *N. gruberi* strains in culture collections could not be from a single species, all strains appear to have conserved some common enzymes which could be used when combined with other methods for identification of *Naegleria* spp. These enzymes could be encoded by conserved genes and transcribed in all strains of *N. gruberi*. The companion bands of proteinases in different strains of *N. gruberi* could be suggested as a result of posttranscriptional modification to fit several requirements of the amoeba to live in diversified environments or they could be from different gene products.

From electrophoretic patterns of some enzymes in *Naegleria* including *N. gruberi*, suggestions have been made that diploidy and genetic recombination might occur in *Naegleria* (Cariou and Pernin, 1987; Pernin and Cariou, 1989). There is also a possibility in this study that genetic recombination might have occurred between strains in *N. gruberi*. The proteinase profile for strain 1518/1A observed in this study could be obtained by adding the proteinase profiles for strains 1518/1G and 1518/7. Data obtained in this study however, are not sufficient to provide evidence that genetic exchange has actually taken place between strains of *N. gruberi*.

3.4.3 ***Proteinases in pathogenic Naegleria fowleri***

Pathogenic *Naegleria fowleri* seems to posses at least two high molecular weight proteinases on gelatin gels, at pH 5.5. Their apparent M_r are 170 kDa and 128 kDa. The 170 kDa band enzyme appears to be inactivated at pH 8.0, and in this way is similar to the band B enzyme in *N. gruberi* strain 1518/1A. The activity of band 128 kDa enzyme on the other hand, was observed to be higher at pH 8.0, resembling the doublet DE in *N. gruberi*, strain 1518/1A. The activity of band 170 kDa enzyme was observed to be partially inhibited by inhibitor E-64 but markedly inhibited by antipain. The activity of band 128 kDa enzyme seemed to be stimulated by DTT in the gel incubation buffer, at pH 5.5. So at pH 5.5 without DTT even in the control, the activity of this enzyme is low, so the inhibition effect of inhibitors on this enzyme could not be observed. Based on sensitivity towards E-64 and antipain, and also on its DTT-dependent activity at pH 5.5, the band of 170 kDa enzyme, although having relatively high apparent M_r , could be a lysosomal cysteine proteinase. Most lysosomal cysteine proteinases found in mammalian cells have apparent M_r between 20 kDa and 35 kDa (Barret *et al*., 1988). The result from the present proteinase study gives strong evidence that *N. fowleri* and *N. gruberi* are not the same species, as they do not have common enzymes, in contrast to what has been observed for different strains of *N. gruberi*. The similarity in properties of the enzymes in both species at different pH and the fact that they were inhibited by the same inhibitors could be indicative that they belong to the same group of enzymes.

The lysate of *Naegleria fowleri* has been observed to cause tissue destruction *in vitro* (Dunnebacke and Schuster, 1974; Fulford *et al*., 1985; Marciano-Cabral and Fulford, 1986). Some of the enzymes identified (both in lysate and cell free-medium of *N. fowleri*) are lipolytic enzymes such as phospholipase A and sphingomyelinase (Hysmith and Franson, 1982) which probably act as aggressors in promoting primary amoebic meningoencephalitis (Curson and Brown, 1978). Proteinases in *N. fowleri* observed in this study could also be suggested to be involved in pathogenesis of this amoeba both *in vivo* and *in vitro* since they are present in the cell lysate of the amoeba. The involvement of proteinases in the pathogenicity of some parasitic protozoa has been proven by stage-specific proteinases in *Leishmania m. mexicana* promastigotes (Robertson and Coombs, 1992), correlation between cytopathic effect of *Entamoeba histolytica* with secretion of a cysteine proteinase (Keene *et al*., 1990) and the coincident inhibition of the trophozoite proteinases and *Plasmodium falciparum* development by the use of lysosomal cysteine proteinases inhibitors (Rosenthal *et al*., 1989). A membrane-associated metallocollagenase in *Entamoeba histolytica* has been proposed to play a role in degradation of extracellular matrix molecules during invasion of this amoeba (Munöz *et al.*, 1982) so the 128 kDa enzyme in *N. fowleri* might also play a vital role in *Naegleria* pathogenicity.

Proteinases in *Naegleria* spp observed in this study appear to be high molecular weight enzymes whereas proteinases reported from other protozoa generally have their apparent molecular weight in the range of 20 kDa to 96 kDa (Keene *et al.*, 1990; North *et al.*, 1990b; Robertson and Coombs, 1992). Despite being high in apparent molecular weight, some of the proteinases in *Naegleria* spp are of the cysteine proteinase type. This finding provides further evidence that these enzymes are common in a wide range of protozoa (North, 1982: 1992) and that they are not only present in parasitic forms. It is interesting to speculate why there are not many forms of proteinases present in pathogenic *N. fowleri* compared with other parasitic protozoa such as *Trichomonas* spp (Lockwood *et al.*, 1987) and *Leishmania mexicana mexicana* (Robertson and Coombs, 1992). Are the multiple forms of proteinases in these protozoa simply due to the presence of multiple genes or are they the result of posttranslational modifications so they are not related to pathogenicity? Details on functional aspects of proteinases in protozoa need to be carried-out in future studies. This study suggests that the amino acid sequence of proteinases in *Naegleria* spp, especially the doublet DE enzymes (since their association with both lysosomes and membrane-associated) in *N. gruberi*, should be examined further to see if they belong to the papain superfamily of cysteine proteinases. This information could aid understanding, the characteristics of enzymes belong to this proteinase group in protozoa.

3.5.0. SUMMARY

1. *Naegleria gruberi* seems to posses proteinase enzymes either retained intracellularly or secreted into the culture medium or membrane-associated. The pattern of intracellular proteinases in SDS-PAGE gelatin gel was observed to be different in different stages of the life cycle of *N. gruberi* strain 1518/1A and is suggested to be correlated to the feeding activity of this amoeba. At least 5 enzymes were detected in actively mutiplying amoebae; they are referred to as bands A, B, C and DE enzymes. The apparent M_r of band A is ~200 kDa, band B is ~148 kDa, band C is ~116 kDa, band D is ~98 kDa and band E is ~92 kDa. Bands DE gave the most prominent bands in gels and were also membrane-associated. Flagellates appear to posses enzymes A and DE, and cysts only band C.

2. The activities of *N. gruberi* proteinases except band A, were inhibited by common cysteine proteinase inhibitors such as antipain and E-64, which suggests they belong to the cysteine proteinase group, although inhibition of doublet DE enzymes was also observed by other inhibitors such as APMSF and 3,4-DCI, specific for different groups of proteinases. At lower pH (pH 5.5), their activities were DTT-dependent; at higher pHs (such as at pH 8.0), only the activity of doublet DE enzymes was commonly observed and this activity was not DTT-dependent. The preferences of the different enzymes for various peptidyl chromogenic substrates vary, although all proteinases in *N. gruberi* strains seem to have high activities towards the substrate Bz-Pro-Phe-Arg-Nan.

3. Gel filtration through a Superose 12 column on FPLC can only partially purify the individual enzymes in cell lysates of *N. gruberi*, strain 1518/1A. Band A enzyme appears to co-fractionate with band B enzyme, or bands DE enzymes during fractionation, but it is also free of other detected activities in earlier fractions.

4. Proteinase patterns in gelatin SDS-PAGE gels for amoebae grown axenically in liquid medium seems to be different from patterns for amoebae grown on agar with live bacteria. The absence of bands B and C from the latter culture has been taken to indicate they may not be involved in digestion of bacteria while the amoebae were growing in these cultures.

5. A similar pattern of proteinases in gelatin SDS-PAGE gels has been found for different stages of growth in culture, but the intensity of each band was different. Since cysts are not so readily lysed by Triton-X-100-treatment as trophozoites, and flagellates revert to the amoeboid stages so quickly, the difference in intensity may be due to the condition of the trophozoites in cultures during growth. As the cultures grew older, the number of trophozoites was reduced, and the number of cysts and non-viable cells was increased. The pH of the medium was observed to increase during growth. These factors indicate that the culture medium changes during growth, and so affects the growth of trophozoites in cultures thus causing the different intensity of proteinase bands on the gel.

6. *N. gruberi* strain 1518/1A secretes proteinases into the culture medium and these enzymes could be essential for food digestion outside the cell. Secretion of these enzymes might also be related to cytopathogenicity of this amoeba *in vitro* reported by other studies.

7. Different patterns of proteinases observed in different strains of *N. gruberi* may be indicative of their genetic, physiological and morphology heterogeneity within the species. Some of the enzymes however, have been conserved in all strains thus they could be used for identification of *Naegleria gruberi* as a species. There is also a possibility that genetic exchange might have taken place between strains of *N. gruberi*.

8. *N. fowleri* lysates posses at least two proteinase activities whose apparent M_r is 170 kDa and 128 kDa. Band of 128 kDa-enzyme is membrane-associated and its activity is higher at alkaline pH compared with lower pH; at

lower pH its activity is greatly stimulated by DTT. The activity of band 170 kDa enzyme is higher at pH 5.5 and is stimulated by DTT, its activity is inactivated at pH 8.0. The activity of this enzyme is inhibited by antipain and slightly inhibited by E-64 indicating it belongs to the cysteine proteinase group.

Chapter 4

Pathogenicity of Hartmannella sp.

Chapter 4

PATHOGENICITY OF *HARTMANNELLA SP.*

4.1. INTRODUCTION

Acanthamoeba spp have been found to be capable of invading the human cornea and destroying it, should they be introduced onto the cornea by soft contact lens wear (John, 1991). Isolates of amoebae from contact lens cases during a survey of microbial contaminants of contact lens cases in the West of Scotland (Devonshire *et al.*, 1993) proved to include several *Acanthamoeba* and one *Hartmannella*. This part of my thesis concerns an investigation of the possibility that this *Hartmannella sp.* may be capable of inflicting similar damage to *Acanthamoeba* when it comes into contact with the cornea.

Amoebae of the genus *Hartmannella* superficially resemble those of *Naegleria* in that they are small and monopodial with a vesicular nucleus containing a large nucleolus, and a posterior contractile vacuole near the uroid. The pattern of pseudopod formation however, is not eruptive in *Hartmannella* and other genera of the Hartmannellidae, while it is eruptive in *Naegleria* and the Vahlkampfiidae. Nuclear division in the two families is markedly different, hartmannellids having an 'open' mitosis with breakdown of the nucleolus and nuclear envelope (Page and Blanton, 1985; Page, 1987), quite unlike the promitosis of the Vahlkampfiids. Finally, the mitochondria of the hartmannellids have tubular cristae while those of *Naegleria* (and all the Heterolobosea) are flattened and plate-like (Page, 1974; 1985; Page and Blanton, 1985).

The five species of freshwater *Hartmannella* recognised at present are *Hartmannella hyalina* (Dangeard, 1900), *Hartmannella agricola* (Goodey, 1916), *Hartmannella vermiformis* Page, 1967, *Hartmannella cantabrigiensis* Page, 1974, and *Hartmannella crumpae* Singh and Hanumaiah, 1979. All species have been isolated from soil, freshwater and stagnant water reservoirs such as drains (Page, 1967a; Page, 1988; Breiman *et al.*, 1990). It should be noted that in the past there has been confusion of the genus *Hartmannella* with the genus *Acanthamoeba*. For example, *Acanthamoeba culbertsoni* was initially designated *Hartmannella culbertsoni* but this confusion has now been clarified by Page (1967b). *Hartmannella vermiformis* in particular has been suspected of tissue invasive potential. Thus Cerva *et al.*, (1973) found it in the human nasal mucosa and Kadlec (1978) in the bronchi of the dog and trachea and intestine of turkeys. Kadlec (1978) failed to demonstrate pathogenicity of his isolates to mice and guinea pigs and tests of freshwater isolates by Cerva (1971) were likewise negative.

A crucial requirement for establishing corneal infection by opportunistic free-living amoebae such as *Acanthamoeba castellanii*, is the ability of the amoebae to bind to the corneal surface. The amoebae apparently adhere, invade and produce damage only on human, pig and Chinese hamster corneas, not on the corneas of other animals (Niederkorn *et al.*, 1992). The objectives of the present study are: (1) to identify further the *Hartmannella sp.* which was isolated from a contact lens case and has been cultured *in vitro* and (2) to investigate if this amoeba could bind and cause damage to human corneal tissue *in vitro*.

4.2. MATERIALS AND METHODS

4.2.1. *Isolation and identification of the amoeba*

Method of isolation

Hartmannella sp. (designated as WI isolate in this study) was obtained from Dr P. Devonshire, Department of Bacteriology, Western Infirmary, Glasgow, after isolation from a contact lens case. Briefly, the amoeba was isolated by taking one drop of solution from the contact lens case and inoculating it onto non-nutrient agar plates seeded with *Escherichia coli* (Devonshire *et al.*, 1993). The agar plates were incubated either at 37°C or at 30°C and were examined every day for the presence of amoebae for seven days.

Identification

Identification of the amoeba to genus and species level was made on the basis of locomotion and morphology of the trophozoite forms and cysts following the Key of Page (1988). Observations of the locomotive form, nuclear structure and cyst morphology were made by phase contrast (Leitz) and bright field light (Leitz) microscopy.

A slab of agar (5 mm x 5 mm) containing some cysts or trophozoites was excised from an agar plate (about 3 to 4 days old), placed face up on a glass slide and a cover slip added for observation by bright field light microscopy. Sometimes a drop of Page's amoeba saline (PAS) was placed on the agar before covering with a cover slip. Under these conditions, amoebae with normal locomotion were observed. The amoebae and cysts were also observed in simple contact preparation. In this preparation, a drop of PAS suspension containing amoebae and cysts taken from agar plates flooded with PAS, were placed on a glass slide and observed by phase constrast microscopy. Measurements of lengths and breadths of moving amoebae were made from at least 30 amoebae, using a microscope eye graticule. Nuclear measurements were made only for cysts. Measurements of trophozoites and cysts were also made from light micrographs. Observations on mitochondrial cristae were made by transmission electron microscopy (Zeiss 902) of sections of amoebae from agar plate cultures. *Hartmannella vermiformis* obtained from the Culture Collection of Algae and Protozoa (CCAP strain 1534/7A), Windermere was used for comparison in identifying the amoeba.

4.2.2. *Cultivation of Hartmannella sp.*

Monoxenic cultivation

Hartmannella sp. was grown on non-nutrient agar, streaked with living *Escherichia coli* strain NCTC W3110 at 25°C. A small piece of agar, containing a few cysts of uniform morphology was transferred onto a new non-nutrient agar plate, seeded with bacteria. After several passages made in the same way, cultures still contained amoebae and cysts similar to the original.

Attempts at axenic cultivation

Attempts to grow the amoeba in axenic liquid medium were made following the techniques described in 2.2.1. Once the amoeba was observed to grow semi-confluently in saline solution (PAS) with heat-killed *Escherichia coli* as food supply, the PAS was gradually replaced by ATCC medium 1034 (see the following section for detailed formulation of the medium). The medium was replaced every three days to dilute out the bacteria. The amoebae, however, adapted to grow in the medium for only one generation. It was later discovered that this amoeba requires heat-killed bacteria to support growth in the liquid medium. So in this study, *Hartmannella sp* (WI isolate) was grown either on agar with live bacteria, or in liquid medium with heat-killed bacteria at 25°C.

ATCC medium 1034

The formulation of this medium was obtained from the American Type Culture Collection, Maryland, USA and was modified from the PYNFH medium of Laverde and Brent (1980).

The medium formulation was as follows: peptone (DIFCO 0118) 10.0 g, yeast extract (DIFCO 0127) 10.0 g, yeast nucleic acid (SIGMA) 1.0 g, folic acid 15.0 g and haemin 1.0 mg, all dissolved in 880 ml of distilled water. All the ingredients were autoclaved for 15 min at 121°C. Before use, 20 ml buffer pH 6.5, (made up from KH_2PO_4 18.1 g and Na_2HPO_4 25.0 g in 1000 ml distilled water), 100 ml foetal calf serum and antibiotics streptomycin and penicillin (both at 2000 units ml^{-1} and not included in the original ATCC medium), were aseptically added to the autoclaved ingredients. The complete medium was store at 4°C before use.

4.2.3. *Pathogenicity study*

The pathogenicity of *Hartmannella sp.* (WI isolate) to human cornea was determined by observing the ability of this amoeba to adhere, invade and cause damage to excised cornea *in vitro* following the techniques of Niederkorn *et al.*, (1992) for *Acanthamoeba castellanii*. In this study the invasive behaviour of *A. castellanii* (kindly supplied by Professor J.H. Freer, Department of Microbiology, University of Glasgow) was also examined in comparison with *Hartmannella sp.* The *A. castellanii* has been isolated from a corneal ulcer biopsy (J.H. Freer, personal communication).

Preparation of amoebae

Amoebae either grown on agar or in liquid medium were harvested as described in 3.2.1 and resuspended at a concentration between ~10^5 and10^6 ml^{-1} in Optisol medium containing 2.5% (v/v) chondroitin sulphate (Chiron Ophthalmics, Irvine, UK.) and gentamicin (25 µg ml^{-1}). This medium is used for storing excised corneas for grafting purposes. Before use in experiments, amoeba viability was determined by trypan blue exclusion.

Human cornea

Adult human corneas excised from cadavers were kindly supplied by Professor C. Kirkness, Department of Ophthalmology, Western Infirmary, Glasgow after removal of a central button for grafting purposes. This excised peripheral tissue was stored in Optisol medium at 4°C for not more than two days before use. The full thickness human cornea was cut into segments (~ 2.0 mm x ~ 3.0 mm, for each segment) and placed epithelium side up on the bottom of sterile individual wells of either 96-well (diameter 6.4 mm) or 24-well (diameter 16.0 mm) polystyrene plates. Optisol suspensions of *Hartmannella sp.* and *A. castellanii* which contained ~10^4 amoebae were added to the wells containing corneal segments. A few drops of heat-killed *E. coli* suspension (see 2.2.1) were also added to the wells. The total volume of fluid was ~150 µl in 6.4 mm-diameter wells and ~450 µl in 16.0 mm-diameter wells. Corneas, inoculated with the amoebae were incubated either at 25°C or 35°C for 24 h. The controls consisted of similar corneal specimens incubated in Optisol medium in the absence of amoebae and heat-killed bacteria.

Light and Transmission Electron Microscopy

Corneal segments were fixed in 2% (v/v) gutaraldehyde in 0.1 M phosphate buffer, pH 7.4, at the experimental temperature for 1 h and processed for transmission electron microscopy as described in 2.2.7. omitting those steps which involved pelleting and agar encasing the pellets of amoebae. Embedding was either in Araldite or Spurr's epoxy resin. Thick sections (~0.35 µm thick) were stained with toluidine blue containing 1% (w/v) toluidine blue and 1% (w/v) borax in distilled water. During staining, the stained sections were left briefly on a hot plate before rinsing with distilled water. The stained sections were mounted on a glass slide in DPX and examined by bright field light microscopy. Ultrathin sections were stained with uranyl acetate and Reynolds' lead citrate and viewed in a Zeiss 902 transmission electron microscope operating at 80 kV.

Scanning electron microscopy

Specimens were fixed and postfixed as previously mentioned and dehydrated by transfer through a graded series of acetone (30-100%). Dehydrated specimens were dried in a CO_2 critical point drier and mounted on aluminium stubs with silver conducting paint. Specimens were coated with a thin (20nm) film of gold-palladium using a sputter-coater (Polaron SC 515 SEM coating system) and were observed in a Phillips scanning electron microscope operating at 20 kV.

4.3.0. RESULTS

4.3.1. *Identification of Hartmannella sp.*

Trophozoites of the amoeba

Trophozoites and cysts of *Hartmannella sp.* (WI isolate) were examined both at light and electron microscopy levels. On the agar surface in the presence of living bacteria, *Hartmannella sp* (WI isolate) trophozoites exhibited two types of morphology which were related to its pattern of movement (Figure 4.1A to D). The trophic amoeba had a striking elongate, often wavy body form appearing round in cross section and progressing usually via a single pseudopodium. Occasionally the pseudopodium was bifurcated (Figure 4.1C). A hyaline cap was always present at the anterior tip of the pseudopodium; the rest of the cytoplasm was faintly granular. Contractile vacuoles which were observed as clear vacuoles by light microscopy were observed in the moving amoebae. When settling on the substratum, however, the amoeba appeared more flattened and had several pseudopodia (Figure 4.1A).

The measurement of the elongated forms of both *Hartmannella* (*Hartmannella sp*. (WI isolate) and *H. vermiformis*) and the ratio of their length to their breadth measurement are given in Table 4.1. Data obtained from *Hartmannella sp*. (WI isolate) agreed with those from *H. vermiformis* CCAP strain 1534/7A.

Under transmission electron microscopy (TEM) of thin sections, both branched and elongated profiles of the amoeba were observed (Figure 4.2). At the ultrastructural level, the nucleus with a double membrane (~30 nm in width), a central spherical electron dense nucleolus and chromatin bodies was observed. The chromatin bodies were scattered in the nucleoplasm and attached to the inner membrane of the nuclear envelope. Short lengths of endoplasmic reticulum with ribosomes were abundant in the cytoplasm. Mitochondrial profiles were oval to elongate, with tubular cristae. The cytoplasm of the trophozoite of *Hartmannella sp*. (WI isolate) was occupied by various types and sizes of vacuoles. Some of the vacuoles contained electron dense material, probably derived from ingested bacteria and therefore could be food or digestive vacuoles. A Golgi body was not evident in the amoeba. Under TEM, there was no distinction between hyaloplasm and the granular cytoplasm of the rest of the amoeba.

Figure 4.1. Cysts and trophozoites of *Hartmannella sp.* (WI isolate) observed on agar prepared as described in 4.2.1. by bright field microscopy. The stages of the trophozoite transformation from flattened to elongated form is illustrated clockwise (A to D). Note the contractile vacuoles shown as clear vacuoles (v) and the hyaloplasm (at longer arrow) at the anterior tip of moving amoebae. n, the cyst nucleus. Arrows indicate direction of movement. Scale bar = 10 µm.

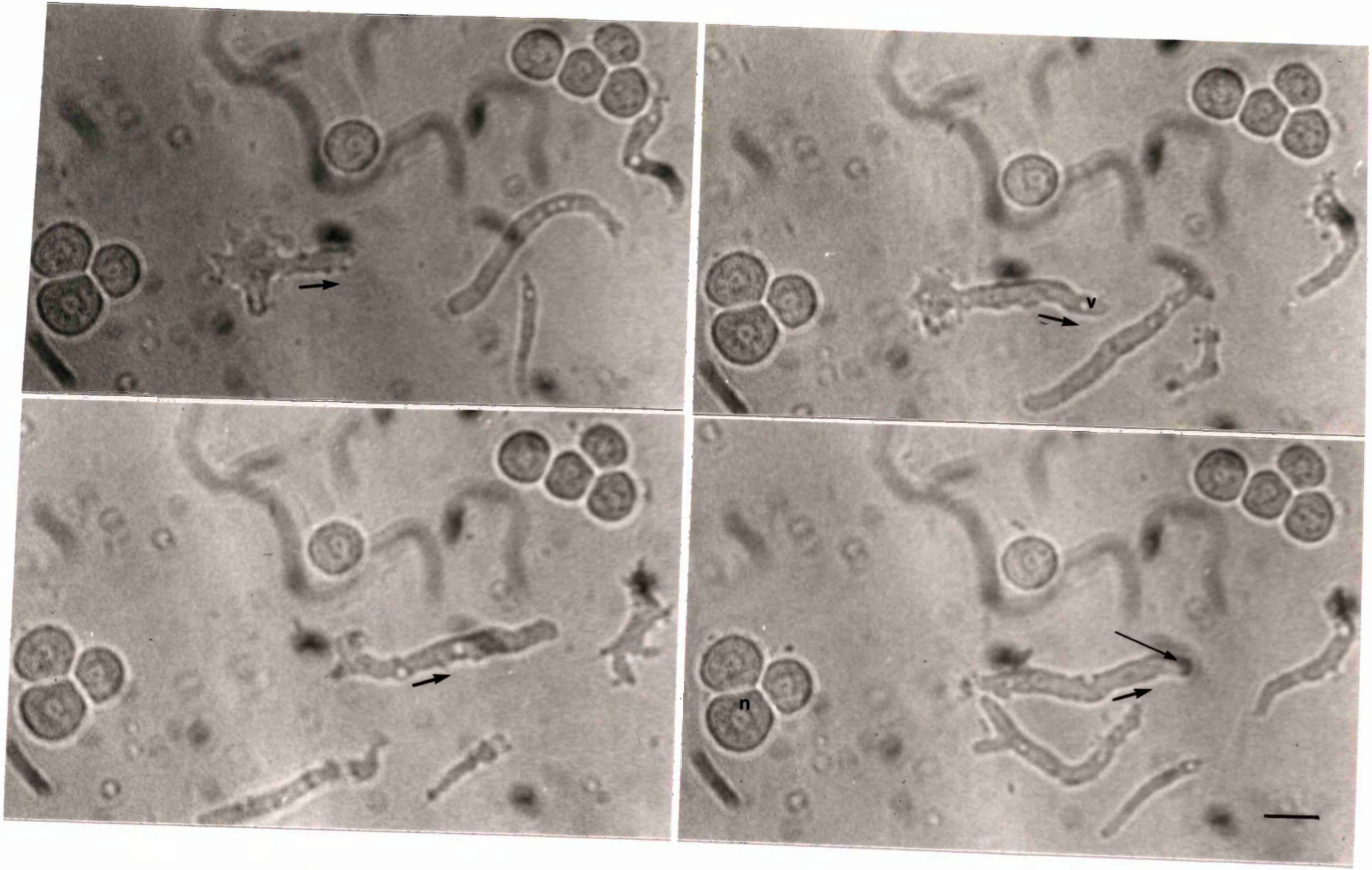
v
n

Figure 4.2. Transmission electron micrographs of flattened (branched) (A) and elongated (B) profiles of *Hartmannella sp*. (WI isolate). The cytoplasm of the amoebae is packed with vacuoles of various sizes. The nucleus has a double membrane and a central electron dense nucleolus. Chromatin bodies occupy the nucleoplasm of the amoeba. Note that short straight lengths of endoplasmic reticulum (ER) with ribosomes are abundant in the cytoplasm. V, vacuole, FV, food vacuole, N, nucleus, n, nucleolus, M, mitochondria. Scale bar = 1 μm.

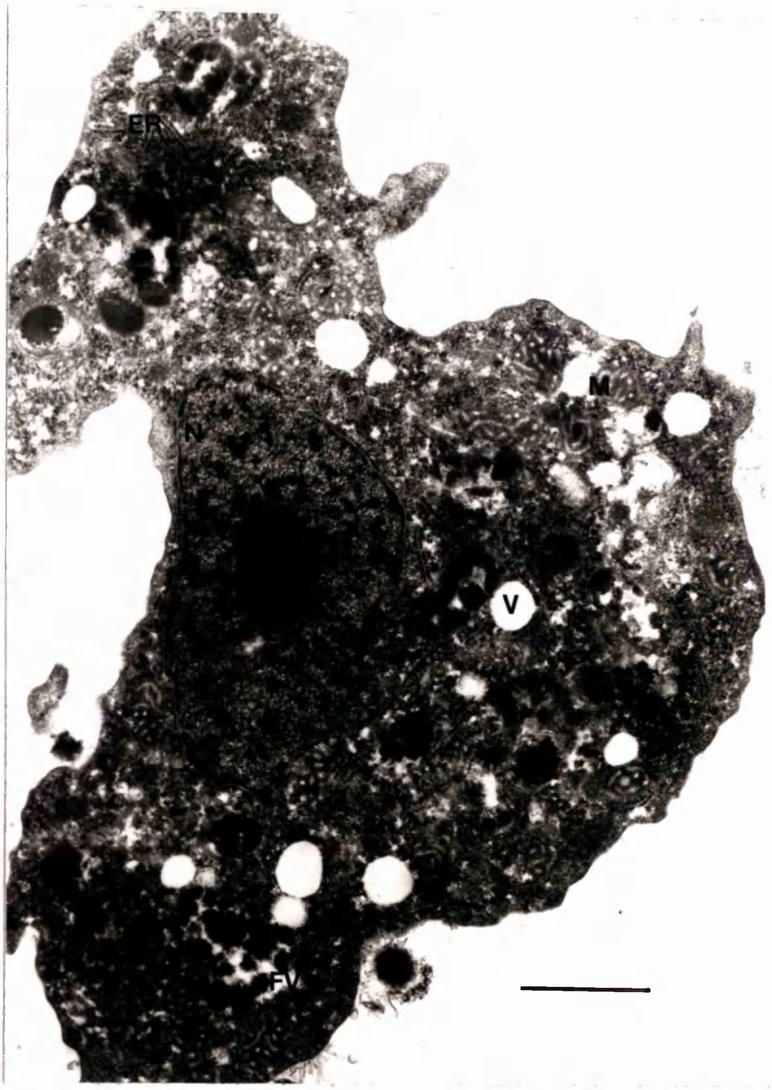
ER
M
N
V
FV

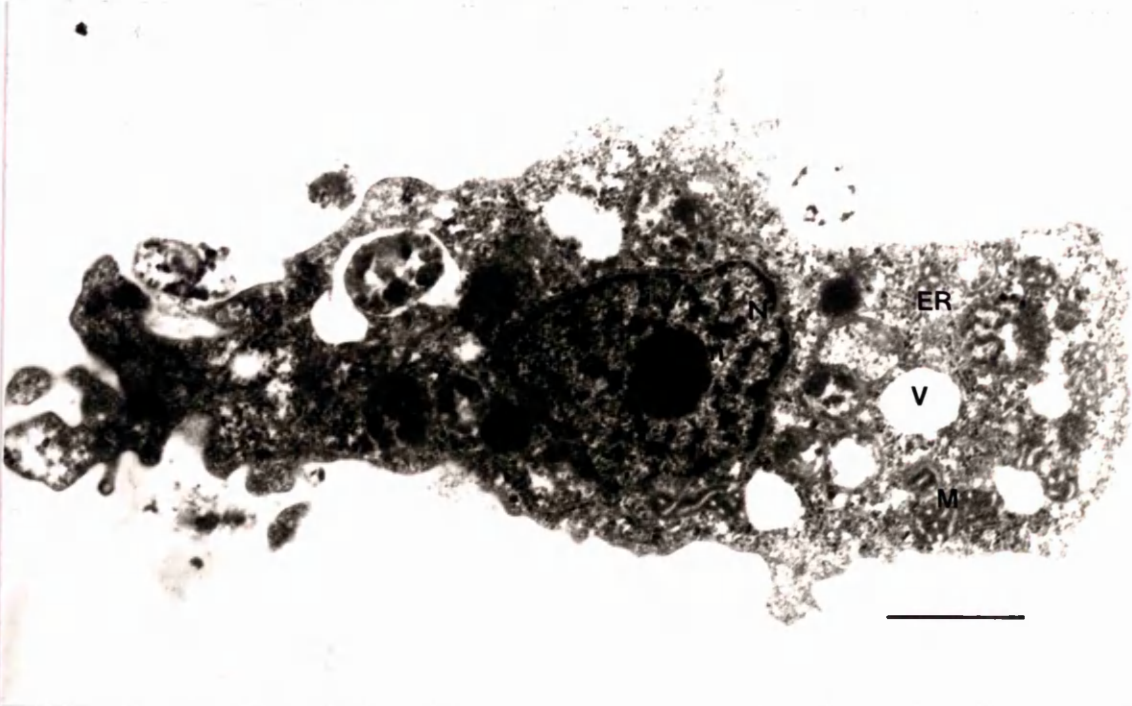
N
ER
V
M

Cysts of the amoeba

Hartmannella cysts appeared to be spherical or ovoid with the single nucleus (diameter between 2 μm and 3 μm) in the centre (Figures 4.1, 4.3). The cyst diameters were 7.9 ± 2.1 μm (Table 4.1). Under light microscopy, the cysts appeared to have a single thin wall (less than 1 μm). The cyst morphology of *Hartmannella sp.* (WI isolate) was similar to that of *Hartmannella vermiformis* CCAP strain 1534/7A (Figure 4.4). As with the trophozoites, data obtained for cysts of *Hartmannella sp.* (WI isolate) agreed with those for *H. vermiformis* CCAP strain 1534/7A (Table 4.1).

At the ultrastructural level, in sections of cysts a thick inner and a thin more electron dense outer wall were observed (Figure 4.3). The inner wall appeared to be made up by fibrous material (Figure 4.3A). The thickness of each wall was not uniform and measured between 200 nm and 500 nm for the inner wall, and between 20 nm and 100 nm for the outer wall. The two walls were occassionally separated by a space as in Figure 4.3B but sometimes they were markedly separated by a space of up to 1.8 μm (Figure 4.3A). The nucleus was round in appearance with chromatin bodies occupying the nucleoplasm as in trophozoites. In some cysts, the profile of the nucleus seemed distorted perhaps due to cytoplasmic shrinkage during cyst formation (Figure 4.3A). The cyst cytoplasm was vacuolar in appearance and mostly occupied by numerous lipid globules (Figure 4.3A). The remains of digestive vacuoles were also recognisable in cysts. Other cytoplasmic organnelles were not readily observed. In some cysts which might represent much later stages of cyst development, mitochondria were found clustered around the nuclear perimeter (Figure 4.3B). In such cysts lipid globules were observed to be reduced in number and the cyst cytoplasm more compact.

Table 4.1. Comparative measurements for trophozoites and cysts of *H. vermiformis* CCAP strain 1534/7A with *Hartmannella sp.* (WI isolate)

Feature	*H. vermiformis* *CCAP strain 1534/7A*	*Hartmannella sp.* *WI isolate*
Trophozoite		
Length	34.2±9.0 µm	35.2±9.6 µm
Length/width	9 to 10	9 to 10
Cyst (diameter)	7.7±1.2 µm	7.9±2.1 µm

Notes:

Means ± standard deviations of measurements were obtained from 50 individuals for cysts and 30 individuals for trophozoites.

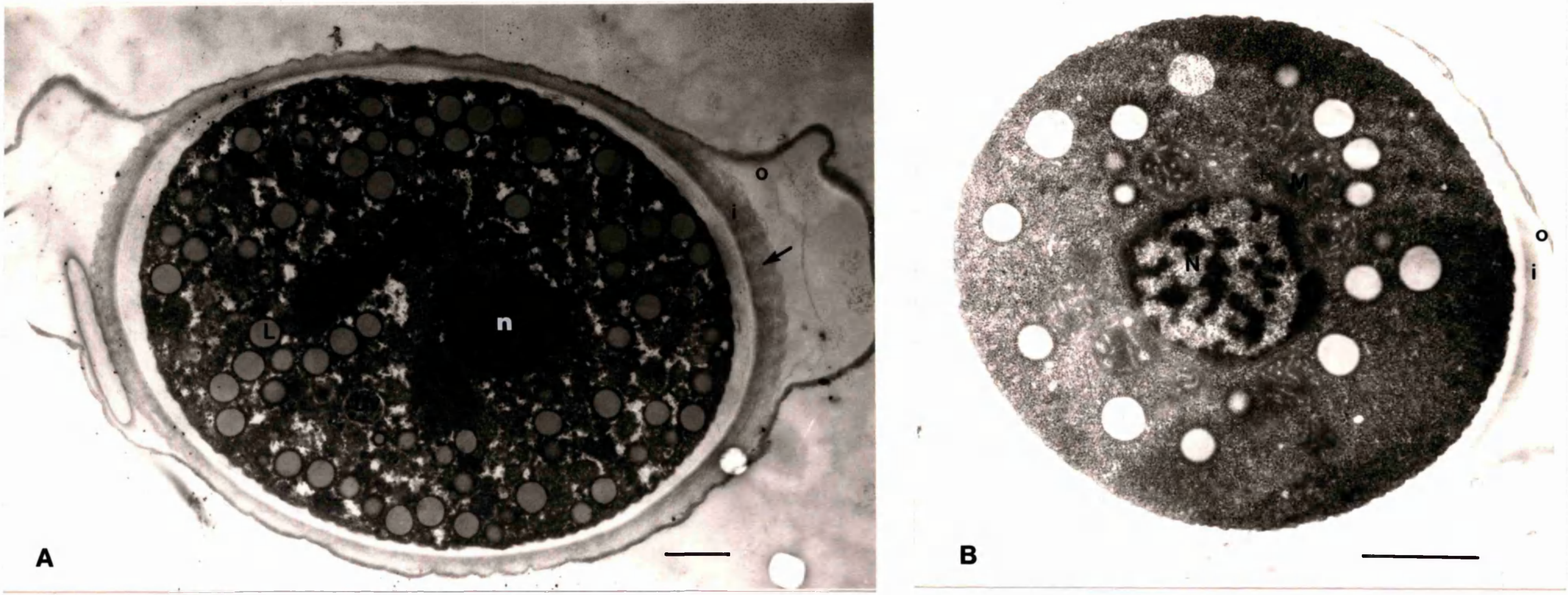

Figure 4.3. Section through whole cysts of *Hartmannella sp*. (WI isolate). The inner (i) wall of the cyst is made up from fibrous material (arrow). The outer wall of cysts (o) usually shows separation from the inner wall at some points as in B, but sometimes the two two walls are markedly separated as in A. The nucleus, as in the trophozoite contains a nucleolus (n) and bodies of extranucleolar chromatin. Lipid globules are abundant in the cyst cytoplasm (in A). The mitochondria (M) are found at the periphery of the nucleus (in B). Dv, digestive vacuole, L, lipid globule. Scale bar = 1 μm.

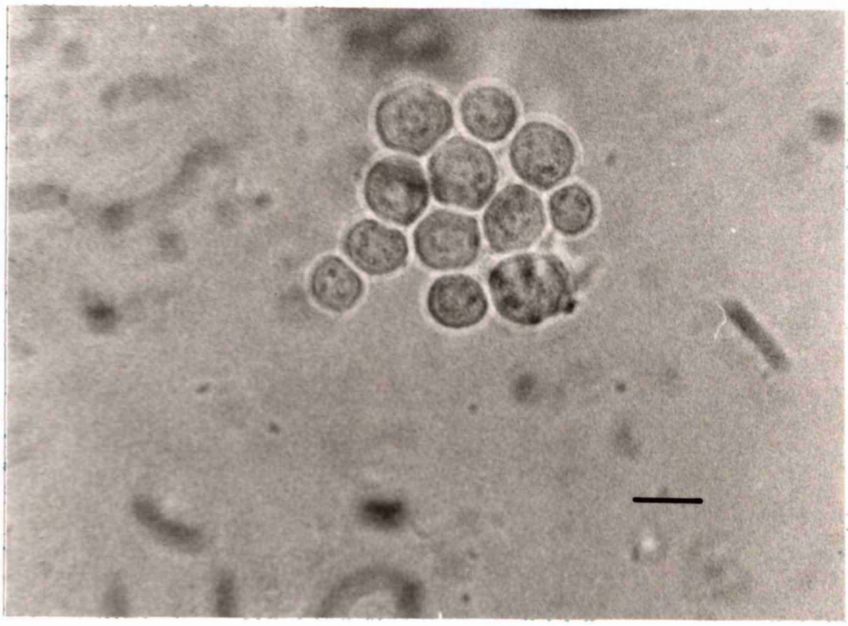

Figure 4.4. Light micrograph of cysts of *Hartmannella vermiformis* (CCAP strain 1534/7A). Note the cysts morphology is identical to that of cysts of *Hartmannella sp.* (WI isolate) in Figure 4.1. Scale bar = 10 μm.

4.3.2. *Evidence of pathogenicity*

The human corneas either used as controls or inoculated with *Hartmannella sp.* (WI isolate) were incubated at 25°C and 35°C. Corneas which were inoculated with *Acanthamoeba castellanii* were incubated only at 35°C. Possible signs of invasiveness and pathogenicity of the amoebae towards human corneas *in vitro* were looked for by bright field light microscopy, transmission electron microscopy (TEM) and scanning electron microscopy (SEM).

a) Control corneas

The stratified epithelium and stroma of human cornea including Bowman's zone and keratocyte layers in a control sample are shown in the light micrograph of Figure 4.5. The surface of the cornea appeared not to be smooth; some of the epithelial cells were not intact and were observed to be in the process of sloughing off from the epithelial layer. The epithelial cells close to Bowman's zone appeared to stain darker than cells near the surface. The thickness of the epithelial layer was between 26 μm and 41 μm, and the thickness of Bowman zone measured ~13 μm. The thickness of the entire stroma was not measured but it represents 90% of the corneal thickness (Casey and Meyer, 1984). Although the stroma keratocytes were observed clearly in this sample, they were not well preserved. Compression artifacts of sectioning detract from the appearance of the stroma.

At the ultrastructural level, at least three layers of nucleated cells were observed in the corneal epithelium (Figure 4.6). Each cell was observed to have a microplicate surface with short projections which appeared to serve for attachment with adjacent cells. The cells stained darker and close to Bowman's zone, seemed to have columnar form, whereas the lightly stained cells near to the corneal surface appeared to be more flattened. These cells were closely packed. The epithelial cells seemed to have a large nucleus with chromatin bodies in the nucleoplasm. The shape of the nucleus appeared to correspond to the shape of the cell; flattened cells had elongate nuclei. The cells had various discernible cytoplasmic organelles such as mitochondria, Golgi bodies and smooth endoplasmic reticulums. The size of these organelles was minute compared with the size of the nucleus. Beneath the epithelial layer, there was an acellular layer of Bowman's zone, separated by a basement membrane (~92 nm in width).

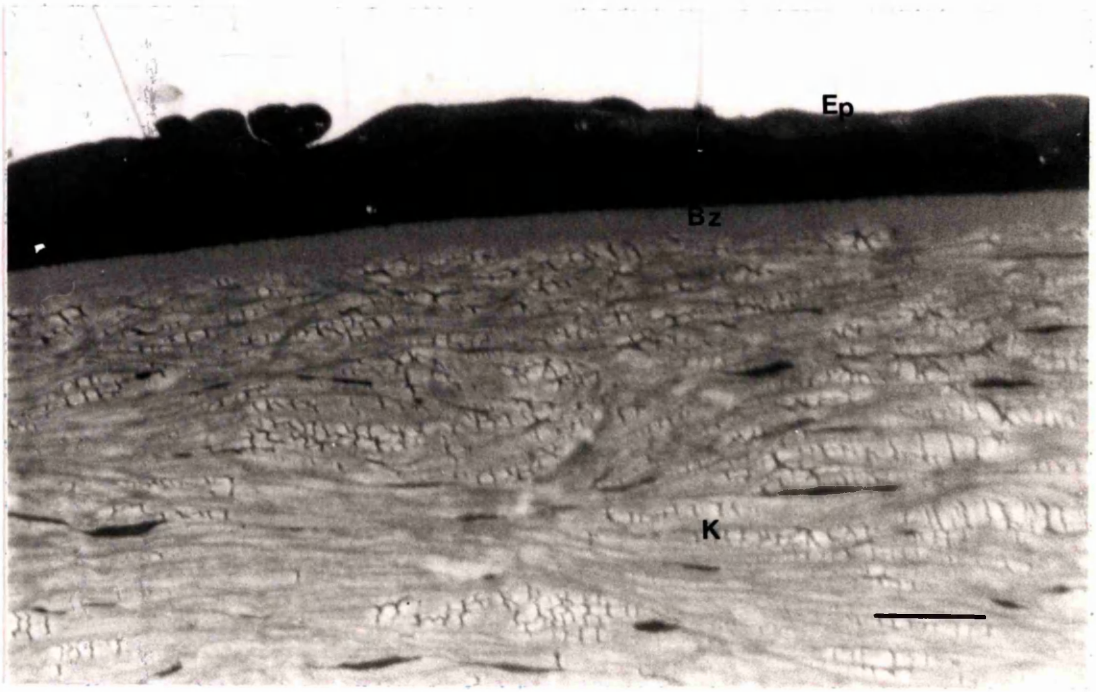

Figure 4.5. Light micrograph of sectional view of control human cornea. This sample was incubated at 25°C and embedded in Araldite. The thickness of the section was 0.35 μm. The section was stained with toluidine blue. The multilayer epithelium (Ep), the acellular Bowman's zone (Bz) and the stroma containing keratocytes (K) are shown. Compression artifacts are evident in the stroma layers. The epithelial cells which are near to Bowman's zone appear to stain darker compared with the cells near the cornea surface. Also the cornea surface was observed not to have smooth in appearance and some of the epithelial cells seemed to be lifted away form the corneal surface. Scale bar = 30 μm.

Figure 4.6. Transmission electron micrograph showing three layers of intact epithelial cells of control human cornea. Each cells has several small projections (at small arrows) on its surface. Nucleus (N) and other cytoplasmic organelles such as Golgi bodies (G), mitochondria (M) and smooth endoplasmic reticulum (ER) are visible in the cell. Note the huge size of the nucleus compared with the size of other cytoplasmic organelles. The basal epithelial layer is separated from Bowman's zone (Bz) by a basement membrane (arrowhead). Scale bar = 2 μm.

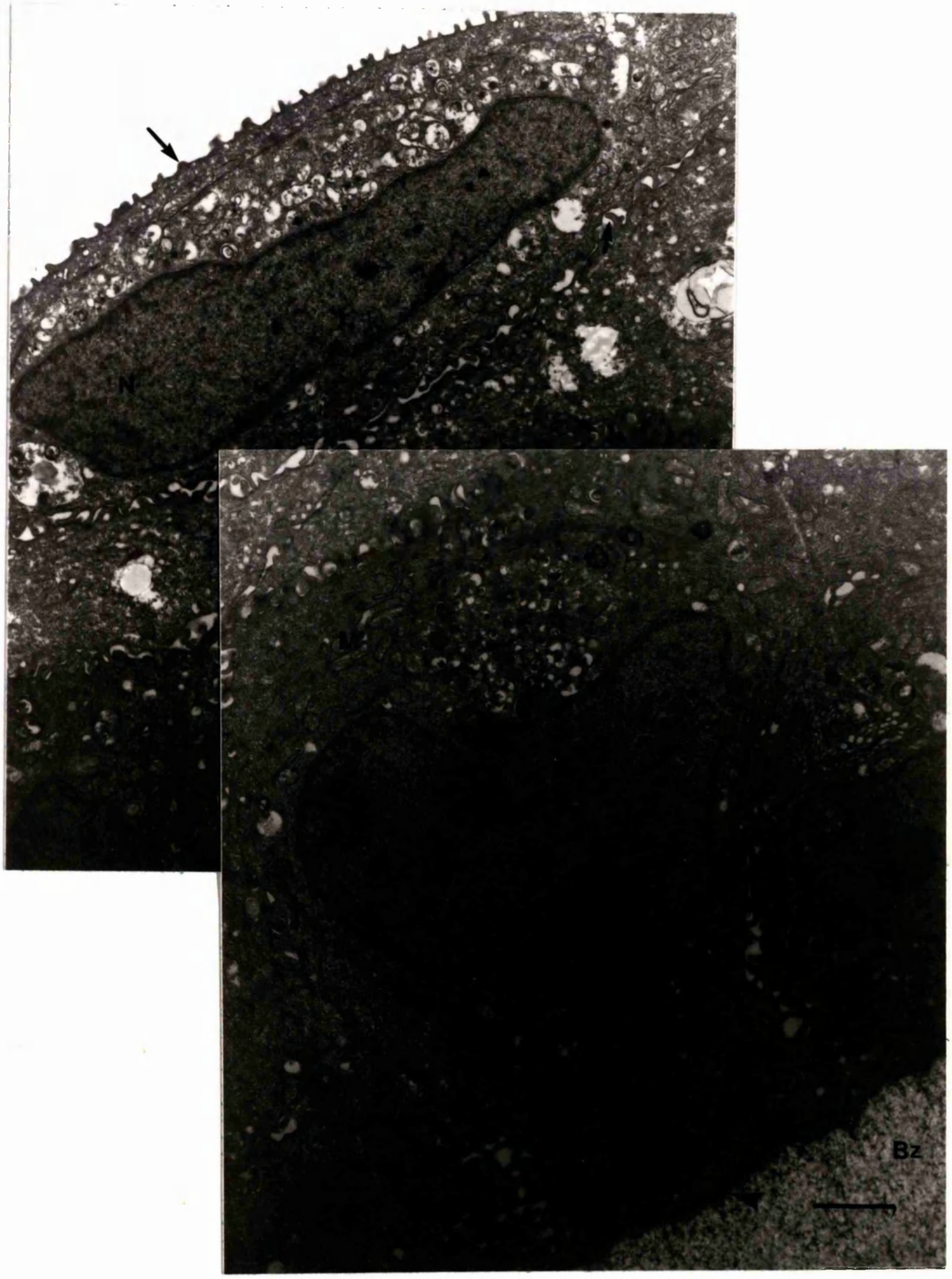
N
M
Bz

The surface of the control cornea under SEM was not smooth and could be seen to be composed of multilayers of various morphology and sizes of cells (Figure 4.7). Small rounded cells (between 8.0 µm and 10 µm in diameter) were observed at the corneal surface. Flattened and elongated cells were also observed. The eroded epithelial surface seemed to be affected probably by dehydration during sample preparation, so the shape of most cells in this sample was distorted and some cells appeared to be lifted away from the corneal surface. The human corneas which were used in this study even as controls thus did not have an intact corneal epithelium.

b) Experimental corneas

Incubated with Hartmannella sp.

Cornea, when incubated for 24 h either at 25°C or 35°C, with *Hartmannella sp.* appeared in section to have lost the entire epithelial layer or only fragmentary remnants of the epithelial layer were observed (Figure 4.8). No amoebae were observed in the corneal stroma.

In TEM sections of human corneas incubated with *Hartmannella sp.* at 25°C or 35°C, an intact layers of the epithelial cells was not observed (Figure 4.9A). In some sections, only the remnants of the epithelium were observed (Figure 4.9B). The shape of the remaining cells of the epithelium was flattened and elongated thus differing markedly from any of the epithelial cells in control (Figure 4.6). The cell in Figure 4.9B appeared not to have many tiny projections on its surface but from the size of its cytoplasmic organelles and its plate-like mitochondrial cristae could be identified as an epithelial cell. The supporting basement membrane of the epithelium was not evident in these samples. There was no evidence for the attachment of the trophozoites of *Hartmannella* on the eroded cornea surface. A

Harmannella cyst however, was observed adhering to the surface of stroma near the cut edge (Figure 4.9C).

Under SEM, in the presence of *Hartmannella*, only one layer of the epithelial cells was observed and only on some parts of the corneal surface (Figure 4.10A). The cells had a flattened shape which are concave at their top sides and these cells measured between 25 μm and 40 μm in length. The remaining surface of the cornea seemed to be devoid of any kind of cells. This observation contradicted to what had been observed in a control sample (Figure 4.10B). In this figure, although some cells had been lifted away from the corneal surface, the remaining cells were still intact and being part of the epithelial layer. *Hartmannella* was not recognised on the cornea surface by scanning electron microscopy so the possibility of its attachment to the corneal surface can not be observed.

Figure 4.7. Scanning electron micrograph of control human corneal surface after incubation at 25°C for 24 h. Some of the epithelial cells appeared to have been removed from the corneal surface, as the epithelial surface is not smooth in appearance. Epithelial cells of various shapes and sizes are visible.
Scale bar = 30 μm.

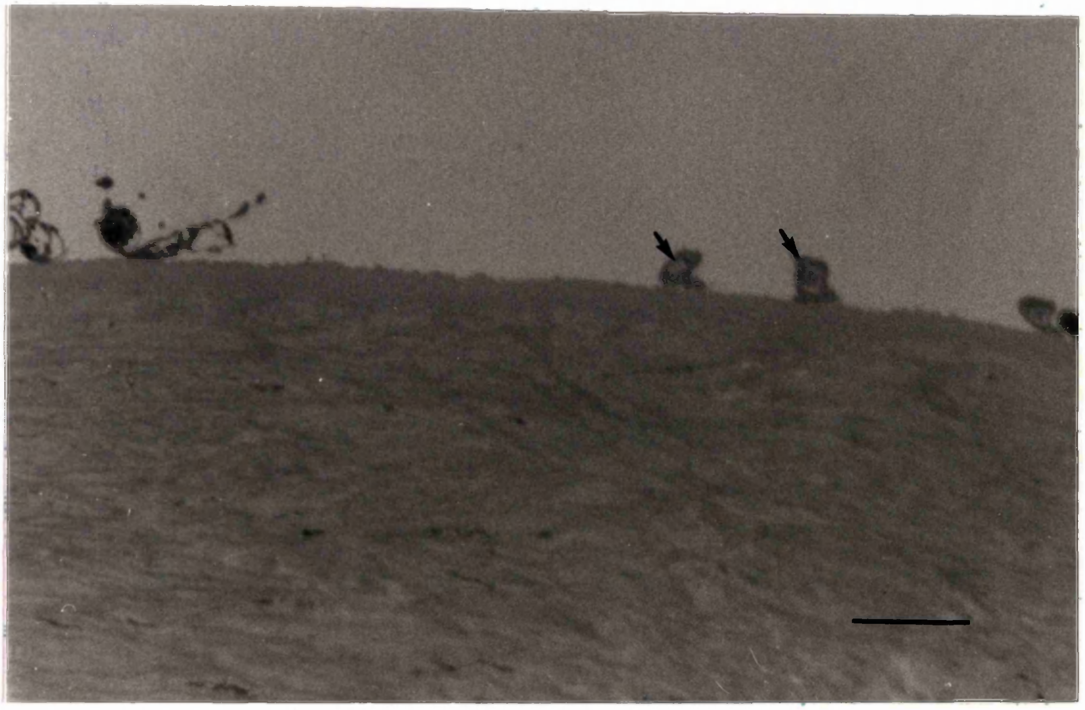

Figure 4.8. Light micrograph of thick (0.35 µm) vertical section of human cornea incubated with *Hartmannella sp.* at 25°C and embedded in Araldite and stained with toluidine blue. Note that in some parts of the cornea surface, the stratified epithelium is completely absent or only represented by a few distorted remnant cells (arrows) overlying Bowman's zone. Bz, Bowman's zone, K, stroma containing keratocytes. Scale bar = 30 µm

Figure 4.9. Transmission electron micrographs of human cornea when incubated with *Hartmannella sp.* (WI isolate) for 24 h at 25°C. A. The epithelial layer is completely absent. B. In this section, a single remaining epithelial cell is observed overlying the Bowman's zone (Bz). Note the cell in this figure is more flattened and looks different from any of the epithelial cells observed in a control cornea (Figure 4.6). There is no evidence of a basement membrane in these specimens. Scale bar = 2 μm.

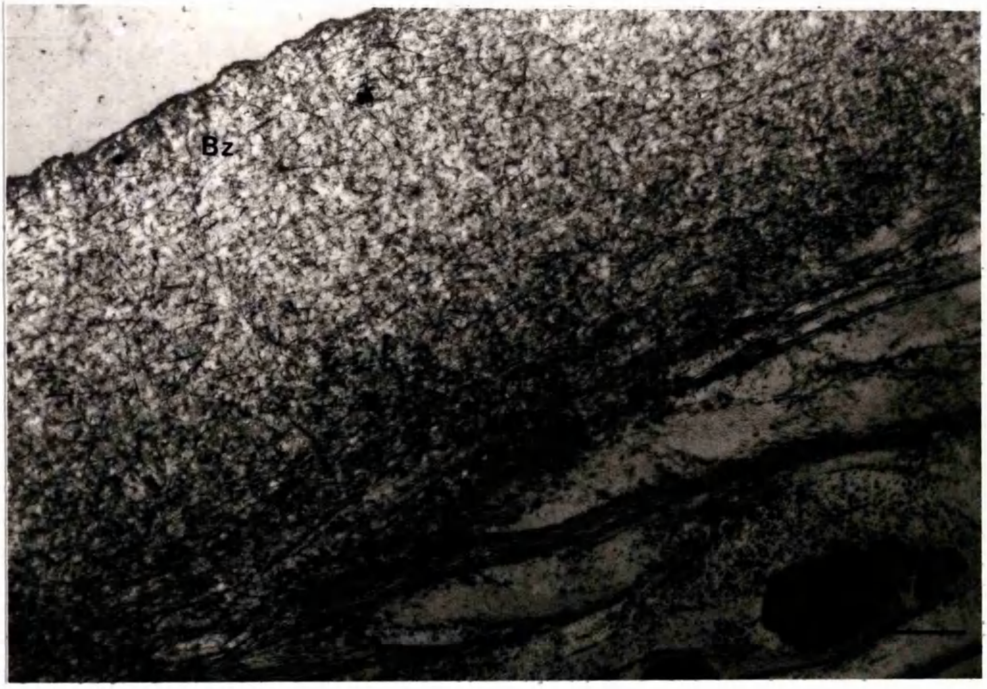
Bz

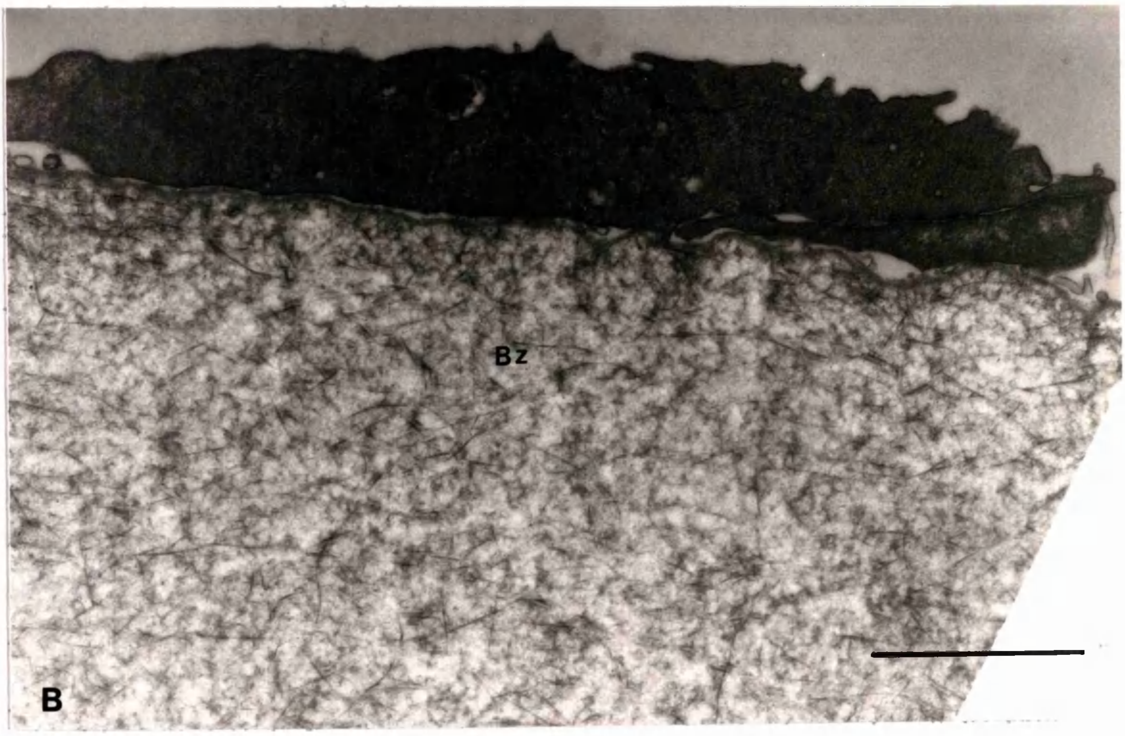
Bz
B

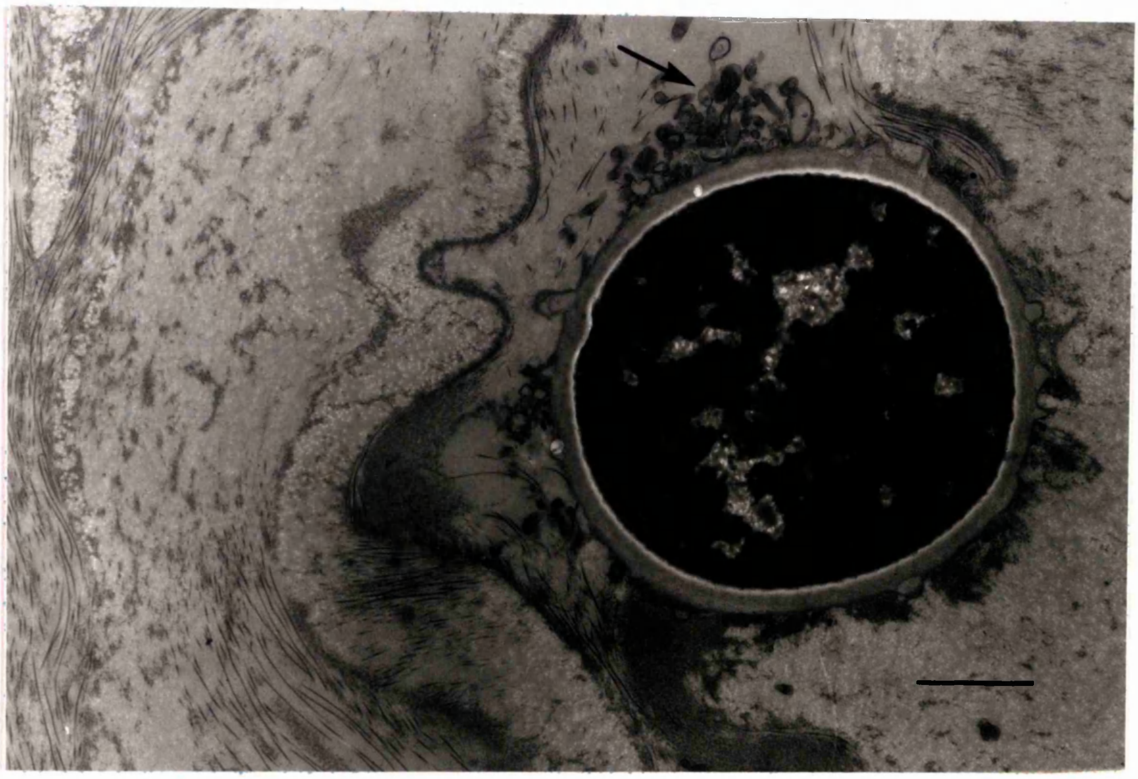

Figure 4.9C. A vertical section of the human corneal stroma showing a cyst of *Hartmannella sp*. (WI isolate) adhering to the surface of stroma near the cut edge. The cornea was incubated for 24 h at 25°C after inoculated with amoebae. Note the minute cytoplasmic inclusions (arrow) resembling the inclusions of the epithelial cells; they could be as the result of epithelial cell lysis due to the presence of *Hartmannella sp*. The cyst cytoplasm was densely stained and the cyst outer wall was spiky in appearance. Scale bar = 2 μm.

Figure 4.10. Scanning electron micrograph of human corneal surface when incubated for 24 h at 25°C with *Hartmannella sp.* (WI isolate). Only scattered flattened cells (arrows) are visible (A). The other part of the cornea surface seems to be exposed so the surface of Bowman's zone is seen (arrowhead). In this specimen, the trophozoites of *Hartmannella* were not readily recognised so the possible attachment of the amoebae could not be detected. Scale bar = 30 µm. In control corneal surface (B), although some epithelial cells had been lifted away from the corneal surface, the underlying epithelial cells (arrow) were still intact so the surface of Bowman's zone is not seen. Scale bar = 10 µm.

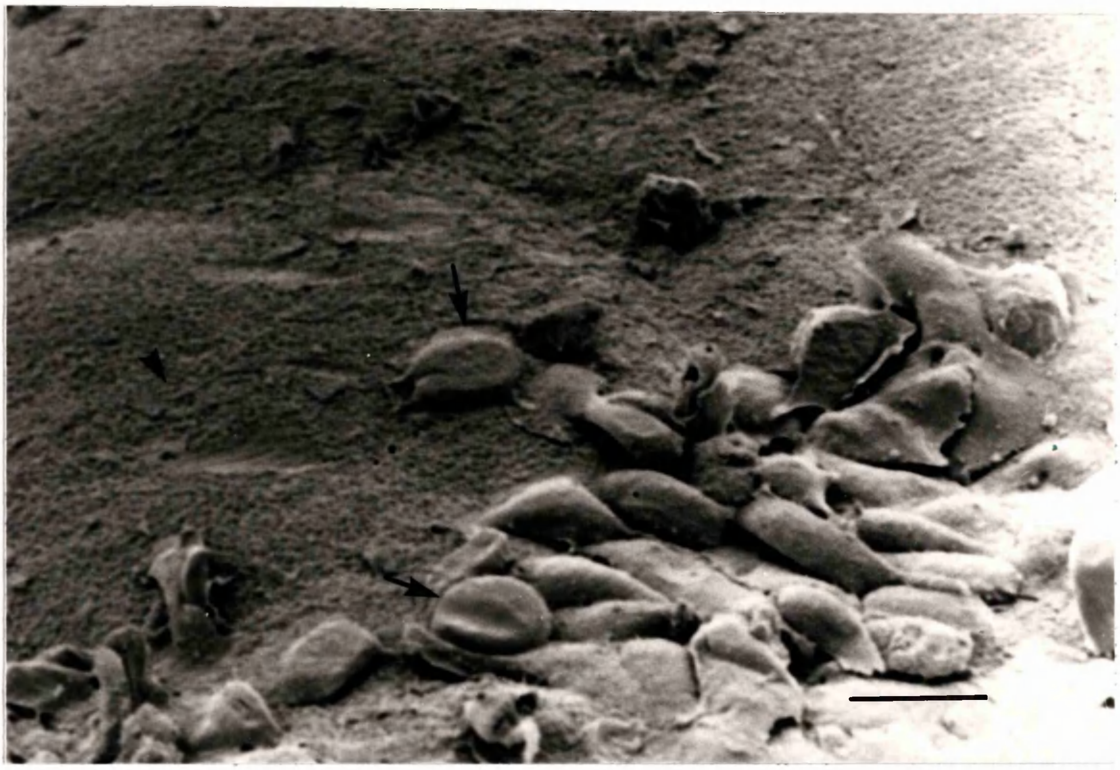

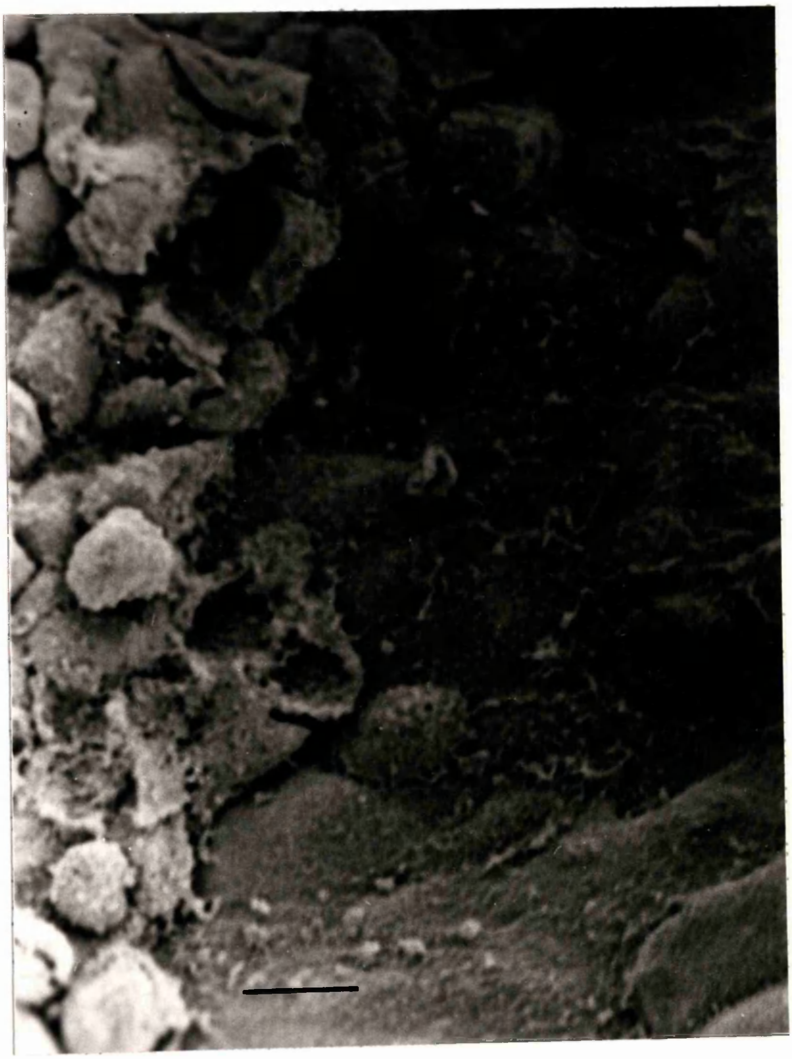

Incubated with Acanthamoeba castellanii

Human cornea, when incubated with *Acanthamoeba castellanii* for 24 h, was observed to have a relatively intact epithelial layer as in the control (Figure 4.11A compared with Figure 4.5) but in the same specimen the amoebae were observed in the cornea stroma near the cut edge (Figure 4.11B).

Evidence for *A. castellanii* invasion of the cornea stroma under TEM is shown in Figure 4.12A. The amoebae were observed between layers of the corneal stroma. In the same specimen, only one layer of flattened epithelial cells was observed. On some parts of the corneal surface which was incubated with *Acanthamoeba*, the remaining epithelial cells were observed to be more rounded and they looked swollen (Figure 4.12B). Although the appearance of these epithelial cells and their attachment to the Bowman's zone looked different from control epithelial cells as they lacked a supporting basement membrane, they could still be recognised as epithelial cells from the shapes and sizes of their cytoplasmic organelles.

In the corneal stroma, *Acanthamoeba* was observed as branched (Figure 4.12C) or entire profile (Figure 4.12D), depending on how the amoebae tried to accomodate themselves in spaces between collagen layers. The amoebae were distinguished from the keratocyte cells by having mitochondria with tubular cristae and characteristic intracrystal inclusions. There was no evidence of amoeba attachment to the corneal surface in sections though possible such attachments were observed under SEM (data not shown).

Figure 4.11. Light micrographs of thick (0.35 μm) vertical sections of human cornea after incubation with *Acanthamoeba castellanii* for 24 h at 35°C. The cornea was embedded in Spurr's resin and the sections were stained with toluidine blue. A. Section to show intact stratified epithelium (arrow). The distruption of the stroma layers is mechanical as the micrograph was taken close to the cut edge of the corneal segment. B. Section near cut edge of stroma showing *Acanthamoeba* within the stroma (arrows). Scale bar = 20 μm.

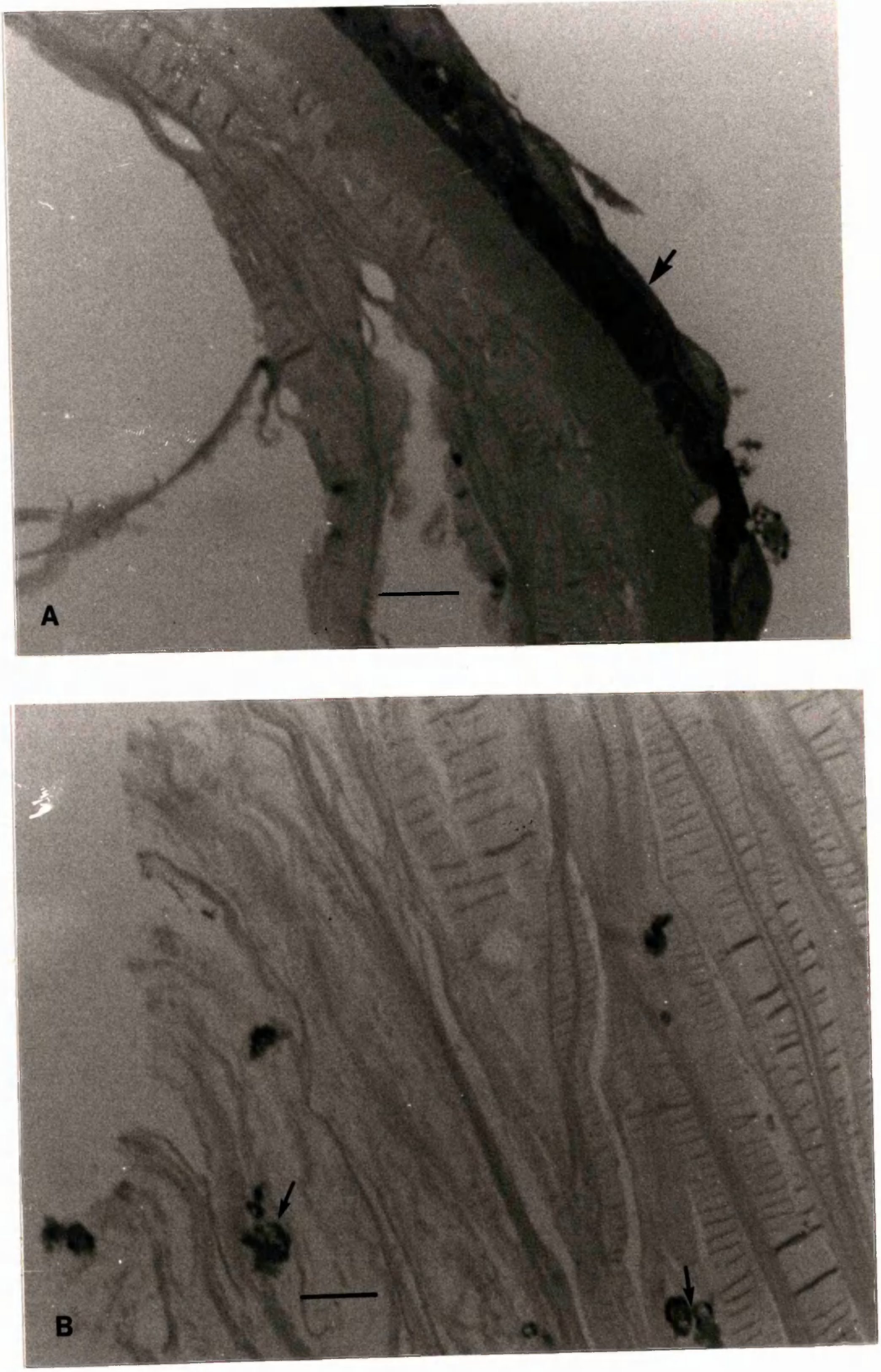
A
B

Figure 4.12. Transmission electron micrographs (A to D) of human cornea showing evidences of *Acanthamoeba castellanii* intrusion in the corneal stroma without completely damaging the epithelium. A. One layer of epithelial cells was observed on the corneal surface whereas the amoebae (arrows) were seen within the stroma. B. Three of the remaining epithelial cells observed on the corneal surface. The cells appeared rounded and swollen compared with the epithelial cells in control cornea (Figure 4.6). Note also the attachment of the cells to the Bowman's zone in B. Lipid globules were observed in these cells. Bz, Bowman's zone; K, keratocyte layer; L, lipid globules, N, nucleus. Scale bar = 5 μm.

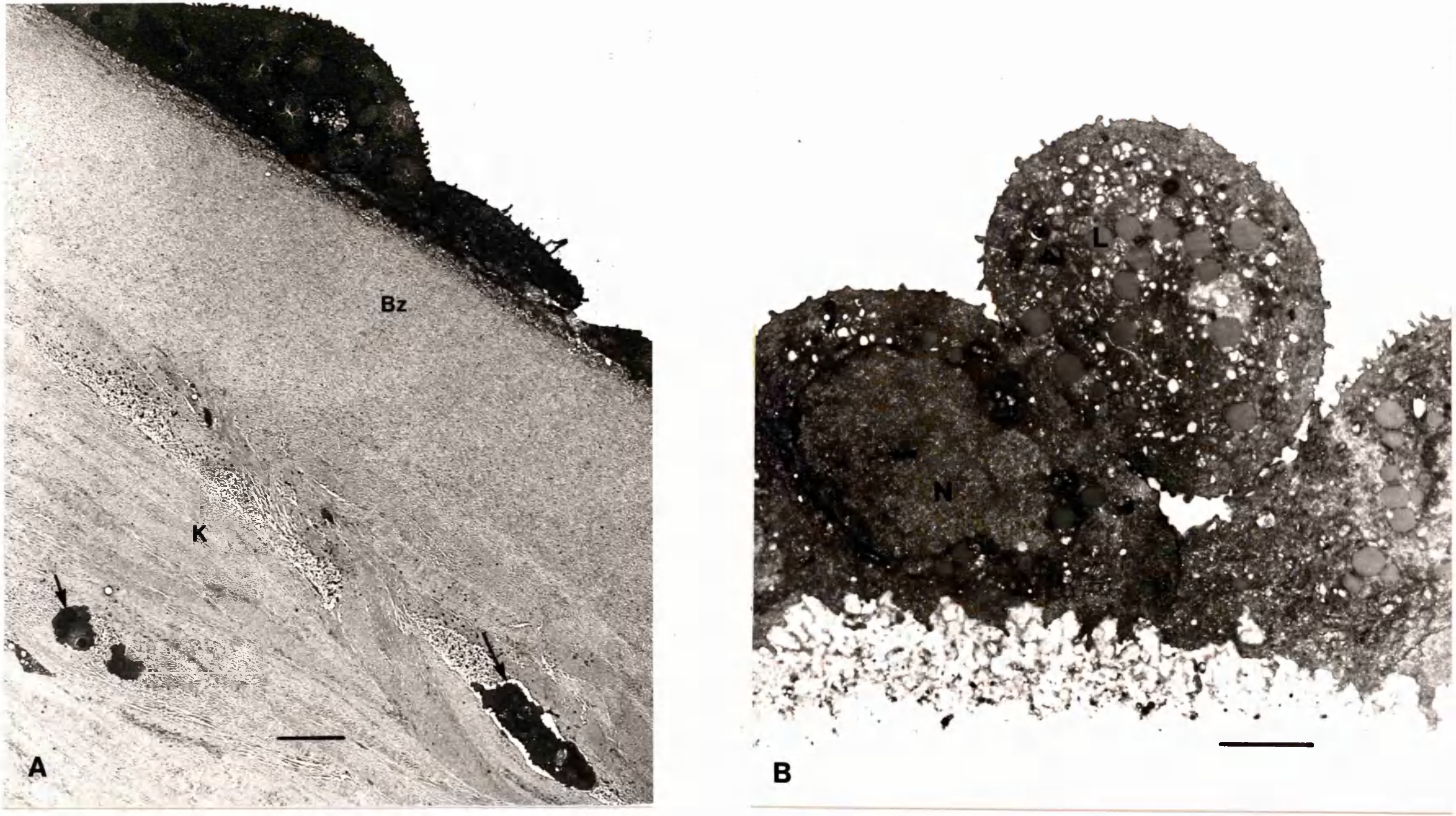
Bz
K
A
L
N
B

Figure 4.12. Transmission electron micrographs (A to D) of human cornea showing evidences of *Acanthamoeba castellanii* intrusion in the corneal stroma without completely damaging the epithelium. A. One layer of epithelial cells was observed on the corneal surface whereas the amoebae (arrows) were seen within the stroma. B. Three of the remaining epithelial cells observed on the corneal surface. The cells appeared rounded and swollen compared with the epithelial cells in control cornea (Figure 4.6). Note also the attachment of the cells to the Bowman's zone in B. Lipid globules were observed in these cells. Bz, Bowman's zone; K, keratocyte layer; L, lipid globules, N, nucleus. Scale bar = 5 µm.

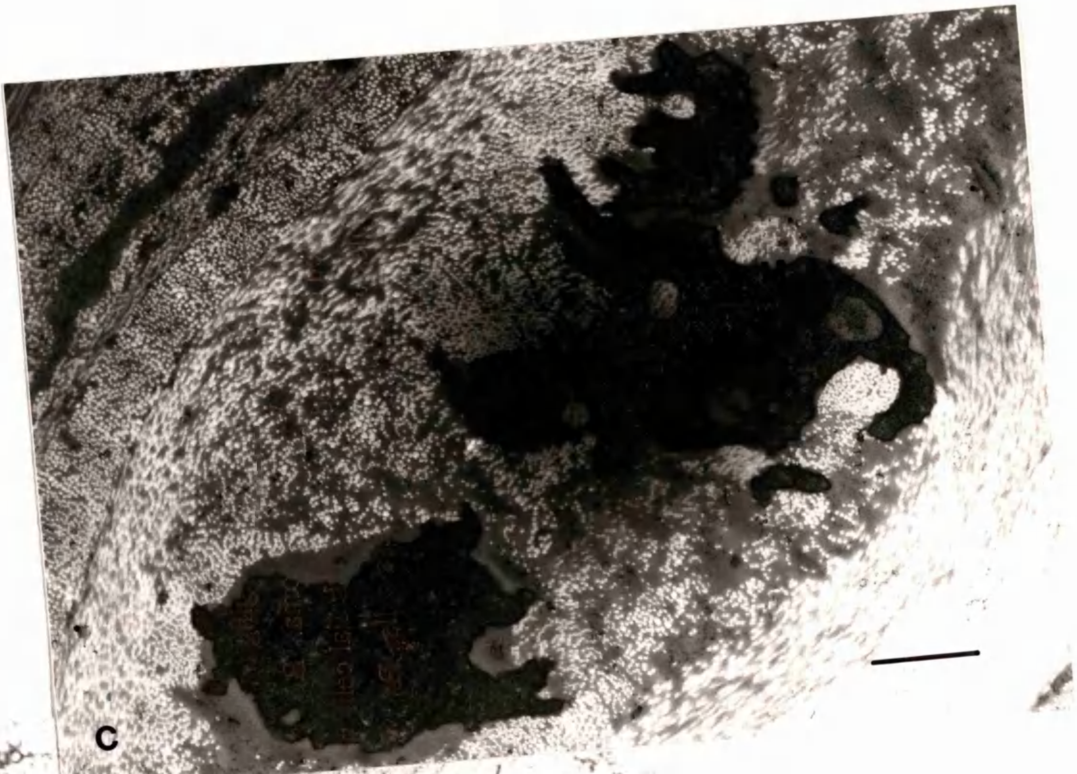
C

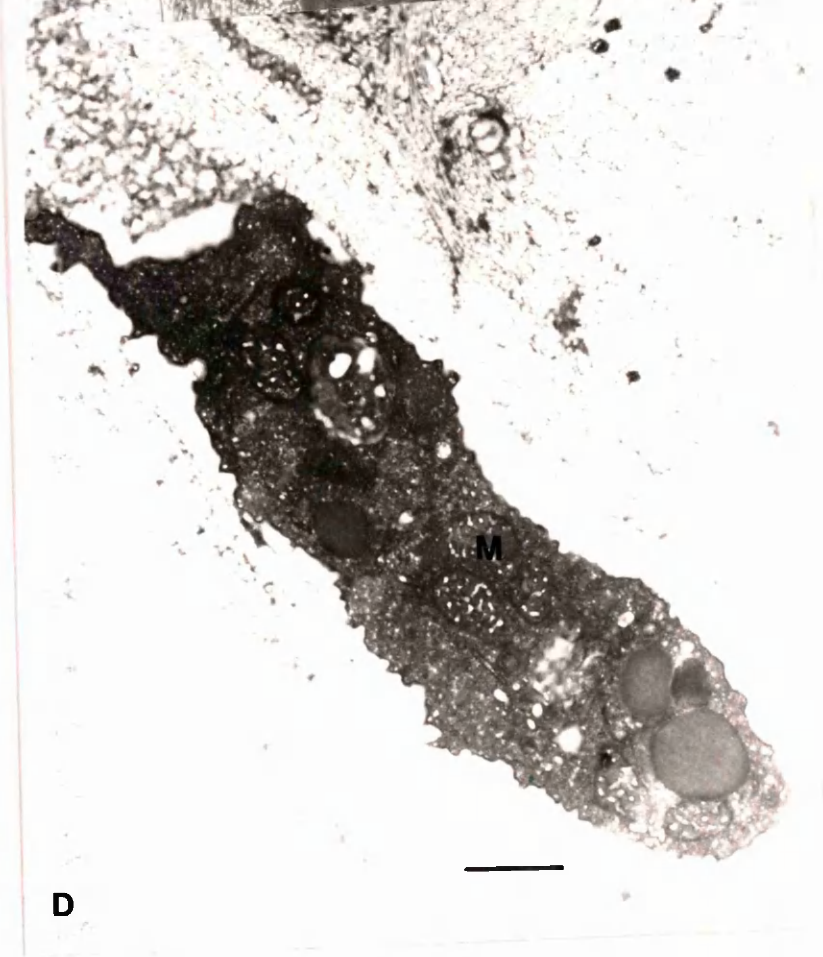
M
D

4.4.0. DISCUSSION

4.4.1. *Identification of Hartmannella sp.*

Measurements and morphological features of the cysts and trophozoites of *Hartmannella sp.* (WI isolate) (Table 4.1) agreed with those of the type strain *Hartmannella vermiformis* (CCAP strain 1534/7A) examined here and also described by Page (1985; 1988), at both light and electron microscope levels. The measurements of cyst diameters, the lengths and breadths of the trophozoites obtained from the present study however, differed slightly from those of Page who found cyst diameters between 4.0 µm and 9.5 µm, length of the trophozoite between 12 µm and 33 µm, and the maximum of trophozoite length/width 8.4. Comparable variations in cyst and trophozoite measurements have been reported for *H. vermiformis* (Cerva, 1971; Cerva and Huldt, 1974). The difference in size between my specimens and those of Page (who also studied strain 1534/7A), can probably be attributed to the growth conditions of the amoebae and also techniques used for measuring the amoebae. For example, cysts in contact preparations become progressively more flattened and hence increased in diameter as a result of compression (Page, 1988). In the present study, the measurements of both cysts and trophozoites of *H. vermiformis* CCAP strain 1534/7A and *Hartmannella sp.* (WI isolate) were almost identical. The *Hartmannella sp.* (WI isolate) isolated from a contact lens case can therefore be assigned with confidence to the species *Hartmannella vermiformis.*

H. vermiformis recently isolated and identified from a hospital water supply was found to be associated with *Legionella pneumophila*, the aetiological agent of Legionaire's disease (Fields *et al.*, 1990). This finding suggests that this amoeba is widely distributed in the environment and is a potential harbourer of pathogens, therefore the amoeba is of medical importance. The ability of the amoeba to grow at both temperatures 25°C and 35°C observed in the present study shows its wide temperature tolerence. *Hartmannella* also was observed to be still viable in Optisol medium but containing killed bacteria after incubation at 35°C for ~24 h, proves its adaptability to survive in a variety of media but only in the presence of living or killed bacteria.

The flattened multipseudopodial form of the amoeba was not described in *A New Key to Freshwater and Soil Gymnamoebae* by Page (1988), but in the present study, this form of *Hartmannella vermiformis* was always observed on agar and co-existed with the elongated form. The living flattened form of the amoeba exhibiting several tiny pseudopodial projections on its surface might cause confusion when identifying *Hartmannella* spp. by light microscopy. It is suggested that for identification of *Hartmannella* spp. the two forms of amoebae should be taken into account together with their cyst morphology. The nucleus of *Hartmannella* which contains extranucleolar chromatin bodies in the nucleoplasm is the main criterion for recognising this amoeba by transmission electron microscopy. Other limax amoebae such as *Naegleria* do not have chromatin bodies in their nucleoplasm (Schuster, 1975b; Page, 1985). At the ultrastructural level, the cyst morphology can be recognised and identified easily. For example, the cyst of *Hartmannella,* under TEM was observed with a double wall but by light microscopy the cyst appeared to have but a single wall. This study proves that both light microscopy and transmission electron microscopy examinations are essential for identification of amoebae. Mitotic patterns (Singh, 1952) have proved to cause confusion while identifying the amoebae especially *Hartmannella sp.* since several genera of small amoebae have a similar pattern of nuclear division. Alloenzyme electrophoretic patterns for different strains of *H. vermiformis* have been found to be similar, suggesting that they could also be used in identification of *Hartmannella vermiformis* (Fields *et al.*, 1990).

4.4.2. *Evidence of pathogenicity*

In vitro at the temperature indicated, *Hartmanella vermiformis* (WI isolate) seemed unable to penetrate and invade isolated corneal tissue, though under comparable conditions *Acanthamoeba castellanii* appeared able to do so. *A. castellanii* used for comparison in *in vitro* invasion studies on *H. vermiformis* in human corneas, was originally isolated from a corneal ulcer biopsy so its pathogenicity is guaranteed. *Hartmannella* however, appeared to denude the corneal surface of stratified epithelium while in the control this surface remained covered with multilayered epithelial cells. The removal of most epithelial cells when the cornea was incubated with *H. vermiformis* suggests that the amoeba might have a different mechanism for damaging the cornea. *Hartmannella* perhaps secretes lytic enzymes which cause the epithelium to dissociate. *Acanthamoeba* on the other hand, seems to invade the corneal stroma without necessarily damaging the overlying epithelium. The amoeba may have invaded the stroma in the present study by entering at the cut edge of the cornea tissue, and this route of invasion might be different from invasion of the amoeba *in vivo*. Although both trophozoites and cysts of *Acanthamoeba* have been observed to adhere to the epithelial surface of the cornea *in vitro* (Niederkorn *et al.*, 1992), such attachment of *Acanthamoeba* in the present study was not observed.

The remnants of the epithelium observed on the corneal surface in the presence of either *Hartmannella* or *Acanthamoeba*, exhibited different cell morphology and attachment to the Bowman's zone surface compared with epithelial cells in the control. In the presence of *Hartmannella*, the epithelial cells were more flattened with no evidence of being attached to the basement membrane. In the presence of *Acanthamoeba*, some epithelial cells became more rounded and looked swollen. The attachment of such cells to the Bowman's zone appeared not to be through a basement membrane. What induces the epithelial attachment to the

Bowman's zone is not known but the attachment is firm and could explain why some of the epithelial cells were intact on the corneal surface in the presence of *Acanthamoeba* compared with the corneal epithelium in the presence of *Hartmannella*.

It has been suggested that epithelial ulceration in human cornea exposed to *Acanthamoeba castellanii* is due to enzymes secreted by the amoeba as the initial step in preparing the host epithelium for phagocytosis. Through this mechanism, the amoeba could move deeper through the corneal surface (Moore *et al.*, 1991). If the invasion of *Acanthamoeba* involves enzyme secretions, the amount of enzymes being secreted must be in small quantities so that only a small part of the epithelium would be affected, the rest of the epithelium remaining intact. In the present study, however, a relatively intact epithelium might be expected if the amoebae did not invade the corneal stroma through the epithelium but via the cut edge of the stroma. Erosion of the epithelial layer of the cornea when exposed to *Hartmannella* was possibly due to the enzymes secreted by the amoeba. Although scanning electron microscopy showed an irregular surface of the cornea in controls, this irregularity could be due to the lack of removal of surface dead cells by the flushing actions of tears in the stored stroma.

Despite being unable to invade the corneal stroma, *Hartmannella* may still be able to threaten human vision. By destroying the epithelial layer which serves as the main refracting interface, the light entering the eyes will be scattered and this will create an irregular astigmatism (Casey and Mayer, 1984). Intact epithelium, through the small projections (plicae) on its exposed cell surfaces, is also essential as a barrier to fluid and small water-soluble molecules (Casey and Mayer, 1984). If the epithelium was not present, such activities would not take place and so the stroma would not function properly.

In *in vivo* studies using a pig model for *Acanthamoeba* keratitis induced by contact lens' wear, three distinct stages of the disease have been observed. The stages are 1) acute infection, 2) condensed infiltrate, and 3) resolution (YuGuang *et al.*, 1992). Histological examination of each stage described by the authors showed that at the first stage of infection, 50% of the experimental animals had intact corneal epithelium but the remaining animals displayed irregular superficial intactness of the cornea. Inflammatory infiltrate in the stroma at this stage was composed of neutrophils. In the second stage, erosions in the corneal epithelium occurred which progressed to stroma disintegration. Blood vessels penetrated the stroma, eventually invading the entire stroma. In the last stage, reestablishment of epithelial integrity, reduction of edema and infiltration, and restoration of corneal clarity occurred. An inflammatory and vascular response to *Acanthamoeba* invasion of the human cornea could not occur *in vitro* but results obtained in the present study might parallel some stages of acute infection. Within 24 h, the acanthamoebae were found to penetrate the corneal stroma. Observations on pathogenicity of *Acanthamoeba* or *Hartmannella* in this study were conducted *in vitro* and did not permit observation longer than 24 h. If the observation time is longer, the cornea tends to disintegrate even in the absence of amoebae, since there is no blood or tear film supply to provide oxygen and nutrients to the cornea.

In *in vitro* studies of corneal pathogenicity of *Acanthamoeba*, cytopathic effects have been observed at 26 h when inoculated with 10^2 amoebae and at 1½ h when inoculated with 10^3 or greater amoebae (Larkin *et al.*, 1991). In the present study, $\sim 10^4$ amoebae per well (not including cysts and non-viable cells) were used for both *Hartmannella sp.* and *Acanthamoeba castellanii* to observe their invasion of human corneas. The effective size of inoculum for *Hartmannella* in order to produce a massive cornea tissue destruction could not be determined due to limitation of the supply of human corneas. Nevertheless, with the size inoculum used, *Hartmannella* appears to be able to cause destruction of the corneal epithelium within 24 h.

The presence of *Hartmannella vermiformis* (WI isolate) in one of the contact lens cases during a survey of microbial contaminants may be related to bacteria presence as a food source. The non-pigmented Enterobacteriaceae *Escherichia coli* and *Klebsiella aerogenes* are excellent food for *H. vermiformis* (Weekers *et al.*, 1993). Other bacteria such as *Arthrobacter simplex, Agrobacterium tumefaciens, Bacillus megaterium, B. subtilis*, and *Pseudomonas fluorescens* are also utilised by the amoeba (Weekers *et al.*, 1993). *E. coli, P. fluorescens* and *Klebsiella pneumoniae* are among other bacteria isolated and identified from contact lens cases (Devonshire *et al.*, 1993) indicating a possible association between *Hartmannella* and the bacteria. The ability of some bacteria to adhere to ocular biomaterials such as soft contact lenses and their interactions with amoebae (*Acanthamoeba*) on soft contact lens surfaces, leading to *Acanthamoeba* keritītis have been documented by John (1991). The possibility that *Hartmannella vermiformis* could cause damage to the human cornea after introduction on a contaminated contact lens becomes more evident.

Although cytopathogenicity of an amoeba *in vitro* does not always correlate with *in vivo* (Marciano-Cabral and Fulford, 1986), the results from the present study suggesting ability of *Hartmannella* to damage the epithelium of the human cornea cannot be ignored. Further investigations such as using a pig model could be useful to observe the amoeba's pathogenicity to the cornea *in vivo* since living pig eyes have been found to provide the most suitable model system for studying *Acanthamoeba* infection (Niederkorn *et al.*, 1992), and keratitis observed in this animal clinically and hispathologically mimics the human counterpart (YuGuang *et al.*, 1992).

4.5.0. SUMMARY

1. *Hartmannella sp* isolated from a contact lens case could be assigned to the species *H. vermiformis* Page, 1967 due to its similarities in locomotion, and morphology (including measurements of cysts and trophozoites) with *Hartmannella vermiformis* CCAP strain 1534/7A. The isolate is therefore designated *H. vermiformis* (WI isolate).

2. The ability of *H. vermiformis* to cause damage to human cornea *in vitro* was tested. Presence of the amoeba diminished the epithelial layer of the cornea within 24 h at 25°C or 35°C. Unlike *Hartmannella*, *Acanthamoeba castellanii* was observed in the corneal stroma within the same period of observation. *Acanthamoeba* appears not to cause destruction to the epithelium while invading the stroma *in vitro*. Results form this study suggest that *Hartmannella* and *Acanthamoeba* have different mechanisms for destroying the human cornea.

Chapter 5

List of references

List of References

ALEXEIEFF, A. (1912). Sur les caractères cytologiques et la systematique des amibes du groupe *limax* (*Naegleria* nov. gen. et *Hartmannia* nov. gen.) et des amibes parasites du vertébrés (*Proctamoeba* nov. gen.). *Bull. Soc. Zool. Fr.*, **37**: 55-74.

ADAMS, M., ANDREWS, R.H., RIBINSON, B., CHRISTY, P.,BAVERSTOCK, P.R., DOBSON, P.J and BLACKLER, S.J. (1989). A genetic approach to species criteria in the amoeba genus *Naegleria* using allozyme electrophoresis. *Int. J. Parasitol.,* **19:** 823-835.

ALONSO, P., and ZUBIAUR, E. (1989). Determination of free and bound amino acids in three strains of *Naegleria. Acta Protozoologica.*, **28:** 111-120.

AMSTRONG, L. and SNYDER, J. A. (1989). Selective reduction of anaphase B in quinacrine-treated PtK_1 cells. *Cell Motil. Cytoskel.,* **14:** 220-229.

ANDERSON, K, JAMIESON, A, JADIN, J.B. and WILLAERT, E. (1973). Primary amoebic meningoencephalitis. *Lancet* **1**: 627.

ANDREU, J.M. and TIMASHEFF, S.N. (1982). Tubulin bound to colchicine forms polymer different from microtubules. *Proc. Natl. Acad. Sci, USA.,* **79:** 6753-6756.

AURAN, J.D., STARR, M.B. and JACOBIEC, F.A. (1987). *Acanthamoeba* keratitis. A review of the literature. *Cornea.*, **6**: 2-26.

AVERNER, M. and FULTON, C. (1966). Carbon dioxide: signal for excystment of *Naegleria gruberi. J. Gen. Microb.*, **42**: 245-255.

BALAMUTH, W. (1964). Nutritional studies on axenic cultures of *Naegleria gruberi. J. Protozool.,* **11**: 19-20.

BALAMUTH, W., BRADBURY, P.C and SCHUSTER, F.L. (1983). Ultrastructure of the amoeboflagellte *Tetramitus rostratus. J. Protozool.,* **30**: 445-455

BAND, R.N. and S. MOHRLOK, S. (1973). Observations on induced amitosis in *Acanthamoeba. Exp. Cell Research.,* **79**: 327-337

BARRETT, A.J. and MCDONALD, J.K (1986). Nomenclature: protease, proteinase and peptidase. *Biochem. J.*, **237**: 935.

BARRETT, A.J., BUTTLE, D.J. and MASON, R.W. (1988). Lysosomal cysteinase. *ISI Atlas Sci: Biochem 1:* 256-260

BENSCH, K.G. and MALAWISTA, S.E (1969). Microtubular crystals in mammalian cells. *J. Cell. Bio.*, **40**: 95-106

BEYNON, R.J. and SALVESEN, G. (1989). Commercially available protease inhibitors. In *Proteolytic enzymes: a practical approach* (Beynon, R.J. and Bond, J.S., eds). IRL Press, Oxford University Press. pp 241-249.

BEZT, H. and WEISER, U. (1979). Protein degradation and proteinases during yeast sporulation. *Eur. J. Biochem.*, **62**: 65-76.

BIDDICK, C.J., ROGERS, L.H. and BROWN, T.J. (1984). Viability of pathogenic and non-pathogenic free-living amoebae in long term storage at a range of temperatures. *Appl. Environ. Microbiol.*, **48**: 859-860.

BINET, S., CHAINEAU, E., FELLOUS, A., LATASTE, H., KRIKORIAN, A., COUZINIER, J.P. and MEININGER,V.(1990). Immunofluorescence study of the action of navelbine, vincristine and vinblastine on mitotic and axonal microtubules. *Int. J. Cancer.*, **46**: 262-266.

BORISY, G.G., and TAYLOR, E.W. (1967). The mechanism of action of colchicine. Binding of colchicine-^{3}H to cellular protein. *J. Cell Biol* **34**: 525-533

BOUVIER, J., SCHNEIDER, P. ETGES, R. and BORDIER, C. (1990). Peptide substrate specificity of the membrane-bound metallo-protease of *Leishmania. Biochemistry.*, **29**: 10113-10119.

BRENT, P.W. (1958). A study of the mechanism of pinocytosis. *Exp. Cell Res.*, **15**: 300-313.

BRANDT, F.F., WARE, D.A. and VISVESVARA, G.S. (1989). Viability of *Acanthamoeba* cysts in ophthalmic solutions. *Appl. Env. Microb.*, **55:** 1144-1146.

BREIMAN, R.F., FIELDS, B.S., SANDEN, G.N., VOLMER, L., MEIER, A and SPIKA, J.S. (1990). Association of shower use with Legionnaires' disease: possible role of amoebae. *J.A.M.A.*, **263**: 2924-2926.

BRINKLEY, B.R. (1985). Microtubule organising centres. *Ann. Rev. Cell Biol.*, **1**: 145-172.

BRINKLEY, B.R. (1990). Toward a structural and molecular definition of the kinetochore. *Cell Motil. Cyto.*, **16:** 104-109.

BROWN, T. (1979). Observations by immunofluorescence microscopy and electron microscopy on the cytopathogenicity of *Naegleria folweri* in mouse embryo cultures. *J. Med. Microbiol.*, **12**: 363-371.

BRYAN, J. and WILSON, L.(1971). Are cytoplasmic microtubules heteropolymers? *Proc. Nat. Acad, Sci. USA.*, **8:** 1762-1766.

BYERS, T.J., AKINS, R., MAYNARD, B., LEFKEN, R. and MARTIN, S. (1980). Rapid growth of *Acanthamoeba* in defined media: induction of encystment by glucose-acetate starvation. *J. Protozool.*, **27:** 216-219.

CANDE, W.Z. and HOGAN, C.J. (1989). The mechanism of anaphase spindle elongation. *Bioessays.*, **11**: 5-9.

CARIOU, M.L. and PERNIN, P. (1987). First evidence for diploidy and genetic recombination in free-living amoebae of the genus *Naegleria* on the basis of electrophoretic variation. *Genetics.*, **115**: 265-270.

CAROSI, G., SCAGLIA, M., FILICE, G. and WILLAERT, E. (1976). An electron microscope study of *Naegleria jadini* nov. sp. (Wallaert-Le Ray, 1973) in axenic "medium". The amoeboid stage. *Prototislogica.,* **12**: 31-36.

CAROSI,G., SCAGLIA, M., FILICIE, G. and WILLAERT, E. (1977). A comparative electron microscope study of axenically cultivated, trophozoites of free-living amoebae of the genus *Acanthamoeba* and *Naegleria* with special reference to the species *N. gruberi* (Schardinger 1899), *N. fowleri* (Carter 1970) and *N. jadini* (Willaert and Le Ray 1973). *Arch. Protistenkd.,* **273**: 264-273.

CARTER, R.F. (1970). Description on a *Naegleria* species isolated from two cases of primary amoebic meningoencephalitis, and of the experimental pathological changes by it. *J. Patho.*, **100**: 214-244.

CASEY, T.A. and MAYER, D.J. (1984). Cornea Grafting: Principle and practice. W.B. Saunders Company, London. pp 17-25.

CERVA, L. (1969). Amoebic meningoencephalitis: axenic culture of *Naegleria. Science.*, **163**: 576.

CERVA, L. (1971). Studies of limax amoebae in a swimming pool. *Hydrobiologia*, **38:** 141-161.

CERVA, L. and HULDT, G. (1974). Limax amoebae in five swimming pools in Stockholm. *Folia Parasitol. (Praha)*, **21**: 71-75.

CERVA, L., SERBUS, C. and SKOCIL, V. (1973). Isolation of limax amoebae from the nasal mucosa of man. *Folia Parasitol. (Praha).*, **20**: 97-103.

CHANG, S.L. (1974). Etiological, pathological, epidemiological, and diagnostical considerations of primary amoebic meningoencephalatis. *Crit. Rev. Microbiol.,* **3**: 135-159.

CHANG, S.L. (1978). Resistance of pathogenic *Naegleria* to some common physical and chemical agents. *Appl. Environ. Microbiol.*, **35**: 368-375.

CHANG, S.L. (1979). Pathogenesis of pathogenic *Naegleria* amoeba. *Folia Parasitol. (Prague).*, **26**: 195-200.

CHAPMAN-ANDRESEN, C. (1973). Endocytic processes. In *The Biology of Amoeba.* (JEON,K.W., ed). Cell Biology. A series of monographs. Academic Press. New York. pp 319-348.

CLARK, C.G. (1990). Genome structure and evolution of *Naegleria* and its relatives. *J. Protozool. (suppl.).*, **37**: 2-6.

CLARK, C.G., LAI, E.Y., FULTON, C. and CROSS, G.A.M. (1990). Electrophoretic karyotype and linkage groups of the amoeboflagellate *Naegleria gruberi. J. Protozool.,* **37**: 400-408.

CLINE, M., CARCHMAN, R. and MARCIANO-CABRAL, F. (1986). Movement of *Naegleria fowleri* stimulated by mammalian cells *in vitro. J. Protozool.*, **33**: 10-13.

COOMBS, G.H. and NORTH, M.J. (1983). An analysis of the proteinases of *Trichomonas vaginalis* by polyacrylamide gel electrophoresis. *Parasitol.*, **86**: 1-6

CURSONS, R.T.M., and BROWN, T.J. (1978). Use of cell cultures as indicator of pathogenicity of free-living amoebae. *J. Clin. Pathol.*, **31**: 1-11.

CURSONS, R.T.M., BROWN, T.J. and KEYS, E. A. (1978). Virulence of pathogenic free-living amoebae. *J. Parasitol.,* **64**: 744-745.

DAGGETT, P.M. and NERAD, T.E. (1983). The biochemical identification of vahlkampfiid amoebae. J. *Protozool.,* **30:** 126-128.

DE JONCKHEERE, J.F. (1977). Use of an axenic medium for differentiation between pathogenic and non-pathogenic *Naegleria fowleri* isolates. *Appl. Environ. Microb.,* **33**: 751-757.

DE JONCKHEERE, J.F. (1979). Differentiation in virulence of *Naegleria fowleri. Pathol. Biol.,* **27**: 453-458.

DE JONCKHEERE, J.F. (1981). *Naegleria australiensis* sp. nov., another pathogenic *Naegleria* from water. *Protistologica.*, **17**: 423-429.

DE JONCKHEERE J.F. (1982). Isoenzme patterns of pathogenic and non-pathogenic *Naegleria spp* using agarose isoelectric focusing. *Ann. Microbiol.,*(Inst.Pasteur), **133**: 319-342.

DE JONCKHEERE, J.F. (1987). Characterisation of *Naegleria* species by restriction endonuclease digestion of whole-cell DNA. *Mol. Biochem. Parasitol.*, **24**: 55-66.

DE JONCKHEERE, J.F. (1988). *Naegleria andersoni n. sp.*, a cosmopolitian amoeboflagellate, with two subspecies. *Eur. J. Protis.*, **23**: 327.

DE JONCKHEERE, J.F. (1989). Variation of electrophoretic karyotypes among *Naegleria spp*. *Parasitol. Res.*, **76**: 55-62.

DE JONCKHEERE, J.F. and MICHEL, R. (1988). Species identification and virulence of *Acanthamoeba* strains from human nasal mucosa. *Parasitol. Res.*, **74**: 314.

DE JONCKHEERE J.F., DIVE, D.G., PUSSARD, M and VICKERMAN, K (1984a). *Willaertia magna* gen nov., sp. nov. (Vahlkampfiidae), a thermophilic amoeba found in different habitats. *Protistologica.*, **20**: 5-13.

DE JONCKHEERE, J.F., and VAN DE VOORDE, H. (1976). Differences in destruction of cysts of pathogenic and non-pathogenic *Naegleria* and *Acanthamoeba* by chlorine. *Appl. Environ. Microbiol.*, **31:** 294-297.

DE JONCKHEERE, J.F., and VAN DE VOORDE, H. (1977). The distribution of *Naegleria fowleri* in man-made thermal waters. *Am. J. Trop. Med. Hyg.*, **26**:10-15.

DE JONCKHEERE J.F., VAN DIJCK, P and VAN DER VOORDE, H (1974). Evaluation of indirect fluorescent-antibody technique for identification of *Naegleria* species. *Appl. Microbiol.*, **28**: 159-164

DE JONCKHEERE J.F., VAN DIJCK, P and VAN DER VOORDE, H (1975). The effect of thermal pollution on the distribution of *Naegleria folweri. J. Hyg. Camb.*, **75:** 7-13.

DE JONCKHEERE, J.F., PERNIN, P., SCAGLIA, M. and MICHEL, R. (1984b). A comparative study of 14 strains of *Naegleria australiensis* demonstrates the existence of a highly virulent subspecies: *N. australiensis italica* n. spp. *J. Protozool.*, **31**: 324-331.

DE MEESTER, F., SHAW, E., SCHOLZE, H., STOLARSKY, T and MIRELMAN, D. (1990). Specific labelling of cysteine proteinases in pathogenic and non-pathogenic *Entamoeba histolytica. Infect. Immun.*, **58**: 1396-1401.

DEVONSHIRE, P., MUNRO, F.A. ABERNETHY, C. and CLARK, B.J. (1993). Microbial contamination of contact lens cases in the west of Scotland. *Brit. J. Ophthalmol.*, 77: 41-45.

DINGLE, A.D and FULTON, C (1966). Development of the flagellar apparatus of *Naegleria*. *J. Cell Biol.*, **31**: 43-54

DODGE, J.D. and VICKERMAN, K. (1980). Mitosis and meiosis: nuclear division mechanisms. In *The Eukaryotic Microbial Cell* (Gooday, G.W. and Trinci, A.P.J.,eds). Cambridge University Press. pp 77-102

DUNNEBACKE, T.H. and DIXON, J.S. (1989). NACM, a cytopathogen from *Naegleria* amoeba: Purification, production of monoclonal antibody and immunoreactive material in NACM-treated vertebrate cell cultures. *J. Cell Sci.*, **93**: 391-402.

DUNNEBACKE, T.H. and DIXON, J.S. (1990). NACM, A cytopathogenic protein from *Naegleria gruberi*, EG_S; purification, production of monoclonal antibody, and the immunoidentification of a product that develops in NACM-treated vertebrate cultures. *J. Protozool (suppl.).*, **37:** 11-16.

DUNNEBACKE, T.H. and SCHUSTER, F.L. (1974). An infectious agent associated with amoebae of the genus *Naegleria*. *J. Protozool.*, **21**: 327-329.

DUSTIN, P (1984). Microtubules and mitosis. In *Microtubules* (2nd edit). Springer-Verlag, Berlin, Tokyo. pp 354-399.

ERICSSON, J.L.E. (1969). Studies on induced cellular autophagy. II. Characterisation of the membrane bordering autophagosomes in parenchymal liver cells. *Exp. Cell Res.*, **56:** 393-405.

EUTENUER, U. and McINTOSH,.J.R. (1981). Structural polarity of kinetochore microtubules in PtK_1 cells. *J. Cell. Biol.*, **89**: 338-345.

FELDMAN, M. R. (1977). *Naegleria fowleri*: Fine structural localisation of acid phosphatase and heme proteins. *Exp. Parasitol.*, **41**: 290-306.

FERRANTE, A (1988). Elastase in the pathogenic free-living amoeba *Naegleria* and *Acanthamoeba sp*. *Infect. Immun.*, **56**: 3320-33201.

FERRANTE, A. (1991). Free-living amoebae: pathogenicity and immunity. *Parasit. Immunol.*, **13**: 31-47.

FERRANTE, A. and BATES, E.J. (1988). Elastase in the pathogenic free-living amoebae *Naegleria* and *Acanthamoeba* spp. *Infect. Immunity.*, **56**: 3320-3321.

FIELDS, B.S., BARBAREE, J.M., SHOTTS, E.B., FEELEY, J.C., MORRILL, W.E., SANDEN, G.N. and DYKSTRA, M.J. (1986). Comparison of guinea pig and protozoan models for determining virulence of *Legionella* species. *Infect. Immun.*, **53**: 553-559.

FIELDS, B.S., NERAD, T.A., SAWYER, T.K., KING, C.H., BARBAREE, J.M., MARTIN, W.T., MORRILL, W.E. and SANDEN, G.N. (1990). Characterisation of an axenic strain of *Hartmannella vermiformis* obtained from an investigation of nocosomal Legionellosis. *J. Protozool.,* **37:** 581-583.

FOWLER, M. and CARTER, R.F. (1965). Acute pyogenic meningoencephalitis probably due to *Acanthamoeba sp.*: a preliminary report. *Brit. Med. J.,* **3:** 740-742.

FORSBURG, S.L. and NURSE, P. (1991). Cell cycle regulation in yeast *Saccharomyces cerevisiae* and *Schizosaccharomyces pombe. Ann. Rev. Cell Biol.,* **7**: 227-257.

FULFORD, D.E. and MARCIANO-CABRAL, F (1987). Cytolytic activity of *Naegleria fowleri* cell-free extract. *J. Protozool.,* **33**: 498-502.

FULFORD, D.E., BRADLEY, S.G. and MARCIANO-CABRAL,F. (1985). Cytopathogenicity of *Naegleria fowleri* for cultured rat neuroblastoma cells. *J. Protozool.*, **32**: 176-180.

FULTON, C (1970). Amoeboflagellates as research partners: The laboratory biology of *Naegleria* and *Tetramitus*. In *Methods in Cell Physiology* (Prescot, D.M, ed). **4**: 314-476.

FULTON, C. (1971). Centrioles. In *Origin and Continuity of Cell Organnelles* (Reinert, J. and Ursprung, H., eds). Springer-Verlag, New York. pp 170-221.

FULTON, C (1977). Cell differentiation in *Naegleria gruberi*. *Ann. Rev. Microbiol.,* **31**: 597-629.

FULTON,C. and DINGLE, A.D. (1971). Basal bodies, but not centrioles in *Naegleria*. *J. Cell Biol.*, **51**: 826-836

FULTON, C and GUERRINI. A.M (1969). Mitotic synchrony in *Naegleria* amoebae. *Exp. Cell Research.*, **56**: 194-200

FULTON,C., KANE, R.E. and STEPHENS, R.E. (1971). Serological similarity of flagellar and mitotic microtubules. *J. Cell Biol.,* **50:** 762-773.

GADASI, H. and KESSLER, E. (1983). Correlation of virulence and collagenolytic activity in *Entamoeba histolytica. Infect. Immun.*, **39:** 528-531.

GARDINER, P.R., MILLER, R.H. and MARSH, C.P. (1981). Studies on the rhizoplast from *Naegleria gruberi. J. Cell Sci.,* **47**: 277-293.

GEAHLAN, R.L. and HALEY, B.E. (1979). Use of GTP photoaffinity probe to resolve aspects of the mechanism of tubulin polymerisation. *J. Biol. Chem.*, **254:** 11982-11987.

GICQUAUD, C. and TREMBLAY, N. (1991). Observations with hoechst staining of amitosis in *Acanthamoeba castellanii*. *J. Protozool.*, **38**: 221-224.

GIESE, A.C. (1979). Bulk Transport. In *Cell Physiology*. W.B. Saunders Company. pp 410-426.

GRIFFIN, J.L. (1972). Temperature tolerance of pathogenic and non-pathogenic free-living amoebas. *Science.*, **178**: 869-870.

GRIFFIN, J.L (1978). Pathogenic free-living amoebae. In: *Parasitic Protozoa.*(Kreier, J.P, ed). Academic Press, NY. pp 508-544.

GRIFFIN, J.L. (1983). The pathogenic amoeboflagellate *Naegleria fowleri*: environmental isolations, competitors, ecologic interactions, and the flagellate-empty habitat hypothesis. *J. Protozool.*, **30**: 403-409.

GUTMANN, E.J., NILES, J.L., McCLUSKEY, R.T. and BROWN, D. (1989). Colchicine-induced redistribution of an apical glycoprotein (gp330) in proximal tubules. *Am. J. Physiol.*, **257**: 397-407.

HENDRY, K.A.K (1987). Studies on the flagellar attachment on African Trypanosomes. A PhD Dissertation. Department of Zoology, University of Glasgow. pp 145-146.

HESSE, J., MARUTA, H. and ISENBERG, G. (1985). Monoclonal-antibosies localise the exchangeable GTP-binding site in β-tubulins and not α-tubulins. *FEBS Lett.*, **179**: 91-95.

HOGAN, C.J. and CANDE, W.Z. (1990). Antiparallel microtubule interactions: Spindle formation and Anaphase B. *Cell Motil. Cyto.*, **16**: 99-103.

HORIO, T.,UZAWA,S.,JUNG,M.K, OAKLEY,B.R., TANAKA, K. and YANAGIDA, M. (1991). The fission yeast γ-tubulin is essential for mitosis and is localised at microtubule organsing centres. *J. Cell Sci.*, **99**: 693-700.

HOLTZMAN, E. (1989). *Lysosomes.* (Siekevitz, P., ed.). Plenum Press, New York, London. 439 pp.

HU, W.N., BAND, R.N. and KOPACHIK, W.J. (1991). Virulence-related protein synthesis in *Naegleria fowleri*. *Infect. Immun.*, **59**: 4278-4282.

HYSMITH, R.M. and FRANSON, R.C. (1982). Elevated levels of cellular and extracellualr phospholipase from pathogenic *Naegleria fowleri. Biochim. Biophys. Acta.,* **711**: 26-32.

JARROLL, E.L. (1991). *Giardia* cysts: their biochemistry and metabolism. In *Biochemical Protozoology* (Coombs, G.H. and North, M., eds). Taylor and Francis, London. pp 52-60.

JOHN, D.T. (1982). Primary amoebic meningoencephalitis and the biology of *Naegleria fowleri. Ann. Rev. Microb.,* **36**: 101-123.

JONES, D.B. (1986). *Acanthamoeba*-the ultimate opportunist? *Amer. J. Ophthamol.*., **102**: 527.

JOHN, D.T., COLE, J.R., and MARCIANO-CABRAL, F. (1984). Sucker-like structures on the pathogenic amoeba *Naegleria fowleri. Appl. Environ. Microbiol.*, **47:** 12-14.

JOHN, D.T., COLE, T.B. and BRUNER, R.A. (1985). Amoebastomes of *Naegleria fowleri. J. Protozool.*, **32**: 12-19.

JOHN, T. (1991). Interactions of bacteria and amoebae with ocular biomaterials. *Cells and Mat.,* **1**: 129-139.

JOHN, T., and DESAI, D. (1991). Adherence of *Acanthamoeba castellanii* cysts and trophozoites to worn hydrogel cantact lenses. *Invest. Ophthalmol. Vis. Sci (Suppl.).,* **32**: 728.

JOHN, T., DESAI, D. and SAHM, D. (1989). Adherence of *Acanthamoeba castellanii* cysts and trophozoites to unworn soft contact lenses. *Am. J. Ophthalmol.,* **108**: 658-664.

KADLEC, V. (1978). The occurrence of amphizoic amoebae in domestic animals. *J. Protozool.*, **25**: 255-237.

KALT, A. and SCHLIWA, M. (1993). Molecular components of the centrosome. *Trends. Cell Biol.*, **3**: 118-128.

KANE, R.E.(1965). The mitotic apparatus: Physical-chemical factors controlling stability. *J. Cell Biol.*, **25:** 137

KAUFMAN, S.S., BLAIN, P.L., PARK, J.H.Y. and TUMA, D.J. (1990). Microtubular response to colchicine in adult and foetal-rat hepatocytes. *Comp. Biochem. Physiol.*, **95**: 281-290.

KAUSHALL, D.C., and SHUKLA, O.P. (1976). Release of certain extracellular enzymes during excystment of axenically produced cysts of *Hartmannella culbertsoni*. *Indian J. Exp. Biol.,* **14**: 498-499.

KAWAMOTO, F. and KUMADA, N. (1987). Fluorescent-probes for detection of protozoan parasites. *Parasitol. Today.*, **3**: 284-286.

KEENE, W.E., HIDALGO, M.E., OROZCO,E and McKERROW, J.H. (1990). Correlation of the cytophathic effect of virulent trophozoites with the secretion of a cysteine proteinases. *Exp. Parasitol.*, **71:** 199-206.

KILVINGTON, S., MANN, P.G. and WARHURST, D.C. (1984). Differentiation between *Naegleria fowleri* and *Naegleria lovaniensis* using isoenzyme electrophoresis of aspartic aminotransferase. *Trans. R. Soc. Trop. Med. Hyg.*, **78**: 562-563.

KING, C.A., PRESTON, T.M., MILLER, R.H. and GROSE,C. (1982). The cell surface in amoeboid locomotion-studies on the role of cell-substrate adhesion. *Cell Biol. Int. Rep.*, **6**: 893-900.

KING, C.A., COOPER, L. and PRESTON, T.M. (1983a). Cell-substrate interactions during amoeboid locomotion of *Naegleria gruberi* with special reference to alterations in temperature and electrolyte concentration of the medium. *Protoplasma.*, **118**: 10-18.

KING, C.A., PRESTON, T.M., and MILLER, R.H. (1983b). Cell-substrate interactions in amoeboid locomotion -a matched reflexion interference and transmission electron microscopy. *Cell Biol. Int. Rep.*, **7**: 641-649.

KIRCHNER, K. and MANDELKOW, E. (1985). Tubulin domains responsible for assembly of dimers and protofilaments. *EMBO J.*, **4**: 2397-2402.

KIRSCHKE, H. and BARRETT, A.J. (1987). The chemistry of lysosomal proteases. In *Lysosomes: their role in protein breakdown* (Glaumann, H. and Ballard, F.J., eds). New York Academic Press. pp 193-238.

KLAR, A.J.S. and HALVORSON, H.O. (1975). Proteinase activities of *Saccharomyces cerevisiae* during sporulation. *J. Bacteriol.*, **124**: 863-869.

KLUGH, H.E. (1974). Statistics. The essentials for research. John Wiley and Sons. pp 264-266.

KREZEL, L.S., GILICINSKI, M.D., BURLAND, T.G. and DOVE, W.F. (1990). Variable pathways for developmental changes in compostion and organisation of microtubules in *Physarum polycephalum. J. Cell Sci.* **96**: 383-393.

LAFONTAINE, J.G. and CHOUINARD. L. A. (1963). A correlated light and electron microscope study of the nucleolar material during mitosis in *Vicia faba. J. Cell. Biol.,* **17**: 167-200.

LARKIN, D.F.P., BERRY, M. and EASTLY, D.L. (1991). *In vitro* corneal pathogenicity of *Acanthamoeba*. *Eye*., **5:** 560-568.

LASTOVICA, A.J. (1974). Scanning electron microscopy of pathogenic and non-pathogenic *Naegleria* cysts. *Int. J. Parasitol*., **4**: 139-142.

LASTOVICA, A.J. (1976). Microfilaments in *Naegleria fowleri* amoebae. *Z. Parasitenk*., **50**: 245-250.

LASTOVICA, A.J. and DINGLE, A.D. (1971). Superprecipitation of an actomyosin-like complex isolated from *Naegleria gruberi* amoebae. *Exptl. Cell Res*., **66**: 337-345.

LARSON, D.E. and DINGLE, A.D. (1981). Isolation, ultrastructure and protein composition of the flagellar rootlet of *Naegleria gruberi*. *J. Cell Biol*., **89**: 424-432.

LAVERDE, D.E. and BRENT, M.M. (1980). Simplified soluble media for axenic cultivation of *Naegleria*. *Protistologica*., **16**: 11-15.

LAWANDE, R.V., ABRAHAM, S.N., JOHN, I. and EGLER, L.J. (1979). Recovery of soil amoebae from the nasal passages of children during the dusty hatmattan period in Zaria. *Am. J. Clin. Patho*., **71**: 201-203.

LAWANDE , R.V., MACFARLANE, J.T., WEIR, W.R.C. and AWUNOR-RENNER, C. (1980). A case of primary amoebic meningencephalatis in a Nigerian farmer. *Am. J. Trop. Med. Hyg*., **29**: 21-25.

LOCKWOOD, B.C., NORTH, M.J. and COOMBS, G.H. (1984). *Trichomonas vaginalis, Trichomonas foetus* and *Trichomonas batrachorum*; comparative proteolytic activity. *Exp. Parasitol*., **58**: 245-253.

LOCKWOOD, B.C., NORTH, M.J., SCOTT, K.I., BREMNER, A.F. and COOMBS, G.H. (1987). The use of a highly sensitive electrophoretic method to compare the proteinases of trichomonads. *Mol. Biochem. Parasitol.,* **24**: 89-95.

LOWREY, D.M. and McLAUGHLIN, J. (1985a). Activation of a heat-stable cytolytic protein associated with the surface membrane of *Naegleria fowleri*. *Infect. Immun*., **50**: 478-482.

LOWREY, D.M. and McLAUGHLIN, J. (1985b). Subcellular distribution of hydrolases in *Naegleria fowleri*. *J. Protozool*., **32**: 616-621.

LUFTIG, R.B., McMILLAN, P.N., WEATHERBEE, J.A. and WEIHING, R.R. (1977). Increased visualization of microtubules by an improved fixation procedure. *J. Histochem. Cytochem*., **25**: 175-187.

McDONALD, K (1989). Mitotic spindle ultrastucture and design. In. *Mitosis: Molecules and Mechanisms* (Ed. Hyams, J.S and Brinkley, B.R). AP. London. pp 1-38.

McEWEN, B. and EDELSTEIN, S.J. (1980). Evidence for a mixed lattice in microtubules reassembled *in vitro. J. Mol. Biol.*, **139**: 123-143.

McINTOSH, J.R. and HERING, J.E. (1991). Spindle fibre action and chromosome movement. *Annu. Rev. Cell Biol.*, 7: 403-426.

McKERROW, J.H. (1988). The role of proteinases in the pathogenesis of parasitic diseases. *Contemp. Issue Infect. Disease.*, 7: 51-57.

MAITRA, S.C., KRISHNA PRASAD, B.N., AGARWALA, S.C. and DAS, S.R. and (1976). Ultrastructural studies on experimental primary amoebic meningoencephalitis (PAME) of mouse due to *Naegleria aerobia* and *Hartmannella culbertsoni. Int. J. Parasitol.*, **6**: 489-493.

MANDELKOW, E., THOMAS, J. and COHEN, C. (1977). Microtubule structure at low resolution by x-ray diffraction. *Proc. Natl. Acad. Sci. USA.*, **74**: 3370-3374.

MARCIANO-CABRAL, F. (1988). Biology of *Naegleria* spp. *Microb. Rev.*, (*Am. Soc. Microb).*, **52**: 114-133.

MARCIANO-CABRAL, F. and BRADLEY, S.G. (1982). Cytopathogenicity of *Naegleria gruberi* for rat neuroblastoma cell cultures. *Infect. Immun.,* **35**: 1139-1141.

MARCIANO-CABRAL, F., and FULFORD, D.E. (1986). Cytopathology of pathogenic and non-pathogenic *Naegleria* species for cultured rat neuroblastoma cells. *Appl. Environ. Microbiol.,* **51**: 1133-1137.

MARCIANO-CABRAL, F. and JOHN, D.T. (1983). Cytopathogenicity of *Naegleria fowleri* for rat neuroblastoma cell cultures: scanning electron microscopy study. *Infect. Immun.*, **40**: 1214-1217.

MARCIANO-CABRAL, F., PATTERSON, M., JOHN, D.T. AND BRADLEY, S.G. (1982). Cytopathogenicity of *Naegleria fowleri* and *Naegleria gruberi* for established mammalian cell cultures. *J. Parasitol.*, **68**: 1110-1116.

MARGOLIS, R.L. and WILSON, L. (1977). Addition of colchicine-tubulin complex to microtubule ends. Mechanism of substoichiometric colchicine poisoning. *Proc. Natl. Acad. Sci. USA.*, **74**: 3466-3470.

MARTINEZ, A.J. (1983). Free-living amoebae, pathogenic aspects: a review. *Protozool. Abstr.,* 7: 293-306.

MARTINEZ, A.J. (1985). Free-living amoebae: natural history, prevention, diagnosis, pathology and treatment of disease. CRC Press, Boca Raton, Fla. pp 1-156.

MARTINEZ, A.J., DUMA, R.J., NELSON, E.C and MORETTA, F.L. (1973). Experimental *Naegleria* meningoencephalitis in mice. Penetration of the olfactory mucosal epithelium by *Naegleria* and pathologic changes produced: by light and electron microscopic study. *Lab. Invest.*, **29**: 121-133.

MARTINEZ, A.J., NELSON, E.C., JONES, M.M., DUMA, R.J. and ROSENBLUM, W.I. (1971). Experimental *Naegleria* meningoencephalitis: an electron microscope study. *Lab. Invest.*, **25**: 465-475.

MASON, R.W. (1991). Proteinases of mammals: an overview. In Biochemical Protozoology (Coombs, G.H. and North, M.J., eds.). Taylor and Francis, London. pp 168-179.

MAST, S.O. and DOYLE, L (1934). Ingestion of fluid by *Amoeba. Protoplasma.*, **20:** 555-560.

MATHERS, W., STEVENS, G. Jr., RODRIGUES, M., CHAN, C.C. GOLD, J., VISVESVARA, G.S., LEMP, M.A. and ZIMMERMAN, L.L. (1987). Immunopathology and electron microscopy of *Acanthamoeba keratitis. Am. J. Ophthalmol.,* **103**: 626-635.

MERDES, A., STELZER, E.H.K. and DEMEY, J. (1991). The 3-dimentional architecture of the mitotic spindle, analysed by confocal fluorescence and electron microscopy. *J. Elect. Micros. Tech.*, **18**: 61-73.

MERTENS, E. (1990). Occurence of pyrophosphate: fructose 6-phosphate 1-phosphotransferase in *Giardia lamblia* trophozoites. *Mol. Biochem. Parasitol.*, **40:** 147-150.

MERTENS, E., DE JONCKHEERE, J. F. and VAN SCHAFTINGEN, E. (1993). Pyrophosphate-dependent phosphofructokinase from the amoeba *Naegleria fowleri*, an AMP-sensitive enzyme. *Bichem. J.*, **292**: 797-803.

MITCHISON, T.J. (1988). Microtubule dynamics and kinetochore function in mitosis. *Annu. Rev. Cell Biol.*, **4**: 527-550.

MITCHISON, T.J. and KIRSCHNER, T.J. (1984). Dynamic instability of microtubule growth. *Nature (London).*, **312**: 237-242.

MITCHISON, T.J. and SAWIN, K.E. (1990). Tubulin flux in the mitotic spindle: where does it come from, where is it going? *Cell Motil. Cytoskel.*, **16**: 93-98.

MITCHISON, T.J., SCHULZE, E. and KIRSHCHNER, M. (1986). Sites of microtubule assembly and disassembly in the mitotic spindle. *Cell.*, **45**: 515-527.

MOORE, M.B., UBELAKER, J.E., MARTIN, J.H., SILVANY, R., DOUGHERTY, J.M., MEYER, D.R. and McCULLEY, J.P. (1991). *In vitro* penetration of human corneal epithelium by *Acanthamoeba castellanii*: a scanning and transmission electron microscopy study. *Cornea.*, **10:** 291-298.

MOSS, D.M., BRANDT, F.H., MATHEWS, H.M. and VISVESVARA, G.S. (1988). High-resolution polyacrylamide gradient gel electrophoresis (PPGE) of isoenzymes from five *Naegleria* species. *J. Protozool.*, **351**: 26-31.

MÜLLER, M., RÖHLICH,P., TÓTH, J and TÖRÖ, I. (1963). Fine structure and enzymic activity of protozoan food vacoules in lysosomes. C.I.B.A. Foundation Symposium on lysosomes (DEREUCK, A.V.S. and CAMERON, M.P.,eds). pp 201-216.

MULLINS, J.M. and SNYDER, J.A (1989). Introduction of random microtubule polymerization in cold and drug-treated ptK$_1$ cells following hyperosmotic shock treatment. *Eur. J. Cell Biol.*, **49**: 149-153.

MUNÖZ, M.L., CALDERON, J. and ROJKIND, M. (1982). The collagenase of *Entamoeba histolytica. J. Exp. Med.*, **155**: 42-51.

NAEGLER, K (1909). Entwicklungsgeschichtliche studien uber Amoben. *Arch. Protistenk.*, **15**: 1-53.

NAGAYAMA, A. and DALES, S. (1970). Rapid purification and the immunological specificity of mammalian microtubular paracrystals possessing an ATPas activity. *Proc. Nat. Acad. Sci.*, **66**: 464-471.

NAKANO, Y., SUDATE, Y. and KITAOKA, S. (1979). Purification and some properties of extracellular protease of *Euglena gracilis. Z. Agric. Biol. Chem.*, **43**: 223-229.

NERAD, T.A., VISVESVARA,G. and DAGGETT, P.M. (1983). Chemically defined media for the cultivation of *Naegleria*: pathogenic and high temperature tolerant species. *J. Protozool.*, **30:** 383-386.

NERAD, T.H. and DAGGET, P.M (1979). Starch gel electrophoresis: and effective method for separation of pathogenic and non-pathogenic *Naegleria* strains. *J. Protozool.*, **26**: 613-615.

NIEDERKORN, J.Y., UBELAKER, J.E., McCULLEY, J.P., STEWART, G.L., MEYWR, D.R., MELLON, J.A., SILVANY, R.E., YUGUANG and PIDHERNEY, M. (1992). Susceptibility of corneas from various animal species to *in vitro* binding and invasion by *Acanthamoeba castellanii. Invest. Ophthalmol. Vis. Sci.*, **33**: 104-112.

NORTH, M.J (1982). Comparative biochemistry of the proteinases of eucaryotic microorganisms. *Micro. Rev.(Am. Soc. Mic).*, pp 308-340

NORTH, M.J. (1989). Prevention of unwanted proteolysis. In *Proteolytic enzymes: a practical approach* (Beynon, R.J. and Bond, J.S., eds). pp 105-124.

NORTH, M. J. (1992). The characteristics of cysteine proteinases of parasitic protozoa. *Bio. Chemist. Hoppe-Sayler.*, **373**: 401-406.

NORTH, M.J., COOMBS, G.H. and BARRY, J.D. (1983). A comparative study of the proteolytic enzymes of *Trypanosoma brucei, T. equiperdum, T. evansi, T. vivax, Leishmania tarentolae* and *Crithidia fasciculata. Mol. Biochem. Parasitol.*, **9**: 161-180.

NORTH, M.J., SCOTT, K.I. and LOCKWOOD, B.C. (1988). Multiple cysteine proteinase forms during the life cycle of *Dictyostelium discoideum* revealed by electrophoretic analysis. *Biochem. J.*, **254**: 261-268.

NORTH, M.J., MOTTRAM, J.C. and COOMBS, G.H. (1990a). Cysteine proteinases of parasitic protozoa. *Parasit. Today.*, **6**: 270-275.

NORTH, M.J., ROBERTSON, C.D. and COOMBS, G.H. (1990b). The specificity of trichomonad cysteine proteinases analysed using fluorogenic substrate and specific inhibitors. *Mol. Biochem. Parasitol.*, **39**: 183-194.

OAKELY, B.R., OAKELY, C.E., YOON, Y. and JUNG, M.K. (1990). Gamma-tubulin is a component of the spindle pole body that is essential for microtubule function in *Aspergillus nidulans. Cells.*, **61**: 1289-1301.

O'DELL,W.D., and STEVENS,A.R. (1973). Quatitative growth of *Naegleria* in axenic culture. *Appl. Microbiol.*, **25**: 621-627.

O'DELL, W.D. and BRENT, M.M. (1974). Nutritional study of three strains of *Naegleria gruberi*. *J. Protozool.*, **21**: 129-133.

OLMSTED, J.B. and BORISY, G.G. (1973). Characterization of microtubule assembly in porcine brain extracts by viscometry. *Biochem,*. **12**: 4282-4289.

OROZCO, E., SOLIS, F.J., DOMINGUEZ, J. CHAVEZ, B. and HERNANDEZ, F. (1988). *Entamoeba histolytica:* Cell cycle and nuclear division. *Exp. Parasitol.*, **67**: 85-95.

PAGE, F.C. (1967a). Taxonomic criteria for limax amoebae with descriptions of three new species of *Hartmannella* and three of *Vahlkampfia*. *J. Protozool.*, **14**: 499-521.

PAGE, F.C. (1967b). Re-definition of the genus *Acanthamoeba* with descriptions of three species. *J. Protozool.*, 14: 709-724.

PAGE, F.C. (1974). A further study of taxonomic criteria for limax amoebae, with descriptions of new species and a key to genera. *Arch. Protistenk.*, **116**: 140-184.

PAGE, F.C (1975). Morphological variation in the cyst wall of *Naegleria gruberi* (Amoebida, Vahlkampfiidae). *Protistologica.,* **11**: 195-204.

PAGE, F.C. (1976). An illustrated key to freshwater and soil amoebae. Scientific Publication no. 34. Freshwater Biological Association, Kendal, Cumberland, United Kingdom. 155 pp.

PAGE, F.C. (1985). The limax amoebae: Comparative fine structure of the Hartmannellidae (lobosea) and further comparisons with the Vahlkampfiidae (Heterolobosea). *Prototislogica.*, **21**: 361-383.

PAGE, F.C. (1987). The classification of 'naked' amoebae (Phylum Rhizopoda). *Arch. Protistenk.*, **133**: 199-217.

PAGE, F.C (1988). A new key to freshwater and soil gymnamoebidae. Culture Collection of Algae and Protozoa. Freshwater Biological Association. 121 pp.

PAGE, F.C. and BLANTON, L (1985). The Heterolobosea (Sarcodina: Rhizopoda). A new class uniting the Schizopyrenida and the acrasidae (Acrasida). *Protistologica.*, **21**: 121-132.

PALADE, G.E. (1975). Intracellular aspects of the processes of protein synthesis. *Science.*, **189**: 347-358.

PERNIN, P. and CARIOU, M.L. (1989). Large genetic heterogeneity within amoebas of the species *Naegleria gruberi* and evolutionary affinities to the other species of the genus. *J. Protozool.,* **36**: 179-181.

PERNIN, P., CARIOU, M.L. and JACQUIER, A (1985). Biochemical identification and phylogenetic relationships in free-living amoebae of the genus *Naegleria*. *J. Protozool.*, **32**: 592-603.

PFEIFER, U. (1987). Functional morphology of the lysosomal apparatus. In *Lysosomes: their role in protein breakdown.* (Glaumann, H. and Ballard, F.J., eds). Acad. Press Inc. (London). pp 3-59.

PITT, D. (1975). *Lysosomes and Cell Function.* Longman, London and New York. 165 pp.

PRESTON, T.M. and O'DELL, D.S. (1973). Deuterium oxide-induced reversion of *Naegleria gruberi* flagellates. *J. Gen. Microbiol.*, **57**: 351-361.

PRESTON, T.M. and O'DELL, D.S. (1974). Studies on the amoeboid and flagellates of *Naegleria.* In *Primary amoebic mengingoencephalitis and free-living amoebae. Proc. Int. Colloq. Antwerp.* pp 55-61.

PRESTON, T.M. and KING, C.A. (1978). An experimental study of the interaction between the soil amoeba *Naegleria gruberi* on a glass substrate during amoeboid locomotion. *J. Cell Sci.*, **34**: 145-158.

PRESTON, T.M., COOPER, L.G. and KING, C.A. (1990). Amoeboid locomotion of *Naegleria gruberi*: the effects of cytochalasin B on cell-substratum interactions and motile behaviour. *J. Protozool. (suppl.)*, **37**: 6-11.

PUPKIS, M.F. and COOMBS, G.H. (1984). Purification and characterisation of proteolytic enzymes of *Leishmania mexicana* amastigotes and promastigotes. *J. Gen. Microbiol.*, **130**: 2375-2383.

RAFALKO, J.S (1947). Cytological observations on the amoebo-flagellate, *Naegleria gruberi* (protozoa). *J. Morph.*, **81**: 1-44.

RAIKOV, I.B. (1982). The protozoan nucleus. Morphology and Evolution (translated by Bobrov, N and Verhovtseva, M.). Cell Biology Monograph, volume 9 (Alfert, M., Beermann, W., Goldstein, l., porter, K.R and Sitte, P, eds). Springer-Verlag Wien NY. pp 72-130.

REED, S.L, KEENE, W.E. and McKERROW, J.H. (1989). Thiol proteinase expression and pathogenicity of *Entamoeba histolytica. J. Clin. Microb.*, **27:** 2772-2777.

RIEDER, C.L. and PALAZZO, R.E. (1992). Colcemid and the mitotic cycle. *J. Cell Sci.*, **102**: 387-392.

ROBERTSON, C.D. and COOMBS, G.H. (1990). Characterisation of three groups of cysteine proteinases in the amastigotes of *Leishmania mexicana mexicana. Mol. Biochem. Parasitol.*, **42:** 269-276.

ROBERTSON, C.D. and COOMBS, G.H. (1992). Stage-specific proteinases of *Leishmania mexicana mexicana* promastigotes. *FEMS Microb. Lett.*, **94:** 127-132.

ROBINSON, B.S., CHRISTY, P. HAYES, S.J. and DOBSON, P.J. (1992). Discontinuous genetic variation among mesophilic *Naegleria* isolates: Further evidence that *Naegleria gruberi* is not a single species. *J. Protozool.*, **39**: 702-712.

RODESCH, F. R., NEVE, P. and DUMONT, J. E. (1970). Phagocytosis of latex beads by isolated thyroid cells. *Exp. Cell Res.,* **60:** 354-360

ROSENTHAL, P.J., McKERROW, J.H., RASNICK, D. and LEECH, J.H. (1989). *Plasmodium falciparum:* inhibitors of lysosomal cysteine proteinases inhibit a trophozoite proteinase and block parasite development. *Mol. Biochem. Parasitol.,* **35**: 177-184.

ROTH, L.E. and DANIELS, E.W. (1962). Electron microscopic studies of mitosis in amoebae. II. The giant amoeba *Pelomyxa carolinensis. J. Cell Biol.*, **12**: 57-78.

ROTHE, G. KLINGEL, S. ASSFALG-MACHLEIDT, I., MACHLEIDT, W., ZIRKEL-BACH, C., BANATI, R.B., MANGEL, W.F. and VALET, G. (1992). Flow cytometric analysis of protease activities in vital cells. *Biol. Chem. Hoppe-Seyler.*, **373**: 547-554.

SALTARELLI, D. and PANTALONI, D. (1982). Polymerisation of the tubulin-colchicine complex and guanosine 5'-triphosphate hydrolysis. *Biochemistry.*, **21:** 2996-3005.

SANTAVY (1978). Colchicine alkaloids and related substances-their chemistry and biology. *Acta Univ. Palach. Olum,* **90**: 15-44.

SAWIN, K.E. and SCHOLEY, J.M. (1991). Motor proteins in cell division. *Trend. Cell Biol.*, **1**: 122-129.

SCHARDINGER, F. (1899). Entwicklungskreis einer *Amoeba lobosa* (Gymnamoeba): *Amoeba gruberi. S.K. Acad. Wiss. Wien.,* **108:** 713-734.

SCHECHTER, J., YANCEY, B. and WEINER, R. (1976). Response of tanycytes of rat media eminence to intraventtricular administration of colchicine and vinblastine. *Anat. Rec.,* **184**: 233-250.

SCHUSTER, F. (1961). Axenic cultivation of *Naegleria gruberi. J. Protozool. (suppl.).*, **18**: 19.

SCHUSTER, F. (1963). An electron microscope study of the amoeboflagellate, *Naegleria gruberi* (Schardinger). 1. The amoeboid and flagellate stages. *J. Protozool.*, **10**: 297-313 2. The cyst stage. *J. Protozool.*, **10**: 313-320.

SCHUSTER, F. (1969). Intranuclear virus-like bodies in the amoeboflagellates *Naegleria gruberi*. *J. Protozool.*, 16: 724-727.

SCHUSTER, F. (1975a). Ultrastructure of cysts of *Naegleria* spp.: A comparative study. *J. Protozool.*, **22**: 352-359.

SCHUSTER, F. (1975b). Ultrastucture of mitosis in the amoeboflagellate *Naegleria gruberi*. *Tissue and Cell.*, 7: 1 12

SCHUSTER, F.L. and SVIHLA, G. (1968). Ribonucleoprotein-containing vesicles in cysts of *Naegleria gruberi*. *J. Protozool.*, **15:** 752-758.

SEDMAK, J.J. and GROSSBERG, S.E. (1977). A rapid, sensitive and versatile assay for protein using Coomassie brilliant blue G250. *Analitic. Biochemi.*, **79**: 544-552

SINGH, B.N. (1950). A culture method for growing small free-living amoebae for the study of their nuclear division. *Nature, London.*, **165**: 65-6.

SINGH, B.N (1952). Nuclear division in nine species of small free-living amoebae and its bearing on the classification of the order amoebida. *Phil. Trans. R. Soc .London.*, **236**: 405-461.

SINGH, B.N AND DAS, S.R. (1970). Studies on pathogenic and non-pathogenic small free-living amoebae and the bearing of nuclear division on the classification of the order Amoebida. *Phil. Trans. R. Soc. London.*, **259**: 435-476.

STARLING, D. (1976). The effects of mitotic inhibitors on the structure of vinblastine-induced tubulin paracrystals from sea-urchin eggs. *J. Cell Sci.*, **20**: 91-100.

STEHR-GREEN, J.K., BAILEY, T.M. and VISVESVARA, G.S. (1989). The epidemiology of *Acanthamoeba* keratitis in the United States. *Am. J. Ophthalmol.*, **107**: 331-336.

STERNLICHT, H. and RINGEL, I. (1979). Colchicine inhibition of microtubules assembly via copolymer formation. *J. Bio. Chem.*, **254**: 10540-10550.

STEVENS, A.R., TYNDALL, R.L., COUTANT, C. and WILLAERT, E. (1977). Isolation of the aetiologic agent of primary amoebic meningoencephalatis from artificially heated waters. *Appl. Environ. Microbiol.*, **34**: 701-705.

STEVENS, A.R., DE JONCKHEERE, J.F. and WILLAERT, E. (1980). *Naegleria lovaniensis* new species: isolation and identification of six thermophilic strains of a new species found in association with *Naegleria fowleri. Int. J. Parasitol.*, **10**: 51-64.

TANNICH, E., SCHOLZE, H., NICKEL, R. and HORSTMANN, R.D. (1991). Homologous cysteine proteinases of pathogenic and non-pathogenic *Entamoeba histolytica*: differences in structure and expression. *J. Biol. Chem.*, **266**: 4798-4803.

TARATUTO, A.L., MONGES, J., ACEFE, J.C., MELI, F., PAREDES, A. and MARTINEZ, A.J. (1991). Leptomyxid amoeba encephalitis: report of the first case in Argentina. *Trans. R. Soc. Trop. Med. Hyg.*, **85**: 77.

TAYLOR, E.W. (1965). The mechanism of colchicine inhibition of mitosis. I. Kinetics of inhibition and the binding of H^3-colchicine. *J. Cell Biol.*, **25**: 145-160.

THONG, Y.H. and FERRANTE, A. (1986). Migration patterns of pathogenic and non-pathogenic *Naegleria. Infect. Immun.*, **51**: 177-180.

THONG, Y.H. and FERRANTE, A. (1987). Experimental pharmacology. Amphizoic amoebae human pathology. *Infect. Dis. Colour Monographs.* (Rondanelli, E.G., ed). Piccin, Padua. 251 pp.

TODD, S.R. and KITCHING, J.A. (1973). Effects of high hydrostatic pressure on morphogenesis in *Naegleria gruberi* (Schardinger). *J. Protozool.*, **20**: 421-424.

UBELAKER, J.E. (1990). *Acanthamoeba sp* trophozoites: *In vitro* adherence and penetration of human corneas. *Bull. Soc. Française Parasitol. Supplement* 1.VII. International Congress of Parasitology, Paris, supplement 1.

VANDRE, D.D. and BORISY, G.G. (1989). Anaphase onset and dephosphorylation of mitotic phosphoprotein occur concomitantly. *J. Cell Sci.*, **94**: 245-258.

VICKERMAN, K. (1962). Patterns of cellular organisation in limax amoebae. *Exp. Cell Res.*, **26**: 497-519.

VISVESVARA, G.S. and CALLAWAY, C.S. (1974). Light and electron microscopic observations on the pathogenesis of *Naegleria fowleri* in mouse brain and tissue culture. *J. Protozool.*, **21:** 239-250.

VISVESVARA, G.S.and STERN-GREEN, K. (1990). Epidemiology of free-living amoeba infection. *J. Protozool. (suppl.),* **37**: 25-33.

VISVESVARA, G.S. , SCHUSTER, F. and MARTINEZ, A.J. (1993). *Balamuthia mandrillaris*, Ng, N-sp, agent of amoebic meningoencephalitis in humans and other animals. *J. Eukaryot. Microb.*, **40**: 504-514.

WARHURST, D.C. (1985). Pathogenic free-living amoebae. *Parasit. Today.*, **1**: 24-28.

WARHURST, D.C. (1988). *Acanthamoeba* keratitis. *Brit. Med. J.*, **296:** 568.

WARHURST, D.C. and THOMAS, S.C. (1978). An isoenzyme different between a smooth (s) and a rough (r) strain of *Naegleria gruberi*. *Protistologica.*, **14**: 87-89.

WEBER, K., BIBRING, T. and OSBORN, M. (1975a). Specific visualisation of tubulin-containing structures in tissue culture cells by immunofluorescence. *Exp. Cell. Res.*, **95:** 111-120.

WEBER, K., POLLACK, R. and BIBRING, T. (1975b). Antibody against tubulin: the specific visualisation of cytoplasmic microtubules in tissue culture cells. *Proc. Nat. Acad. Sci.*, **72:** 459-463.

WEEKERS, P.H.H, BODELIER, P.L.E., WIJEN, J.P.H. and VOGELS, G.D. (1993). Effects of grazing by free-living soil amoebae *Acanthamoeba castellanii, Acanthamoeba polyphaga and Hartmannella vermiformis*. *Appl. Environ. Microb.*, **59**: 2317-2319.

WEIK, R.R. and JOHN, D.T. (1977). Agitated mass cultivation of *Naegleria fowleri*. *J. Parasitol.*, **63**: 868-871.

WILEY, C.A., SAFRIN, R.E., DAVIS, D.E., LAMPERT, P.W., BRAUDE, A.A., MARTINEZ, J. and VISVESVARA, G.S. (1987). *Acanthamoeba* meningoencephalitis in a patient with AIDS. *J. Infect. Disease.*, **155**: 130

WONG, M.M., KARR, S.L. and CHOW, C.K. (1977). Changes in the virulence of *Naegleria fowleri* maintained *in vitro*. *J. Parasitol.*, **63**: 872-878.

WOODS, A., SHERWIN, T., SASSE, R., MACRAE, T.H., BAINES, A.J. and GULL, K. (1989). Definition of individual components within the cytoskeleton of *Trypanosoma brucei* by a library of monoclonal antobodies. *J. Cell Sci.*, **93**: 491-500.

WRIGHT, P. AND BUCKLEY, R.J. (1988). *Acanthamoeba* keratitis. *Brit. Med. J.*, **296**: 568-569.

YUGUANG, H., MCCULLEY, J.P., ALIZADEH, H., PIDHERNEY, M., MELLON, J. UBELAKER, J.E., STEWART, G.L., SILVANY, R.E. and NIEDERKORN, J.Y. (1992). A pig model of *Acanthamoeba* keratitis: transmission via contaminated contact lenses. *Invest. Ophthalmol. Vis. Sci.*, **33:** 126-133.

YUMURA, T.K. and FUKUI, Y. (1987). Reorganisation of microtubules during mitosis in *Dictyostelium:* Dissociation from MTOC and selective assembly/disassembly *in situ*. *Cell Motil. Cytoskel.*, **8**: 106-117.

GLASGOW
UNIVERSITY
LIBRARY